Ollscoil Chathair
Bhaile Átha Cliath
Dublin City University

Investigating the inhibitory effect of *Candida parapsilosis* on *Staphylococcus aureus* biofilm formation

A thesis submitted for the award of Doctor of Philosophy (PhD) by

Ciara Furlong

B.A. (Mod) Microbiology

Supervised by Dr Linda Holland

Dublin City University

Faculty of Science and Health, School of Biotechnology

January 2024

Declaration

I hereby certify that this material, which I now submit for assessment on the programme of study leading to the award of Doctor of Philosophy, is entirely my own work, and that I have exercised reasonable care to ensure that the work is original and does not to the best of my knowledge breach any law of copyright, and has not been taken from the work of others save and to the extent that such work has been cited and acknowledged within the text of my work.

Signed: _____ 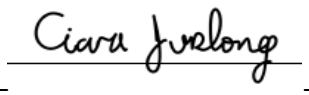 _____

ID No.: 19215463

Date: 08/01/2024

Acknowledgements

Thank you to my supervisor Dr Linda Holland for her guidance and support.

Thank you to my friends and colleagues in DCU, Katie, Yongda, Dearbhla, and Helena. Of course, there's a special thank you to Katie. I am so glad we both had each other, and I will miss our chats, especially the coffee walks around Albert College Park.

Thank you to Roberta for sharing the lab with me for the final stretch of our projects. Especially after having spent so much time alone in that lab. You really helped keep me sane and focused on the end goal.

To Mom, Dad, Eoin, Eimear, and Nana.

I wouldn't have completed my PhD without the support and encouragement of my parents, so this is for them. They've been with me every step of the way. Thank you for all the tea and hugs when I needed them. I love you both. A special thank you and all my love to my Nana, and especially for all the lit candles. Living together for 8 years flew by.

Ciara

Contents

List of Figures

List of Tables

List of Abbreviations

AMR	Antimicrobial resistance
AIP	Auto-Inducing Peptide
BHI	Brain heart infusion
CaSN	*Candida albicans* supernatant
CDC	Centre for disease control
CFS	Cell-free supernatant
CFU	Colony forming units
CP	*Candida parapsilosis*
CV	Crystal violet
CWA	Cell Wall Anchored
DEG	Differentially expressed gene
DRI	Device Related Infection
ECM	Extracellular matrix
eDNA	Extracellular DNA
EPS	Extracellular polymeric substance(s) or exopolysaccharide
ICU	Intensive care unit
LAB	Lactic acid bacteria
MDR	Multi-drug resistance
MRSA	Methicillin-resistant *Staphylococcus aureus*
MSCRAMM	microbial surface components recognizing adhesive matrix molecules
MSSA	Methicillin-sensitive *Staphylococcus aureus*
MWCO	Molecular Weight Cut Off
NEAT	Near iron transporter
PCA	Principal component analysis
PIA	Poly intercellular adhesin
PNAG	Poly-N-acetylglucosamine
RNA-seq	RNA sequencing
RT	Room temperature

SA1	*S. aureus* DSM 799
SN	Supernatant
TSB	Tryptone soya broth
VRSA	Vancomycin-resistant *Staphylococcus aureus*
WHO	World Health Organisation
YPD	Yeast peptone dextrose

Abstract

Investigating the inhibitory effect of *Candida parapsilosis* on *Staphylococcus aureus* biofilm formation

Ciara Furlong

Biofilms are surface-attached communities of microorganisms surrounded by an extracellular matrix. The biofilm matrix plays an integral role in protecting the microorganisms within. Infections associated with biofilms are incredibly difficult to treat. *Staphylococcus aureus* is a major human pathogen and can produce robust biofilm. *Candida parapsilosis* is an emerging fungal pathogen that is frequently isolated as the cause of different types of infection. Its interaction with *S. aureus* has yet to be explored. The exploration of inter-species interaction between microorganisms presents an opportunity to gain insight into novel approaches to combat human pathogens by exploiting natural microbial antagonism.

The aim of this project is to characterise the effect of co-culture with *C. parapsilosis* on *S. aureus* during biofilm formation. Using various *in vitro* techniques, such as a crystal violet biofilm assay, co-culture with *C. parapsilosis* resulted in an inhibition of robust *S. aureus* biofilm formation. Further investigation revealed that cell-free *C. parapsilosis* supernatant could also inhibit *S. aureus* biofilm formation. This result suggested that a fungal-secreted factor was causing the inhibitory effect on *S. aureus* biofilm. Extensive *in vitro* analysis of the bacterial biofilm inhibitory phenotype revealed that the fungal factor(s) exhibit pleiotropic effects and may be targeting various components of the *S. aureus* biofilm matrix. RNA sequencing identified global changes in transcription that occur in *S. aureus* in the presence of *C. parapsilosis* cells or cell-free supernatant. In addition, various *in vitro* techniques have been utilised to characterise the cell-free supernatant of *C. parapsilosis*, indicating that the active factors may be small molecules/metabolites.

Future study is needed to identify the biofilm inhibiting factors produced by *C. parapsilosis* and assess their potential usefulness as an alternative or conjugate therapy against biofilm infections.

Chapter 1 - Introduction

1.1. *Staphylococcus aureus*, a major human pathogen

Staphylococcus aureus is a Gram-positive bacterium with a spherical cocci appearance (Ogston and Witte, 1984; Brown and Grilli, 1998). Alexander Ogston first described *S. aureus'* role in abscess formation and septicaemia in 1880, and it remains a clinically important microorganism more than 100 years later (Ogston and Witte, 1984). *S. aureus* can be found in the environment and is a human commensal organism; however, carriage in humans varies depending on factors such as age, geographic location, and body niche (Sollid *et al.*, 2014). The bacterium colonises the skin and nasal passages of ~30% of the human population, and another third of the population are transient carriers (Thomer, Schneewind and Missiakas, 2016).

S. aureus is recognised as a major human pathogen and is responsible for many different infections in humans (Figure 1.1). It is a leading cause of skin and soft tissue and bloodstream infection (Tong *et al.*, 2015). *Staphylococci* are the leading cause of device-related infections (Weinstein and Darouiche, 2001). *S. aureus* is an opportunistic pathogen, and the increasing risk of antibiotic-resistant isolates is great. The antimicrobial resistance (AMR) crisis was declared as one of the top 10 global health threats, with *S. aureus* among the pathogens of interest (World Health Organization, 2019).

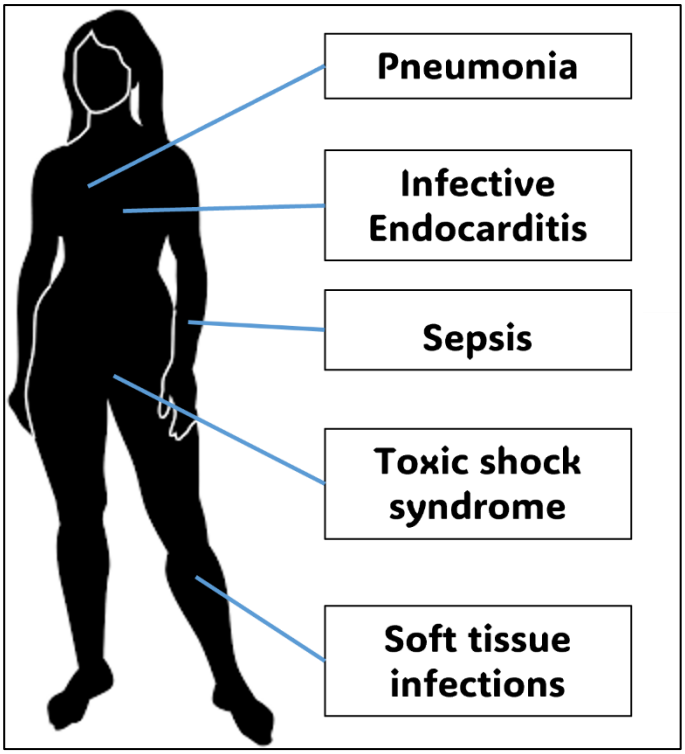

Figure 1.1. – S. aureus can cause infection across multiple sites in the human body. *S. aureus is a well-adapted bacterium that can cause life-threatening infections such as sepsis, endocarditis, osteomyelitis, and skin and soft tissue infections. Figure adapted from* (Salgado-Pabón and Schlievert, 2014)

1.1.1. Methicillin Resistant *S. aureus*

Benzylpenicillin (penicillin G), a β-lactam antibiotic, was used to treat *S. aureus* infections prior to the 1950s (Stapleton and Taylor, 2002). However, resistant strains that produced β-lactamases that inhibited the action of penicillin soon arose. To combat this, methicillin, a penicillin derivative with the ability to inhibit β-lactamase was synthesised. Unfortunately, as soon as Methicillin was used clinically, methicillin resistant *S. aureus* (MRSA) strains were isolated (Chambers, 1997). Methicillin resistance in *S. aureus* isolates is mediated by the presence of *mecA* and *mecC* genes that encode the penicillin-binding protein 2a (PBP2a) and PBP2c enzymes, respectively (Chambers, 1997; García-Álvarez *et al.*, 2011). Recently, a study by Larsen *et al*. tracked the evolution of methicillin resistance for a particular MRSA to the pre-antibiotic era

and that this resistance arose “possibly as a co-evolutionary adaptation of *S. aureus* to the colonization of dermatophyte-infected hedgehogs” (Larsen *et al.*, 2022). The study highlighted the importance of recognising the interconnectivity of wild, agricultural, and human ecosystems in the evolution of antibiotic resistance.

Transient carriage of *S. aureus*, including MRSA, in nasal cavities and on the hands of healthcare workers, is a major route of nosocomial infection (Lowy, 1998; Creamer *et al.*, 2010). MRSA has had a considerable impact across the globe. The incidence of MRSA hospital-acquired infection (HAI) or healthcare associated MRSA (HA-MRSA) varies across countries in the European Union (EU) (reviewed in (Köck *et al.*, 2010)). It was reported in 2001, that 40% to 50% of *S. aureus* isolates that were sampled from bloodstream infections in Irish hospitals were methicillin resistant (Ireland and SARI Infection Control Subcommittee, 2001). From 2016 to 2020 the incidence of HA-MRSA isolates being reported decreased on average across the EU, indicating the success of control measures in healthcare settings (World Health Organization, 2021). In the Republic of Ireland, this was also the case, with the number of HA-MRSA isolates detected from blood cultures decreasing year on year (Health Protection Surveillance Centre, 2022). However, case reporting parameters did not account for repeated infections in a single patient. Furthermore, if a case was first identified as MSSA and then later on as MRSA, only MSSA was recorded and the same vice versa. Therefore, overall infection incidence may be somewhat underestimated. Despite this, MRSA remains an important pathogen for Europe due to isolates that are resistant to at least one other type of antimicrobial compound.

S. aureus’ antibiotic resistant status, it’s inherent ability to evade the host immune system, and its arsenal of virulence factors all contribute to making this bacterium such an effective pathogen. Treatment is made even more difficult due to its capability of colonizing the surface of medical devices by forming a biofilm.

1.2. Biofilms –What are they?

As early as the 17th century, microbiologists have recognized that bacteria tend to associate with surfaces. Early references to what we now know as a 'biofilm' arose in the 1960s in relation to wastewater treatment (Flemming *et al.*, 2021). However, it is often cited that this term was coined by Costerton *et al*. in 1978 (Costerton, Geesey and Cheng, 1978; Donlan and Costerton, 2002). By definition, a biofilm is a surface-attached community of microorganisms where these cells are enclosed within a self-made extracellular polymeric substance (EPS) (Donlan, 2002). Biofilms studied in a laboratory setting are often composed of just a single species. However, in the natural environment, biofilms can contain a mix of many different species of bacteria, fungi, and viruses. Microorganisms can colonise virtually any surface to form a biofilm. Examples include the colourful biofilms that we see in geothermal pools, they form on domestic and industrial infrastructure, rocks in streams, the plaque on human teeth and even on sand (Hall-Stoodley, Costerton and Stoodley, 2004; Liu *et al.*, 2016; Galié *et al.*, 2018).

The ability to form a biofilm is universal in bacteria (López, Vlamakis and Kolter, 2010). It is now known that the majority of bacteria exist in this sessile mode (attached to a surface and or other microorganisms) of growth as opposed to the planktonic (free-floating) state of growth (Costerton *et al.*, 1995). Biofilm formation is a cyclical process that proceeds through various stages. Generally, biofilm development can be divided into at least 3 stages (Figure 1.2). Attachment is the first step, where planktonic cells fix themselves to a surface. Maturation of the biofilm follows where the cells proliferate and begin to secrete molecules to produce a biofilm matrix. The final stage is dispersal, where cells are released from the biofilm and the cycle can begin again (Costerton *et al.*, 1995; Kostakioti, Hadjifrangiskou and Hultgren, 2013).

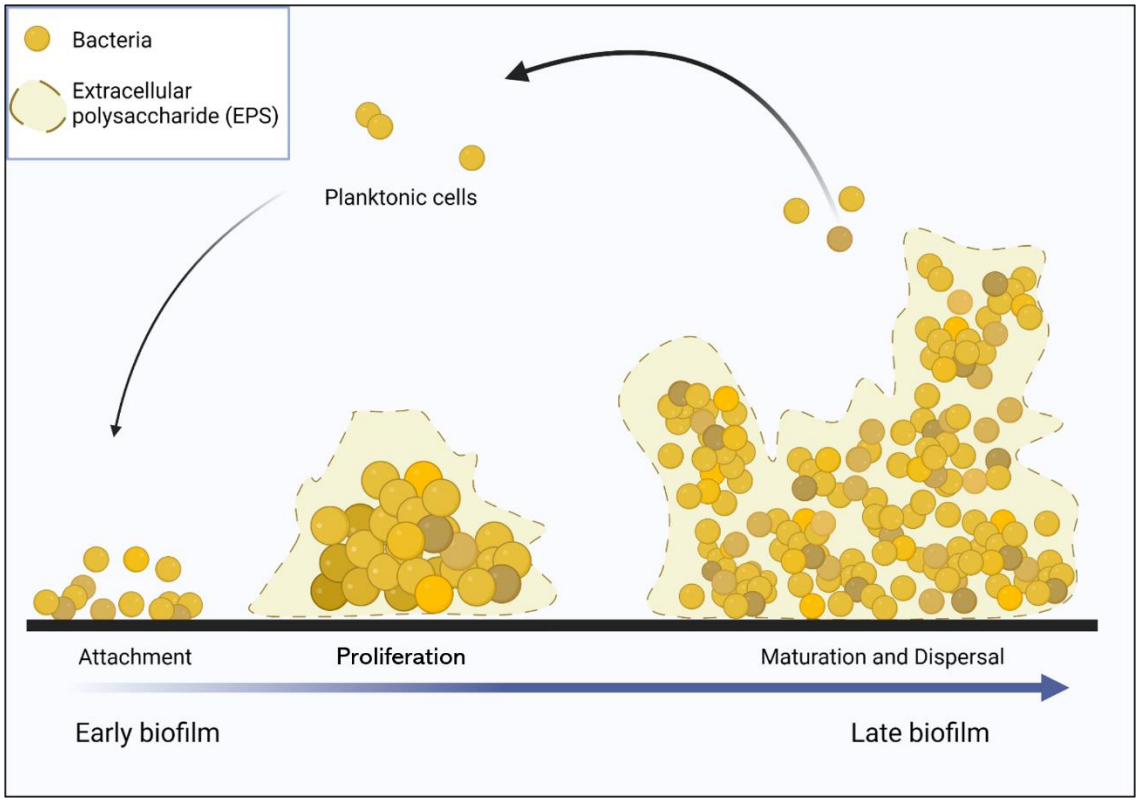

Figure 1.2. The stages of biofilm formation. *During the early stages of biofilm formation, planktonic bacteria attach themselves to a surface. The bacterial cells begin to grow and proliferate to form micro-colonies and produce EPS. The latter stages of biofilm are characterised by a mature biofilm with distinct microbial populations. Finally, cells disperse from the biofilm to colonise other niches. Created with BioRender.com.*

An interest in studying the role of bacteria within a biofilm as the cause of infection arose in the 1970s (Høiby, 2017; Vestby *et al.*, 2020). Perhaps due to this, there is a lag in studying surface-attached sessile bacteria compared to single-species planktonic cultures that have been studied for over 100 years. This is understandable as it is easier to work with homogenous cultures in the laboratory (Hall-Stoodley, Costerton and Stoodley, 2004). Despite this, rapid advances in our understanding of biofilms have been made.

A biofilm can form in response to different signals, and they offer many advantages to the microorganisms that exist in such a community. Changes in the environment like high salt concentration (osmotic stress) can result in the induction of biofilm formation as a defence mechanism (Ferreira *et al.*, 2019). Stimuli that mirror conditions found in the human body, such as iron-deprivation, can also trigger biofilm (Jefferson, 2004). This can then compromise the effectiveness of the host's immune response (Jacques, Marrie and Costerton, 1987). Biofilms have inherent heterogeneity, with sections of the biofilm, even adjacent cells, which vary widely both physiologically and chemically from each other (Stewart and Franklin, 2008). These subpopulations arise due to oxygen and nutrient gradients. Depending on where they are located within the biofilm, cells may be growing aerobically, anaerobically, fermenting, or they even may be dead (Rani *et al.*, 2007). Biofilm formation is also a mechanism to colonise a favourable niche (Jefferson, 2004). When glucose (which is required for EPS production) becomes scarce bacteria become planktonic and move on to a more favourable environment (Hunt *et al.*, 2004).

1.2.1. Antimicrobial-resistant properties of biofilms

The antimicrobial resistance (AMR) crisis is characterised by the increase in infectious human diseases around the globe that cannot be treated with any known antimicrobial agent (Michael, Dominey-Howes and Labbate, 2014). Many of the drugs that are currently used to kill microorganisms are losing their effectiveness, and more species that have evolved multi-drug resistance (MDR) are emerging (Tanwar *et al.*, 2014). This is due in part to overuse and/or inappropriate use of antibiotics. WHO has described this crisis as one of the greatest threats to global human health (World Health Organization, 2021).

As the threat of MDR rises, the WHO has highlighted microbial species of importance based on their threat to human health. The ESKAPE pathogens are among the bacterial species that the WHO has marked as a priority (Tacconelli *et al.*, 2018). ESKAPE is an acronym for an assortment of multi-drug resistant pathogens; they are *Enterococcus*

faecium, *Staphylococcus aureus, Klebsiella pneumoniae*, *Acinetobacter baumannii*, *Pseudomonas aeruginosa*, and *Enterobacter* species (Rice, 2008; Mulani *et al.*, 2019).

Biofilm infections are incredibly difficult to treat (Archer *et al.*, 2011). Biofilm-forming microorganisms are a major concern in healthcare settings and lead to increased morbidity and mortality (Subhadra *et al.*, 2018). Indeed, biofilms can be up to a thousand times more resistant to antibiotics than their planktonic counterparts (Ceri *et al.*, 1999). While planktonic bacteria released from the biofilm can be treated effectively with antibiotics and in combination with the natural immune response of the host.

Biofilms utilise many different resistance mechanisms (reviewed by (Uruén *et al.*, 2020)) (Figure 1.3). Penetration of antibiotics into the biofilm is the first challenge, with select antibiotics (vancomycin and chloramphenicol) shown to be unable to penetrate (Singh *et al.*, 2016). In the case of vancomycin another study has shown that vancomycin can penetrate but the time and concentrations required is not currently achievable by existing treatment methods (Post *et al.*, 2017). The heterogeneity of biofilms is believed to play a role in the inherent resistance to antimicrobial treatment. Oxygen gradients exist in biofilm with some cells existing in oxygen-limited regions. Cells in oxygen-limited conditions are less susceptible to antibiotics (Borriello *et al.*, 2004). Bacteria can produce enzymes that can neutralise the antibiotics. Persister cells are another mechanism. These cells are extremely tolerant of antibiotic clearing. They are dormant cells and many antibiotics require actively respiring cells to be effective (Theis *et al.*, 2023). Furthermore, efflux pump-mediated resistance continues to challenge antibiotic therapy (Dashtbani-Roozbehani and Brown, 2021).

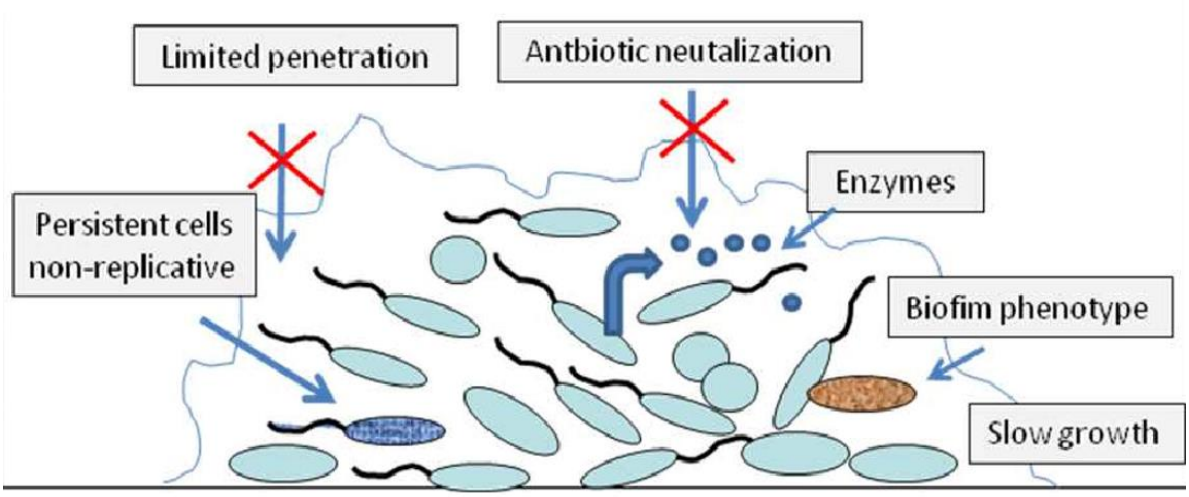

Figure 1.3. Biofilm resistance mechanisms. *Biofilm resistance is a combination of many mechanisms. The extracellular matrix limits drug penetration. Bacterial cells can produce enzymes that inactivate the antibiotic. The inherent heterogeneity of cells within the biofilm, including persister cells also prevents killing by antibiotics. Figure reproduced from* (Laura Estela and Ramos, 2012).

Antibiotic treatment alone is usually insufficient to treat biofilm infections. Following the failure of antibiotic therapy, the recommended method currently used to treat biofilm infections is simply the physical removal of the biofilm (Bhattacharya *et al.*, 2015). This can include debridement of chronically infected wounds, replacement of catheters or surgical removal of other contaminated medical devices or prostheses (Wolcott, Kennedy and Dowd, 2009; Khatoon *et al.*, 2018). The lack of available treatment options only highlights the need for novel therapeutic strategies.

1.3. *Staphylococcus aureus* biofilm regulation and pathogenesis

S. aureus has an arsenal of virulence factors that enable it to colonise host tissues and masterfully evade the host immune system (Gordon and Lowy, 2008). Bacteria rely on cues from the environment and host to coordinate a response. Quorum sensing (QS) was first reported in 1970. It is the intercellular signalling between bacteria that acts by monitoring cell density within microbial populations (Nealson, Platt and Hastings, 1970; Pena *et al.*, 2019). QS systems enable bacteria to react to their environment, specifically in relation to cell or population density. These systems induce a range of physiological responses like virulence, sporulation, motility and biofilm formation (Miller and Bassler, 2001). Two-component signalling systems are an additional method used to perceive and respond to these environmental changes (Stock, Robinson and Goudreau, 2000). These systems can coordinate the expression of *S. aureus* virulence factors such as toxins and surface-attached proteins (Jenul and Horswill, 2018). *S. aureus* produces many toxins. Among these are the membrane damaging toxins (alpha toxin and bicomponent leukotoxins), toxins that interfere with host receptors (e.g. enterotoxins) and secreted enzymes including those that can degrade host molecules (aureolysin) (reviewed in (Otto, 2014)).

The ability of *S. aureus* to form a biofilm has a major impact in clinical settings (Reffuveille *et al.*, 2017). *S. aureus* biofilms are a source of major complications and infection in humans causing a range of issues like endocarditis, osteomyelitis and increased antimicrobial tolerance. In particular, persistent biofilm infections of implanted medical devices are extremely hard to treat (Donlan, 2002; Römling *et al.*, 2014). Biofilms are prevalent in chronic wounds, with *S. aureus* biofilms widely associated with such chronic infections (James *et al.*, 2008; Zhao *et al.*, 2013). Chronic wounds affect up to 2% of the population in developed countries (Fazli *et al.*, 2009). They present significant challenges for treatment when infected and incur high healthcare costs (Gottrup, 2004; Han and Ceilley, 2017). Chronic wounds are characterised by prolonged inflammation and the presence of bacterial communities impairs the healing process (Zhao *et al.*, 2013). *S. aureus* is among the most common

bacterial species present in chronic wounds, with another bacterial pathogen *Pseudomonas aeruginosa* (*P. aeruginosa*) found deep in the tissue while *S. aureus* colonises the uppermost layers (Fazli *et al.*, 2009). *S. aureus* is present in just over 90% of chronic venous leg ulcers and often as a biofilm (Gjødsbøl *et al.*, 2006). *S. aureus* biofilm can impair wound healing by altering host gene expression and the production of inflammatory cytokines. Furthermore, *in vitro* analysis has shown that *S. aureus* biofilm induces a lower level of cytokine production in human keratinocytes when compared to planktonic *S. aureus* (Secor *et al.*, 2011). It has been demonstrated that *S. aureus* biofilm resists phagocytosis by host macrophages and has the ability to attenuate inflammation *in vivo* (Thurlow *et al.*, 2011).

1.3.1 Mechanisms of *S. aureus* biofilm formation.

The processes that lead to the formation of the *S. aureus* biofilm are complex and tightly regulated (Hall-Stoodley, Costerton and Stoodley, 2004). Figure 1.4 provides an overview of the most important biofilm regulators. These include, SarA, LytSR, MgrA, SaeRS, Sigma B, and Agr. Changes in the environment can trigger biofilm formation in *S. aureus* (reviewed in (Liu, Zhang and Ji, 2020)). *S. aureus* can adapt to diverse physiological niches. For example, *S. aureus* can lower the pH of its extracellular environment by metabolising glucose. Previous studies have noted this lowered pH (to around pH 5.5) during biofilm formation (Liu, Zhang and Ji, 2020; Fernández *et al.*, 2021). A low pH prevents *agr* expression, the main QS system in *S. aureus* that is key for biofilm repression and dispersal via the production of proteases (discussed further in this introduction) (Regassa, Novick and Betley, 1992; Boles and Horswill, 2011). There are two main mechanisms of biofilm formation in *S. aureus*. Ica-dependent and ica-independent biofilm formation.

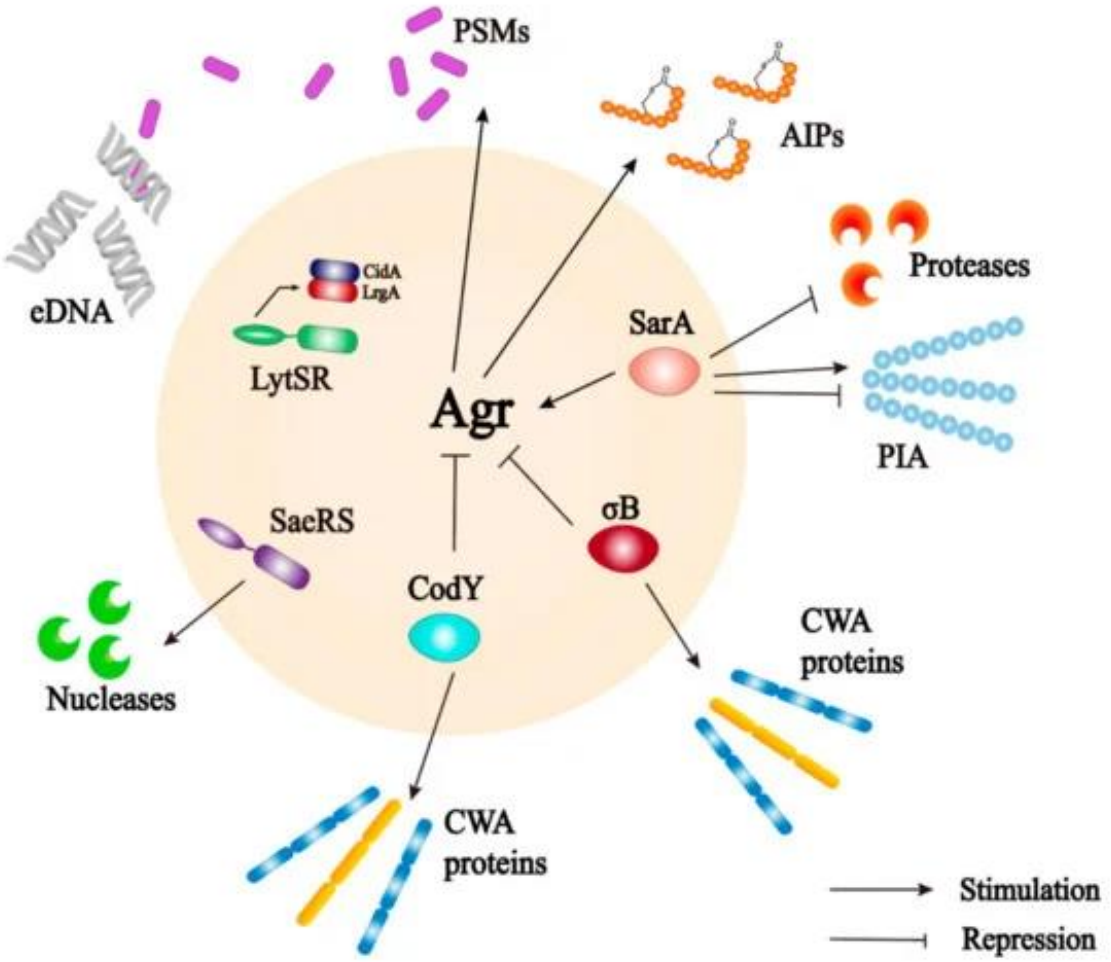

Figure 1.4. A complex network of regulators control S. aureus biofilm formation. *S. aureus employs a vast network of interconnected regulatory pathways to control biofilm formation. Shown are the important regulators Agr, LytSR, SigB, CodY, SaeRS, and SarA. These regulators are responsible for the activation and/or the repression of various effectors of biofilm, such as proteases, nucleases, PSMs and AIPs. They are also responsible for the production of biofilm matrix components PIA and CWA proteins. Black arrows indicate stimulation, and red blunted arrows indicate repression. CWA; cell wall anchored proteins. AIP; autoinducing peptides. PSMs; Phenol soluble modulins. PIA; polysaccharide intercellular adhesin. eDNA; extracellular DNA. Figure reproduced from* (Peng *et al.*, 2023).

1.3.1.1. Ica-dependent biofilm formation

Initially, it was believed that biofilm formation in *S. aureus* required the presence of poly-intercellular adhesion (PIA) or poly-β-1-6-N-acetylglucosamine (PNAG) which is encoded by the *icaADBC* locus (O'Gara, 2007). PIA is a cationic and partially deacetylated molecule. It is one of the main components of the *Staphylococcal* biofilm, in both *S. aureus* and *Staphylococcus epidermidis* (*S. epidermidis*). The *ica* locus was first identified in *S. epidermidis* (Heilmann *et al.*, 1996; Mack *et al.*, 1996).

PIA plays a significant role in bacterial aggregation and a structural role in the biofilm matrix (Heilmann *et al.*, 1996). Many bacteria across different species (including gram-negative species like *Escherichia coli*) produce PIA orthologues, highlighting its importance in biofilm formation (Wang, Preston and Romeo, 2004; Ganeshnarayan *et al.*, 2009). The expression of *icaADBC* is regulated by different factors including the global regulatory proteins SarA and Sigma B (Cue, Lei and Lee, 2012). The presence of NaCl has been correlated with PIA production in MSSA (methicillin-sensitive *S. aureus*) isolates also (O'Neill *et al.*, 2007).

The *SarA* locus is required for PIA production in *S. aureus* by directly binding to the *icaADBC* promoter and positively regulating the expression of the *ica* operon (Valle *et al.*, 2003; Tormo *et al.*, 2005). The gene product of *SarA* is the *Staphylococcal* accessory regulator (SarA) protein and is a major regulator of a wide range of virulence factors (Cheung and Zhang, 2002). A mutation of *SarA* results in limited biofilm formation (Beenken, Blevins and Smeltzer, 2003). Sigma B is a stress response regulator that controls over 100 genes in response to environmental changes (Pané-Farré *et al.*, 2006). *SarA* expression is controlled by Sigma B and is essential for surface attachment (Valle *et al.*, 2003). Therefore, sigma B is an indirect regulator of the *ica* locus. It has been noted that the mechanisms governing the expression of this locus vary between species (*S. aureus* vs *S. epidermidis*) and between strains of the same species (Cue, Lei and Lee, 2012).

There is contradictory reports on the role of Sigma B in *S. aureus* biofilm formation. Lauderdale *et al*., showed that Sigma B is essential for *ica*-independent biofilm formation (Lauderdale *et al.*, 2009). Valle *et al*. had originally reported that sigma B was

not required for biofilm formation (Valle *et al.*, 2003), however, it was later demonstrated that the strain used in that study was an *agr* mutant and that the defective Agr QS system masked the Sigma B biofilm phenotype (Lauderdale *et al.*, 2009). In addition, it has been reported that sigma B can also inhibit PIA synthesis and biofilm in *S. aureus* (Valle, Echeverz and Lasa, 2019)**.**

The regulation of the *ica* operon is carefully controlled in order to prevent wasteful production of metabolically expensive PIA. IcaR is the transcriptional repressor for *icaADBC* (Conlon, Humphreys and O'Gara, 2002). Interestingly, SarA and Sigma B are required for *icaR* expression. In addition, Cerca *et al.* noted that IcaR only had weak repressive effect on *icaADBC* expression (Cerca, Brooks and Jefferson, 2008).

1.3.1.2. Ica-independent biofilm formation

It is now known that *ica*-independent biofilm phenotypes exist that depend on alternative mechanisms that require different proteins. These include the fibronectin-binding proteins (FnBPA and FnBPB), SarA, and the major autolysin (Atl) (Fitzpatrick, Humphreys and O'Gara, 2005). Evidence for alternate mechanisms of biofilm formation first arose when MRSA clinical isolates produced increased biofilm in the presence of glucose, despite *icaA* expression being induced in the presence of NaCl. This suggested little correlation between biofilm development and the expression of the *ica* operon in *S. aureus* clinical isolates. This is further evidenced by the fact that *S. aureus* with a mutation in the *ica* locus has the ability to produce a biofilm (Fitzpatrick, Humphreys and O'Gara, 2005).

While SarA is required for the positive expression of the *ica* locus, it also activates transcription of the *bap* gene and is consequently a positive regulator of Bap-mediated biofilm formation (Trotonda *et al.*, 2005). The *rbf* gene (regulator of biofilm formation) encodes a transcriptional regulator of *S. aureus* biofilm (Lim *et al.*, 2004). This araC-type

regulator does not regulate the *ica* operon suggesting that Rbf may induce biofilm by some other independent pathway.

The *S. aureus* surface protein G (SasG) is a novel adhesin with sequence similarity to the Aap (accumulation association protein) of *S. epidermidis* (Roche, Meehan and Foster, 2003). Its role in biofilm formation, independently of *ica,* has been demonstrated (Corrigan *et al.*, 2007; Geoghegan *et al.*, 2010). SasG promotes adhesion to the desquamated epithelial cells of the nasal passage and plays a role in the accumulation phase of biofilm formation (Geoghegan *et al.*, 2010). The B repeats of SasG are vital to its ability to help form a biofilm. Specifically, the number of B repeats, where 8, 6 and 5 repeats result in biofilm. Whereas 4, 2 or 1 repeats did not form biofilm. Interestingly, SasG masks the effect of some MSCRAMMS (microbial surface component recognizing adhesive matrix molecules), such as ClfB, due to its size, but the adhesion ability of *S. aureus* is compensated for by SasG (Corrigan *et al.*, 2007; Geoghegan *et al.*, 2010).

Another mechanism by which *S. aureus* can form a biofilm is by incorporating host molecules. *S. aureus* is unique in its ability to coagulate blood (Crosby, Kwiecinski and Horswill, 2016). This ability helps researchers to distinguish *S. aureus* from coagulase negative *Staphylococci* (Kateete *et al.*, 2010). Hijacking of the host coagulation enables *S. aureus* to subvert the ancient innate immune response to invading bacteria (McAdow, Missiakas and Schneewind, 2012). It secretes the traditional staphylococcal coagulase (Coa) and the von Willebrand factor-binding protein (vWbp) (Friedrich *et al.*, 2003; Kroh, Panizzi and Bock, 2009). *S. aureus* can utilise Coa and vWbp to non-proteolytically activate prothrombin to form fibrin fibrils, thus hijacking the host clotting cascade (Friedrich *et al.*, 2003). As soon as a medical device is inserted into the body, it is immediately coated with host plasma proteins and other elements that condition the surface (MacKintosh *et al.*, 2006; Gee Neoh *et al.*, 2017). Upon attachment to the surface, *S. aureus* can use its ability to coagulate blood and create the biofilm scaffold from fibrin. Thus, Coa-mediated biofilm is dependent on the availability of fibrinogen and the proteins FnBPA/FnBPB (Thomer, Schneewind and Missiakas, 2016; Zapotoczna, O'Neill and O'Gara, 2016). *S. aureus* coagulases have been reported to be critical for biofilm formation under physiologically relevant conditions (Zapotoczna *et al.*, 2015). This biofilm can also protect the bacteria from phagocytosis, playing an important role

in its evasion of the host immune system (Guggenberger *et al.*, 2012; Thomer, Schneewind and Missiakas, 2016).

1.4. The *S. aureus* biofilm life cycle

As stated previously, biofilm formation proceeds through three main stages: Attachment, proliferation/maturation and dispersal (Otto, 2013) (Figure 1.2). Using microfluidic technology, the biofilm formation of *S. aureus* can be separated into five stages (Moormeier *et al.*, 2014). These include the addition of multiplication and exodus stages that follow the attachment stage. Multiplication stage was described as immediately following attachment, where a lawn of cells is rapidly grown. At this stage the cells have yet to begin to produce the membrane-like extracellular matrix (ECM) but produce a variety of factors that help to stabilise cell-cell adherence that protect them from shear forces (Moormeier *et al.*, 2014; Moormeier and Bayles, 2017). Following the multiplication stage, a subpopulation of cells is released through a mechanism known as "exodus" aided by a *Staphylococcal* nuclease (Moormeier *et al.*, 2014). This model is relatively new, so for the purpose of this introduction, the more established three-stage model is used.

1.4.1. *S. aureus* Attachment

Biofilm attachment is the first crucial step in establishing the biofilm community (Figure 1.2). To initiate attachment, planktonic bacteria must first come into contact with a biotic (living) or an abiotic (artificial) surface. While some bacteria are motile through the use of flagella e.g. *Escherichia coli* (Kumar and Philominathan, 2009; Nakamura and Minamino, 2019), *S. aureus* usually relies on Brownian movement or spreading motility to come into contact with a surface (Pollitt, Crusz and Diggle, 2015). Biofilm attachment can be categorised into two stages: an initial reversible attachment stage and an irreversible attachment stage (Renner and Weibel, 2011). Furthermore, depending on the surface type, the mechanisms used by *S. aureus* can differ.

For an abiotic surface, initial attachment is facilitated by non-specific interactions like van der Waals and electrostatic and hydrophobic forces (Bos, van der Mei and Busscher, 1999; Dunne, 2002). Teichoic acids are highly charged polymers that are involved in cell division (Brown, Santa Maria and Walker, 2013). Lipoteichoic acids (LTA) are anchored in the cell membrane and wall teichoic acids (WTA) are covalently linked to the peptidoglycan of gram-positive bacteria. Teichoic acids contribute to the initial stages of *S. aureus* biofilm formation in several ways. Teichoic acids have been shown to play a key role in adherence to hydrophobic surfaces like polystyrene and glass due to their net charge. Gross *et al*. (2001) showed that a *dltA* mutant, which resulted in a lack of D-alanine esters (positively charged residues) in the teichoic acids, had an increased negative charge that led to reduced bacterial adhesion. The reduction in attachment observed was most likely due to an increase in repulsive forces between the increased negative *S. aureus* cell surface charge and the slightly negative surface charge of the polystyrene and glass (Gross *et al.*, 2001).

S. aureus possesses an arsenal of surface proteins to help it irreversibly attach to living surfaces in particular (Moormeier and Bayles, 2017). Many of the surface proteins involved in attachment are cell wall anchored (CWA) proteins that are covalently linked to the cell wall. These include the MSCRAMMS, the near iron transporter (NEAT) family motif proteins, three helical bundles and the G5/E repeat proteins and are the subject of many detailed reviews (Paharik and Horswill, 2016; Foster, 2019). These proteins, including FnBPA, FnBPB (O'Neill *et al.*, 2008), ClfA and ClfB (Abraham and Jefferson, 2012; Herman-Bausier *et al.*, 2018), and the major autolysins (AltA and AltE) (Houston *et al.*, 2010). These proteins enable the bacteria to anchor themselves to the surface by binding host matrix components (e.g fibronectin) and initiate biofilm formation (Moormeier and Bayles, 2017).

1.4.2. *S. aureus* Biofilm Accumulation, Maturation, and the Biofilm Matrix

Following attachment, cells begin to proliferate and produce a self-made EPS that will surround the cells. This is known as biofilm accumulation/maturation. These substances are what form the matrix of the biofilm, also known as a 3D ECM. The biofilm matrix can

also be described as the space between the cells. It is a structural scaffold for adhesion between cells and with a surface. The bacterial biofilm with a mature matrix is a dynamic environment with fluid-filled channels that enable the movement of nutrients and resources, such as iron, throughout the biofilm structure. It is thought that water accounts for most of the biofilm mass (Quan *et al.*, 2021). The *S. aureus* matrix is typically composed of carbohydrates, proteins (lysis-derived and secreted) and extracellular DNA (eDNA) (Fitzpatrick, Humphreys and O'Gara, 2005).

1.4.2.1. PIA in biofilm

The production of PIA by the *ica* operon, which was discussed above, plays an important structural role in the matrix of *Staphylococcal* biofilms. This is evidenced by the fact that its locus is conserved across numerous *S. aureus* strains (Cramton *et al.*, 1999). *S. aureus* biofilms are known for their distinct establishment of tower-like columns (Moormeier *et al.*, 2013) (Figure 1.5). The structure of the biofilm also aids in resisting shear stress, which is presumably critical for infection sites that are exposed to strong blood flow, e.g., endocarditis infection (Rupp, Fux and Stoodley, 2005).

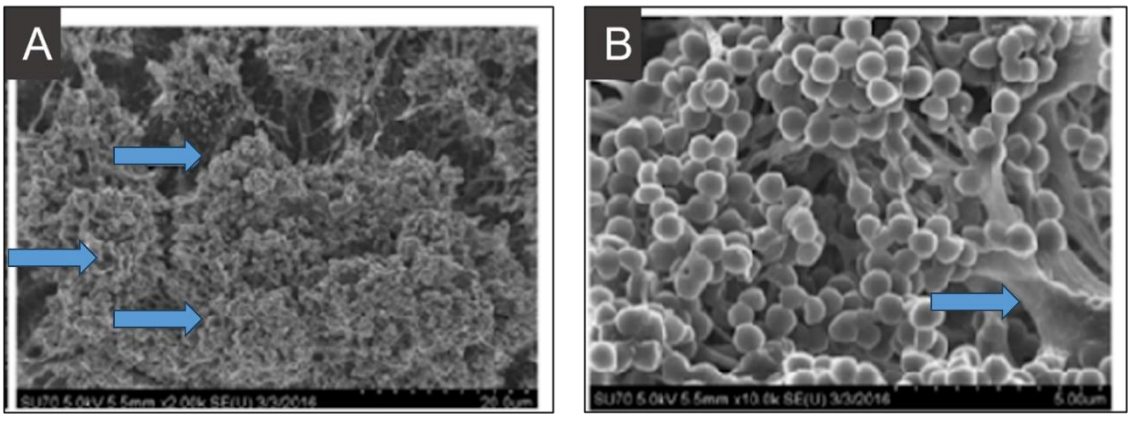

Figure 1.5. A scanning electron microscopy image of S. aureus biofilm. *Where (A) arrows indicate the tower-like structures, indicative of S. aureus biofilm, and (B) arrow indicates the biofilm matrix that connects the bacterial cells. Image reproduced from (Reddinger et al., 2016). The arrows included in the original image were enlarged for ease of viewing.*

1.4.2.2. Surface-attached and secreted matrix proteins

Some of the proteins that are involved with bacterial attachment also play a role in biofilm accumulation and matrix development. These include the CWA proteins FnBPAB, SasG, SasC, SdrC, Ebh, and Bap and the role of each is reviewed by (Speziale *et al.*, 2014) but is briefly touched on here. FnBPA and FnBPB have both been independently linked to biofilm accumulation and contain subdomains N2N3 which has been identified as being involved in biofilm accumulation (Geoghegan *et al.*, 2013). As stated previously, SasG B repeats are required for the role of SasG in biofilm (Geoghegan *et al.*, 2010). By a similar approach, the role of the N2 subdomain of SdrC was determined to play a role in biofilm accumulation (Barbu *et al.*, 2014). SdrC is a multifunctional adhesion which promotes intercellular adhesion by low affinity homophilic bonds (Feuillie *et al.*, 2017). SasC is also involved in cell aggregation, confirmed by heterologous expression in *Staphylococcus carnosus* (Schroeder *et al.*, 2009).

Secreted and cytoplasmic proteins also contribute to biofilm formation and are important for cell-cell adhesion. While the exact composition of the biofilm matrix is uncertain as it can be highly variable, cytoplasmic proteins are abundant and have been shown to reversibly attach to the *S. aureus* cell wall in response to decreasing pH (Foulston *et al.*, 2014). These multifunctional proteins are recycled from the cytoplasm and "moonlight" as matrix proteins. These included proteins that are involved in central metabolism: enolase, acetolactate synthase, GAPDH (glyceraldehyde-3-phosphate dehydrogenase), and transketolase (Foulston *et al.*, 2014).

Also present are the secreted proteins such as alpha toxin (Hla), beta toxin (Hlb) and extracellular adherence protein (Eap) that play a role in maturation (Caiazza and O'Toole, 2003; Johnson, Cockayne and Morrissey, 2008; Yonemoto *et al.*, 2019). Eap plays an important role in biofilm formation under certain conditions, for example, in low-iron environments (Johnson, Cockayne and Morrissey, 2008). SasG along with Eap are implicated in biofilm thickness, with a single deletion of *eap* resulting in reduced ruggedness and thickness of the biofilm (Yonemoto *et al.*, 2019). Hla is a haemolytic

toxin and a *hla* mutant was unable to colonise plastic under static or flow conditions (Caiazza and O'Toole, 2003). The beta-toxin is a neutral sphingomyelinase and a known virulence factor of *S. aureus*. It forms cross-links with itself in the presence of DNA and therefore assists in the formation of an insoluble nucleoprotein biofilm matrix (Huseby *et al.*, 2010). Phenol soluble modulins (PSMs) are a group of peptides with surfactant characteristics. PSMs also play a role in the stabilization and structuring of biofilms, by producing amyloid fibrils that contribute to this stabilization (Periasamy *et al.*, 2012; Hobley *et al.*, 2015).

1.4.2.3. The role of extracellular DNA in the biofilm matrix

Extracellular DNA (eDNA) is the most recently identified component of the biofilm matrix. It has become almost ubiquitous in bacterial biofilms, and a recent review has updated our understanding of its role in biofilm formation (Campoccia, Montanaro and Arciola, 2021). A major route of eDNA release in *S. aureus* is from the autolysis of bacterial cells. This is the function of the major autolysin (Atl) in *S. aureus* (Houston *et al.*, 2010). eDNA is thought to provide a cellular scaffold, contributing to the structure of the biofilm, such as the tower-like structure of *S. aureus* biofilm (Mann *et al.*, 2009). Furthermore, its negative charge creates an electrostatic force that binds cells and host factors together (Thomas and Hancock, 2009).

The best-characterized example of eDNA's interaction with *S. aureus* proteins during biofilm development is the beta toxin, encoded by the *hlb* gene, which is structurally related to DNase I and enables it to bind DNA (Huseby *et al.*, 2010). The mechanism of DNA release to maintain biofilm integrity is facilitated by hydrolases and regulated by the *cidABC* and *lrgAB* operons, which have opposing activities (Sadykov and Bayles, 2012). In particular, cidA promotes cell lysis and eDNA release during biofilm formation (Rice *et al.*, 2007). eDNA is the most common component of the biofilm matrix and would be a promising target for biofilm eradication (Sugimoto *et al.*, 2018). This is evidenced by successful treatment of biofilm-associated *P. aeruginosa* in a patient with CF with a combination of antibiotics and DNase I (Gibson, Burns and Ramsey, 2003).

Recently, it has been proposed that lipoproteins have a DNA-binding capacity (Kavanaugh *et al.*, 2019). SaeP is a lipoprotein and an auxiliary protein of the SaeRS two-component system, a system involved in controlling virulence factors and pathogenicity (Novick and Jiang, 2003; Arya and Princy, 2016; Haag and Bagnoli, 2017). When SaeP is produced, there is an increase in high-molecular weight DNA on the surface of the bacterial cell. Suggesting lipoproteins may play a role in anchoring the bacterial cell surface to the biofilm matrix (Kavanaugh *et al.*, 2019). Recently, environmental RNA has been implicated in *S. aureus* polysaccharide-dependent biofilms (Chiba *et al.*, 2022).

1.4.3. Biofilm dispersal in *S. aureus*

The dispersal step of the biofilm formation cycle can be the most dangerous for those infected. During this step, cells are released from the biofilm into the surrounding environment or bloodstream, enabling the bacteria to colonise new areas and consequently cause systemic infection (Fux, Wilson and Stoodley, 2004; Fleming and Rumbaugh, 2018). *S. aureus* produces various exo-enzymes and surfactants that degrade the matrix for cells to escape and disperse (Figure 1.6). It is important to understand that enzymes that target the protein and/or DNA components are not effective at degrading PIA/PNAG biofilms and likewise mechanisms that target PIA/PNAG are not effective at dispersing ica-independent biofilms (Chaignon *et al.*, 2007). For example, whilst proteinase K can degrade protein-based biofilms, metaperiodate is ineffective, as they do not contain high levels of PIA, (Kogan *et al.*, 2006).

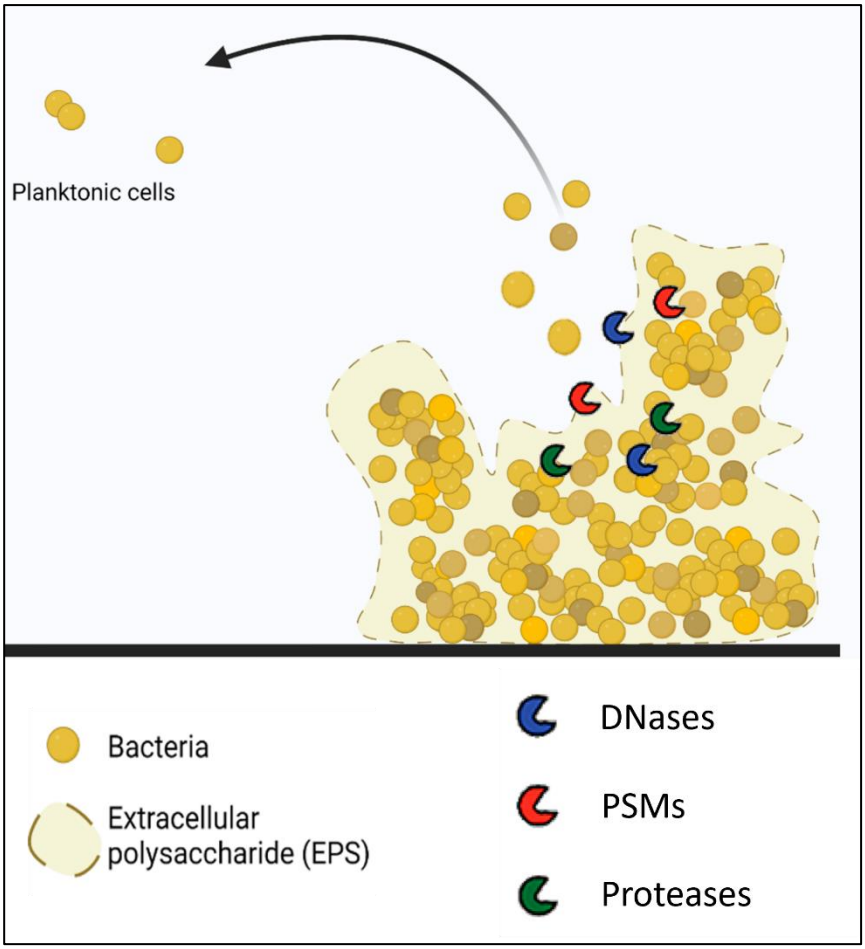

Figure 1.6. S. aureus biofilm dispersal. *Biofilms are dispersed by breaking down the extracellular polysaccharide matrix. Proteases, nucleases, and phenol soluble modulins (PSMs) degrade protein eDNA and carbohydrate (PIA) matrices. This figure was made, in part, using Biorender.com.*

As previously mentioned, the accessory gene regulator or Agr QS system contributes to biofilm development in *S. aureus* (Yarwood *et al.*, 2004). Agr QS system is a negative regulator of biofilm, and its repression is necessary for biofilm growth. This QS system is the main *S. aureus* system (reviewed in depth by (Thoendel *et al.*, 2011)), and it plays an important role in biofilm dispersal. Agr is activated when autoinducing peptides (AIP) generated by *S. aureus* reach a certain concentration (Tan *et al.*, 2018). AIP binds AgrC

and the regulatory cascade is initiated. Agr is activated in response to certain environmental cues or stresses such as pH (Regassa, Novick and Betley, 1992).

The Agr-regulated proteases' destruction of the proteinaceous biofilm components is one of the main factors influencing the transition between biofilm development and detachment (Lauderdale *et al.*, 2009; Martí *et al.*, 2010; Boles and Horswill, 2011). Agr is responsible for the upregulation of protease production and other enzymes that are involved in the structuring and restructuring of the matrix. It also down-regulates the expression of surface factors (Tegmark, Karlsson and Arvidson, 2000; Cheung *et al.*, 2001). This allows bacterial cells to be released from the biofilm and colonise new niches. PSMs, also regulated by the Agr QS system, are critical for the detachment of bacteria from the biofilm and dissemination (Periasamy *et al.*, 2012). *agr* repression is critical for biofilm growth and this can be achieved by a decrease in pH due to acidic metabolites derived from glucose catabolism (Regassa, Novick and Betley, 1992).

S. aureus produces two extracellular nucleases, Nuc and Nuc2 (also known as thermonucleases). Nuc is the main nuclease and plays two major roles. It aids in avoiding the host immune system by degrading neutrophil extracellular traps (NETs) (Thammavongsa, Missiakas and Schneewind, 2013). It also degrades eDNA within biofilms and a mutation in *nuc* results in enhanced biofilm formation (Mann *et al.*, 2009). *nuc/nuc2* are complementary genes. This means that their products can interact to express a certain trait. However, Nuc2 plays a lesser role in virulence and is not involved in immune evasion (Yu *et al.*, 2021).

Finally, dispersin B can degrade PIA in *S. aureus* and *S. epidermidis* biofilms. Dispersin B is isolated from *Actinobacillus actinomycetemcomitans,* however, no homologue has been found in *S. aureus* (Kaplan *et al.*, 2003). Therefore, an alternate mechanism of biofilm dispersal that targets carbohydrate must be utilised.

1.5. Therapies to inhibit or disperse *S. aureus* biofilm formation.

1.5.1 A need for new therapies to treat *S. aureus*

The treatments currently available for *S. aureus* biofilm infections are the debridement (removal) of the biofilm or removal of the colonised surface/medical device as soon as detected, along with treatment with high local concentrations of antibacterial drugs (Høiby *et al.*, 2015). There are many side effects associated with antibiotic therapy of high dosages and even after such therapy the clinical cure rate for *S. aureus* biofilm infections is low (Maya *et al.*, 2007). Furthermore, the removal or replacement of medical devices is expensive and puts patients at a higher risk of complications. These patients can be medically vulnerable and additional surgeries could expose them to further risk.

To avoid this, researchers are looking to alternative therapies that may be used instead of, or in conjunction with, traditional antimicrobial therapy. Researchers are exploring new treatments such as bacteriophage therapy, small molecules, and enzymes (Kelly *et al.*, 2012; Alves *et al.*, 2014; Ghosh, Jayaraman and Chatterji, 2020; Liu *et al.*, 2021). Preventative measures, including vaccines and surface modification of medical devices, are also being investigated. Reviews into these strategies and more have been previously published (Bhattacharya *et al.*, 2015; Khatoon *et al.*, 2018; Suresh, Biswas and Biswas, 2019).

1.5.2. Microbial Cell-free Supernatants against *S. aureus* biofilm

Supernatants from various bacteria and fungi have been shown to have the potential to disrupt existing, or prevent the formation of *S. aureus* biofilms. These supernatants can contain a variety of active biomolecules that may have therapeutic value.

One example is the use of cell-free supernatants (CFS) from *Bacillus subtilis* (*B. subtilis*), which killed both planktonic and biofilm *S. aureus* cells (Zhang *et al.*, 2021). The

supernatant increased the susceptibility of *S. aureus* to conventional antibiotics like penicillin. Overcoming bacterial resistance to antibiotics is obviously a major area of interest and highlights the importance of researching natural products from bacteria, fungi, and plants.

The serine protease, Esp, of some *S. epidermidis* isolates can prevent *S. aureus* colonisation and biofilm formation (Iwase *et al.*, 2010). Purified Esp inhibited and destroyed pre-existing *S. aureus* biofilm. Interestingly, Iwase *et al*. 2010 conducted an epidemiological study which showed that the presence of Esp-secreting *S. epidermidis* correlated with a lack of *S. aureus* colonisation. *S. epidermidis* has also been reported to produce small molecules capable of inhibiting and dispersing preformed biofilm (Glatthardt *et al.*, 2020). While not identified, the molecule(s) were resistant to various biochemical stresses and were effective against MSSA and MRSA isolates.

An example of fungal supernatant with anti-biofilm properties has been reported. CFS from *Saccharomyces cerevisiae* showed anti-biofilm action by preventing EPS formation and auto-aggregation of *S. aureus* (Kim *et al.*, 2020). Biofilm-related gene expression was also altered, specifically the *icaADBC* operon that mediates PIA biosynthesis. These biomolecules represent a potential source of therapeutics that can disrupt *S. aureus* biofilm.

1.5.2.1. Lactic acid bacteria supernatants

Lactic acid bacteria (LAB) are bacteria that can ferment lactic acid and they are used widely throughout the food industry (Wang *et al.*, 2021). LAB are found within the human gut and are increasingly recognised for their potential to fight against pathogens or act as a probiotic (Pessione, 2012; Colombo *et al.*, 2018). LAB CFS can have antibacterial activity due to organic acids, protein and other compounds (Mani-López, Arrioja-Bretón and López-Malo, 2022). There are many different strains, and each may affect the target pathogen in a different way. A recent study screened different LAB strains for antibacterial activity against *S. aureus* associated with atopic dermatitis. Their activity varied between strains and the authors suggested this was indicative of different modes of action. These included expression of bacteriocins and the production of

specific organics compounds. However, the acidification of its surroundings was the main inhibitory factor (Christensen *et al.*, 2021). The authors concluded that live LAB or CFS could potentially be used as a treatment against *S. aureus*. Biofilm inhibition without killing may also be beneficial as *S. aureus* may be slower in developing resistance against such non-lethal treatments. LTA released from *Lactobacillus plantarum* was able to inhibit biofilm formation and aggregation in various *in vitro* and *in vivo* models, without affecting *S. aureus* growth (Ahn *et al.*, 2018).

In general, supernatants and natural products from various bacteria and fungi have the potential to disrupt or prevent *S. aureus* biofilms by inhibiting growth, attachment, and EPS matrix formation. Treating the EPS is of particular importance as a previous study suggested that even after the bacteria have been destroyed, the EPS may remain and act as a foot-hold for re-colonisation by the same or a different bacterial species (Maya *et al.*, 2007). More research is needed to understand the specific mechanisms involved and to develop effective treatments based on these supernatants or natural products.

1.6. *S. aureus* and polymicrobial biofilm.

Biofilms can be polymicrobial in nature, meaning different species of both bacteria and/or fungi may be present. The interactions between the species present may be synergistic or antagonistic. Fungi have only been acknowledged as a significant source of infection since the 1980s, with immunocompromised individuals usually being the most at risk (Pfaller and Diekema, 2007). While less frequent than bacterial infections, the mortality rate associated with fungal infections is comparable (Bongomin *et al.*, 2017) and *Candida* spp. are the leading cause of invasive fungal infections (Guinea, 2014).

1.6.1. *S. aureus* interactions with *Candida albicans*.

Many studies on bacterial-fungal interactions have focused on the interaction between *S. aureus* and *Candida albicans* or *Aspergillus fumigatus* [reviewed in (Lohse *et al.*, 2018; Kumari and Singh, 2019)]. *S. aureus* is frequently co-isolated with *C. albicans* as the cause of infection (Klotz, Chasin, *et al.*, 2007). Examples of such infections include oral and vaginal candidiasis and invasive candidiasis (Calderone and Clancy, 2011). The *S. aureus* interaction with the major human fungal pathogen *C. albicans* is among the best characterised.

S. aureus interaction with *C. albicans* can be described as broadly synergistic. *S. aureus* can adhere to *C. albicans* hyphae and result in a dual-species biofilm (Peters *et al.*, 2012). Increased virulence is a consequence of *S. aureus* – *C. albicans* dual species infection (Todd *et al.*, 2019). Increased tolerance of *S. aureus* to antimicrobials such as vancomycin has also been observed as a consequence of dual-species biofilm (Kong *et al.*, 2016). The interaction between *S. aureus* and *C. albicans* can be physical and chemical (Figure 1.7).

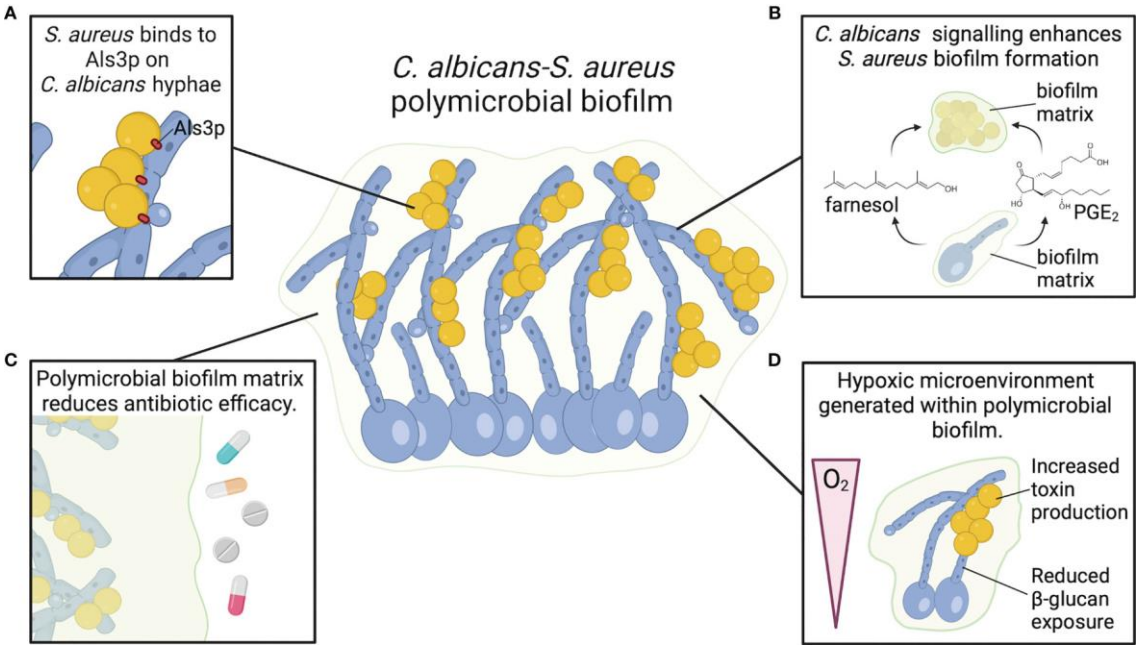

Figure 1.7. Illustrated summary of the interaction between C. albicans and S. aureus during polymicrobial biofilm. *(A) Physical interaction where S. aureus can bind to the Als proteins on C. albicans hyphae. (B) Enhanced biofilm formation due to C. albicans quorum sensing molecules (chemical signal) like farnesol. C) Enhanced drug resistance and (D) increased virulence expression. PGE2; immune system signalling compound prostaglandin E2. Als3p; hyphal adhesin protein. Figure reproduced from* (Eichelberger and Cassat, 2021) *as originally published in Frontiers.*

Our knowledge of the interaction of *S. aureus* with other human disease-causing *Candida* species (*C. parapsilosis*, *C. tropicalis* and *C. auris*) is limited. A recent study demonstrated the antagonistic behaviour of *S. aureus* towards *C. glabrata* whereby *S. aureus* cell-free supernatant killed *C. glabrata* via an apoptotic mechanism (Camarillo-Márquez *et al.*, 2018). As non-*albicans Candida* are being increasingly identified as sources of human infection (Manfredi *et al.*, 2002; Taei, Chadeganipour and Mohammadi, 2019), the risk of co-infection with major pathogens like *S. aureus* increases. More research is needed to characterise the mechanisms that govern these inter-species interactions.

1.7. *Candida parapsilosis* - a major fungal pathogen.

Non-albicans *Candida* species, such as *C. parapsilosis*, *C. tropicalis*, *C. auris*, and *C. glabrata* (now named *Nakaseomyces glabrata)* are under increasing scrutiny for their role in human infection (Berkow and Lockhart, 2017; CDC, 2021). *Candida parapsilosis* is emerging as a significant human pathogen, such that it is now the leading cause of vulvovaginal candidiasis in Europe (Trofa, Gácser and Nosanchuk, 2008; Borges *et al.*, 2018). *C. parapsilosis* is a fungal yeast species that exists in the natural environment such as in soil, and domestic animals, and is typically a commensal of human skin. The main mode of transmittance is by human hands, and it is known to primarily cause severe disease in neonates of low birth weight (Trofa, Gácser and Nosanchuk, 2008).

A contributing risk factor to the heightened incidence of *C. parapsilosis* infections is its ability to grow on prosthetic materials and intravenous catheters (Trofa, Gácser and Nosanchuk, 2008). *C. parapsilosis* is frequently isolated from oral infections and is associated with increased mortality in neonatal ICU. *C. parapsilosis* has three secreted aspartyl proteases, which are major virulence factors in many other fungal species (Naglik, Challacombe and Hube, 2003; Singh *et al.*, 2019). These proteases may contribute to the invasiveness of *C. parapsilosis* during infection of low-birth weight neonates (Singh *et al.*, 2019). A recent review outlined their role in fungal pathogenesis (Kulshrestha and Gupta, 2023).

Candida infections can range from superficial infections of the skin and hair to life-threatening systemic infections (Silva *et al.*, 2012). Historically, *C. albicans* is the most common fungal species to infect humans (Calderone and Clancy, 2011), and this is reflected in the literature as the focus of many studies. Like antibiotic resistance, antifungal resistance is a major problem. The wide usage of fluconazole to treat candidiasis, which is also commonly prescribed prophylactically, has increased selective pressure resulting in resistant strains (Berkow and Lockhart, 2017). Antimicrobial resistance is also widely present in *C. parapsilosis* strains. A study found that 5 out of 10 clinical isolates tested overexpressed at least one gene responsible for drug efflux of azoles (CDR1, MDR1 and MRR1) and fluconazole resistance (ERG 11) (Neji *et al.*, 2017). Fungi are eukaryotic and so share many similarities with human host cells. This in turn

hinders the development of effective antifungal treatments (Rodrigues and Nosanchuk, 2020).

1.7.1. Physical characteristics and biofilm formation in *C. parapsilosis*

C. parapsilosis, *C. orthopsilosis* and *C. metapsilosis* are closely related species and are collectively known as the *C. parapsilosis sensu lato* species complex (Nemeth, Gacser and Nosanchuk, 2018). Unlike *C. parapsilosis*, *C. orthopsilosis* and *C. metapsilosis* are less clinically encountered. *C. parapsilosis sensu strictu* is referred to here as *C. parapsilosis*. *C. parapsilosis* exists in either yeast or pseudohyphal form. *C. parapsilosis* yeast cells may be round, oval, or cylindrical (Trofa, Gácser and Nosanchuk, 2008). Unlike *C. albicans*, *C. parapsilosis* does not form true hyphae (Laffey and Butler, 2005). Pseudohyphae are formed by budding and can be distinguished from true hyphae by the lack of cytoplasmic connection between cells or branching. The formation of pseudohyphae is one of the most important virulence factors of *C. parapsilosis*. Proteins with similarity to the *C. albicans* hyphal Als protein have been identified in these cells and may aid in the first step of host cell invasion (Kozik *et al.*, 2015).

Like other *Candida* species, *C. parapsilosis* can form a biofilm, however, this ability is strain dependent, with the capacity to form biofilm also varying depending on the media used (Silva *et al.*, 2009; Lattif *et al.*, 2010; Pannanusorn, Fernandez and Römling, 2013; Pannanusorn *et al.*, 2014). Pseudohyphae play a significant role in *C. parapsilosis* biofilms and biofilms produced by strong-biofilm forming strains were composed of yeast and pseudohyphae, while weak-biofilm forming strains produced biofilm composed of yeast cells (Laffey and Butler, 2005; Pannanusorn *et al.*, 2014).

Candida biofilm formation progresses along three stages of biofilm formation. Generally, yeast cells first attach to a substrate, followed by a period of biofilm initiation. During biofilm maturation, hyphae/pseudohyphae are formed and the cells begin to produce an extracellular matrix (Gulati and Nobile, 2016). The final stage is dispersal where yeasts can then migrate to and colonise other areas (Sellam *et al.*, 2009). The structure of *Candida spp.* biofilms are highly variable.

In particular, the *C. parapsilosis* biofilm matrix is mainly composed of carbohydrates with some protein (Silva *et al.*, 2009). Conversely, biofilm matrices of *C. tropicalis* have low levels of carbohydrates and protein. Transcription factors Cph1 and Bcr1 are major biofilm regulators in *C. parapsilosis,* while transcription factors Tec1 and Bgr1 identified as playing a role in *C. albicans* biofilm did not share the same function in *C. parapsilosis* (Holland *et al.*, 2014). The reverse was also true with regulators of biofilm identified with a major role in *C. parapsilosis* only.

1.7.2. *C. parapsilosis* interactions with other microorganisms

There are a small number of studies that focus on the interaction between *C. parapsilosis* and other microorganisms (Bandara *et al.*, 2009; Gonia *et al.*, 2017; Garcia *et al.*, 2020). The lipopolysaccharide of *Escherichia coli* has been shown to modulate *C. parapsilosis* biofilm formation *in vitro* (Bandara *et al.*, 2009). Post co-incubation on polystyrene plates resulted in a significant reduction in colony forming unit (CFU) counts of *C. parapsilosis*. A separate study investigated the potential modulating effect of *C. parapsilosis* on *C. albicans* interaction with premature intestinal epithelial cells (Gonia *et al.*, 2017). *C. parapsilosis* protected host cells from invasion via secreted molecules as well as physical interaction with *C. albicans* cells.

Dermatomycoses are infections of the skin, hair, and nails and *C. albicans*, *C. parapsilosis* and *Trichophyton rubrum* are common causes of such infections. *C. parapsilosis* and C. albicans were examined with *T. rubrum* in a model of dual species biofilm (Garcia *et al.*, 2020). It was found that the *Candida* became dominant within the biofilm when added to pre-adhered and matured *T. rubrum* biofilms and an antagonistic behaviour of *T. rubrum* was observed whereby it prevented *C. albicans* filamentation and *C. parapsilosis* development (Garcia *et al.*, 2020).

Few studies investigate the interaction of *C. parapsilosis* with *S. aureus*. In a mixed-species model of infection, various *Candida* species were screened for their ability to protect *S. aureus* within a mouse model (Carlson and Johnson, 1985). When mice were inoculated with *S. aureus* the bacteria could not be detected in the mice post 48 hours.

When the mice were inoculated with both *S. aureus* and *C. albicans*, increased survival of the bacteria was noted. *C. parapsilosis* was less effective in protecting *S. aureus* compared to *C. albicans* and *C. glabrata* (Carlson and Johnson, 1985). A second study with a similar experimental set-up also came to the same conclusion, whereby, co-infection with *C. parapsilosis* did not result in synergistic mortality (Nash *et al.*, 2015). This may suggest a general lack of synergistic interaction between these two microorganisms. At present, only one study has looked at *S. aureus*' ability to form a dual-species biofilm with *C. parapsilosis*, with the view to investigating a novel treatment against *S. aureus and C. albicans/C. parapsilosis* dual biofilms (She *et al.*, 2020). The authors report that *S. aureus* can form a biofilm with both *Candida* species.

More research into emerging important microbial species such as *Candida parapsilosis* is needed. Looking at the interaction between these different species can give us a greater understanding of microbial pathogens in general and potentially enable us to use the products of these organisms to create new treatments or improve existing ones.

1.8. Thesis Objectives.

S. aureus is a leading cause of infection worldwide. A fundamental virulence trait is the production of a biofilm. The interaction between *S. aureus* and *C. parapsilosis*, to our knowledge, has not been characterised. Our data suggests that *C. parapsilosis* produces molecules with anti-biofilm activity. Understanding the antagonistic relationship between these two human pathogens during biofilm formation may give insight into the underlying mechanisms which underpin the inability of certain microbes to co-exist or form multi-species biofilms. This will allow us to identify novel targets for alternative biofilm treatments or discover novel anti-biofilm molecules.

1.8.1. Thesis Aims.

1. Characterisation of the interaction between *Staphylococcus aureus* and *Candida parapsilosis*.
2. Characterisation of the mechanism of action exhibited by *C. parapsilosis* cell-free supernatant on *S. aureus* biofilm formation.
3. Characterisation of the *C. parapsilosis* cell-free supernatant.

Chapter 2 – Materials and Methods

2.1. Strains and growth conditions

The *S. aureus* isolates DSM 799 and DSM 1104, *S. epidermidis* (DSM 28319) and *C. albicans* (DSM 1386) were obtained from Leibniz Institute DSMZ-German Collection of Microorganisms and Cell Cultures GmbH (https://www.dsmz.de/). All strains and the *Candida parapsilosis* clinical isolates used in this study are listed in Table 2.1 below. Further information on the clinical isolates of *C. parapsilosis* is included in the Appendix (Table A1).

Table 2.1. List of S. aureus, S. epidermidis, C. albicans and clinical C. parapsilosis isolates used in this study.

Abbreviation	Isolate Name	Abbreviation	Isolate Name
SA1	*S. aureus,* DSM 799		
SA2	*S. aureus,* DSM 1104		
SH1000	*S. aureus*, SH1000		
S. epidermidis	DSM 28319		
C. albicans	DSM 1386		
C. parapsilosis (CP)			
CP1	CLIB214	CP13	81/041
CP2	CDC317	CP14	CDC177
CP3	CDC173	CP15	90-137
CP4	711701	CP16	02-203
CP5	CDC167	CP17	73-107
CP6	J961250	CP18	CDC165
CP7	CDC179	CP19	81/253
CP8	J930733	CP20	81/040(C)
CP9	103	CP21	J931058
CP10	J930631/1	CP22	J951066
CP11	J960578	CP23	J950218
CP12	81/040(S)	CP24	J931845

All strains were stored at -80°C in 15% glycerol stock. *S. aureus* and *S. epidermidis* strains were maintained at 4°C on Tryptone soy broth (TSB) agar (Oxoid, UK). *C. parapsilosis* and *C. albicans* were maintained at 4°C on Yeast peptone dextrose (YPD) agar

(Formedium). For overnight cultures, single colonies of *C. parapsilosis* were picked and grown in YPD media at 30°C shaking at 160 rpm. Bacterial cells were grown in TSB media overnight at 37°C with shaking at 180 rpm.

2.2. 96-well Polystyrene Plate Biofilm assay

S. aureus and *C. parapsilosis* cells from overnight cultures were centrifuged, washed with 1 x Phosphate buffered saline (PBS), centrifuged again, and re-suspended in PBS (Thermo-Fischer Scientific, Denmark). Cells were resuspended to an OD_{600} of 1 (*C. parapsilosis)* and 0.1 (*S. aureus*) (approx. 10^7 CFU/mL) in the relevant medium, TSB, TSB supplemented with 0.2% glucose (TSB-0.2G), TSB supplemented with 1% glucose (TSB-1G), TSB supplemented with 1% NaCl (TSB-1N). For single species biofilm assays, 100 µL of cells was added to a well in a Nunclon Delta 96 well plate (Thermo-Fischer Scientific, Denmark) with 100 µL of the relevant medium. Mixed species biofilms were prepared by adding 100 µL of *S. aureus* and 100 µL of *C. parapsilosis* to the same well. The total volume in each well was 200 µL. Plates were incubated for 24hr or 48 h at 37°C in a static incubator. The supernatant was removed, and the plates were gently washed twice with 100 µL of 1 x PBS to remove non-adherent cells and allowed to dry overnight at room temperature (RT). In general, each 96-well plate biofilm assay was carried out with three biological replicates and eight technical replicates.

2.3. Crystal violet measurement of biofilm biomass

50 µL of 0.4% crystal violet stain (Sigma-Aldrich) was added to each well and allowed to stand at RT for approximately 10 min. Excess dye was removed by gently washing with PBS. An image of the plate was taken once dry. Dye bound to the biofilm was solubilised by adding 50 µL of 33% (v/v) acetic acid (Sigma-Aldritch) to each well and allowed to stand at RT for 15 min. The dissolved dye was transferred to a new 96-well plate where a 1 in 20 (or appropriate) dilution was made in dH_2O. The absorbance was read at 595nm in a plate reader (Tecan Infinite M200 Pro).

Crystal violet-stained biofilm absorbances are (where appropriate) displayed using boxplots. The boxes represent the interquartile range (IQR). The centre line in each box represents the median (50th percentile). The whiskers represent the largest or smallest absorbance values within 1.5 IQR above the 75th percentile or below the 25th percentile, respectively. The jitter points represent each single data point (n=12). Black dots represent points that have been identified as outliers, these points are also represented by a coloured point and are therefore duplicated.

2.4. *C. parapsilosis* heat-kill biofilm assay

Biofilm assays were set up as described above (section 2.2), with the following addition. *C. parapsilosis* cells diluted to an OD of 1 in TSB-0.2G and were heat-killed in a water bath for 15 min at 80°C. 100 µL of heat-killed cells were added to wells of a 96-well plate containing 100 µL of *S. aureus* and to wells containing 100 µL TSB-0.2G to act as a negative growth control. Plates were incubated at 37°C for 24 h. Plates were washed twice with 100 µL of PBS and then allowed to dry overnight before being stained with crystal violet as described above (section 2.3). This assay was repeated with three biological replicates and at least eight technical replicate wells.

2.5. Preparation of fungal cell-free supernatant (CFS) from static culture

Overnight cultures of *C. parapsilosis* or *C. albicans* were washed by first pelleting the cells by centrifugation and resuspending in 1 x PBS. Cells were then diluted to an OD of 1 (approx. 10^7 CFU/mL) in TSB-0.2G. In a 6 well Nunclon plate (Thermo Fischer Scientific, Denmark), 2.5 ml of diluted cells was added to 2.5 ml of TSB-0.2G and incubated for 24 hr at 37°C in a static incubator. The CFS was collected in 50 ml falcon tubes and centrifuged for 5 min at 4500 rpm (5000 x *g*) (Rotanta 460 R, Hettich). With care not to disturb the pellet, the CFS was filter sterilised (Corning^{TM}, 0.2 µm filter pore) before storage at -20°C or used immediately. The CFS collected from CP1 and CP6 is referred to as SN1 and SN6, respectively.

2.6. Collection of fungal CFS from shaking cultures.

10 mL of TSB-0.2G was inoculated with CP1, CP6, or *C. albicans* and incubated at 37°C shaking overnight. The tubes were then centrifuged for 5 min at 4500 rpm (5000 x *g*) (Rotanta 460 R, Hettich). The CFS was then filter sterilised (Corning™ ,0.2 µm filter pore) before storage at -20°C or used immediately. The CFS collected from *C. albicans* is named CaSN.

2.7. Investigating the effect of fungal CFS on bacterial biofilms.

The biofilm assay was set up as described in section 2.2, with 100 µL of *C. parapsilosis* or *C. albicans* CFS replacing *Candida parapsilosis* cells. In a 96-well plate, 100 µL of *S. aureus* or *S. epidermidis* (OD_{600} of 0.1 in TSB-0.2G) was added to 100 µL of CFS (SN1, SN6, or CaSN) for a final CFS concentration of 50% (v/v) (% of total well volume). The plate was incubated for 24 h at 37°C in a static incubator. The plates were washed twice with PBS and allowed to dry before staining with 0.4% crystal violet (section 2.3). In general, each experiment was carried out with three biological replicates and eight technical replicate wells.

2.8. CFS MBIC

Testing the minimum biofilm inhibition concentration (MBIC) of *Candida* CFS against *S. aureus* biofilm. In a 96-well plate, the *C. parapsilosis* CFS (SN1 or SN6) was two-fold serially diluted in TSB-0.2G. The final CFS concentrations ranged from 50% to 0.19% (% of total well volume). 100 µL of SA1 in TSB-0.2G (OD of 0.1) was then added to each well. Wells that contained only *S. aureus* and TSB-0.2G or only TSB-0.2G and CFS acted as controls. 200 µL of *S. aureus* diluted to an OD of 0.1 in SN1 or SN6 was added to test biofilm development in 100% (v/v) SN. The assays were incubated at 37°C for 24 h. The assays were then washed twice with 100 µL of PBS. Once dry, the plates were stained, and the absorbance read as described in section 2.3.

2.9. Growth kinetic study with *C. parapsilosis* CFS

To test if the *C. parapsilosis* CFS affected *S. aureus* growth, a growth kinetic experiment was run. Overnight cultures of *S. aureus* were washed in PBS and diluted to an OD of 0.2 in TSB-0.2G, TSB-0.2G+50% (v/v) SN1 or SN6, TSB-0.2G+70% (v/v) SN1 or SN6. The cultures were incubated at 37°C at 180 rpm. Optical density readings were taken at hourly intervals from time 0 h to 8h and at 24 h using a spectrophotometer (UV-3100 PC, VWR) at 600nm (OD_{600}). A graph was plotted with OD against time. Results are combined from at least three biological replicates.

2.10. Resazurin viability assay

Biofilm viability was measured using resazurin sodium salt (Thermofisher Scientific, Denmark). A 10X stock of resazurin (200 µM) was prepared in sterile PBS. The solution was filter-sterilized and stored at 4 °C in the dark. Biofilms were grown in TSB-0.2G as in section 2.2. After non-adherent cells were washed away, 20 µL of 10X resazurin in 180 µL of TSB was added to each well. The final concentration of resazurin was 20 µM. pates were incubated at 37°C for 30 min in the dark. An image was taken. Pink indicated live growing cells and blue indicated no growth. This experiment was repeated in triplicate.

2.11. Primary attachment assays

To investigate if *C. parapsilosis* supernatant reduced *S. aureus* attachment, biofilm assays were set up as described in section 2.2. with adjustments. The assays were incubated for 1.5 h at 37°C before being washed gently with 100 µL of PBS twice. The assays were visualised using crystal violet staining and the absorbance measured as previously described (section 2.3). To calculate the CFU/mL, wells were scraped, and the biofilms resuspended in 100 µL of PBS and serially diluted. The drop method was used whereby 10 µL of sample was plated onto TSA (agar) in triplicate. Plates were incubated at 37°C for 24 h before CFU was calculated.

2.12. *S. aureus* biofilm formation on silicone squares.

Overnight cultures *of S. aureus* and *C. parapsilosis* were diluted in TSB-0.2G to an OD of 0.1 and 1, respectively. For single species biofilms, 500 µL of *S. aureus* or *C. parapsilosis* was added to wells in a 24-well Nunclon plate containing 500 µL TSB-0.2G. For mixed species wells, 500 µL of *S. aureus* was added to 500 µL of *C. parapsilosis* cells. Sterile squares of silicone measuring 1 cm^2 were placed at the bottom of the wells, fully submerged. Plates were incubated statically for 24 h at 37°C. The squares were removed gently using tweezers and dipped into PBS to wash off non-adherent cells before being allowed to dry fully at RT. For staining, the squares were covered in 0.4% crystal violet for approx. 10 min. To wash off the crystal violet, the squares were dipped into PBS and swirled gently. This was repeated until the PBS was clear. An image was taken.

To test the effect of *C. parapsilosis* supernatant on *S. aureus* biofilm formation on silicone, the method above was repeated with *C. parapsilosis* cells substituted for an equal volume of supernatant, SN1, resulting in a 50% (v/v) concentration of supernatant in each well.

2.13. Collection and storage of biofilm samples for RNA extraction

Single-species (SA1), dual-species (SA1 and CP1), and CFS-treated (SA1 and SN1) biofilms in TSB-0.2G media and SA1 and CFS-treated biofilms in TSB-1G were set up in 6-well Nunclon plates. After 24 h of growth at 37°C, wells were washed twice with PBS, then scraped and re-suspended in 1mL PBS. This was then added to 2mL bacteriaProtect™ reagent (Qiagen, Germany), vortexed, then immediately put on ice for 5 min. The cells were then centrifuged at 5000 *x g* for 10 min (Rotanta 460 R, Hettich). All liquid was poured off, with care not to disturb the pellet. At this stage, the pellets were either stored at -80°C or continued immediately on to the RNA extraction steps described below.

2.14. RNA extraction, library preparation and sequencing (RNA-seq method)

Following from section 2.13. Pellets were re-suspended in TE buffer (30 mM Tris-Cl, 0.5 M EDTA, pH 8) containing 50 µL of lysostaphin (1 mg/mL). The samples were incubated for 10 min in a water bath at 37°C. Samples were vortexed for 10s every 2 minutes during incubation. For biofilms grown in TSB-1G, 50 µL of proteinase K (20 mg/ml) (Qiagen) was also added prior to incubation. Total RNA extraction was then carried out using the Qiagen RNA mini-Kit (Qiagen, Germany) according to the manufacturer's instructions.

The RNA extraction protocol ensured that only bacterial cells were lysed, and that no RNA was released from the fungal cells in the mixed species samples. This was later confirmed by the Agilent 2100 bioanalyzer (Agilent Technologies Inc.). RNA samples were eluted in dH_20 and then stored at - 80°C immediately. 5 µL of the final RNA sample was aliquoted separately for sample quality analysis. RNA concentration and quality was first quantified using a Nanodrop 2000 (Thermo Scientific). Only samples with an A260/A280 ratio of above 2.0 and a concentration of > 50 ng/µL were accepted. To determine total RNA integrity, samples were run on an Agilent 2100 Bioanalyzer or Qubit 4 (Invitrogen). The RNA samples were prepared and run on the Bioanalyzer or Qubit according to the manufacturer's instructions.

Sample quality control (QC), Library preparation, sequencing, and library QC was carried out by Novogene (Novogene, UK). Illumina 150 paired-end sequencing produced a stranded library (this preserved strand information). Raw reads were generated and stored as FastQ files. Each library produced between 26 and 37 million reads for the TSB-0.2G media condition and between 4 and 25 million reads for the TSB-1G media condition. The number of raw reads for each sample in the two separate RNA-seq experiments is listed below in Table 2.2. For the TSB-1G media condition samples the forward and reverse reads are separated and idicated by '_1' and '_2', respectively.

Table 2.2. Raw reads per RNA library

Sample	# Raw reads
TSB-0.2G media condition	
Control_1	28452422
Control_2	31694370
Control_3	35047670
Cells-1	37634046
Cells-2	32543986
Cells-3	31427988
SN-1	26544510
SN-2	31273846
SN-3	32532648
TSB-1G media condition	
SA1.1_G_1	23776546
SA1.1_G_2	17629882
SA1.2_G_1	15389636
SA1.2_G_2	11880514
SA1.3_G_1	17646224
SA1.3_G_2	17821376
SN1.1_G_1	25110636
SN1.1_G_2	4325110
SN1.2_G_1	20751708
SN1.2_G_2	8810252
SN1.3_G_1	17493668
SN1.3_G_2	10973318

2.15. Identification of differentially expressed genes (DEGs) and Statistical analysis.

RNA data analysis was carried out with the aid of Dr. Emma Finlay (bioinformatician) using the analysis platform Galaxy (Afgan *et al.*, 2016). FASTQC (Galaxy Version 0.72+galaxy1) and MultiQC were used to assess the quality of the reads. Any reads containing adapter contamination were trimmed using Cutadapt (version 4.0). The reads were aligned to the reference genome of *Staphylococcus aureus* NCTC 8325 (NCBI Reference Sequence: NC_007795) using HISAT2 (Galaxy Version 2.2.1+galaxy0) (Kim *et al.*, 2019). The overall alignment rate for each sample was >94%. This reference genome was chosen as it has greater annotation than the DSM799 genome and increased compatibility with downstream analysis tools. Gene counts were generated by HtSeq-Count (Galaxy Version 0.9.1) using Union mode (Anders, Pyl and Huber, 2015). A counts matrix was produced and exported to R (version 4.2.2), where the EdgeR Bioconductor package was used for the annotation and creation of a DEG output table (Robinson, McCarthy and Smyth, 2010; Chen, Lun and Smyth, 2016). User manual can be accessed at: https://www.bioconductor.org/packages/release/bioc/vignettes/edgeR/inst/doc/edgeRUsersGuide.pdf. Genes with a *P* value < 0.05 and a Log2 fold change (LogFC) >|1.5| were considered as being significantly differentially expressed. Figures depicting differential gene expression of *S. aureus* biofilms were created using the 'EdgeR', 'gplots', 'ggven', 'RColorBrewer' and 'ggplot2' packages in RStudio, R version 4.2.2.

2.16. pH measurement of biofilm supernatant

Biofilms were set up in TSB-0.2G and TSB-1G media as described in section 2.2 using 6-well Nunclon plates. After 2, 6, and 24 h of incubation, the biofilm supernatant was removed from each well and sterilised using a 0.2 µm filter. pH measurements were taken using a pH meter (8691 AZ IP65 pH pen) at the indicated times and at 0 h prior to incubation. Measurements were taken in triplicate and the average value was used. This was repeated for each of the three biological replicates for each media condition.

2.17. Cell aggregation assays

Auto-aggregation assays were carried out as described by Kaplan *et al.* with some adjustments (Kaplan *et al.*, 2012). Bacteria were cultured in 6 well plates (10^7 CFU/mL) with an equal volume of SN1 or TSB-0.2G media. The final volume in each well was 4 mL. After static incubation at 37°C for 24 h, the broth was carefully removed and 500 µL of PBS was added. The biofilms were re-suspended and transferred into a 1.5 mL microcentrifuge tube. The cells were resuspended by pipetting and the tubes were incubated statically at room temperature and photographed at 15 and 30 min. Where indicated, biofilms were incubated with 10 µL of DNase I (0.5 mg/mL) for 10 min prior to resuspension.

2.18. Biofilm dispersal by sodium metaperiodate, proteinase K and DNase I.

To examine the matrix components over time, bacterial biofilms were grown as described in section 2.2. At 2, 6, 16 and 24 h of growth, the biofilms were washed twice and 50 µL of proteinase K (100 µg/mL), sodium meta-periodate (NaIO4) (10 mM) or DNase I (200 µg/ml) was added to degrade protein, carbohydrate, and extracellular DNA respectively. The plates were incubated for 2 hr at 37°C. The wells were washed once with PBS and allowed to dry before staining with 50 µL of 0.4% crystal violet as described in section 2.3.

2.19. Protease assay using Skimmed milk agar

Protease activity of biofilm cultures was assessed by growth on 2% skimmed milk agar plates. Skimmed milk agar was made by autoclaving skimmed milk solutions (Sigma) separately to TSA agar and then mixing to a final concentration of 2% skim milk. Once cooled enough to handle (about 50°C). Control and SN1-treated (50% v/v) *S. aureus* biofilms were set up in 24-well Nunclon plates. 500 µL of cells, diluted to an OD of 0.1

in TSB-0.2G or TSB-1G was added. 500 µL of TSB-0.2G or TSB-1G was added to control biofilms and 500 µL of SN1 was added for the treated wells. Samples of the biofilm supernatants were taken at 6 h and 24 h and spun to pellet and remove any cells. Twenty µL of this biofilm (cell-free) supernatant was added into wells made in the agar. Plates were incubated for 24 h at 37°C and protease activity was assessed by measuring zones of proteolysis (clearing) on the agar. The experiment was completed in triplicate (three biological replicates and three technical).

2.20. DNase agar

Biofilms were set up as in section 2.19. DNase activity of biofilm cultures was assessed by incubation on DNase agar plates (Oxoid). Samples of the biofilm supernatants were taken at 6 h and 24 h and spun to pellet any cells. Biofilm supernatant (20 µL) was added into wells made in the agar. Plates were incubated for 24 h at 37°C and the plates were flooded with 1N HCL and allowed to stand for about 10 minutes. DNase activity was assessed by zones of clearing on the agar. The experiment was completed in triplicate (biological and technical).

2.21. Preformed biofilm assay

S. aureus or *S. epidermidis* biofilm assays were set up in 96 well plates as previously described in section 2.2. without *C. parapsilosis* CFS. Following 24 h incubation at 37°C, the plates were washed twice with 100 µL PBS. For testing 100% (v/v) CFS, 200 µL of TSB-0.2G, SN1 or SN6 was added to appropriate wells. For 50% (v/v) CFS, 100 µL of TSB-0.2G or TSB-1G was added to each well and 100 µL of TSB-0.2G (control), SN1 or SN6 (treated) was added to appropriate wells. The plates were incubated for a further 24 h at 37°C. The assays were washed and visualised using crystal violet staining as described in section 2.3. The experiment was completed in triplicate (biological and technical).

2.22. Biofilm dispersal assay with decreasing concentrations of CFS

Biofilm assays were set up as described in section 2.21. After the first 24 hrs of growth, all liquid was removed from each well and the biofilms were washed gently with PBS. In a sterile plate, the CFS was serially diluted 2-fold in TSB-0.2G to get a range of concentrations in a final volume of 200 µL. This was transferred into the initial biofilm assay plate then incubated for another 24 h. The assays were then washed twice with 100 µL of PBS. Once dry, the plates were stained, and the absorbance measured as described in section 2.3.

2.23. Minimum inhibitory concentration (MIC) of oxacillin

The MIC of oxacillin was determined by the broth microdilution method according to Clinical and Laboratory Standards Institute (CLSI) guidelines. Briefly, in a 96 well Nunclon plate, oxacillin was diluted 2-fold in TSB media. 100 µL of TSB media containing SA1 at an OD of 0.1 (10^7 CFU/ml) was added. Plates were incubated at 37°C for 24 h. The absorbance (600nm) was read in a plate reader (Tecan M200 pro). The MIC was recorded as the last well where there was no visible growth. The MIC_{90} was recorded as the minimum concentration of oxacillin that reduced the absorbance by at least 90%. The MBC was assessed by using a pin replicator to transfer the contents of the wells onto TSA agar. The agar plates were incubated for 24 h. The MBC was recorded as the minimum concentration required to inhibit all growth. The experiment was completed in triplicate (biological and technical).

2.24. Biofilm susceptibility testing (MBIC) to oxacillin

The minimum biofilm inhibition concentration (MBIC) was tested. Oxacillin was diluted 2-fold in TSB broth media or SN1. 100 µL of TSB-0.2G media containing SA1 at an OD of 0.1 (10^7 CFU /ml) was added. The plates were incubated for 24 h at 37°C. The wells were washed with PBS and the biofilm biomass was quantified as described in section 2.3.

2.25. Dry weight of biofilm

Biofilm assays were conducted in 6-well Nunclon microtiter plates. For biofilm inhibition, 2.5 mL of bacteria were diluted in the relevant media to an OD 0.1 (roughly 10^7 CFU/mL) and 2.5 mL of cell-free supernatant (CFS), or the relevant media was added. After 24 h of static growth, the biofilms were washed gently with PBS twice. 1 mL of PBS was added, and biofilms were removed using a cell scraper and transferred into a pre-weighed micro-centrifuge tube. The cells were pelleted by centrifugation, and the supernatant was discarded. The tubes were left to dry overnight in an oven (60°C). The tubes were weighed, and the initial weight of the empty tube was deducted from the final weight to calculate the dry weight of biofilm biomass.

For measuring the effect on preformed biofilm, 2.5 mL of bacteria were diluted in the relevant media to an OD of 0.1 and 2.5 mL of the relevant media was added. Following incubation for 24 h at 37°C, the biofilms were washed twice with 1 mL PBS to remove non-adherent bacteria. 2.5 mL of *C. parapsilosis* cell-free supernatant and 2.5 mL of the relevant media was added. For sterility controls, 5 mL of media was used. Plates were again incubated for 24 h. The biofilms were washed, dried, and weighed as described above. For SN1-treated biofilms, results represent 3 wells combined. For CaSN-treated biofilms, results represent the weight of biofilm from a single well.

To ensure all wells were scraped adequately, crystal violet staining was used to visualise any leftover adherent cells.

2.26. *C. parapsilosis* growth curve

The *C. parapsilosis* growth curve was set up as described for SA1 in section 2.9. Briefly, TSB-0.2G media was inoculated to an OD 0.2. The cultures were grown in a shaking incubator 180 rpm at 37°C. OD_{600} readings were taken at hourly intervals from time 0 h to 8h and at 24 h and 28 h. A graph was plotted with OD against time.

2.27. Treatment of *C. parapsilosis* CFS

To test the effect of various treatments on the activity of *C. parapsilosis* CFS on bacterial biofilm *C. parapsilosis* CFS was treated with Proteinase K (100 µg/mL), pepstatin A (10 µg/mL), and heat treated. For heat treatment the SN1 was boiled for 15 minutes prior to use in the biofilm assay. Proteinase K (Qiagen) at a final concentration of 100 µg/mL was added to SN1 and incubated shaking for 1 h before inactivating by heat treatment. Pepstatin A (Thermofisher Scientific, Denmark) (10 µg/mL) suspended in ethanol was added to the SN to inactivate the activity of aspartyl proteases. Treated CFS (100 µL) was added to wells of a 96-well plate containing 100 µL of *S. aureus* (10^7 CFU/mL) suspended in TSB-0.2G media. Wells containing *S. aureus* and untreated CFS acted as controls. As pepstatin A was suspended in ethanol, an equal volume of ethanol was included in control wells to account for its presence in the test wells. The plates were incubated for 24 h at 37°C. The wells were washed with PBS and the biofilm biomass was quantified as described in section 2.3.

2.28. Supernatant size fractionation.

C. parapsilosis CFS was prepared as described in section 2.6. The CFS was fractionated by centrifugation using Amicon filters (Merck Millipore, MA, USA) with 5 kDa cutoff membranes for 25 min at 5,000 × g. 100 µL of each fraction was added to wells containing 100 µL of SA1 suspended in TSB-0.2G media (OD_{600} 0.1 – approx. 10^7 CFU/mL). Wells containing 100 µL of S. aureus (SA1) and 100 µL of TSB-0.2G acted as a control. The microtiter plates were incubated for 24 h at 37°C before washing twice with 100 µL of 1 x PBS. The plates were dried at RT and the absorbance measured as described in section 2.3.

2.29. Metabolomic sample preparation and analysis

Cell-free supernatant from *C. parapsilosis* CP1, CP6 and *C. albicans* was collected as described in section 2.6. Samples were frozen and stored at -80°C. Targeted

metabolomics, quality control, data processing and metabolite quantification was performed by the Conway Metabolomic Facility at University College Dublin.

The supernatant samples were analysed using a targeted metabolomic platform and were prepared according to the MxP® Quant 500 assay manual (Biocrates Life Sciences, Innsbruck, Austria). This kit has been previously used for targeted metabolomics in *Candida* species (Begum *et al.*, 2022). 10 µL of sample was loaded into a 96 well plate and dried for 30 mins, and subsequently derivatised using 50 µL of derivatization solution (5% phenyl isothiocyanate in ethanol/water/pyridine (volume ratio 1/1/1)). The plate was then dried for 60 mins under nitrogen. A total of 300 µL of 5 mM ammonium acetate in methanol was added to each well and the plate was placed on a shaker for 30 mins. The plate was centrifuged at 500 g for 2 mins, and 150 µL of high-performance liquid chromatography (HPLC)-grade water was added for liquid chromatography tandem mass spectrometry (LC- MS/MS) analysis. Additionally, 10 µL of eluate was diluted with 490 µL of methanol running solvent for flow injection analysis tandem mass spectrometry (FIA-MS/MS) analysis.

The prepared 96 well plate was analysed by a Sciex ExionLC series UHPLC system coupled to a Sciex QTRAP 6500+ mass spectrometer. The mobile phase A and B were 100% water and 95% acetonitrile (both added 0.2% formic acid), respectively. In the LC-MS/MS analysis, amino acids (n=20), amino acid related (n=30), bile acids (n=14), biogenic amines (n=9), carboxylic acids (7), hormones and related (n=4), indoles and derivatives (n=4), nucleobases and related (n=2), fatty acids (n=12), trigonelline, trimethylamine N-oxide, p-Cresol sulfate, and choline were quantified. Lipid classes such as lysophosphatidylcholines (n=14), phosphatidylcholines (n=76), sphingomyelins (n=15), ceramides (n=28), dihydroceramides(n=8), hexosylceramides (n=19), dihexosylceramides (n=9), trihexosylceramides (n=6), cholesteryl esters (n=22), diglycerides (n=44), triglycerides (n=242), were semi-quantified in FIA-MS/MS analysis, furthermore acylcarnitines (n=40) and the sum of hexose were also semi-quantified in FIA-MS/MS analysis. The multiple reaction monitoring (MRM) method was used to acquire data for the metabolites.

2.30 Data processing and metabolite quantification

Data were processed using MetIDQ software provided by Biocrates Life Sciences. Amino acids and part of amino acid related metabolites and biogenic amines were quantified based on isotopically labelled internal standards and seven-point calibration curves. All other metabolites were semi-quantified by using internal standards. Data quality was assessed by investigating the accuracy and reproducibility of QC sample, provided with Quant 500 assay. Metabolites were included for further statistical analyses only when their concentrations were above the limit of detection (LOD) in more than 50% of samples.

Principal component analysis (PCA) was performed using the 'mixOmics' R package to distinguish between *Candida* samples and the control (TSB-0.2G media). For the normalization process used to create a heatmap, the data were mean-centred and divided by the standard deviation of each metabolite (autoscaling). Students T-test was used to identify significant increases in the concentration of a metabolite compared to the media control. Differential metabolites were identified based on threshold *P*-value (< 0.05).

2.31. General Data analysis

Results were considered significant if $P < 0.05$. The p-value was calculated using students' t-test (two-tailed) using excel or R (version 4.2.2) unless otherwise stated (R Core Team, 2022). All experimental figures were created using R Studio or Microsoft PowerPoint. R Packages used: 'tidyverse', 'ggplot2', 'gplots', 'RColourBrewer', 'reshape2', 'dplyr', 'ggarange', 'ggpubr', 'cairo', 'Limma' 'DEseq', 'mixOmics' and 'edgeR'.

Chapter 3 – Characterising *S. aureus* biofilm formation during co-culture with *Candida parapsilosis*

3.1. Introduction

The *Staphylococcus aureus* biofilm is complex, and treatment of biofilm infections is made more difficult due to the inherent resistance that biofilms have against antibiotics (Donlan and Costerton, 2002; Moormeier and Bayles, 2017). Novel treatments and prevention strategies are needed to target these biofilms. *S. aureus* is a model organism whose interaction with bacterial and fungal species has been documented. This includes interactions during dual-species biofilm formation (Orazi and O'Toole, 2017; Carolus, Van Dyck and Van Dijck, 2019). Biofilms at the site of infection are commonly polymicrobial (Wolcott *et al.*, 2013). It is becoming increasingly clear that the disease phenotype or the clinical outcome of infection can be shaped by interactions between pathogenic bacteria and other microbial species present at the site of infection (Amador, Sternberg and Jelsbak, 2018).

Although there is a significant body of work that relates to the synergistic interaction of *S. aureus* and *Candida albicans* (reviewed in (Carolus, Van Dyck and Van Dijck, 2019)), the cross-kingdom interaction of *S. aureus* with the lesser-studied *Candida parapsilosis* has not, to our knowledge, been fully explored. *S. aureus* forms a dual-species biofilm with *C. albicans* by adhering to the Als membrane proteins that *C. albicans* expresses on its hyphae (Klotz, Gaur, *et al.*, 2007). This dual-species biofilm is clinically relevant as both have been co-isolated from sites of infection (Haiko *et al.*, 2019; Kumari and Singh, 2019).

C. parapsilosis is the second most commonly isolated *Candida* species from bloodstream infections (Bassetti *et al.*, 2015). Interestingly, despite its prevalence, there is a lack of studies that explore its interaction with other microbial species. *C. parapsilosis* does not form true hyphae and instead produces pseudohyphae (Laffey and Butler, 2005). *S. aureus* may therefore be unable to interact with *C. parapsilosis* in the same way as with *C. albicans*.

To our knowledge, this is the first study to focus on characterising the interaction between *S. aureus* and *C. parapsilosis* during biofilm formation. This chapter characterised the effect of co-culture with *C. parapsilosis* on *S. aureus*. Biofilm formation

was qualitatively and semi-quantitatively assessed using the crystal violet staining method and absorbance measurements. Tryptone soya broth (TSB) is used to facilitate *S. aureus* biofilm growth. This culture media is the most commonly used for biofilm formation and is usually supplemented with additional glucose (Lade *et al.*, 2019).

A transcriptomic analysis of *S. aureus* response to *C. parapsilosis* was performed using RNA sequencing (RNA-seq). RNA-seq has become a popular method for researchers and an attractive alternative to microarrays as it has increased sensitivity in detecting differentially expressed genes (DEGs) (Rao *et al.*, 2019). It also allows researchers a wide variety of applications, such as the identification of known and novel transcripts, single nucleotide variants and other features without needing prior knowledge. Transcriptomics combined with traditional microbiological *in vitro* techniques allows us to investigate microbe-microbe interactions and how they change the physiology of pathogenic bacteria (Amador, Sternberg and Jelsbak, 2018; Short *et al.*, 2021).

3.2. Results

3.2.1 Co-culture with *C. parapsilosis* cells inhibits robust *S. aureus* biofilm formation.

The effect on *S. aureus* biofilm by *C. parapsilosis* cells was measured using the crystal violet (CV) staining method. Whereby CV binds to the biofilm biomass (both the cells and the biofilm matrix) and can then be solubilised and measured via absorbance. There was a significant decrease (59.2%, $P < 0.001$) in SA1 biofilm when grown in the presence of *C. parapsilosis* isolate CP1 cells compared to the SA1 control (Figure 3.1). CP1 does not form biofilm in the test media, TSB supplemented with 0.2% glucose (TSB-0.2G) (Figure 3.1). This enables the dramatic decrease in *S. aureus* biofilm to be observed. It is important to note that SA1 can form variable amounts of biofilm, visualised by the spread in data points (Figure 3.1B). Further variability is introduced by the nature of the crystal violet assay. Crystal violet can become trapped at the edges of wells leading to inflated values once destained. However, increasing the number of biological and technical replicates within experiments minimises this variability.

The effect of CP1 cells on SA1 biofilm formation on the biologically relevant material silicone was also examined (Figure 3.1C). Similar to the microtiter plate assay, the presence of CP1 cells reduced SA1 biofilm formation on silicone squares.

.

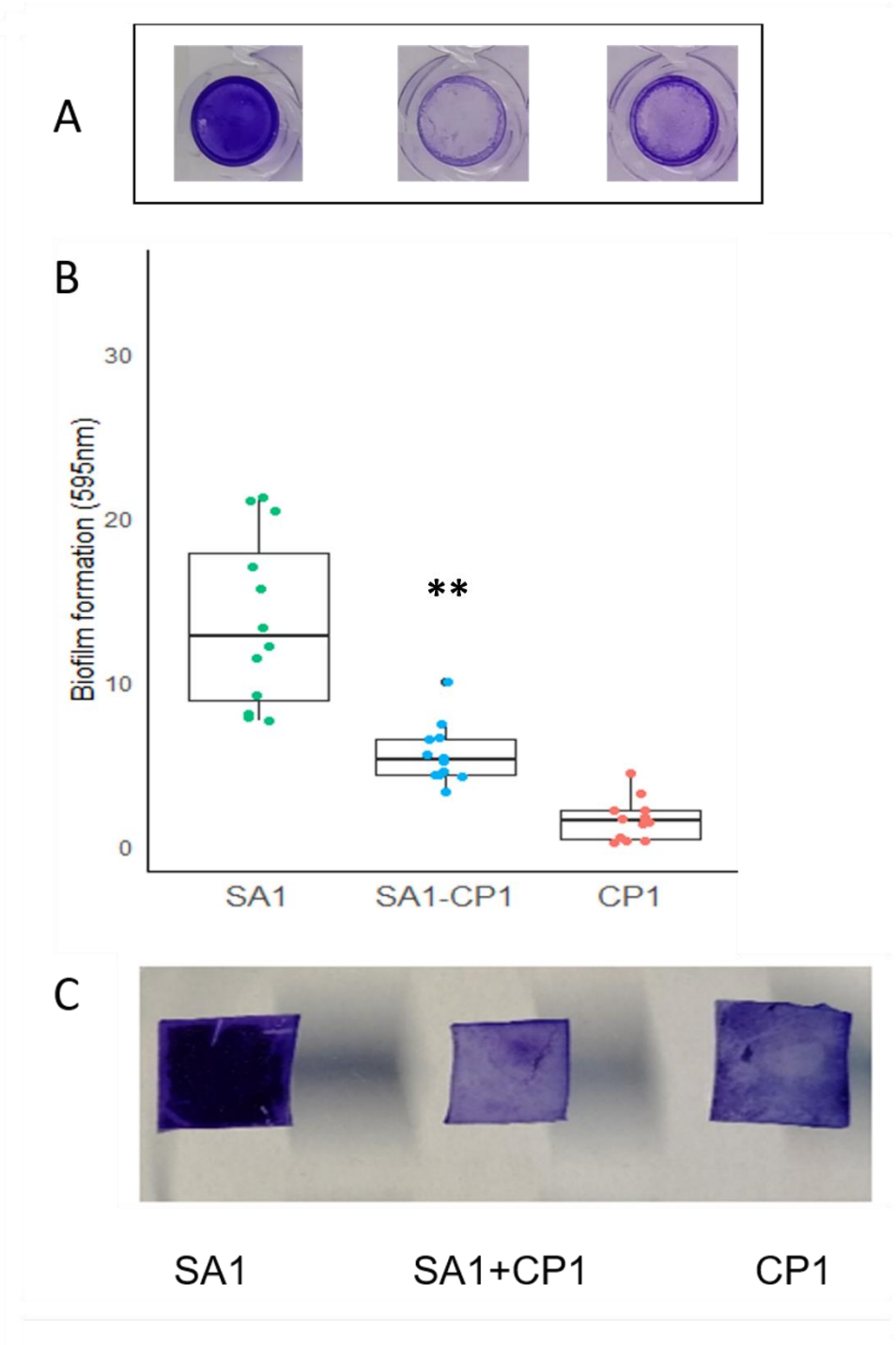

Figure 3.1. C. parapsilosis CP1 inhibits SA1 biofilm formation. *SA1 cells were grown in the presence or absence of CP1 cells at* 37°C *for 24 hr in TSB 0.2% glucose medium in microtiter plates and stained with crystal violet. The presence of CP1 greatly reduced SA1 biofilm formation. (A) from left to right: SA1 biofilm, SA1+CP1 biofilm, and CP1 biofilm. (B) Crystal violet bound to biofilms grown on microtiter plates were destained using 33% acetic acid and measured at an absorbance of 595nm. ** indicates P < 0.001.*

(C) SA1 cells were grown in the presence or absence of CP1 cells for 24 hr in TSB 0.2% glucose medium on silicone squares and stained with crystal violet. CP1 cells inhibit SA1 biofilm formation on this biologically relevant material.

3.2.1.2. CP1 inhibition of SA1 biofilm requires the presence of live fungal cells.

In order to confirm that the decrease in SA1 biofilm was due to the presence of live *C. parapsilosis*, SA1 was grown in the presence of heat-killed CP1 cells (Figure 3.2). There was no decrease in SA1 biofilm due to the presence of the heat-killed CP1 cells. In fact, the average absorbance value was increased compared to the SA1 control biofilm. This was most likely due to the dead fungal cells were being incorporated into the bacterial biofilm.

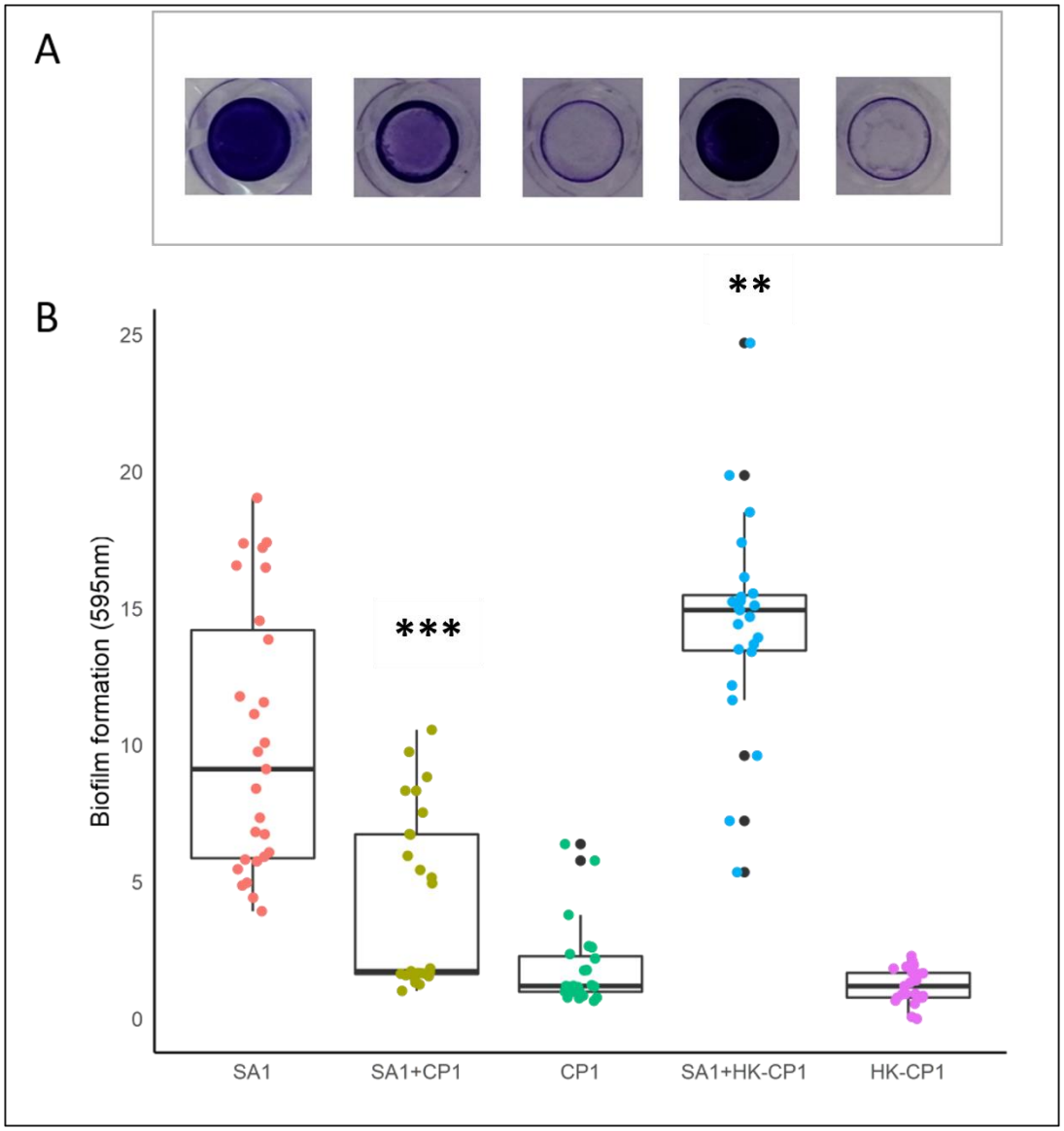

Figure 3.2. Heat-killing C. parapsilosis results in a loss of the inhibitory effect against S. aureus. *S. aureus (SA1) was grown in the presence or absence of CP1 or heat-killed CP1 (HK-CP1) for 24 h at 37°C. Heat-killed CP1 had no effect on S. aureus biofilm formation. (A) Crystal violet-stained biofilm images and (B) the corresponding absorbance values are displayed as boxplots. ** indicates a statistically significant increase in biofilm compared to the control, SA1 (P < 0.001). *** indicates a significant decrease in biofilm compared to the control, SA1 (P < 0.0001).*

3.2.2. Extending the biofilm incubation time yields similar results.

The biofilm assay was extended out to 48 h of growth. SA1 was grown in TSB-0.2G media with or without the presence of *C. parapsilosis* cells (Figure 3.3). *C. parapsilosis* was also grown alone. SA1 biofilm formation was inhibited in the presence of CP1 cells ($P < 0.0001$). Similar results were seen compared to 24 h of growth. Therefore, further experiments used an incubation time of 24 h.

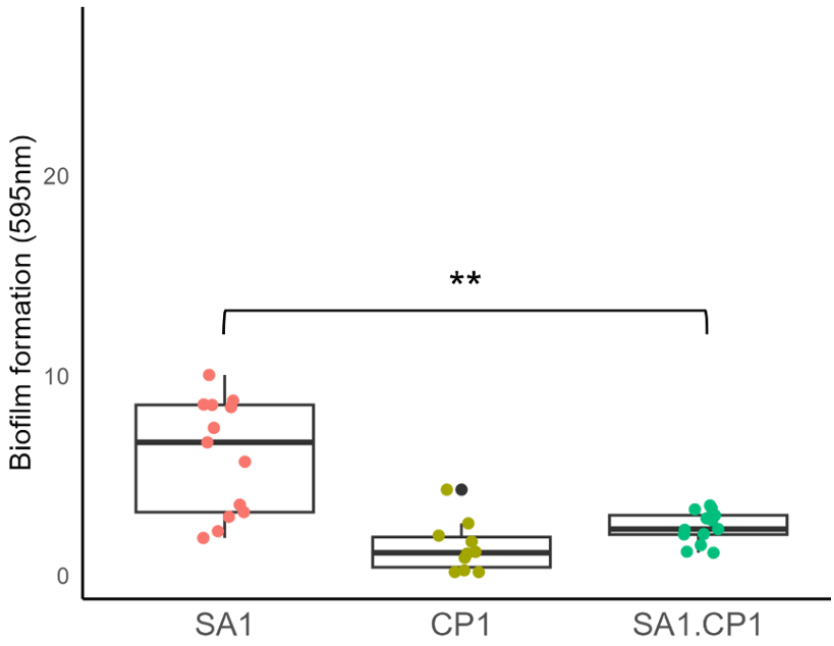

Figure 3.3. C. parapsilosis inhibits S. aureus biofilm over 48 h. *C. parapsilosis CP1 was grown in TSB with 0.2% glucose as single and as dual-species biofilms with S. aureus (SA1). After 48 h of growth at 37°C, the biofilms were washed to remove non-adherent cells. The biofilms were stained with crystal violet and the absorbance read at 595 nm. ** indicates a significant decrease in biofilm compared to the control, SA1 ($P < 0.001$).*

3.2.3. Disparate visual effect on *S. aureus* biofilm is due to *C. parapsilosis* biofilm phenotypes.

A total of twenty-four clinical isolates of *C. parapsilosis* were tested in a biofilm assay and grown as a single species culture or co-cultured with SA1. Two media, TSB supplemented with 0.2% glucose (TSB-0.2G), were used to screen the *C. parapsilosis* isolates. The results of the screening in TSB-0.2G are shown in Figure 3.4. Two biofilm phenotypes emerged; 12 *C. parapsilosis* isolates were biofilm-positive, and 12 were biofilm-negative. Where these isolates formed strong biofilm, no visual decrease compared to SA1 biofilm was observed (Figure 3.4B). Co-culture of SA1 with biofilm-negative *C. parapsilosis* cells results in a visual reduction in SA1 biofilm formation compared to the SA1 control (Figure 3.4A). SA1 co-culture with biofilm-positive *C. parapsilosis* cells does not result in a visual decrease in bacterial biofilm. However, this does not necessarily indicate that these isolates do not affect SA1 biofilm. CP1 (biofilm negative) and CP6 (biofilm positive) isolates were chosen as representatives for further study.

A Biofilm-negative

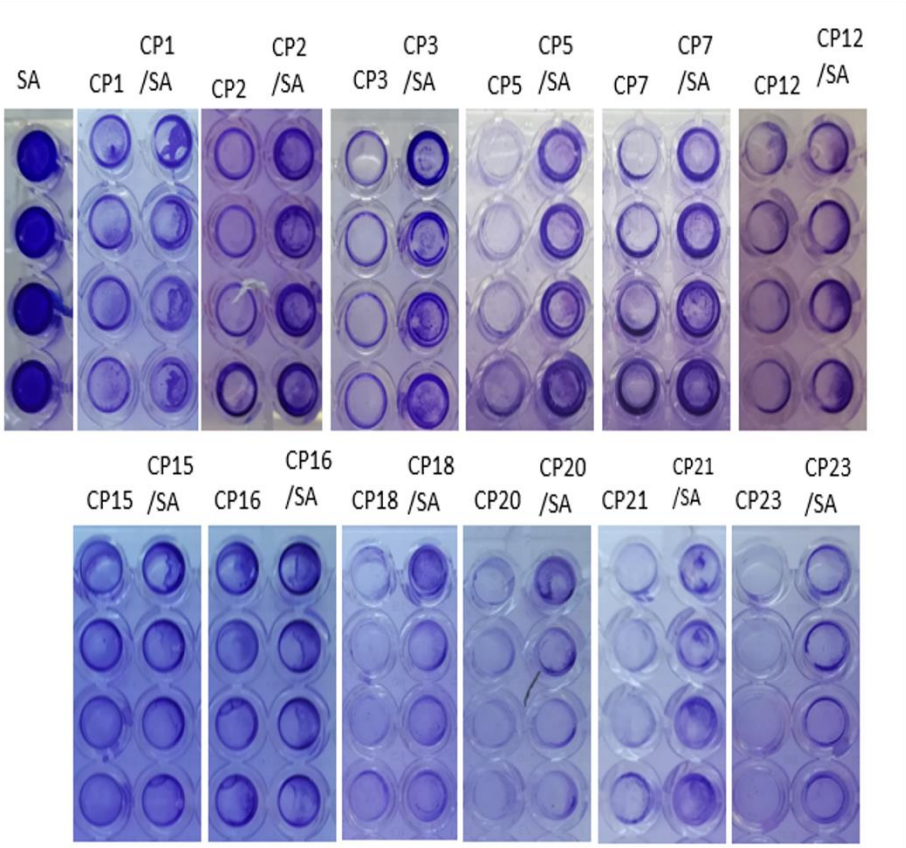

B Biofilm-Positive

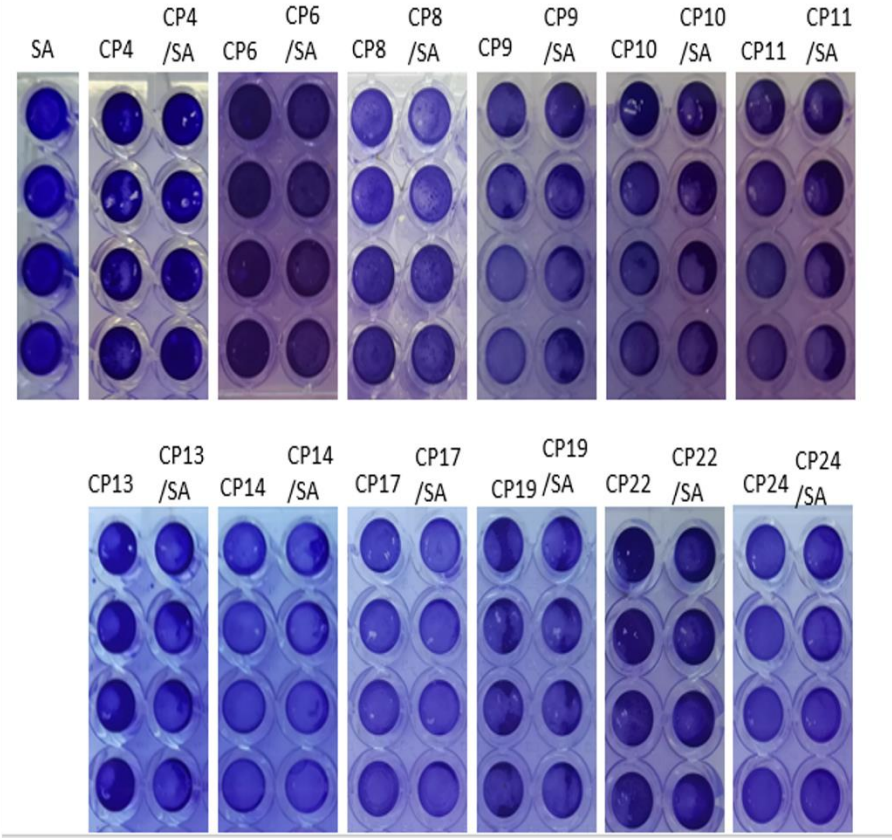

Figure 3.4. Screening of 24 C. parapsilosis isolates. *C. parapsilosis isolates (CP1 to CP24) were grown in TSB with 0.2% glucose as single (CP) and as dual-species biofilms with S. aureus (CP#/SA). Two different phenotypes in C. parapsilosis emerged, A) biofilm negative and B) biofilm positive. Where C. parapsilosis did not form biofilm, a visual decrease in biofilm compared to the S. aureus (SA) control is observable.*

3.2.4 *C. parapsilosis* cell-free supernatant (CFS) inhibits *S. aureus* biofilm formation.

To determine if *C. parapsilosis* was inhibiting *S. aureus* biofilm via a secreted factor, *C. parapsilosis* isolates, CP1 and CP6, were incubated alone, statically for 24 h in TSB 0.2% glucose media at 37°C. Their supernatants were collected, and filter sterilised to ensure that the supernatant was cell-free. The isolates CP1 and CP6 produce the CFS named here as SN1 and SN6, respectively. The CFS at a concentration of 50% (v/v) was chosen for testing against SA1 (Figure 3.5). The CFS was added at time 0 h to the biofilm assay. Both SN1 and SN6, at a 50% concentration, significantly reduced SA1 biofilm formation ($P < 0.0001$). We observed a reduction in SA1 biofilm with the addition of SN1 and SN6 by 58% and 40%, respectively compared to SA1 that produced biofilm without the presence of CFS. These results also indicated that *C. parapsilosis* is secreting an inhibiting factor regardless of the presence of *S. aureus*. The *C. parapsilosis* supernatants SN1 and SN6 also inhibited SA1 biofilm formation on silicone, a clinically relevant surface (Figure 3.5C).

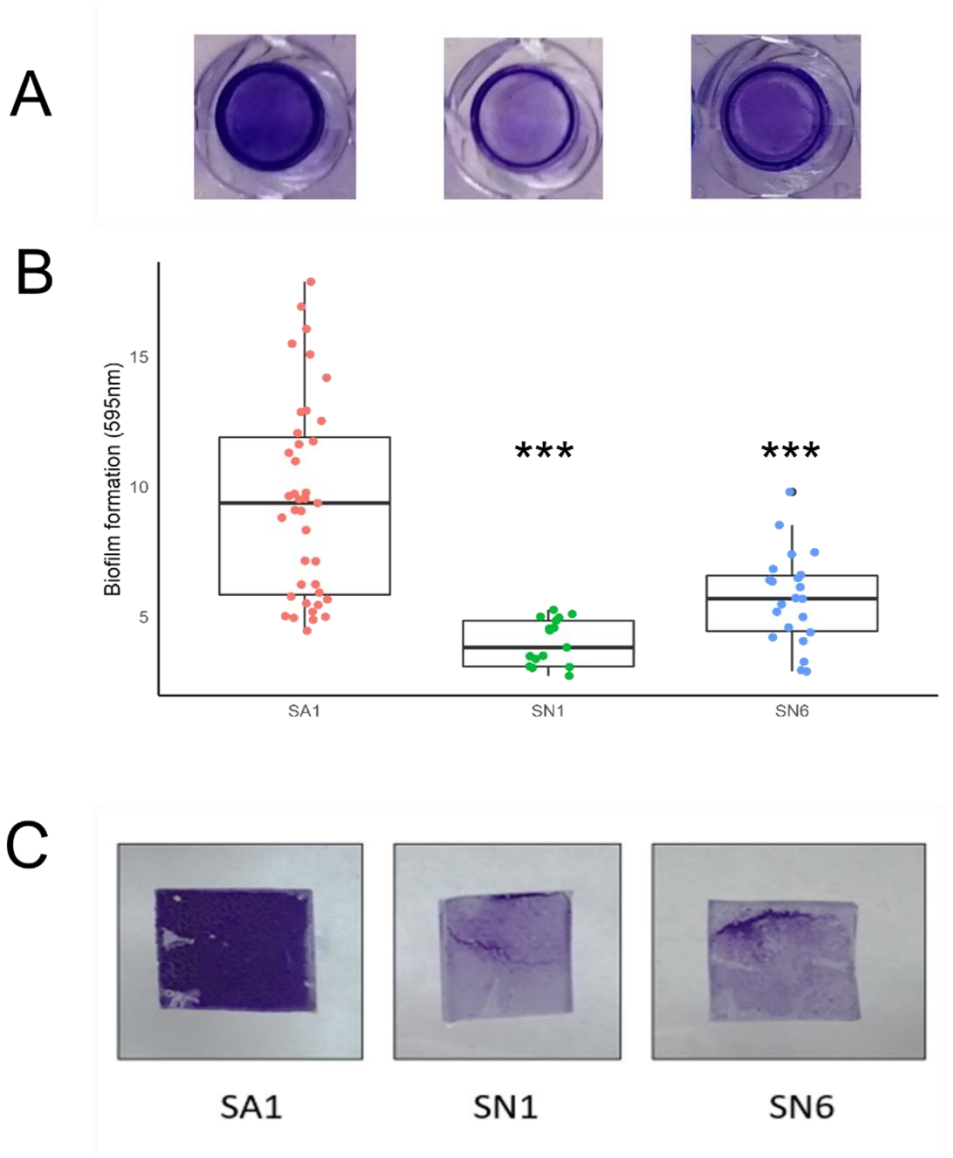

Figure 3.5. C. parapsilosis CFS was tested against S. aureus biofilm formation. *(A) SA1 cells were grown in the presence or absence of C. parapsilosis cell-free supernatant (50% (v/v)), SN1 or SN6, at* 37°C *for 24 hr in TSB 0.2% glucose medium in microtiter plates and stained with crystal violet. The presence of C. parapsilosis CFS greatly reduced SA1 biofilm formation by 58%. (B) SA1 biofilm is inhibited by C. parapsilosis CFS. *** indicates P < 0.0001. (C) SA1 biofilm formation on silicone squares is inhibited by C. parapsilosis CFS.*

3.2.5. Cell-free *C. parapsilosis* supernatant from shaking cultures can inhibit SA1 biofilm formation.

The experiments described above use *C. parapsilosis* CFS collected from cultures grown statically in Nunclon 6 well plates in TSB 0.2% glucose at 37°C for 24 h. CFS, from shaking (180 rpm) overnight cultures grown in TSB-0.2G media at 37°C for approx. 18 h, was assayed for its effect on *S. aureus* biofilm formation.

This shaking supernatant (SN-SH) at a 50% (v/v) concentration was tested against 0 h SA1 biofilm (Figure 3.6). SN1-SH and SN6-SH significantly inhibited the SA1 biofilm in TSB-0.2G media by 48% and 54%, respectively ($P < 0.0001$). Therefore, we concluded that CFS prepared this way had the same effect on SA1 biofilm. For experimental work from this point of the investigation onwards, the *C. parapsilosis* CFS was collected in this way and is referred to, again, as SN1 or SN6 for simplicity.

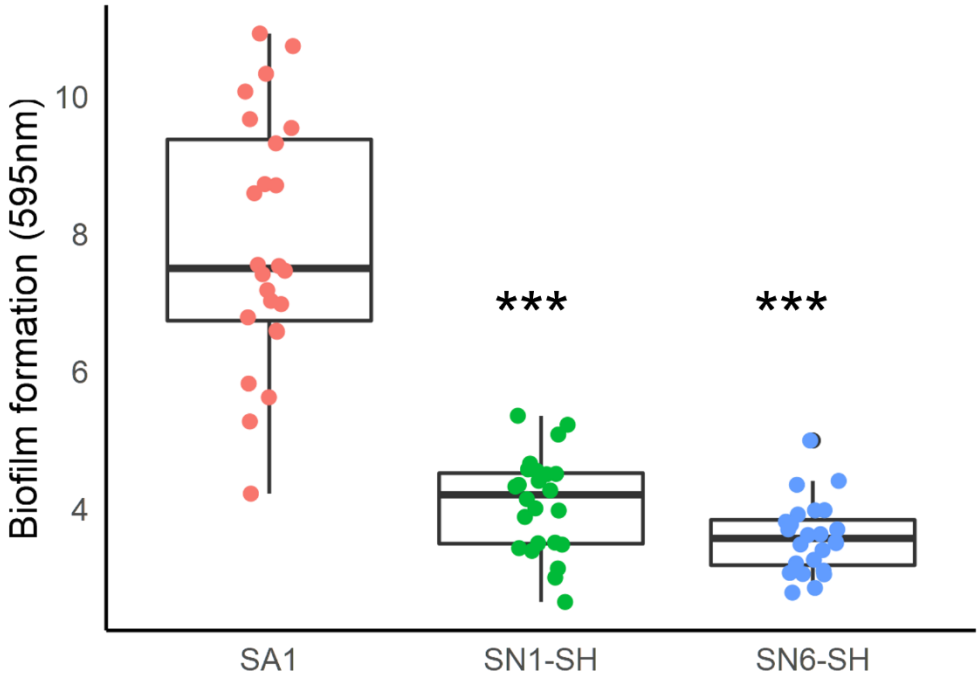

Figure 3.6. C. parapsilosis supernatant collected from shaking cultures inhibits SA1 biofilm. *SA1 cells were grown in the presence or absence of C. parapsilosis cell-free supernatant (50% (v/v)), SN1-SH or SN6-SH, at 37°C for 24 hr in TSB 0.2% glucose medium in microtiter plates and stained with crystal violet. The CFS was prepared from overnight shaking cultures grown in TSB 0.2% glucose. The presence of C. parapsilosis CFS greatly reduced SA1 biofilm formation. *** indicates P < 0.0001.*

3.2.6. *C. parapsilosis* cell-free supernatant inhibits *S. aureus* biofilm in a dose-dependent manner.

The minimum biofilm inhibitory concentration (MBIC) of *C. parapsilosis* CFS against SA1 biofilm was determined by setting up SA1 biofilm assays in the presence of decreasing concentrations of SN1 and SN6 CFS from 100% to 0.78%. Untreated SA1 biofilm was used as a control. SN1 concentrations (expressed as a percentage of total well volume) from 100% to as low as 12.5% significantly inhibited SA1 biofilm ($P < 0.01$) (Figure 3.7A). Significant inhibition of SA1 biofilm at concentrations of SN6 as low as 6.25% was also

observed ($P < 0.01$) (Figure 3.7B). A s the experiments were conducted on different days, SA1 had different growth rates between the SN1 and SN6 treatments. However, the biofilm inhibition trend remained in both cases. These results further indicate that *C. parapsilosis* secretes a factor that inhibits *S. aureus* biofilm and demonstrates that the fungal CFS works to inhibit biofilm in a dose-dependent manner.

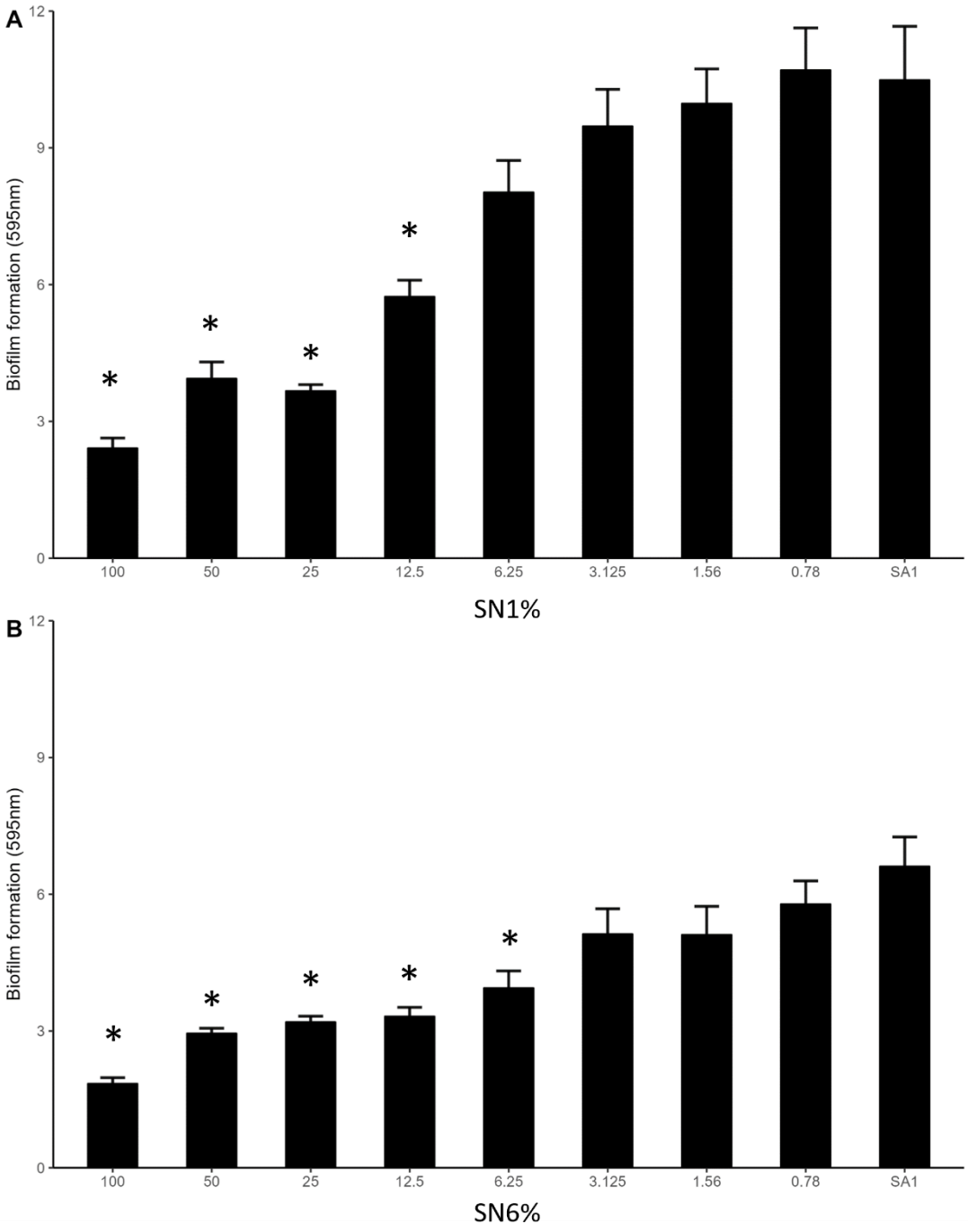

Figure 3.7. SA1 tested against decreasing concentrations of C. parapsilosis supernatant. *C. parapsilosis cell-free supernatants (A) SN1 and (B) SN6 were diluted two-fold across a 96 well plate before SA1 was added, resulting in SN concentrations (expressed as a percentage of total well volume) ranging from 100% to 0.78%. The bar columns represent the mean absorbance values (595nm) of the solubilised crystal violet from three independent experiments. * Indicates P < 0.01.*

3.2.7. *C. parapsilosis* cell-free supernatant does not alter the growth rate of *S. aureus*.

The effect of *C. parapsilosis* CFS on SA1 growth was investigated to determine if the decrease in SA1 biofilm formation was related to a growth defect (Figure 3.8A and B). A growth curve was carried out where SA1 was grown at 37°C shaking in the presence of SN1 and SN6. The CFS concentrations tested were 50% (v/v) and 70% (v/v) in TSB-0.2G. The higher CFS of 70% was included to confidently identify any growth defect that may not be detected with the 50% concentration. No growth defect or inhibition of SA1 growth was observed when grown in a 50% or 70% concentration of CFS SN1 or SN6.

Resazurin dye was used to measure cell viability in the CFS-treated and untreated biofilms. Resazurin is a blue fluorogenic dye used as a redox indicator in cell viability and proliferation assays. The blue dye is irreversibly reduced to a pink dye by viable cells. Resazurin staining of the control and CFS-treated biofilms indicated there was no decrease in cell viability when SA1 was grown in the presence of *C. parapsilosis* CFS. (Figure 3.8C).

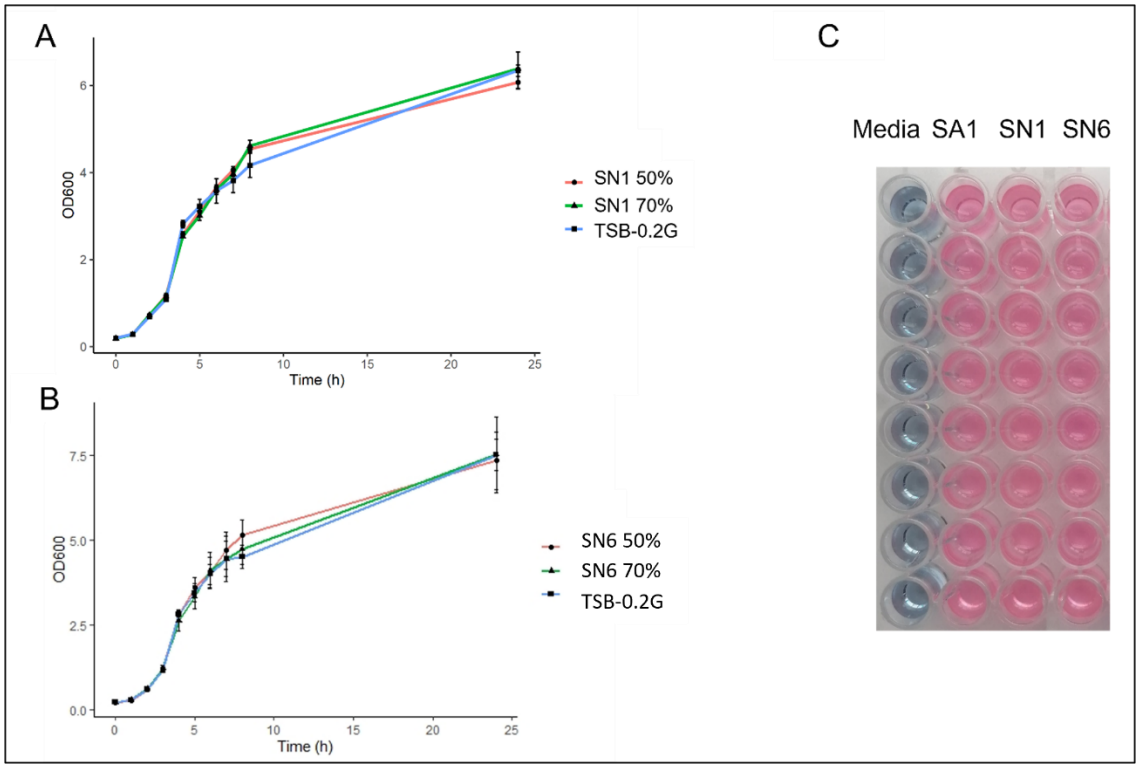

Figure 3.8. S. aureus growth curve and viability in the presence of C. parapsilosis CFS. *The growth of SA1 was tested against (A) SN1 and (B) SN6. SA1 growth was measured over a 24 h period in TSB-0.2G and TSB-0.2G containing different concentrations of C. parapsilosis cell-free supernatant (SN1 or SN6). OD_{600} readings were taken at 0, 2, 4, 6, 8 and 24 h. The results are expressed as the mean OD_{600} value ± SE (n = 3). C) resazurin-stained treated and untreated biofilms. Pink indicates cell growth. Blue indicates no growth. Media; TSB-0.2G sterile control.*

3.2.8. *C. parapsilosis* cell-free supernatant does not affect *S. aureus* primary attachment.

The initial attachment of cells to a biotic or abiotic surface is critical for complete biofilm formation. Therefore, the primary attachment of SA1 cells in the presence of SN1 and SN6 was investigated. Here, SA1 was incubated with SN1 or SN6 for 1.5 h, then non-adherent cells were gently washed away, and attached cells were stained with crystal violet. There was no decrease in bacterial cell attachment, as measured by the absorbance of attached crystal violet ($P > 0.17$) (Figure 3.9A). Enumeration of CFU/mL

via the drop method also indicates that the presence of SN1 or SN6 does not affect cell primary attachment to the polystyrene plates ($P > 0.2$ and $P > 0.15$, respectively) (Figure 3.9B).

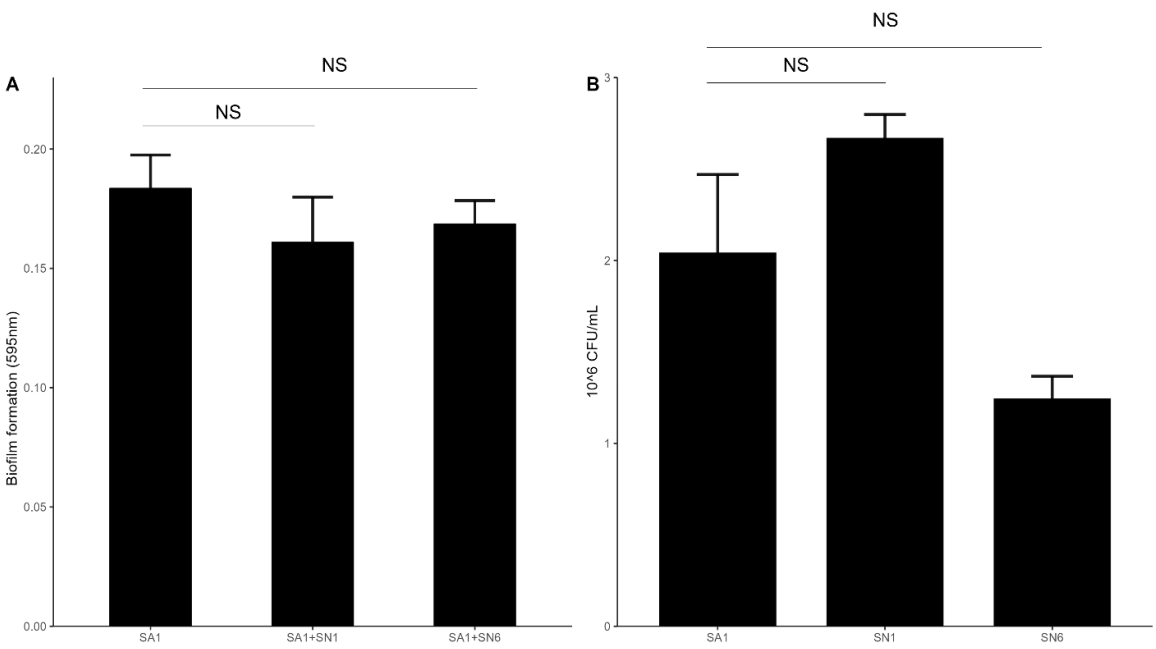

Figure 3.9. Primary attachment of SA1. *The effect on primary attachment of SA1 by C. parapsilosis CFS was measured by A) crystal violet absorbance and B) CFU/mL. Bar columns represent the mean absorbance value of 12 data points from 3 independent experiments. Error bars represent ± SE. NS; No statistically significant decrease in attachment was detected (P > 0.05).*

3.2.9. Global changes in *S. aureus* gene expression during co-culture with *C. parapsilosis* or its supernatant in TSB-0.2G media.

RNA-seq analysis was performed to investigate the transcriptional response of *S. aureus* to co-culture with *C. parapsilosis* cells or its CFS. Total RNA was collected from *S. aureus* (SA1), *S. aureus*-CP1 and *S. aureus*-SN1 biofilms grown for 24 h at 37°C in TSB-0.2G media. These samples are referred to as control, Cells, and SN, respectively.

3.2.9.1. Quality Control of RNA-seq data

Quality control (QC) was carried out by Novogene (UK) at multiple steps. These included sample preparation QC, library QC, and sequencing data QC. A data quality summary of the library data was created (Table 3.1).

Table 3.1. Data quality summary

Sample	Effective(%)	Error(%)	Q20	Q30	GC%
Control_1	99.62	0.03	96.37	90.04	36.64
Control_2	99.62	0.03	97.54	92.30	36.67
Control_3	99.59	0.03	97.22	92.18	35.63
Cells-1	99.45	0.03	97.56	92.80	35.59
Cells-2	99.59	0.03	98.15	93.99	35.62
Cells-3	99.61	0.03	96.50	90.30	36.20
SN-1	99.61	0.02	96.48	90.24	35.27
SN-2	99.59	0.03	97.10	91.78	35.72
SN-3	99.25	0.03	96.50	90.27	36.25

Sample: sample name. Effective: (Clean reads/Raw reads)*100%**.** Error: base error rate**.** Q20, Q30: (Base count of Phred value > 20 or 30) / (Total base count). GC: (G & C base count) / (Total base count).

As described in the methods Chapter 2, section 2.15, FastQC and MultiQC were used to assess the quality of the reads again. The reads were of sufficient quality to proceed with data analysis. Differential gene expression analysis was performed in Galaxy, a user-friendly platform for RNA-seq analysis (Afgan *et al.*, 2016). Then the Bioconductor package edgeR was used in RStudio to take the gene counts, perform statistical analysis,

and produce a list of differentially expressed genes (DEGs) (Robinson, McCarthy and Smyth, 2010).

Principal component analysis (PCA) was used to visualise the relationship between the samples (Figure 3.10). 90% of variance is explained by PC1 and PC2. 83% of variance was described along PC1, the x-axis which separates the Control and *C. parapsilosis*-treated samples (Cells and SN). The Cell and SN sample replicates clustered together and away from the control sample replicates. This indicates that these samples are different from the control samples i.e., genes are differentially expressed. While the control samples seem to be further spread along the Y-axis, indicating greater differences between them, 7% represents a relatively small difference compared to the 83% that separates the controls from the treated groups.

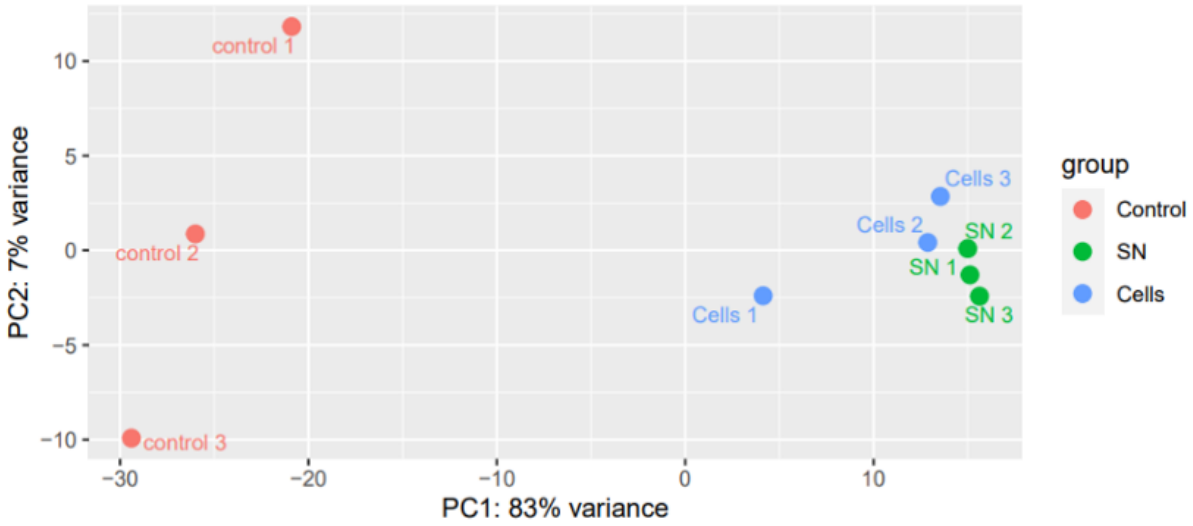

Figure 3.10. Principal component analysis (PCA) plot representing clustering of RNA-seq sample replicates. *Total RNA was collected from S. aureus (control), S. aureus-CP1 (Cells) and S. aureus-SN1 (SN) biofilms. Distinctive clusters formed along the PC1 axis, which demonstrates the effect on the S. aureus transcriptome by C. parapsilosis (cells or CFS).*

3.2.9.2. *C. parapsilosis* cells and CFS regulate a core set of genes.

There were significant (log2FC |>1.5|, adjusted $P < 0.05$) gene expression changes under the conditions tested in TSB-0.2G media. 782 and 892 genes were differentially expressed in the supernatant-treated (SN) and CP1 co-culture (Cells) conditions compared to the control, respectively. 524 and 258 genes were down-regulated and up-regulated in the Cells condition, respectively. In the SN condition, 554 and 338 genes were down- and up-regulated, respectively (Figure 3.11A). These results are also displayed as a volcano plot, with significantly ($P < 0.05$ and Log2FC >1.5 or <-1.5) down-regulated genes shown in blue and up-regulated gene displayed in red (Figure 3.11C).

There was a significant overlap of 712 DEGs (74% of genes) between the two conditions (Figure 3.11B). This indicates that co-culture with *C. parapsilosis* cells or *C. parapsilosis* supernatant has a similar effect on *S. aureus* biofilm formation.

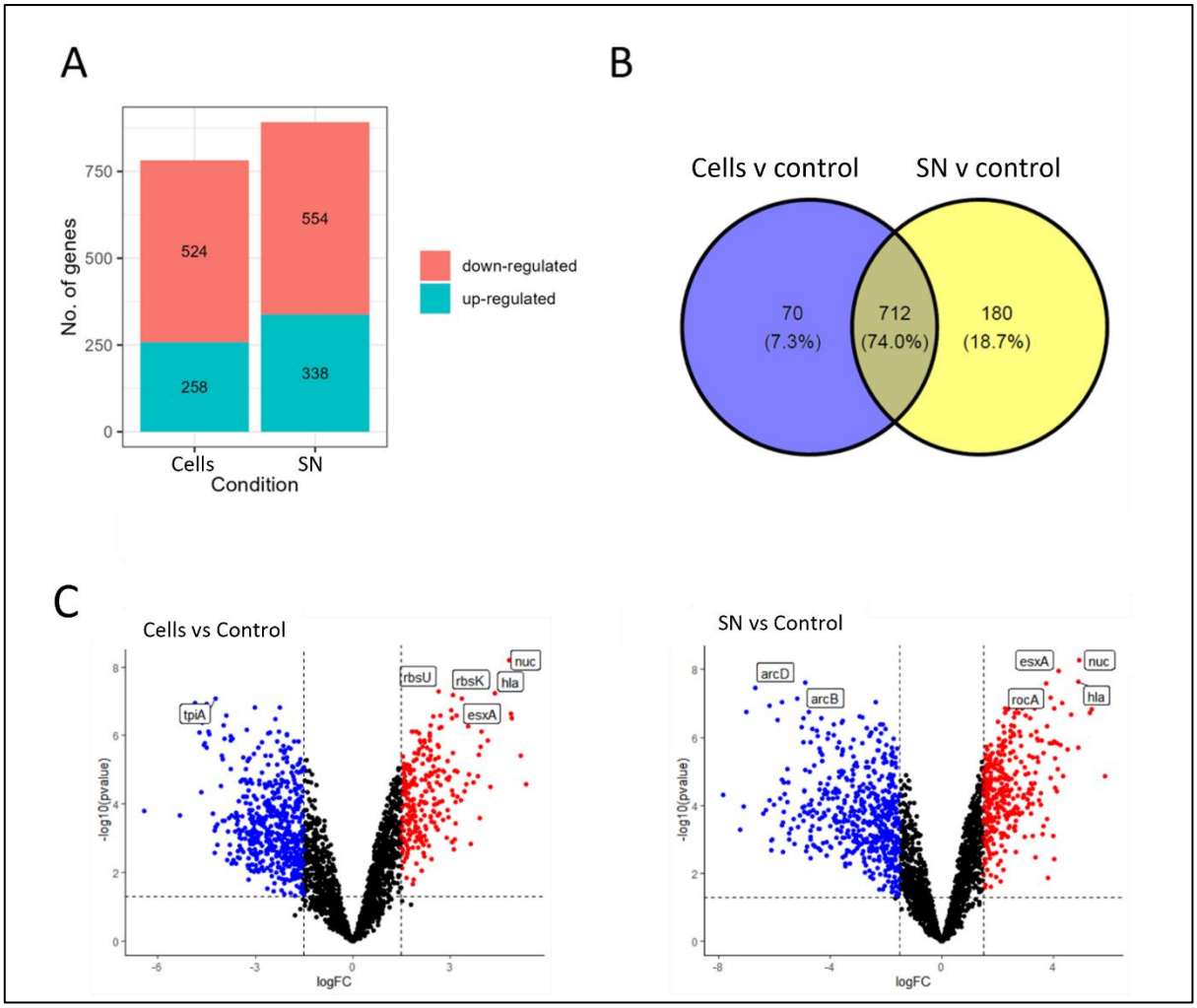

Figure 3.11. Overview of S. aureus biofilm gene expression in the different conditions tested in TSB-0.2G media. *A. The number of significantly differentially expressed genes (DEGs) in S. aureus-C. parapsilosis mixed species biofilm (Cells) and in S. aureus biofilm treated with C. parapsilosis supernatant (SN) in TSB-0.2G media. B. A Venn diagram displaying the percentage overlap in DEGs between the two conditions in comparison to the S. aureus biofilm control. Volcano plots of (C) S. aureus biofilm formed in response to growth with C. parapsilosis (Cells v control) or its supernatant (Supernatant v control) in TSB-0.2G media. The top 6 genes (P value) in each condition are labelled.*

A heatmap of the topmost DE genes across the samples in the TSB-0.2G experiment was created (Figure 3.12). The top genes are sorted by adjusted *P*-value. Clustering of the

sample types shows the similarity of expression within sample groups but differences between the sample types, with Cells and SN being most similar, while the control biofilm samples show a very different profile for these top expressed genes. A comparison between the topmost DE genes in the SN and cells conditions showed a considerable similarity in gene expression profiles. Therefore, co-culture with *C. parapsilosis* or its supernatant induces a change in gene expression of hundreds of genes potentially explaining the biofilm inhibition phenotype.

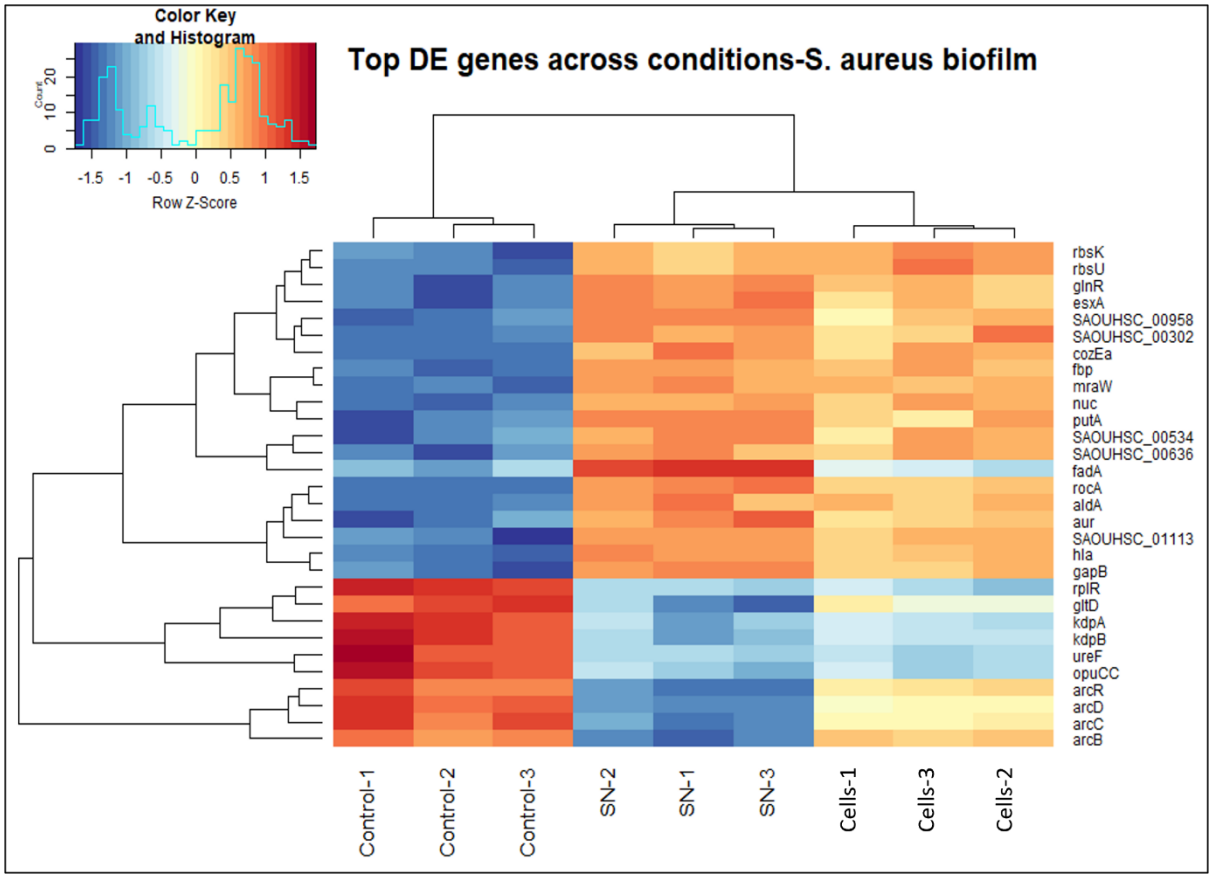

Figure 3.12. Heatmap of the top DE genes across the different conditions in TSB-0.2G media. *The top 30 differentially expressed (DE) genes in each condition are shown and ranked by adjusted P value. Columns represent the samples, while each row represents a different gene. Dendrograms cluster genes by correlation (left) or by sample expression values (top). Rows represent genes and are coloured according to whether they are upregulated (red) or downregulated (blue). Row Z-score scaling method was used. The darker the colour indicates a greater change in gene expression. The contrast used for the creation of this heatmap was Control vs SN.*

3.2.9.3. Top differentially expressed genes in both cells and CFS conditions.

The gene counts data was then re-analysed using a design matrix that took the average gene expression values from cells and SN conditions and compared them against the control samples. This gives an output file with a single value for logFC and adjusted *P*

value for each gene, and the top 10 up- and downregulated DEGs (sorted by LogFC) are shown below (Table 3.2).

Table 3.2. Top differentially expressed genes (up and down) ranked by log fold change. With $|\log_2(\text{fold change})| \geq 1.5$ and p-value < 0.05.

Gene Name	Gene Annotation	LogFC
SAOUHSC_00845	hypothetical protein	5.59
SAOUHSC_02425	hypothetical protein	5.14
nuc	thermonuclease	4.87
hlgA	gamma-hemolysin h-gamma-II subunit	4.77
aur	zinc metalloproteinase aureolysin	4.73
hla	alpha-hemolysin	4.64
SAOUHSC_00622	hypothetical protein	4.38
gapB	glyceraldehyde 3-phosphate dehydrogenase 2	4.29
hutG	formimidoylglutamase	4.2
cspC	hypothetical protein	4.19
hrtA	hypothetical protein	-7.12
rrfA	5S Ribosomal RNA	-6.2
SAOUHSC_02934	hypothetical protein	-5.73
SAOUHSC_02432	hypothetical protein	-5.33
kdpB	potassium-transporting ATPase subunit B	-5.28
kdpC	potassium-transporting ATPase subunit C	-5.19
arcC	carbamate kinase	-5.13
SAOUHSC_02948	hypothetical protein	-5.12
SAOUHSC_01826	hypothetical protein	-5.08
rrfC	5S Ribosomal RNA	-5.05

The *staphylococcal* nuclease gene, *nuc*, is among the most highly upregulated and significant genes (logFC 4.87, $P < 0.0001$). Also, among the top DEGs are various protease-encoding genes, *aur*, *hla,* and *hlgA*.

The most highly up-regulated gene was *SAOUHSC_00845*. This was a hypothetical protein, and its function is unknown. According to a search on Aureowiki, it is located beside genes involved in the cell envelope. It encodes a 7 kDa protein whose sequence homology indicates that it belongs to the UPF0337 family of stress response proteins or the CsbD stress response family. *CspC* was also upregulated. This gene encodes a cold shock protein that is strongly induced by toxic chemicals or antimicrobials (Chanda *et al.*, 2010).

The most downregulated gene was *hrtA*. This encodes an efflux system that relieves the cell of toxic buildup of heme (Stauff *et al.*, 2008). *kdpABC,* which encodes a high-affinity K-specific transport system was significantly downregulated by -4.15, -5.28, and -5.19, respectively. This system also contributes to arginine catabolism-mediated ammonia production. DEGs involved in arginine metabolism and biosynthesis (such as *arcC*) are discussed below.

3.2.9.3. Kyoto Encyclopaedia of Genes and Genomes (KEGG) Biological Pathway Enrichment and Gene Ontology (GO) Functional Enrichment Analysis

Gene ontology analysis enables researchers to identify what biological processes, cellular components and molecular functions DEGs of interest are involved in that may explain a phenotype observed (Ashburner *et al.*, 2000). To understand the function of the identified DEGs in the anti-biofilm effect of *C. parapsilosis* on *S. aureus*, GO analysis was performed.

One GO term in Cellular Component, ‘extracellular region’, was enriched for the upregulated genes. For the downregulated genes, four terms in Biological Process were significantly enriched: ‘nickel cation transport’, ‘macromolecule metabolic process’, ‘cellular component biogenesis’, and ‘cell wall organisation’. One term in Cellular Component, ‘plasma membrane’, was significantly enriched.

KEGG pathway gene enrichment analysis is a tool that allows researchers to link molecular information to higher-order functional information. All identified DEGs in the treated condition were mapped by Kobas against the KEGG database (Bu *et al.*, 2021). The search returned ten KEGG IDs (corrected *P*-value <0.05): “Ribosome”, “Metabolic pathways”, “Purine metabolism”, “Biosynthesis of antibiotics”, “Biosynthesis of amino acids”, “Pyrimidine metabolism”, “Biosynthesis of secondary metabolites”, “Microbial metabolism in diverse environments”, “Histidine metabolism”, and “Arginine metabolism”.

Interestingly, genes involved in arginine metabolism were significantly enriched. DEGs involved in the arginine biosynthesis pathway are shown in Figure 3.13. We report that co-culture with *C. parapsilosis* and its CFS resulted in a downregulation of these same genes by between at least 2- and 5-fold.

Arginine synthesis is coupled with the urea cycle (Cunin *et al.*, 1986). Genes involved in the urea cycle, the *ureABCDEFG* genes, were downregulated in the *C. parapsilosis* co-culture conditions. *argR* (arginine repressor) and *argG* (argininosuccinate synthase) were upregulated by 2- and 1.5-fold, respectively. *rocA*, *rocD*, and *rocF* form part of the arginase pathway and were upregulated.

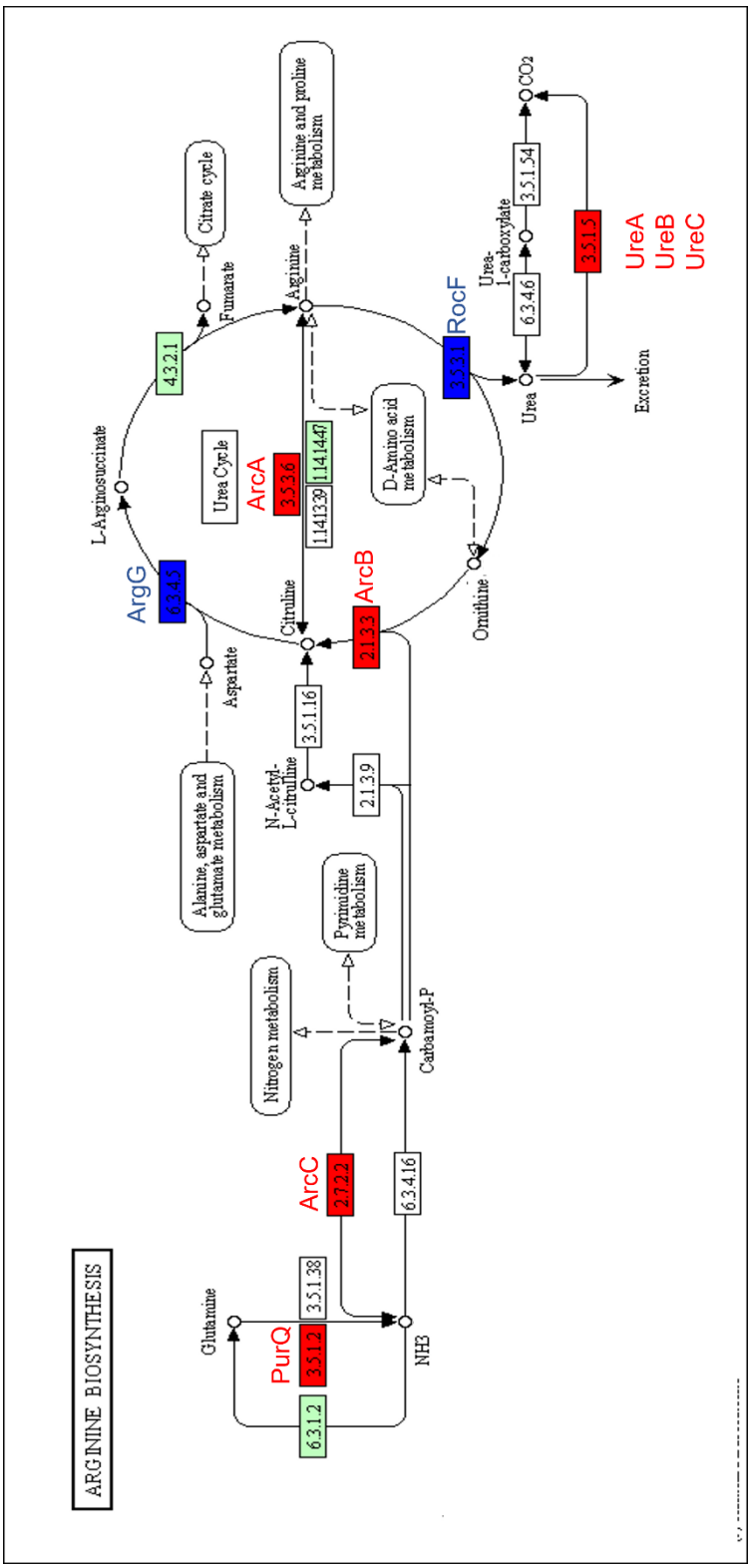

Figure 3.13. Significantly enriched KEGG pathway 'Arginine biosynthesis'. *Red highlights represent down-regulation, and blue highlights represent up-regulation. Green highlights are fully annotated by KEGG. (Kanehisa and Goto, 2000).*

3.2.9.4. Significant DEGs related to biofilm formation, regulation, and virulence.

A biased search for significant DEGs known to be involved in *S. aureus* biofilm and virulence was conducted, and the results are presented in Table 3.3. Various regulators involved in biofilm formation were seen, such as *arlR, arlS, mgrA, sigB, agrA*, and *agrC*.

Genes involved in the production or release of biofilm matrix components were identified. *icaA, icaB,* and *icaC* were downregulated (Table 3.3). These genes encode N-glycosyltransferase, Intercellular adhesion protein B and Intercellular adhesion protein C, respectively. Extracellular DNA (eDNA) is an important matrix component and the *lrgAB* operon was differentially expressed.

The surface protein encoding genes *sasG*, *sasC*, *fnbA*, *fnbB*, and c*lfA* were differentially expressed and each have been linked to biofilm formation. The intracellular protease encoding genes *clpP* and *clpC* were identified. They have opposing functions related to biofilm and repress or enhance it, respectively (Frees *et al.*, 2004). Interestingly the gene *cwrA* was upregulated by more than 3-fold. This gene is upregulated specifically in response to cell wall damage (Balibar *et al.*, 2010).

Table 3.3. DEGs (logFC |≥ 1.5|, *P* <0.05) related to *S. aureus* biofilm regulation, formation, and virulence due to co-culture with *C. parapsilosis* and its CFS. NS; not significant.

Gene Name	Gene Annotation	LogFC
Biofilm regulators		
sigB	RNA polymerase sigma factor SigB	1.75
agrA	Accessory gene regulator protein A	-1.69
agrC	Accessory gene regulator protein C	-1.59
arlRS	ArlRS two-component system	1.82/1.67
mgrA	Hypothetical protein (Global regulator)	2.99
sarT	Accessory regulator T	-4.46
sarU	Hypothetical protein	-3.93
sarX	Hypothetical protein	1.53
Biofilm matrix components		
icaA	N-glycosyltransferase	-3.61
icaB	Intercellular adhesion protein B	-3.6
icaC	Intercellular adhesion protein C	-4.14
lrgA	murein hydrolase regulator LrgA	2.34
lrgB	antiholin-like protein LrgB	-1.45 (NS)
splABCDEF	Serine proteases	2.34 - 3.19
Surface attachment proteins		
clfA	Clumping factor A	2.57
sasG	*S. aureus* surface protein G	-1.95
sasC	*S. aureus* surface protein C	-2.38
fnbAB	Fibronectin-binding proteins	-2.5 / -1.64

Internal proteases and damage response protein		
clpP	ATP-dependent Clp protease proteolytic subunit	2.19
clpC	Endopeptidase	-3.31
cwrA	hypothetical protein	3.81

3.9.3.4. Comparison of genes expressed in the SN or Cells conditions

While Cells and SN treatments resulted in very similar genes expression changes in *S. aureus* during biofilm formation, there is evidence that the Cells and SN groups also differ from each other, and this can be seen in the greater number of DE genes (180) in the SN condition compared to 70 in the Cells condition (Figure 3.11). Differences between the group expression profiles are also displayed in the heatmap (Figure 3.12). For example, *fadA* has increased expression levels under SN treatment, whereas Cells and the Control groups show greater similarity. Likewise, while *arcC*, *arcB*, *arcD*, and *acrR* are highly expressed in the Control group, the SN group shows greater downregulation than the Cells treatment group.

DE genes unique to the Cells or SN conditions were analysed using KEGG and GO analysis. For the Cells condition KEGG analysis showed two terms were significantly (corrected *P* -value < 0.05) enriched, “Ribosome” and “Pyrimidine metabolism”. GO analysis revealed significant enrichment for one term under ‘Biological process’: 'de novo' UMP biosynthetic process. This is in agreement with the KEGG analysis that flagged pyrimidine metabolism.

For the SN condition there were no significant hits when analysed using GO. Using KEGG analysis five terms were significantly enriched for (corrected *P* -value < 0.05). These were Citrate cycle (TCA cycle), “Ribosome”, “Carbon metabolism”, “Biosynthesis of secondary metabolites”, and “Biosynthesis of antibiotics”. Apart from “Ribosome”, the terms that were enriched all contained the following genes: *fumC*, *gcvT*, *sucC*, and *sucA*.

3.3. Discussion

S. aureus DSM 799 (ATCC 6538), here referred to as SA1, is a clinical isolate, and it is used for infectious disease research and quality control. It is a strong biofilm former under *in vitro* conditions (Chen *et al.*, 2019). Data presented in this chapter demonstrate that when SA1 was co-cultured statically with CP1 cells (*C. parapsilosis* isolate CLIB214), a significant decrease in SA1 biofilm was observed (Figure 3.1). Extending the biofilm growth out to 48 h demonstrated the same inhibitory effect on *S. aureus* biofilm by *C. parapsilosis* (Figure 3.3). However, the striking decrease in SA1 biofilm can only be seem when *C. parapsilosis* does not make a biofilm of its own. Biofilm formation in TSB-0.2G media by *C. parapsilosis* isolates was strain dependent and this strain variation has been previously observed (Silva *et al.*, 2009). Whether or not there is a physical interaction between *S. aureus* and *C. parapsilosis* is unclear. Unlike studies that characterise the interaction between *S. aureus* and *C. albicans* (Peters *et al.*, 2012; Schlecht *et al.*, 2015; Carolus, Van Dyck and Van Dijck, 2019; Wu *et al.*, 2021), no such studies have been carried out with *C. parapsilosis*, highlighting the novelty of the research described here. *S. aureus* has been shown to attach to *C. albicans* hyphae and form a dual species biofilm. However, *C. parapsilosis* does not produce true hyphae and instead form pseudohyphae (Laffey and Butler, 2005). It is, therefore, unlikely that *S. aureus* adheres to *C. parapsilosis*. Instead, the bacteria may become trapped within the fungal biofilm matrix. However, further investigation would be needed to confirm this.

It was revealed that regardless of fungal biofilm phenotype, *C. parapsilosis* releases a factor into the supernatant that is responsible for the inhibitory effects on SA1 biofilm (Figure 3.5). The fungal CFS significantly reduced SA1 biofilm both visually and semi-quantitatively. SN1 (biofilm negative phenotype) reduced *S. aureus* biofilm formation by 58%. SN6 (Biofilm positive phenotype) reduced biofilm formation by 40%. Biofilm formation was variable and the percentage reduction in biofilm varied across experiments. However, a reduction was always observed. Both SN1 and SN6 did not exhibit any bactericidal activity against planktonic *S. aureus* and no growth defect was

detected (Figure 3.8). Therefore, the biofilm inhibition is not due to cell death or a growth defect or inhibition.

C. parapsilosis supernatants have been previously shown to reduce the virulence of *C. albicans* by inhibiting its ability to damage premature epithelial cells via a *C. parapsilosis*-secreted factor (Gonia *et al.*, 2017). The *C. parapsilosis* CFS reduced the ability of *C. albicans* to adhere to premature epithelial cells. Many other studies into the effect of microbial supernatants on *S. aureus* have been reported. CFS of *Saccharomyces cerevisiae* decreased extracellular polysaccharide (EPS) production and auto-aggregation in *S. aureus* (Kim *et al.*, 2020). Furthermore, investigation using qRT-PCR revealed significant downregulation of genes involved with EPS production (*icaA* and *icaD*). Lactic acid bacteria (LAB) are a significant group of probiotic organisms and have been shown to benefit human health by displacing pathogens or producing antibacterial products. Their supernatants have a range of abilities from bactericidal effects to growth inhibition. Benmouna *et al*. report that the CFS of *Enterococcus sp.* decreases *S. aureus* biofilm formation by interfering with its adhesion ability (Benmouna *et al.*, 2020). Another study found that CFS of LAB had antibacterial action against multiple pathogens, including *Salmonellae*, *Listeria monocytogenes* and *S. aureus*, all important food-borne pathogens (Mariam *et al.*, 2014).

The initial attachment of bacterial cells to a surface to seed a biofilm is a crucial step in its formation. Therefore, it was plausible to hypothesise that *C. parapsilosis* supernatant may prevent the primary attachment of *S. aureus* cells to the surface of the polystyrene plates resulting in a decrease in overall biomass post-incubation. It was found that the presence of *C. parapsilosis* supernatants SN1 and SN6 had no significant effect on primary attachment (Figure 3.9). This data suggests that the CFS may be affecting biofilm maturation and matrix production.

RNA-seq analysis has provided many insights into *S. aureus* biofilm formation. Previous studies include investigations of the transcriptomes of methicillin-susceptible *S. aureus* during biofilm formation (Tan *et al.*, 2015). RNA-seq has also enabled scientists to gain

insight into the mechanisms of infection by analysing the transcriptomes of pathogens during host infection. Dual-species transcriptomic studies involving *S. aureus* have been conducted (Vandecandelaere *et al.*, 2017; Short *et al.*, 2021). Short *et al*. analysed the transcriptome of *C. albicans* during dual-species biofilm formation with *S. aureus* (Short *et al.*, 2021).

When *S. aureus* was co-cultured with *C. parapsilosis* cells or its CFS, a similar transcriptomic response was observed (overlap of more than 700 genes). A global change in gene expression was seen with hundreds of DEGs identified (Figure 3.11). Despite a 75% overlap in gene expression under CFS-treated conditions. There were 180 and 70 unique genes for the SN and Cells condition, respectively. Analysis of the genes unique to the SN and Cells conditions didn't reveal any obvious links to biofilm formation. KEGG and GO analysis identified enrichment for metabolic and biosynthesis pathways indicating that the CFS is affecting bacterial metabolism.

A core set of overlapping genes became the focus as both the Cells and SN conditions had a similar phenotype (biofilm inhibition). Interestingly, among the top differentially expressed genes were *nuc* and various proteases which can affect components of the biofilm matrix. The *S. aureus* thermonuclease encoded by *nuc* has a role in biofilm formation and maturation whereby it degrades eDNA (Mann *et al.*, 2009). Thermonuclease is involved in biofilm structuring and tower formation during an early biofilm formation stage termed the 'exodus' stage (Moormeier *et al.*, 2014). Also observed was the downregulation of the *ica* operon, which encodes PIA, an important matrix component (Table 3.3). It is possible that the upregulation of thermonuclease is degrading eDNA in the biofilm, preventing biofilm maturation and that this combined with a decrease in PIA production results in impaired biofilm formation.

Many different extracellular proteases were upregulated such as serine proteases and aureolysin. Extracellular proteases are important for biofilm maturation and over expression can result in biofilm dispersal (Martí *et al.*, 2010). The virulence factor, Alpha-hemolysin (*hla*), was significantly upregulated by co-culture with CFS. In contrast, Todd

et al. demonstrated that *hla* expression in *S. aureus* is not significantly altered by co-culture with *C. parapsilosis* cells (Todd, Noverr and Peters, 2019). Though, this was under planktonic conditions. Furthermore, genes of the Agr quorum sensing system were down-regulated (Table 3.3). This is interesting as the hallmark of *agr* activation is the upregulation of virulence factors and increased protease activity that lead to biofilm dispersal (Boles and Horswill, 2008).

Another key global regulator of virulence is MgrA, a member of the SarA protein family. Here, *mgrA* was upregulated by more than 3-fold due to co-culture with CP1 cells and SN1. MgrA is regulated by the two-component system ArlRS. *arlR* and *arlS* were upregulated by 1.8 and 1.6-fold, respectively. ArlRS, in response to an unknown extracellular signal, regulates the expression of adhesins, transcriptional regulators and virulence factors through MgrA (Crosby *et al.*, 2020). MgrA has been demonstrated to play a role as a negative regulator of biofilm and autolysis (Ingavale *et al.*, 2005; Jiang, Jin and Sun, 2018). This may explain the upregulation *nuc* and of the virulence factor, alpha toxin (*hla*). However, the results presented here are in contrast to previous studies, in that no upregulation of *RNAIII* (*hld*) was observed. Therefore, rather than acting via *agr*, MgrA may instead bind directly to the *hla* promoter and induce transcription (Ingavale *et al.*, 2005).

The downregulation of surface protein-encoding genes, *sasC, sasG, fnbA, and fnbB* was also seen. FnbA and FnbB are required for *ica*-independent biofilm formation (O'Neill *et al.*, 2008). SasG plays a role in biofilm accumulation (Geoghegan *et al.*, 2010). Taken together, these results suggest that the *C. parapsilosis* secreted factor is altering gene expression in favour of inhibiting biofilm via gene regulators that target matrix component accumulation or production and the downregulation of various surface proteins. Nevertheless, it cannot be dismissed that the fungal CFS may also directly target the biofilm matrix resulting in the phenotype observed.

As reviewed by Eichelberger and Cassat, co-culture of *S. aureus* with *C. albicans* cells resulted in metabolic adaptations of both pathogens (Eichelberger and Cassat, 2021). Metabolic changes in *S. aureus* are evident from the results presented here. The

heatmap constructed (Figure 3.12) and KEGG analysis showed that among the top DEGs, there were genes involved in arginine biosynthesis and the arginine deiminase (ADI) pathway. The genes of this pathway have been shown to play a role in biofilm in *S. aureus* and other species (Zhu *et al.*, 2007; Lindgren *et al.*, 2014; De Backer *et al.*, 2018). The ADI pathway catabolises arginine to ornithine with the byproducts of ammonia, CO_2 and ATP. Arginine is important for providing energy under anoxic conditions via the catabolism of ammonia through the ADI pathway. The ADI pathway is composed of three enzymes (ArcA, ArcB and ArcC) and their genes are part of the *arc* operon (Cunin *et al.*, 1986). ArcR positively controls the expression of the deiminase operon (Makhlin *et al.*, 2007).

Genes of the ADI pathway (*arcA*, *arcB*, *arcD*, *arcC* and *arcR*) and the connected urea cycle (*ureA*, *ureB*, *ureC*) were significantly downregulated during co-culture with *C. parapsilosis* or CFS. The urease genes are repressed by MgrA (Crosby *et al.*, 2020). The *arc* genes have been previously shown to be upregulated during biofilm formation in *S. aureus* (Vlaeminck *et al.*, 2022). ArcD is an arginine-ornithine antiporter, and Zhu *et al.* revealed that deletion of *arcD* resulted in a decrease in intercellular adhesin (PIA) deposition (Zhu *et al.*, 2007). The arginine deiminase, ArcA, has been demonstrated to have a critical role, where its inactivation results in a marked decrease in biofilm (Vlaeminck *et al.*, 2022). Furthermore, ArcA enables biofilm maturation in *S. epidermidis* by regulating pH homeostasis (Lindgren *et al.*, 2014).

Genes of the Kdp K+ uptake system have been linked to pH homeostasis and are upregulated during *S. aureus* biofilm growth (Beenken *et al.*, 2004; Price-Whelan *et al.*, 2013). Yet, *kdpABC* were significantly downregulated under *C. parapsilosis* co-culture. The results presented here suggest that co-culture with *C. parapsilosis* is repressing the *S. aureus* ADI pathway, which alongside the Kdp K+ uptake system is possibly required for full biofilm formation/maturation via the regulation of cell pH homeostasis.

The aim of this chapter was to characterise the effect of co-culture with *C. parapsilosis* on *S. aureus* biofilm formation. Co-culture with *C. parapsilosis* cells or CFS from *C. parapsilosis* results in the visible and significant inhibition of *S. aureus* biofilm on polystyrene and silicone surfaces. It can be concluded from our results that *C. parapsilosis* is secreting a non-bactericidal anti-biofilm factor that may be targeting a component of the *S. aureus* biofilm matrix and/or altering the transcription of genes involved in biofilm formation, cell metabolism and homeostasis resulting in the inhibition of nascent *S. aureus* biofilm. Further work is required to identify the mode of action of the fungal supernatant and identify potential targets within the biofilm matrix.

Chapter 4 – Characterisation of the mechanism of action exhibited by *C. parapsilosis* CFS on *S. aureus* biofilm formation.

4.1. Introduction

Implantable medical devices have revolutionised medical healthcare across the globe. Attachment to these devices by surface-adhering microbes represents a major challenge to treatment, with device-related infections (DRIs) accounting for almost half of all healthcare-associated infections (VanEpps and Younger, 2016). Biofilms formed by *Staphylococci* have long been recognised as the primary contributor to biofilm-associated infection (Otto, 2013). Research that investigates possible targets within the biofilm is vital in developing new strategies to combat biofilm-associated infections.

Due to the resistance of biofilms to antibiotic treatment, alternative therapies are needed. In recent years, there has been a renewed interest in the anti-pathogenic ability of microbial culture supernatants. Probiotic strains of the genus *Lactobacillus* are attractive to researchers for their potentially bactericidal effect (Benmouna *et al.*, 2020; Christensen *et al.*, 2021). Many studies have identified bacterial and fungal culture supernatants (including supernatants from pathogenic species) that inhibit biofilm formation in various species, even some that have not identified the bioactive compound responsible (Iwase *et al.*, 2010; Kim *et al.*, 2020; Alghofaili, 2022). These compounds represent a potentially viable resource for combating biofilm-related diseases. Natural products are also considered more effective with less side-effects than chemically synthesised counterparts (Mishra *et al.*, 2020).

As introduced in the literature review (Chapter 1), the biofilm matrix is essential for the structural integrity of the biofilm. It acts as the 'glue' that holds it all together. Different strains of *S. aureus* can produce different types of matrices, i.e., containing varying amounts of the main constituents; protein, eDNA and carbohydrate (PIA). It is generally accepted that Methicillin-sensitive *S. aureus* (MSSA) produces a PIA-dependent biofilm. While methicillin-resistant *S. aureus* (MRSA) makes a protein and eDNA biofilm (O'Neill *et al.*, 2007). The addition of glucose is the standard method of increasing biofilm formation by *S. aureus in vitro*. However, additions like glucose or salt (NaCl) to the growth media can induce changes in the biofilm matrix produced (Lade *et al.*, 2019).

In Chapter 3, RNA-seq identified many different DEGs (surface attachment proteins, proteases, nucleases, and genes that encode matrix components) that are involved in biofilm formation and biofilm matrix production. Furthermore, treatment with *C. parapsilosis* CFS did not affect primary attachment or growth rate of *S. aureus*. Our hypothesis is that one or more biofilm matrix components may be the target of *C. parapsilosis* CFS. Therefore, the objective of this chapter is to identify the matrix target(s) by utilising different media to influence the types of biofilm matrices produced. Additional *S. aureus* strains are introduced to the study to explore the CFS effect on a different strain background. Gene expression analysis (RNA-seq) in a medium, where no biofilm inhibition was observed, will be carried out. Also explored is the effect of *C. parapsilosis* CFS on preformed biofilm.

4.2. Results

4.2.1. The effect of *C. parapsilosis* CFS depends on the growth medium.

The effect of *C. parapsilosis* CFS, SN1 and SN6, on *S. aureus* biofilm formation in TSB medium supplemented with 1% NaCl (TSB-1N) or 1% glucose (TSB-1G) was tested. SN1 and SN6 (50% v/v) inhibited SA1 biofilm formation in TSB-1N by 58% and 60% respectively ($P < 0.0001$) (Figure 4.1B). Interestingly, SN1 and SN6 (50% v/v) had no effect on SA1 biofilm formation in TSB-1G. The biofilms produced by SA1 in this media appeared denser than those formed in TSB-0.2G (Chapter 3).

The addition of NaCl is widely used in biofilm studies but the variability due to the addition of NaCl has been previously demonstrated (Lade *et al.*, 2019). Indeed, the addition of 1% NaCl to the growth medium resulted in highly variable biofilms between independent experiments (data not shown). It was therefore excluded from further study.

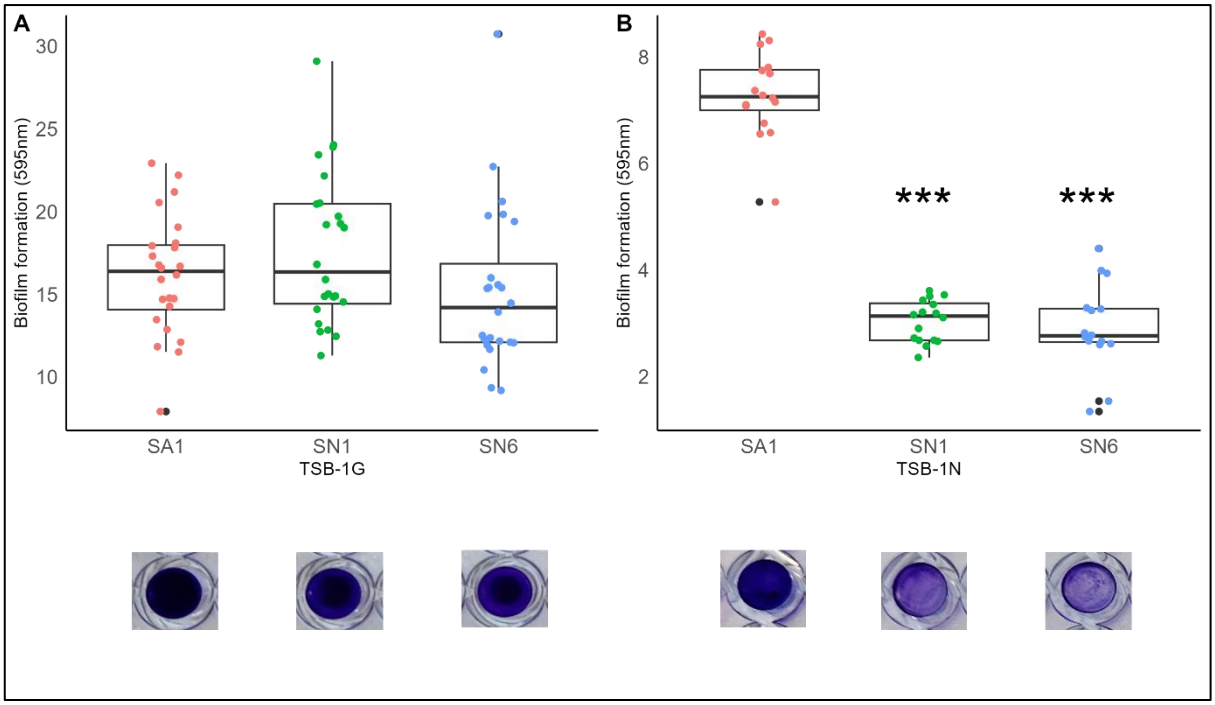

Figure 4.1. The effect on SA1 biofilm inhibition by C. parapsilosis supernatant in different media. *Supernatant (50% v/v) was added at time 0 h to SA1 grown in (A) TSB supplemented with 1% glucose (B) TSB supplemented with 1% NaCl. Representative crystal violet-stained biofilm wells are displayed. The absorbance values are represented by boxplot. The horizontal line bisecting each box represents the median value (50th percentile). The whiskers represent the largest or smallest absorbance values within 1.5 IQR above the 75th percentile or below the 25th percentile respectively. Black dots outside of the whiskers represent outliers. The jitter points represent each single data point. *** indicates a significant result (P < 0.0001).*

4.2.2. Transcriptional response of *S. aureus* to *C. parapsilosis* CFS in TSB-1G media.

In a second RNA-seq experiment, the effect on *S. aureus* during biofilm formation with *C. parapsilosis* CFS, SN1, in TSB-1G media was assessed. Total RNA was collected from *S. aureus* and SN1-treated *S. aureus* biofilms after 24 h of growth.

4.2.2.1. Quality control analysis of TSB-1G condition RNA-seq data

Quality control (QC) was carried out by Novogene (UK) at multiple steps. These included sample preparation QC, library QC, and sequencing data QC. A library data quality summary table was created (Table 4.1).

Table 4.1. Data quality summary (TSB-1G media)

Sample	Effective(%)	Error(%)	Q20	Q30	GC%
SA1.1_G_1	95.09	0.03	97.37	92.55	35.72
SA1.1_G_2	95.35	0.03	97.74	93.30	35.73
SA1.2_G_1	93.66	0.03	97.82	93.48	36.43
SA1.2_G_2	93.27	0.03	97.58	92.90	36.35
SA1.3_G_1	91.44	0.03	97.25	92.30	36.24
SA1.3_G_2	91.71	0.03	97.65	93.10	36.26
SN1.1_G_1	91.89	0.02	98.11	94.24	36.70
SN1.1_G_2	91.72	0.03	96.96	90.64	36.55
SN1.2_G_1	92.43	0.03	97.77	93.37	36.48
SN1.2_G_2	92.13	0.03	97.74	93.33	36.43
SN1.3_G_1	97.92	0.03	97.41	92.41	36.46
SN1.3_G_2	98.03	0.03	97.10	91.59	36.53

Sample: sample name. Effective: (Clean reads/Raw reads)*100%**.** Error: base error rate**.** Q20, Q30: (Base count of Phred value > 20 or 30) / (Total base count). GC: (G & C base count) / (Total base count).

Unlike with the previous RnA-seq experiment described in Chapter 3, the RNA samples here, were split and run on two separate flow cell lanes. This results in two rows per sample in the Table above. Data quality was again checked using FastQC and multiQC as indicated in the methods section 2.15. Reads containing adapter sequences were trimmed (5' Adapter: 5'-AGATCGGAAGAGCGTCGTGTAGGGAAAGAGTGTAGATCTCGGTGGTCGCCGTATCATT-3'.

3'Adapter: 5'-ATCGGAAGAGCACACGTCTGAACTCCAGTCACGGATGACTATCTCGTATGCCGTCTTCTGCTTG-3').

Principal component analysis (PCA) was used to visualise any patterns between the samples (Figure 2.9). 78% of variability is explained by PC1 and PC2. 58% of variability was described along PC1, the x-axis which partially separates the Control and *C. parapsilosis* SN1-treated samples (SN1_G). Therefore, most of the variability can be explained by SN treatment. However, this result does indicate that the SN treatment does not influence gene expression as strongly as the previous experimental condition in Chapter 3.

Figure 4.2 Principal component analysis (PCA) plot representing clustering of RNA-seq sample replicates. *Total RNA was collected from S. aureus (SA1_G) and S. aureus biofilms that were treated with C. parapsilosis CFS (50% v/v) (SN1_G) biofilms grown in TSB 1% glucose.*

4.2.2.2. Significant changes in gene expression in response to *C. parapsilosis* CFS

Genes were considered significantly differentially expressed when log fold change (logFC) of |>1.5| and adjusted $P < 0.05$. In TSB-1G media, only a small number of DEGs were identified compared to the previous RNA-seq experiment. 26 genes were significantly upregulated and 13 were significantly downregulated in the presence of SN1. These results are displayed in a bar plot and as a volcano plot (Figure 4.3A and B).

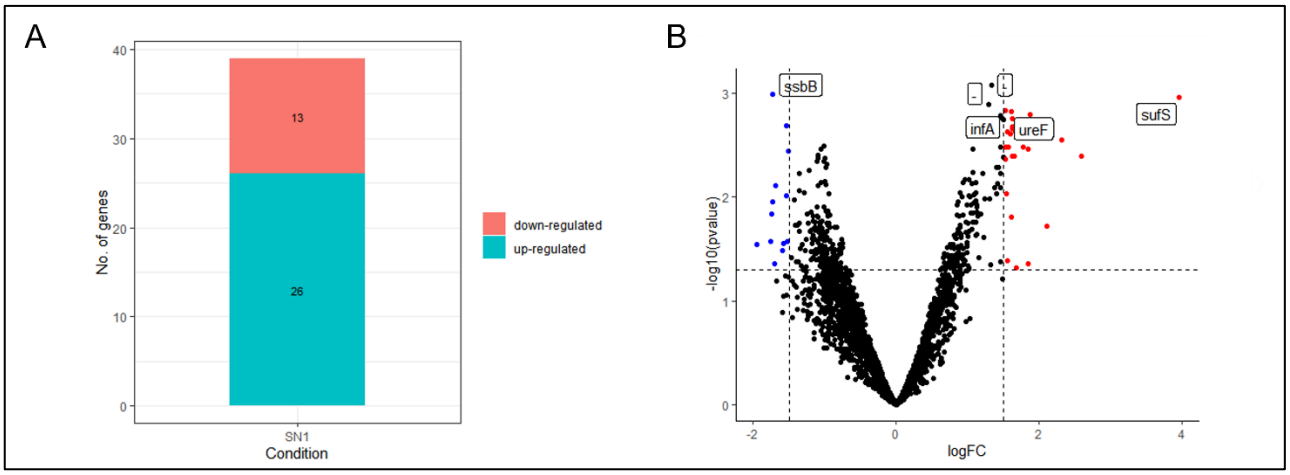

Figure 4.3. ***RNA-sequencing analysis of S. aureus biofilm treated with C. parapsilosis CFS in TSB-1G media.*** *A. The number of genes up- and down-regulated in the SN1 treated condition. B. A volcano plot with the top 6 genes (P value) labelled.*

A heatmap of the topmost DE (differentially expressed) genes sorted by *P*-value across the samples in the TSB-1G experiment was created (Figure 4.4). Clustering of the sample types shows similarity of expression within groups but differences between the sample types. Here samples within the control group (SA1_G) and SN1 group cluster together. However, samples SA1.1_G and SN1.1_G show greater downregulation or upregulation of these genes, respectively, compared to their sample groups. Despite this, they are included in the dataset as their expression profiles, while displaying greater gene expression, are similar to their respective sample group.

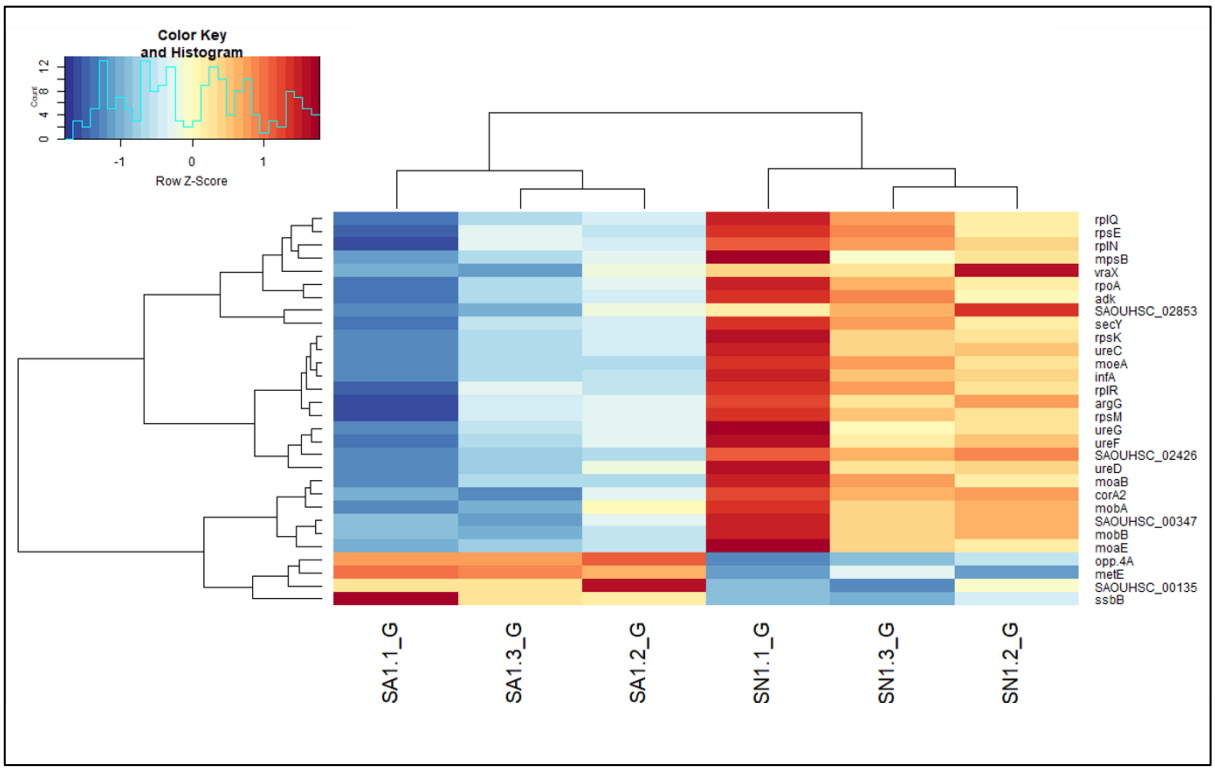

Figure 4.4. Heatmap of the top DE genes across the different conditions in TSB-1G media. *The top 30 differentially expressed (DE) genes sorted by P-value in the S. aureus control (SA1.1_G) and supernatant treated (SN1.1_G) conditions is shown and ranked by P value. Columns represent the samples, while each row represents a different gene. Dendrograms cluster genes by correlation (left) or by sample expression values (top).*

The top twenty genes differentially expressed (|logFC| > 1.5 and $P < 0.05$) in the SN-treated condition in TSB-1G media are shown in Table 4.2. Ten of the genes were hypothetical proteins. Two cysteine proteases are included in the Table. However, within the dataset, three *ssp* genes are significantly upregulated; *sspA*, *sspB* and *sspC* (logFC of 1.5, 1.6, and 1.8, respectively).

ureD and *ureF*, genes of the urease operon were significantly upregulated (logFC 1.6). Genes involved in the arginine biosynthetic pathway *argG* (argininosuccinate synthase)

and *argH* (argininosuccinate lyase) were also significantly upregulated (logFC 1.6 and 1.5, respectively).

Unlike in TSB-0.2G media (Chapter 3), no other annotated biofilm-related genes were differentially expressed. KEGG pathway enrichment analysis was performed using Kobas and only one KEGG term, “sao03010: Ribosome”, was significantly enriched (adjusted *P* value <0.05).

Table 4.2. Top 20 *S. aureus* DEGs (LogFC |> 1.5|, *P* < 0.05) treated with *C. parapsilosis* supernatant in TSB-1G media.

TSB-1G		
Gene Name	Gene Annotation	LogFC
sufS	aminotransferase	3.96
thrB	homoserine kinase	2.59
menB	1,4-dihydroxy-2-naphthoyl-CoA synthase	2.31
SAOUHSC_00661	hypothetical protein	2.11
vraX	hypothetical protein	1.87
sspC	cysteine protease/staphostatin B	1.84
SAOUHSC_02853	hypothetical protein	1.84
mpsB	hypothetical protein	1.78
sspB	cysteine protease/staphopain B	1.68
rplQ	50S ribosomal protein L17	1.67
SAOUHSC_00360	hypothetical protein	-1.95
SAOUHSC_02266	hypothetical protein	-1.76
SAOUHSC_02195	phi PVL orf 3-like protein	-1.74
mepB	hypothetical protein	-1.73
ssbB	bacteriophage L54a single-stranded DNA binding protein	-1.73
SAOUHSC_01296	hypothetical protein	-1.7
opp-4B	oligopeptide ABC transporter permease	-1.68
SAOUHSC_00701	hypothetical protein	-1.59
SAOUHSC_02993	hypothetical protein	-1.58
SAOUHSC_00135	hypothetical protein	-1.53

4.2.3. Altering glucose concentration changes the biofilm matrix composition.

Identifying the composition of the matrix is vital to identify what (if any) matrix component the *C. parapsilosis* supernatant may be targeting. The matrix composition of SA1 biofilm in TSB-0.2G and TSB-1G was determined. Biofilms were grown for 2, 6, 16, and 24 h, after which they were treated with sodium metaperiodate ($NaIO_4$), proteinase K and DNase I to target carbohydrates, protein, and extracellular DNA respectively. The dispersal of biofilm compared to the control gives an indirect measurement of how much protein, carbohydrate and eDNA was present. The percentage (%) dispersal of biofilm post-treatment is displayed (Figure 4.5).

Both biofilm types are abundant in protein. After 24 h of growth, treatment with proteinase K resulted in biofilm dispersal by 94% and 90% in TSB-0.2G and TSB-1G, respectively. The amount of carbohydrate and eDNA increases over time in TSB-0.2G media, while in TSB-1G the inverse is true. Following 24 h of growth in TSB-0.2G, treatment with DNase I and $NaIO_4$ resulted in biofilm dispersal by 60% and 81%, respectively. The same treatment in TSB-1G resulted in biofilm dispersal by 19% and 23%, respectively.

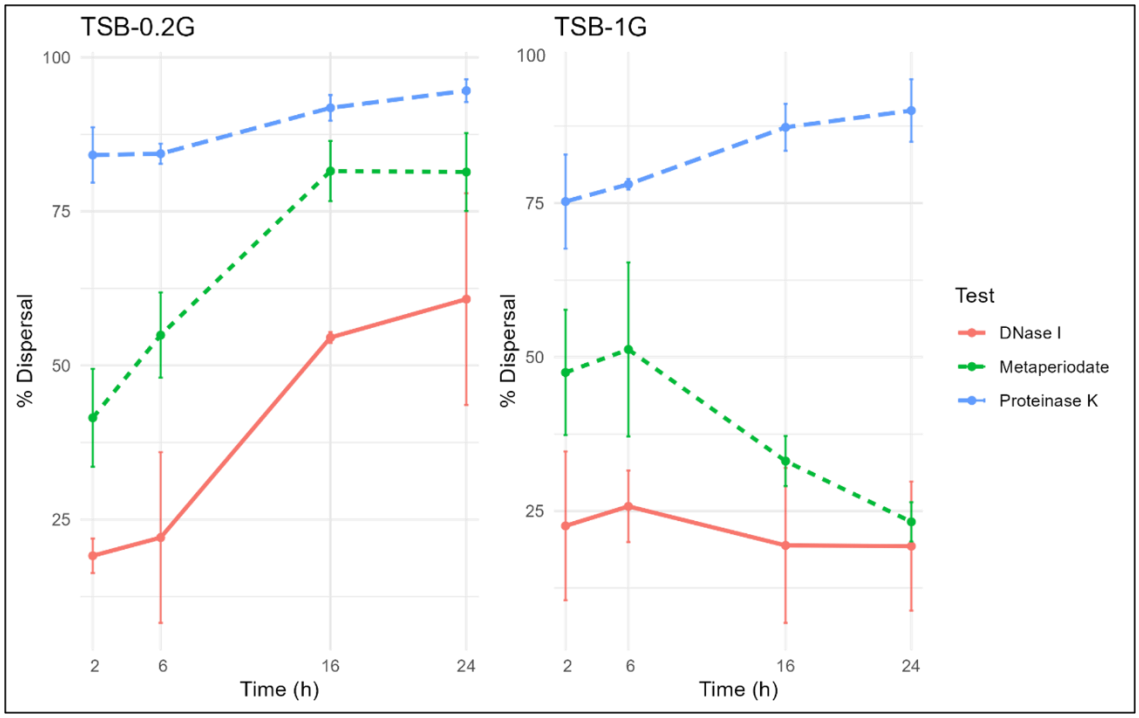

Figure 4.5. The matrix composition of SA1 over time in TSB media supplemented with different concentrations of glucose. *Percentage (%) dispersal in SA1 biofilm over time (h) due to treatment with either DNase I, Sodium metaperiodate (metaperiodate) or proteinase K. TSB-0.2G; TSB supplemented with 0.2% (w/v) glucose. TSB-1G; TSB supplemented with 1% (w/v) glucose.*

4.2.4. *S. aureus* acidification of the extracellular environment during biofilm formation is impacted by *C. parapsilosis* CFS.

To determine if pH played a role in the biofilm inhibition by *C. parapsilosis* CFS, the pH of control and SN treated biofilms was measured at 2, 6 and 24 h. The initial average pH values for TSB-0.2G media, TSB-1G media and SN1 were 7.04, 6.67 and 6.78 respectively. The pH of all biofilm media tested decreased over time (Figure 4.6). This glucose dependent decrease in pH is in agreement with the findings of other research studies (Regassa, Novick and Betley, 1992; Boles and Horswill, 2008; O'Neill *et al.*, 2008).

A lower pH (pH of 4.84) was reached in biofilms grown in a higher concentration of glucose, TSB-1G, and the pH values between the control and SN treated biofilms showed

no difference. Control biofilms grown in TSB-0.2G reached an average pH of 5.04 and the SN treated biofilms in the same media was pH 5.94. This difference was significant $P < 0.01$.

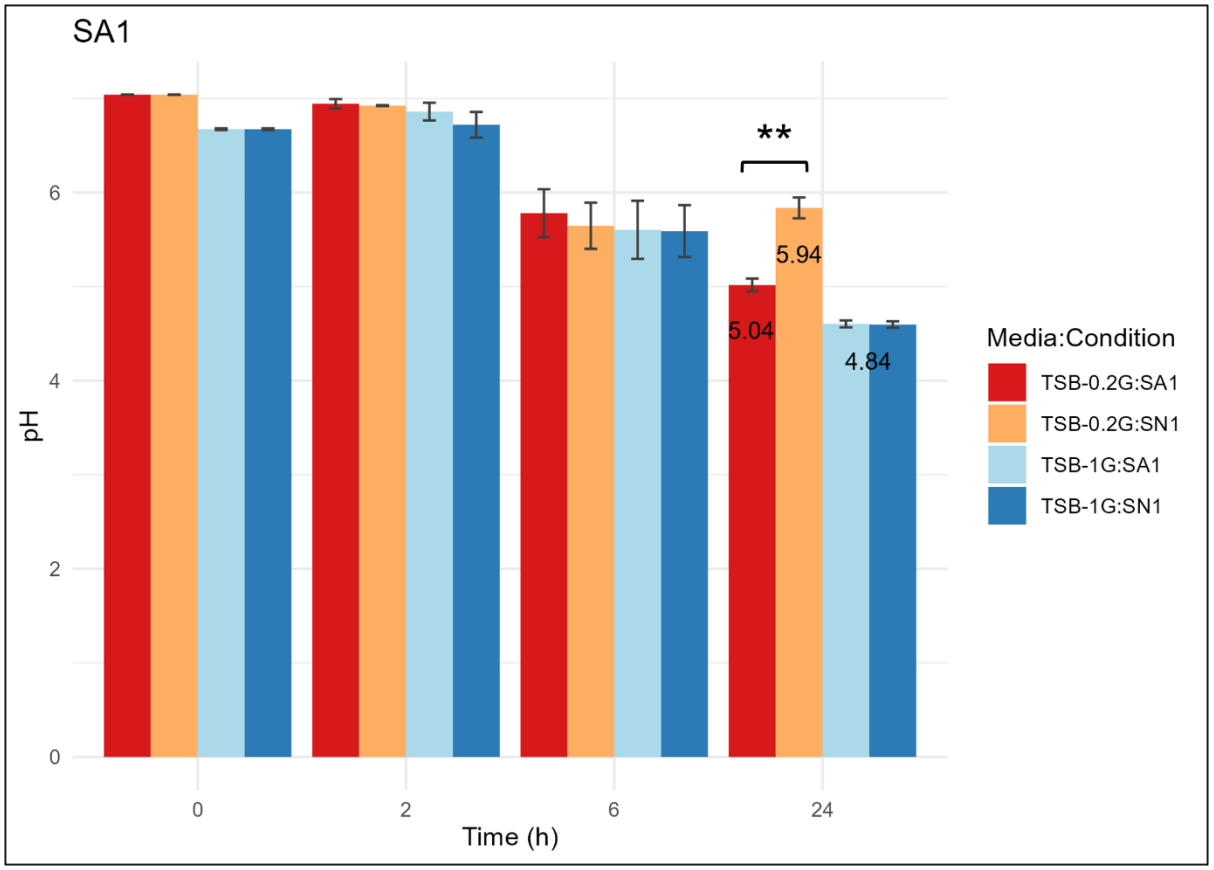

Figure 4.6. Extracellular pH of SA1 biofilm. *The pH of S. aureus biofilm supernatants grown in different concentrations of glucose (0.2% or 1% w/v) with or without C. parapsilosis cell-free supernatant, SN1 (50% v/v), was measured at specific intervals. Error bars show standard deviation. ** represents P < 0.01.*

To investigate the role of pH on biofilm formation further, the pH of *S. aureus* biofilms, both control and CFS-treated, were buffered to pH 6 (Figure 4.7). Following 24 h of growth, the untreated SA1 control produced biofilm at a pH of 6 ± 0.2. *C. parapsilosis* CFS treatment resulted in significant biofilm inhibition. These results demonstrate that

any biofilm inhibition is not solely due to the increase in extracellular pH. However, a role for pH cannot be ruled out altogether.

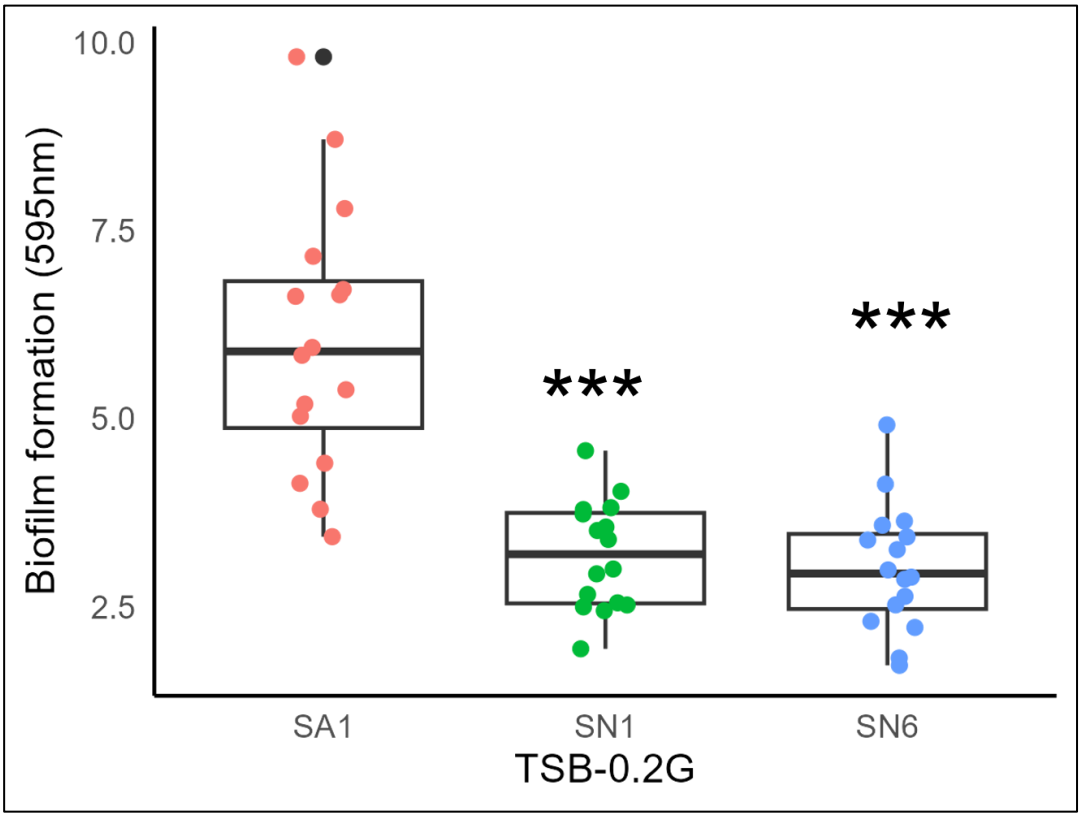

Figure 4.7. SA1 biofilm formation in pH buffered media condition. *SA1 biofilm was grown in TSB-0.2G media and C. parapsilosis CFS, SN1 or SN6 (50% v/v). The biofilm media in each case was buffered to a pH of 6. After 24 h of growth at 37°C the biofilms were stained with crystal violet. The abundance of biofilm is displayed as the absorbance of the crystal violet dye that was bound to the biomass. The jitter points represent each single data point (n=16). This experiment was completed in duplicate, with eight technical replicates in each. *** Indicates P < 0.0001.*

4.2.5. *C. parapsilosis* CFS inhibits the biofilm formation of two other *S. aureus* strains.

The *C. parapsilosis* CFS was tested against two additional *S. aureus* strains. DSM1104 (ATCC 25923 and is also known as Seattle 1945) is a biofilm-forming model strain and is referred to here as SA2. SH1000 is a key model methicillin susceptible *S. aureus* (MSSA) laboratory strain. It is derived from the strain 8325-4 with the *rsbU* gene repaired (Horsburgh *et al.*, 2002). SH1000 is a strong biofilm former (Lamret *et al.*, 2022).

The effect of *C. parapsilosis* CFS on SA2 and SH1000 biofilm formation in TSB-0.2G and TSB-1G was tested (Figure 4.8). The presence of SN1 (50% v/v) inhibited SA2 and SH1000 biofilm formation by 82% and 82% ($P < 0.0001$) in TSB-0.2G, respectively. SN1 had no inhibitory effect on SA2 biofilm in TSB-1G media. In fact, an increase in biofilm can be seen in TSB-1% glucose upon treatment with SN. This may be due to biofilm instability during the washing steps. Increasing the number of replicates may reduce the difference between the control and the test wells.

Interestingly, SN1 inhibited SH1000 biofilm in TSB-1G media by 30% ($P < 0.0001$). SA2 displayed similar results to SA1, while SH1000 biofilm was inhibited in TSB-1G media. Therefore, we chose to continue further work using SA1 and SH1000.

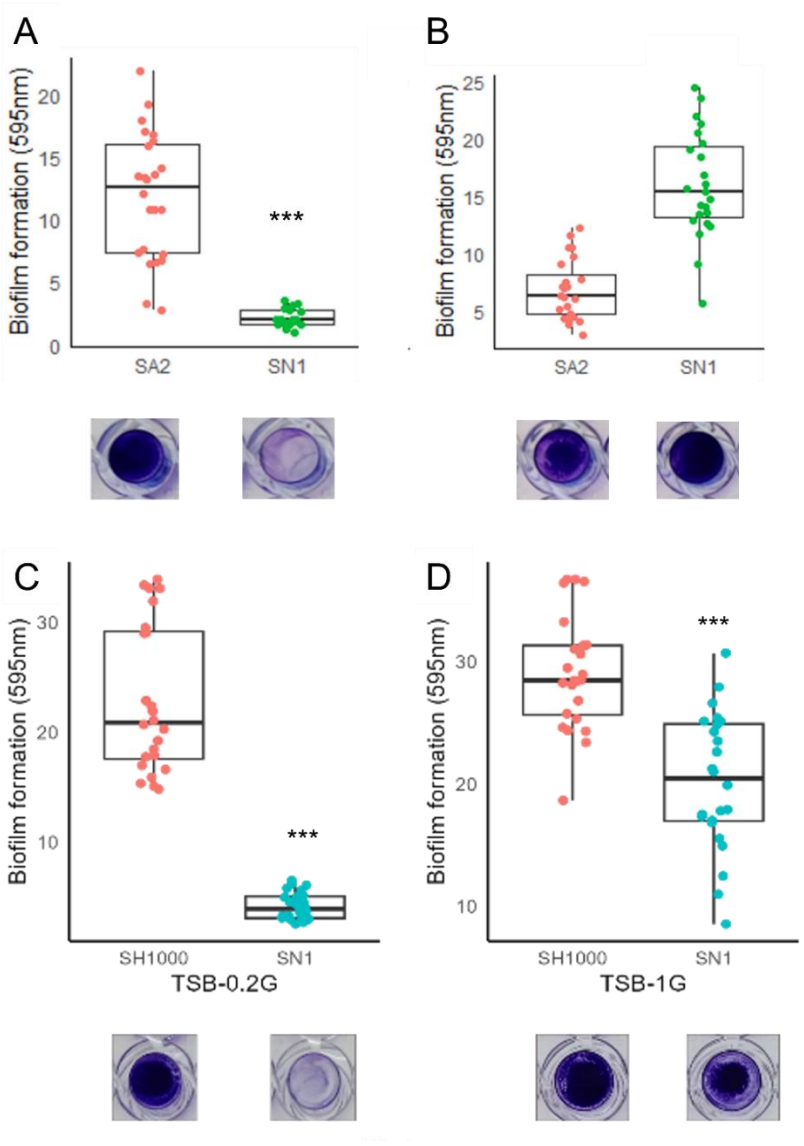

Figure 4.8. SA2 and SH1000 biofilm inhibition by C. parapsilosis CFS. *A) and C) Inhibition of SA2 and SH1000 biofilms grown in TSB media supplemented with 0.2% glucose by C. parapsilosis cell-free supernatant, SN1 (50% (v/v). B) and D) inhibition of SA2 and SH1000 biofilms grown in TSB media supplemented with 1% glucose. The biofilms were stained with crystal violet and the abundance of biofilm is displayed as the absorbance of the crystal violet dye that was bound to the biomass. The boxes represent the interquartile range (IQR). The centre line in each box represents the median (50th percentile). The whiskers represent the largest or smallest absorbance values within 1.5 IQR above the 75th percentile or below the 25th percentile respectively. The jitter points represent each single data point (n=24). *** Indicates P < 0.0001.*

4.2.6 Glucose levels alter the biofilm matrix of SH1000.

The SH1000 biofilm matrix composition was investigated (Figure 4.9). In TSB-0.2G media, initial levels of PIA, eDNA and protein are similar, however by 24 h, protein and eDNA are the important matrix components. Meanwhile, the levels of PIA decrease over time. In TSB-1G, from 2 h the SH1000 biofilm matrix was a complex environment abundant in all three of the major components. Despite some fluctuation over time in the levels of eDNA and PIA, all three constituents remained high. This resulted in a strong, dense, and stable biofilm.

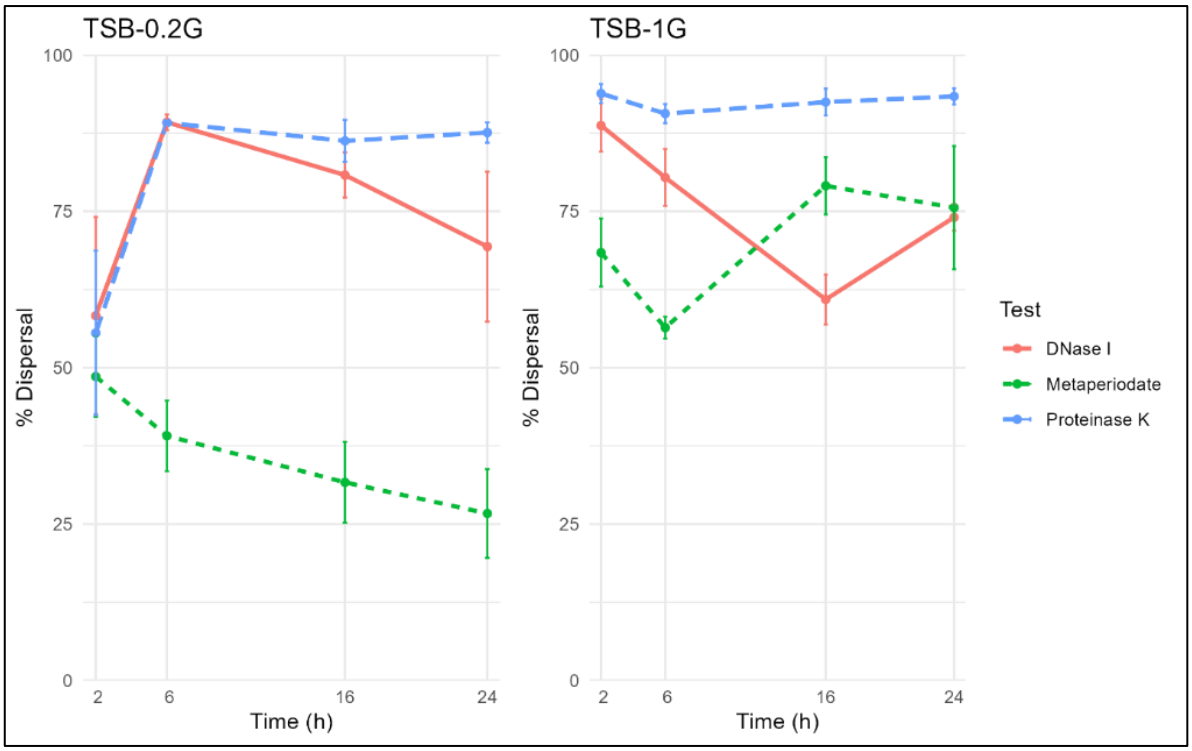

Figure 4.9. SH1000 biofilm matrix composition over time. *Percentage (%) dispersal in SH1000 biofilm over time (h) due to treatment with either DNase I, Sodium metaperiodate (metaperiodate) or proteinase K. TSB-0.2G; TSB supplemented with 0.2% (w/v) glucose. TSB-1G; TSB supplemented with 1% (w/v) glucose.*

4.2.7 CFS modulates the extracellular media pH during SH1000 biofilm formation.

The pH of SH1000 biofilm supernatant was tested over time (Figure 4.10). These results mirrored what was observed in SA1. In TSB-0.2G, SN1 buffered the biofilm environment to a pH of 6.07 while the control pH was 5.2. A more acidic pH was reached in TSB-1G media and there was no effect on extracellular pH exhibited by SN1. The pH values for the control and SN1-treated biofilms 4.7 and 4.68 respectively.

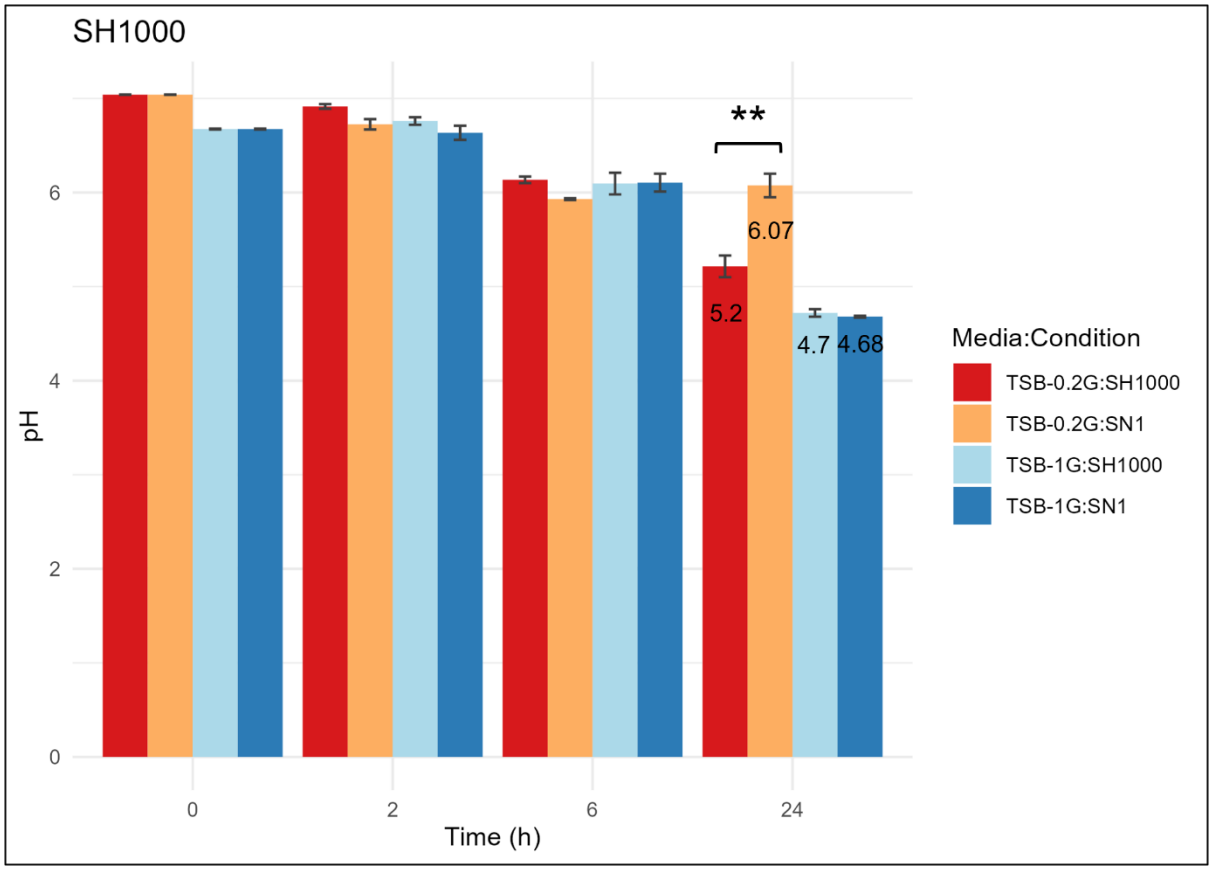

Figure 4.10. Extracellular pH of SH1000 biofilm. *The pH of S. aureus SH1000 biofilm supernatants grown in TSB media supplemented with different concentrations of glucose (0.2% or 1% w/v) with or without C. parapsilosis cell-free supernatant, SN1 (50% v/v). The pH was measured at the indicated times. Error bars show standard deviation. ** represents P < 0.01.*

4.2.8. Protease activity within the biofilm is increased by *C. parapsilosis* CFS treatment.

Results presented in the previous chapter, Chapter 3, showed that there was a significant up-regulation of extracellular proteases in SA1 SN1 treated biofilm cells (Table 3.2 and 3.3). SA1 and SH1000 control and SN1-treated biofilms were grown in TSB-0.2G and TSB-1G. Samples of the biofilm supernatant were taken at 6 h and 24 h and added to wells (5 mm in diameter) in 2% skim milk agar. Skim milk agar can be used to assess protease activity. Zones of clearing or proteolysis indicate protease activity as the opaque casein protein in the skim milk is degraded.

Following incubation, zones of proteolysis were observed around SA1 samples but not for SH1000 (Table 4.3). For SA1, SN1-treated biofilms in TSB-0.2G resulted in slightly larger, but significant ($P < 0.05$) zones of proteolysis and this could be indicative of increased protease activity. Interestingly, SA1 SN1-treated biofilms grown in TSB-1G also showed a significantly larger zone of clearing. The overall levels of protease activity seem to decrease from 6 h to 24 h in this media. Images of the skim milk agar plates are presented in Appendix Figure A1.

Table 4.3. Protease activity of biofilm supernatants on skim milk agar.

Diameter of proteolysis zones are displayed in millimetre (mm).

Diameter of well = 5 mm.

Time (h)	Test	TSB-0.2G		TSB-1G	
		SA1	SH1000	SA1	SH1000
6	Control	11	<6	14	<6
	SN1-treated	14*	<6	14.6	<6
24	Control	14.6	<6	10	<6
	SN1-treated	17.2*	<6	12.6*	<6

* Indicates significance at $P < 0.05$, comparing SN1-treated to control at the same timepoint

TSB-0.2G: TSB supplemented with 0.2% (w/v) glucose; TSB-1G: TSB supplemented with 1% (w/v) glucose. SN1: *C. parapsilosis* CFS 50% (v/v).

4.2.9. DNase activity is increased by *C. parapsilosis* CFS treatment.

S. aureus produces a heat stable DNase enzyme, thermonuclease, encoded by the *nuc* gene. In Chapter 3, *nuc* expression was highly upregulated during biofilm formation in the presence of SN1 (Table 3.2). The DNase activity of biofilm supernatant was assessed for SA1 and SH1000 SN1 treated biofilm using DNase agar. Samples of biofilm supernatants were taken at 6 h and 24 h and added to wells (5 mm in diameter) in DNase agar. Zones of clearing were observed and indicate DNase activity. A significant increase in DNase activity was seen in SA1 at 24 h in both media tested ($P < 0.05$) (Table 4.4). However, the zones of clearing around the SA1 control in TSB-1G at 24 h are smaller than the zones observed from 6 h biofilm supernatant samples ($P < 0.01$). This would

suggest that nuclease activity decreased over time. No significant increase in DNase activity was observed in SH1000 at either timepoint. Images of the DNase agar plates are presented in Appendix Figure A2.

Table 4.4. DNase activity of biofilm supernatants on DNase agar.

Diameter of clearing zones are displayed in millimetre (mm).

Time (h)	Test	TSB-0.2G		TSB-1G	
		SA1	SH1000	SA1	SH1000
6	Control	18.8	10.4	19	11
	SN1-treated	20	10	19	11
24	Control	18.6	10.6	15.8	11
	SN1-treated	21	11.2	18	11

* Indicates significance at $P < 0.05$. ** indicates significance at $P < 0.001$, comparing SN1-treated to control at the same timepoint

TSB-0.2G: TSB supplemented with 0.2% (w/v) glucose; TSB-1G: TSB supplemented with 1% (w/v) glucose. SN1: *C. parapsilosis* CFS 50% (v/v).

4.2.10. *C. parapsilosis* CFS prevents *S. aureus* aggregation.

Aggregation is an important initial step in biofilm formation (Trunk *et al.*, 2018). Different factors contribute to aggregation in *S. aureus*, such as pH, net surface charge and the amount of carbohydrates, eDNA and proteins. The common matrix components carbohydrate, eDNA and protein acts as agglutinins (Trunk *et al.*, 2018). eDNA has been shown to enhance adhesion and surface aggregation (Das *et al.*, 2010). A visual tube assay was used to observe the aggregation of the bacterial cells (Figure 4.11). SA1 or SH1000 was incubated overnight in TSB-0.2G or TSB-1G with/without *C. parapsilosis* SN1 (50% v/v).

In TSB-0.2G, untreated SA1 cells quickly aggregated and settled to the bottom of the tube. Whereas CFS-treated SA1 cells (SN1) remained in suspension (Figure 4.11A). However, the DNase I treated control also resulted in cell aggregation. In TSB-1G, the CFS had no effect on SA1 aggregation, and the bacterial cells quickly settled (Figure 4.11B). This suggests that the mechanism by which SN prevents aggregation may not involve eDNA or that eDNA is not required for aggregation under these conditions.

All three tubes containing SH1000 failed to aggregate within the 30-minute timeframe of this assay, regardless of growth medium or presence of SN1 (Figure 4.11C and D). The cells across all treatments did eventually settle after >3 h (data not shown).

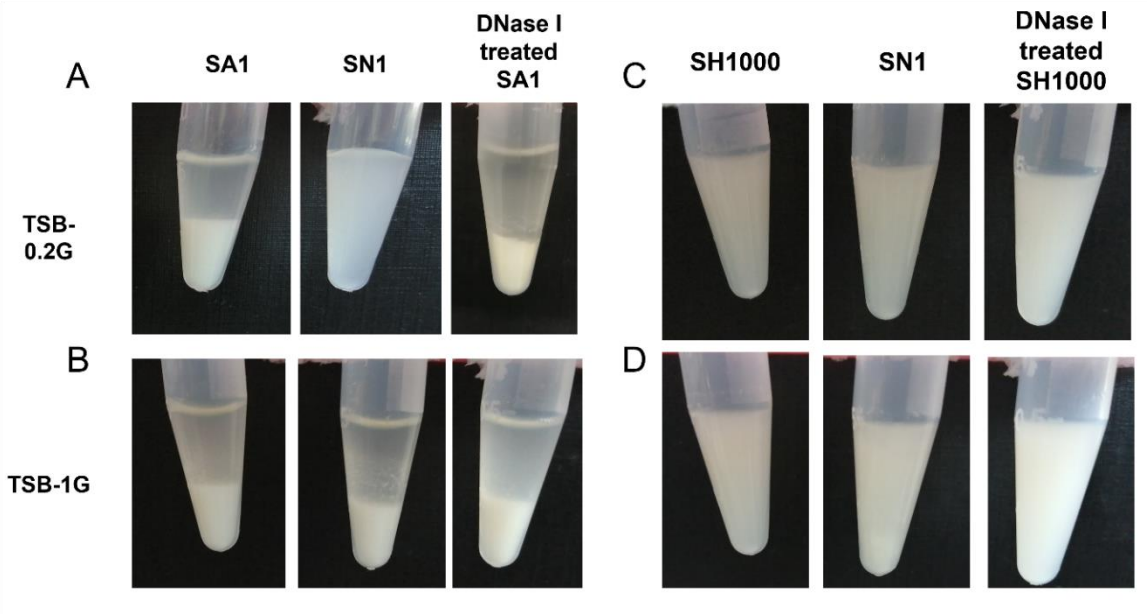

Figure 4.11. The aggregation of S. aureus cells in the presence or absence of C. parapsilosis cell-free supernatant. *S. aureus was grown overnight under biofilm conditions with/without C. parapsilosis supernatant SN1 (50% v/v). The biofilms were scraped, and the cells resuspended in phosphate buffered saline. Where indicated, DNase I was added to the tube and incubated for 10 min prior to resuspension. The biofilm cells were transferred to a tube and allowed to stand. Images were taken after 30 min.*

4.2.11. *C. parapsilosis* CFS reduces sub-inhibitory oxacillin induced SA1 biofilm formation.

The biofilm matrix plays a vital role in the integrity of the biofilm. Biofilms are notoriously recalcitrant to antibiotic therapy. Disrupting the matrix can be an effective strategy to enhance antibiotic treatment of biofilms (Baelo *et al.*, 2015). The hypothesis of whether CFS-treated *S. aureus* biofilms would be more susceptible to antibiotics was investigated using SA1 only (Figure 4.12). The MIC of oxacillin (a beta-lactam antibiotic) against SA1 planktonic cells in TSB-0.2G media was 0.25 µg/mL. This indicates that SA1 is sensitive to oxacillin.

The MBIC (minimum biofilm inhibition concentration) which is defined as the minimum concentration of antibiotic required to inhibit the formation of biofilm was also assessed (Figure 4.12). In TSB-0.2G, the $MBIC_{90}$ was 0.25 ug/mL and the $MBIC_{50}$ was 0.06 ug/mL for both SN1-treated and untreated biofilms ($P < 0.05$). Surprisingly, the *C. parapsilosis* CFS did not seem to have any effect on the antibiotic tolerance of SA1 during biofilm formation.

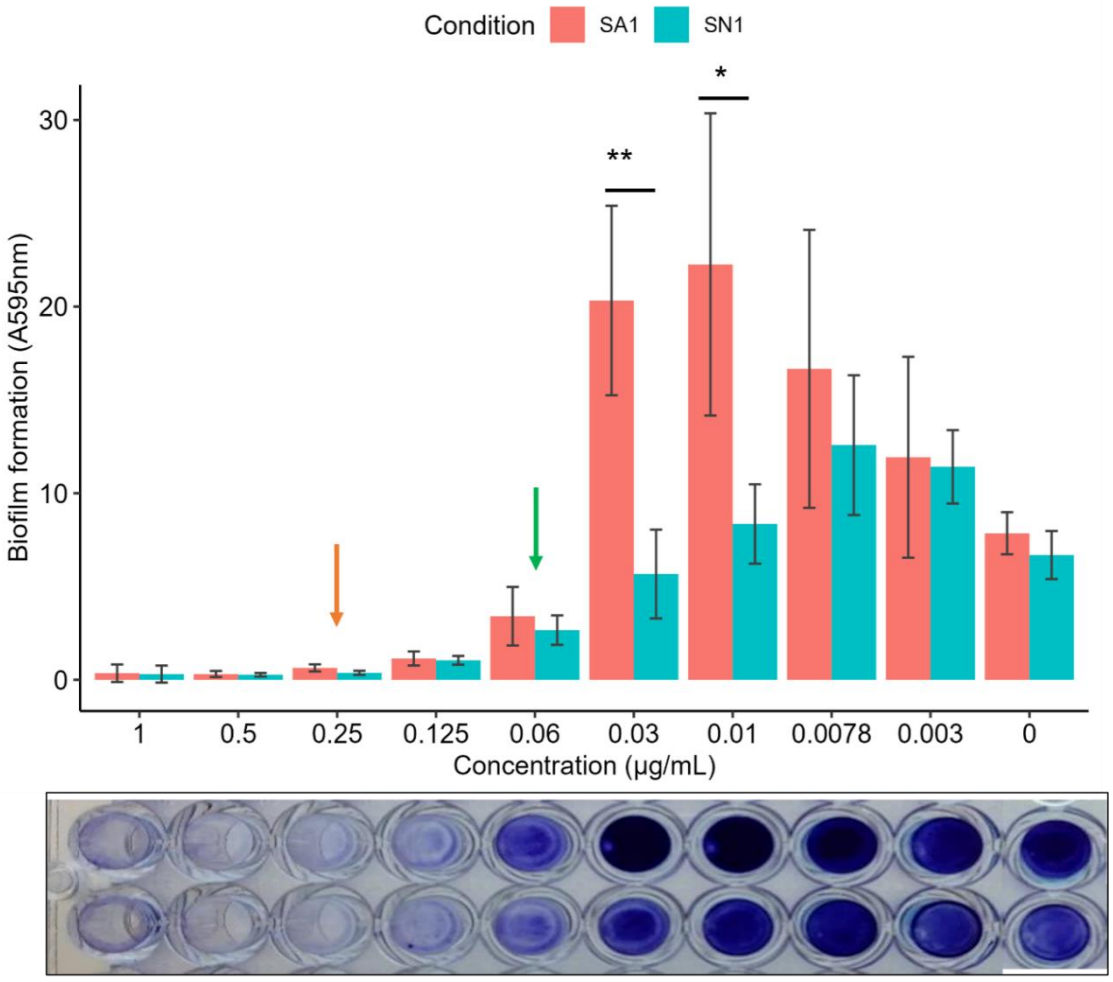

Figure 4.12. Biofilm susceptibility testing. *The MBIC of oxacillin was determined against SA1 biofilm and SA1 biofilm grown in the presence of C. parapsilosis supernatant, SN1 (50% v/v). The crystal violet absorbance is shown as a bar plot, and a representative image of the stained assay is also shown. The $MBIC_{90}$ and $MBIC_{50}$ are marked by an orange or green arrow, respectively. Error bars ± SD (n=4). * Indicates a significance P < 0.05, ** indicates a significance P < 0.01.*

Interestingly, at lower sub-inhibitory concentrations of oxacillin, SA1 biofilm formation was increased compared to the untreated antibiotic control. SA1 biofilm was significantly increased at oxacillin concentrations between 0.03 μg/mL and 0.01 μg/mL ($P < 0.05$) (Figure 4.12). No significant increase was seen at these concentrations in antibiotic treated SA1 biofilms grown in the presence of SN1. The SN1 treated biofilm had significantly lower biomass at oxacillin concentrations of 0.03 μg/mL and 0.01 μg/mL ($P < 0.01$ and $P < 0.05$, respectively) when compared to antibiotic treatment alone. Sub-inhibitory levels of beta-lactam antibiotics have been previously shown to induce biofilm formation in *S. aureus* and that this induction relies on the presence of eDNA (Kaplan *et al.*, 2012). These results may suggest that *C. parapsilosis* CFS is inhibiting the eDNA-dependent increase in biofilm.

4.2.12. *C. parapsilosis* CFS can detach preformed *S. aureus* biofilm.

4.2.12.1 CFS effect on SA1 preformed biofilm

The effect of SN1 and SN6 on preformed/mature biofilm was assessed and the results are displayed in Figure 4.13. SN1 and SN6 (50% v/v) were added to SA1 biofilm grown in TSB-0.2G media for 24 h. SN1 and SN6 dispersed the mature biofilm resulting in a significant decrease of 35% and 22% respectively ($P < 0.0001$ and <0.01 respectively) (Figure 4.13A). SN1 and SN6 (50% v/v) had no effect on SA1 biofilm grown in TSB-1G (Figure 4.13B).

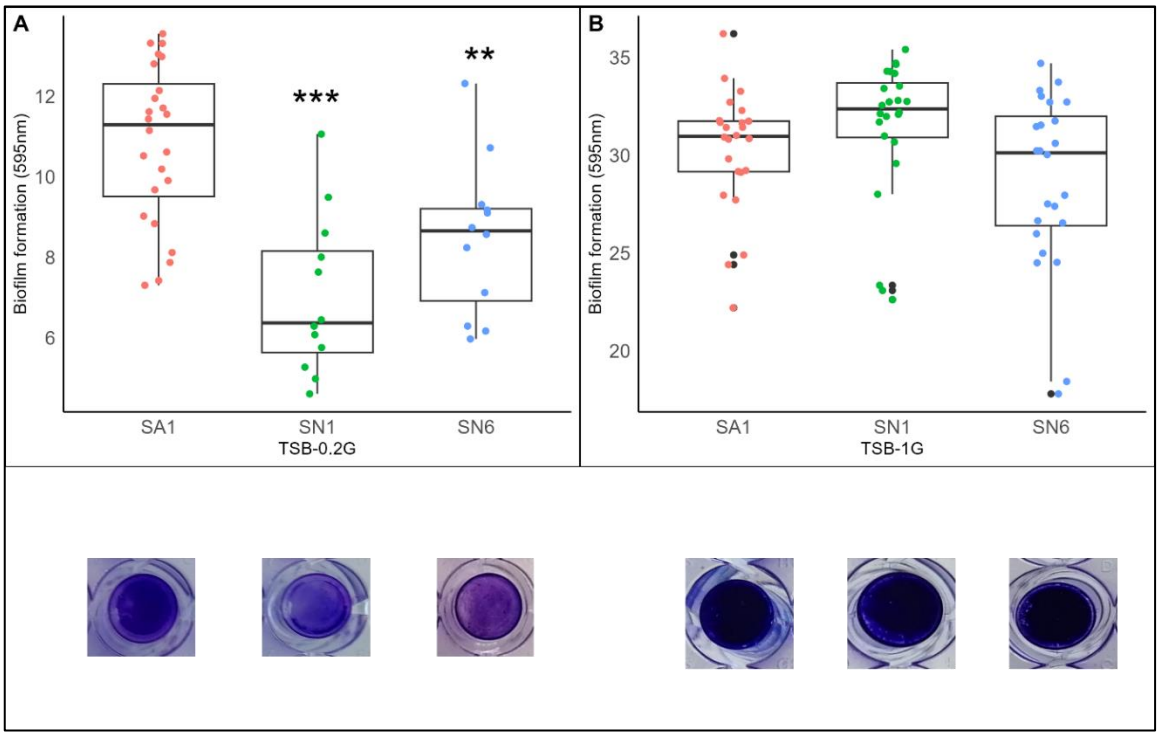

Figure 4.13. C. parapsilosis supernatant tested against SA1 preformed (24 h) biofilm. *The absorbance data displayed as a boxplot of SA1 grown in TSB supplemented with (A) 0.2% glucose and (B) 1% glucose. Representative crystal violet-stained biofilm wells are displayed. The horizontal line bisecting each box represents the median value (50th percentile). The whiskers represent the largest or smallest absorbance values within 1.5 IQR above the 75th percentile or below the 25th percentile respectively. Black dots outside of the whiskers represent outliers. The jitter points represent each single data point. ** indicates a significant result (P < 0.01). *** indicates a significant result (P < 0.0001).*

4.2.12.2 CFS effect on SA1 preformed biofilm is dose dependent.

Decreasing concentrations of CFS were tested against preformed SA1 biofilm (Figure 4.14). Similar to the results seen for biofilm inhibition, the effect of the CFS on preformed biofilm was dose-dependent (Figure 4.14). SN1 significantly dispersed SA1 biofilm at concentrations between 100% - 3.125% (v/v) (Figure 4.14A). SN6 significantly dispersed biofim at concetrations between 100% and 12.5% (v/v) (Figure 4.14B). SN1

and SN6 were tested at different times. There was a difference in *S. aureus* growth between these experiments, however, the biofilm dispersal trend (a reduction in overal biofilm upon treatment) was observed in both cases.

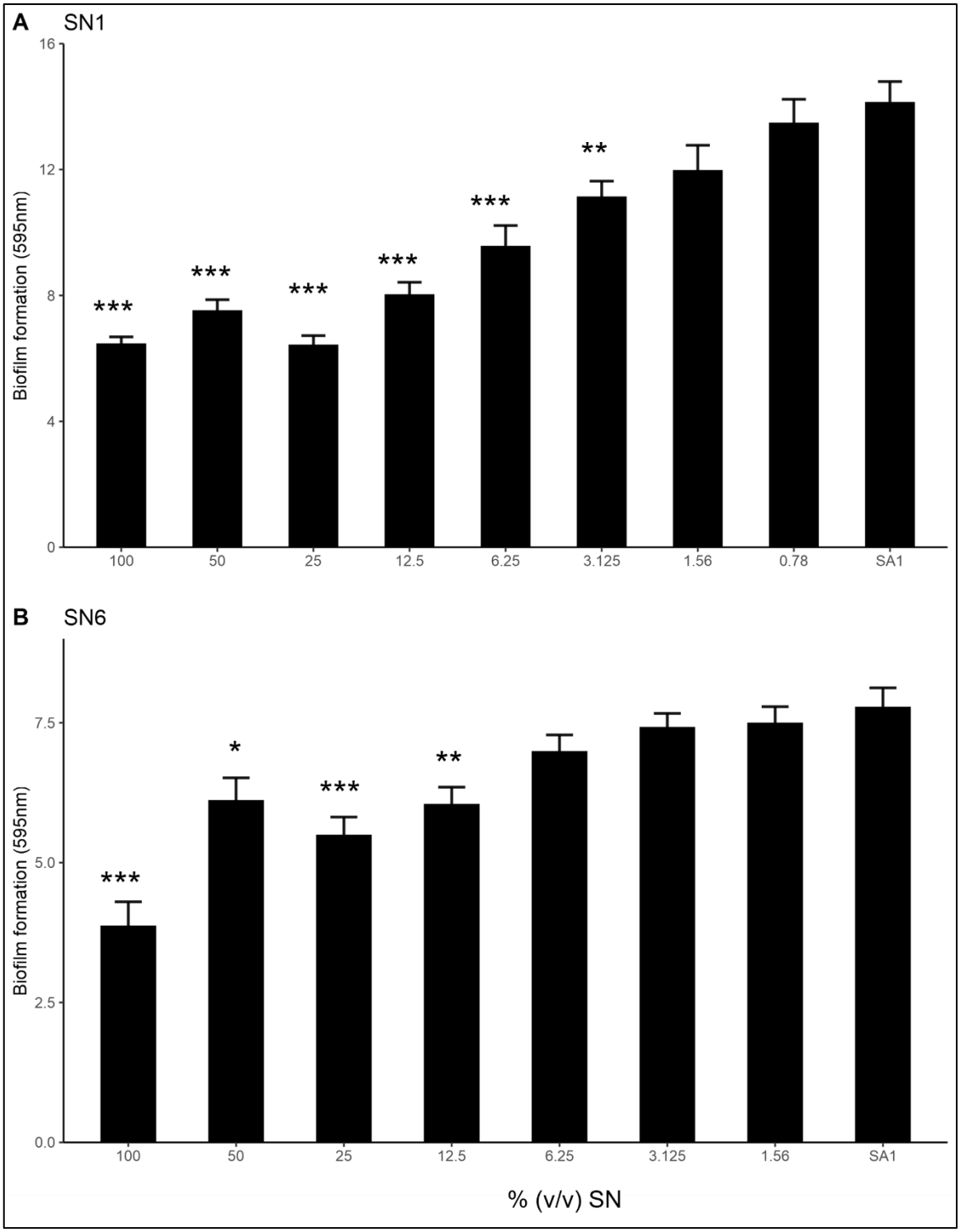

Figure 4.14. Decreasing concentrations of C. parapsilosis CFS were tested against preformed (24 h old) S. aureus biofilm. *The bar columns represent the mean absorbance values of crystal violet-stained biofilms. Error bars represent ± SE.* P < 0.01, ** P < 0.001, *** P < 0.0001 indicates a significant result compared to the SA1 control.*

4.2.12.3 Altering glucose concentration effects dispersal of SA1 biofilm.

Interestingly, the addition of 100% (v/v) *C. parapsilosis* CFS, SN1 and SN6, were able to detach preformed biofilm grown in TSB-1G media by 42% and 33%, respectively (Figure 4.15). The CFS is collected from *C. parapsilosis* grown in TSB-0.2G media. To control for this, TSB-0.2G media was added to the SA1 control for the subsequent 24 h of growth. This suggests that a lower concentration of glucose restores the ability of *C. parapsilosis* CFS to inhibit SA1 biofilm, regardless of the type of matrix already established.

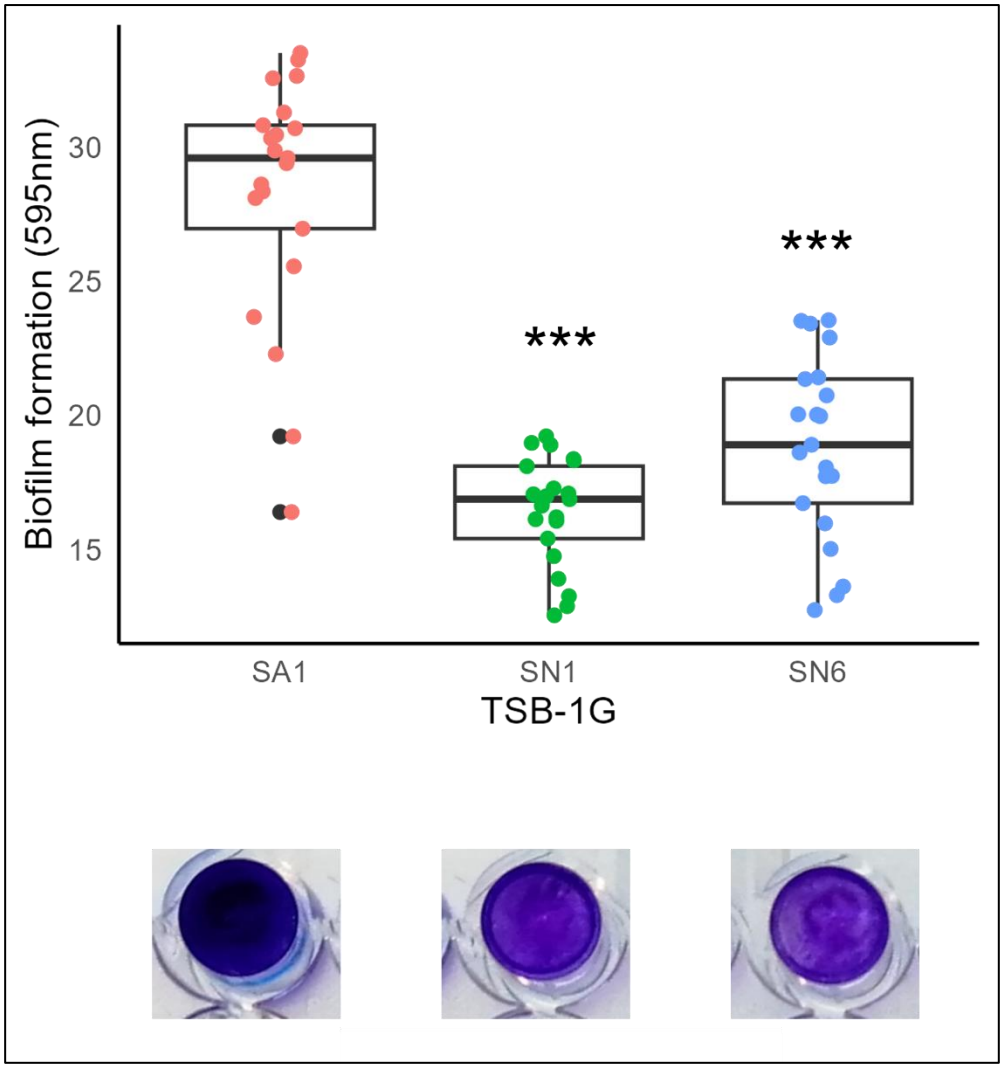

Figure 4.15. 100% (v/v) CFS concentration can detach preformed biofilm grown in TSB-1G. *SA1 biofilm was grown in TSB-1G media for 24 h. Then, 100% (v/v) SN1 or SN6 was added. Representative crystal violet-stained wells are shown. The horizontal line bisecting each box represents the median value (50th percentile). Black dots outside of the whiskers represent outliers. The jitter points represent each single data point. *** indicates a significant result (P < 0.0001) compared to the SA1 control.*

4.2.12.4. CFS effect on SH1000 preformed biofilm

The biofilm dispersal effect on preformed SH1000 biofilms was also investigated (Figure 4.16). Comparable to the results seen with SA1, a decrease of SH1000 biofilm by SN1

was observed in TSB-0.2G (65%, *P* <0.0001). No decrease in biofilm due to *C. parapsilosis* CFS was observed in TSB-1G.

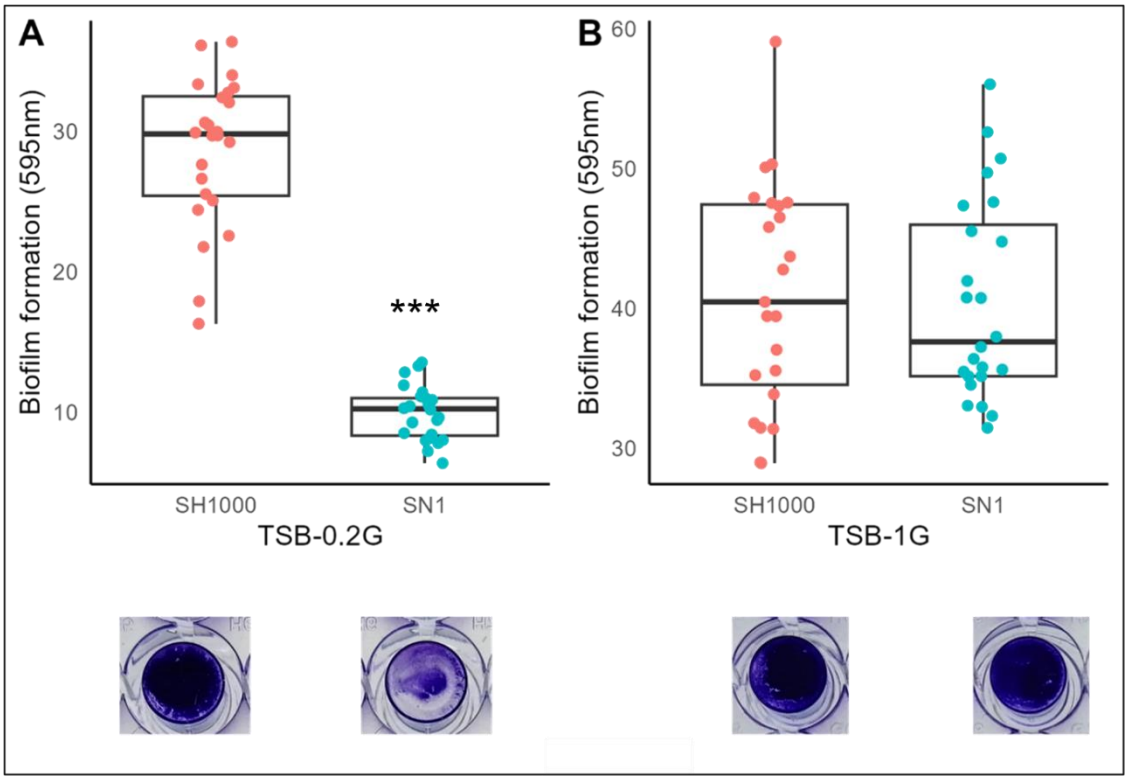

Figure 4.16. SH1000 preformed biofilm dispersal by C. parapsilosis CFS. *(A)Preformed SH1000 biofilms grown in TSB media supplemented with 0.2% glucose (TSB-0.2G). (B) Preformed SH1000 biofilms grown in TSB media supplemented with 1% glucose (TSB-1G). Representative crystal violet-stained wells are shown. The horizontal line bisecting each box represents the median value (50th percentile). The whiskers represent the largest or smallest absorbance values within 1.5 IQR above the 75th percentile or below the 25th percentile respectively. Black dots outside of the whiskers represent outliers. The jitter points represent each single data point. *** indicates a significant result (P < 0.0001).*

4.3. Discussion

A biofilm is a complex and dynamic community. Biofilms studied *in vitro* are influenced heavily by changes in media, surface type, and strain (Hancock, Witsø and Klemm, 2011; Wijesinghe *et al.*, 2019). In this chapter, the ability of *C. parapsilosis* CFS to prevent *S. aureus* biofilm formation (inhibitory effect) and its ability to disperse preformed biofilm (dispersal effect) was investigated using different bacterial strains and different media.

The inhibitory effect of *C. parapsilosis* CFS on *S. aureus* biofilm formation was media dependent. It has been reported that *S. aureus* produces biofilm through two different mechanisms: A polysaccharide-dependent biofilm, where the presence of PIA is needed for the biofilm to form and an extracellular (eDNA) and protein biofilm, where eDNA and protein (not polysaccharide) form the main constituents of the biofilm matrix (Cramton *et al.*, 1999; Fitzpatrick, Humphreys and O'Gara, 2005; O'Neill *et al.*, 2008). Furthermore, MSSA isolates were more often observed to produce polysaccharide biofilms (O'Neill *et al.*, 2007). A recent study suggests that it is not so straightforward. Mlynek *et al.* have shown that eDNA interacts with polysaccharide in the extracellular matrix (Mlynek *et al.*, 2020). Results presented here agree with Mlynek *et al*., as the *S. aureus* strains used in this study produced biofilms with a matrix containing varying amounts of all three major components, protein, PIA (poly intercellular adhesin), and eDNA.

SA1 biofilm formation was inhibited by *C. parapsilosis* CFS by approx. 50% when grown in TSB media supplemented with 0.2% glucose (Chapter 3, Figure 3.4 and Table 4.5). This inhibitory effect was lost when SA1 was grown in TSB media supplemented with 1% glucose (Figure 4.1 and Table 4.5). Similar to SA1, biofilm formation by SH1000 was inhibited by 75% in TSB supplemented with 0.2% glucose. However, unlike the effect in SA1, the *C. parapsilosis* CFS could inhibit SH1000 biofilm formation (inhibition of 30%) when the glucose concentration was increased to 1% (Table 4.5).

Table 4.5. Inhibition of biofilm in different media and the relative abundances (% biomass) of three main biofilm matrix components at 24 h.

	0.2% glucose		1% glucose	
	SA1	**SH1000**	**SA1**	**SH1000**
% inhibition of biofilm	50	75	0	30
% eDNA levels at 24h	60	67	19	74
% PIA levels at 24 h	81	26	23	75
% Protein levels at 24 h	94	87	90	93

The matrix of SA1 in TSB-0.2G media contains high levels of eDNA and PIA, while in TSB-1G media the level of both is lower compared to biofilm formed in TSB-0.2G media (Figure 4.5 and Table 4.5). Protein is the most abundant matrix component of this strain. In SH1000, levels of PIA are low in TSB-0.2G media while eDNA and protein are abundant (Figure 4.9 and Table 4.5). From an early timepoint, SH1000 biofilm matrix in TSB-1G is complex with all three major constituents abundant across the 24 h tested. In agreement with our results, SH1000 has previously been reported to produce PIA-independent biofilms in TSB-0.2G media (Boles and Horswill, 2008). These data indicate that eDNA may be a target of the fungal CFS as there is only a visible inhibitory effect when the levels of eDNA are high in the biofilm matrix.

With an increased concentration of glucose (1%), no biofilm inhibition was observed in SA1 upon treatment with *C. parapsilosis* CFS (Figure 4.1). Investigation of the transcriptome in TSB-1G media of *S. aureus* and SN1-treated biofilms revealed 39 DEGs. Few genes with biofilm related function were identified. Serine (*sspA*) and cysteine proteases (*sspB* and *sspC*) were upregulated by logFC of 1.5, 1.6, and 1.8, respectively. A possible role for these in biofilm formation is biofilm remodelling (O'Neill *et al.*, 2008). *ureD*, *ureF*, *argG*, and *argH* genes were also upregulated. *argG* and *argH* encode proteins (argininosuccinate synthase and argininosuccinate lyase, respectively) that are part of the arginine biosynthetic pathway. Interestingly, *argG* was also upregulated in TSB-0.2G media CFS-treated condition (Chapter 3, Figure 3.11). *ureD* and *ureF* genes

form part of the urease operon and encode urease accessory proteins. Urease is crucial for pH homeostasis under acidic conditions (Zhou *et al.*, 2019; Zhou and Fey, 2020). Overall, when compared to the RNA-seq experiment conducted in TSB-0.2G media (Chapter 3), the relatively small number of bacterial genes impacted by *C. parapsilosis* CFS when grown in TSB-1G may indicate that the biofilm inhibition seen in TSB-0.2G media is in response to global changes in expression.

The presence of glucose mediates the acidification of the biofilm culture. Increasing the concentration of glucose from 0.2% (14 mM) to 1% (55 mM) resulted in greater acidification of the media by *S. aureus* (Figure 4.4 and 4.7). Interestingly, a media dependent effect arose whereby *C. parapsilosis* CFS buffered the biofilm media to a higher pH but only at the lower concentration of glucose. The Agr quorum sensing system (a negative regulator of biofilm) is pH sensitive. A previous study demonstrated that co-culture with *C. parapsilosis* resulted in modest increase in pH but below the threshold of *agr* activation (Todd, Noverr and Peters, 2019). In agreement with Todd *et al.,* the *C. parapsilosis* CFS buffers the media to a pH of 6 and gene expression analysis in this media also rules out *agr* activation (Chapter 3, Table 3.3). A further experiment where the media was buffered to a pH of 6 demonstrated that the biofilm inhibition is not solely due to an increase in pH (Figure 4.7). It cannot be ruled out that the change in pH may be causing other changes within the biofilm.

From Table 4.5, a trend emerges whereby biofilm inhibition is correlated with high levels of eDNA. The inhibition of SA1 biofilm in TSB-0.2G is lost when it is grown in TSB-1G. Therefore, eDNA may be a target of the *C. parapsilosis* CFS. As already stated in Chapter 1, the principal role of eDNA is to secure the bacterial cells together in the biofilm (Dengler *et al.*, 2015). The DNase activity in the biofilm supernatant of treated and untreated SA1 and SH1000 biofilm under both media conditions was tested.

Table 4.6. Percentage (%) increase in DNase activity in SA1 and SH1000 due to treatment with ***C. parapsilosis*** CFS in TSB supplemented with different concentrations of glucose.

	0.2% glucose		**1% glucose**	
	SA1	SH1000	SA1	SH1000
6 h (CFS treated v control)	6% increase	No change	No change	No change
24 h (CFS treated v control)	12.9% increase	5.3% increase (not significant)	13.9% increase	No change

SA1 biofilm supernatant DNase activity was increased at both 6 hours and 24 hours in TSB-0.2G media (Tables 4.3 and 4.6). There was also an increase in DNase activity in SH1000 under the same conditions (5.3%), however this increase was not significant. This correlates with our hypothesis that eDNA is a major component of SA1 and SH1000 TSB 0.2% glucose induced biofilm and that increased levels of DNase activity due to the presence of fungal CFS results in the degradation of this eDNA and reduced biofilm formation.

It is interesting that there was DNase activity in SA1 TSB 1% glucose induced biofilm as no biofilm inhibition is observed under these conditions. Decreased levels of eDNA have been observed at higher concentrations of glucose (Luo *et al.*, 2020). Therefore, the reduced levels of eDNA in TSB-1G could be a consequence of the increase DNase activity or the higher levels of glucose in the media. In turn, as this biofilm is mainly composed of protein, the increased DNase activity would have no effect on biofilm maturation of SA1 under these conditions, resulting in no fungal CFS induced biofilm inhibitory effect.

As discussed above, the presence of glucose mediates the acidification of the biofilm culture. *C. parapsilosis* CFS buffers the biofilm media to a higher pH (Figure 4.4 and 4.7) and nuclease activity is increased at higher pH and decreased at an acidic pH (Luo *et al.*,

2020). DNase activity was increased under CFS treatment in TSB-1G media for SA1. Therefore, it is unlikely to be a pH effect that explains the lack of inhibition by CFS in TSB-1G media for SA1. However, SH1000 biofilm in TSB-1G media is inhibited. This inhibition is lower (only a 30% decrease) and while eDNA is abundant the sheer amount of biofilm could play a role. SH1000 produced more biofilm than SA1. The CFS may not be able to overcome this amount of biofilm.

Further evidence that the *C. parapsilosis* CFS is targeting eDNA was observed while testing the antibiotic tolerance of CFS-treated biofilms. No effect on antibiotic tolerance by *C. parapsilosis* CFS was detected. However, there was biofilm induction at sub-inhibitory concentrations of oxacillin and this induction was prevented in the presence of CFS. This eDNA-dependent biofilm formation under sub-inhibitory levels of beta lactams has been previously described (Kaplan *et al.*, 2012). Kaplan *et al.*, observed an increase in biofilm (as high as 10-fold) when *S. aureus* (MSSA and MSSA strains) was exposed to sub-inhibitory concentrations of bet lactam antibiotics. Biofilm formation induced by low-level methicillin was inhibited by DNase. Furthermore, the biofilm induction phenotype was absent from an *atl* mutant strain (Kaplan *et al.*, 2012). This suggests that the *C. parapsilosis* CFS could be preventing biofilm formation by degrading eDNA, either by increased thermonuclease activity or preventing eDNA release via the anti-holin activity of LrgAB (significantly upregulated in TSB-0.2G, Chapter 3).

Protein is an important matrix component of SA1 biofilm in both media tested here. Similarly, protein is an important matrix component for *S. aureus* strain SH1000. Protein may be the target of the CFS, as an increase in protease expression is observed in SA1 in TSB-0.2G (Chapter 3, Tables 3.2 and 3.3) and TSB-1G media (Table 4.2). Increased zones of proteolysis indicated that protease activity is heightened in both TSB-0.2G (17.8% increase) and TSB-1G (26% increase) in CFS-treated SA1 biofilms at 24 h (Table 4.3). Conversely, no protease activity was observed in SH1000.

PIA or PNAG (polymeric β-1,6-linked N-acetylglucosamine) is the main carbohydrate constituent of the biofilm matrix. It is encoded by the *ica* operon and contributes

significantly to *Staphylococcal* biofilm formation (Cramton *et al.*, 1999). PIA and eDNA are known agglutinins and the interaction between PIA and eDNA has been shown to promote aggregation (Mlynek *et al.*, 2020). *C. parapsilosis* CFS prevents aggregation in SA1 (but not in SH1000) in TSB-0.2G but not in TSB-1G. eDNA is unlikely to be the agglutinin responsible for aggregation as DNase I treatment resulted in aggregation. Instead, the inhibition of aggregation could be due to the downregulation of genes encoding surface proteins (e.g., *sasG and sasC*) or the downregulation of the *icaA, icaB* and *icaC* genes in SA1 that was presented in Chapter 3 (logFC -3.6, -3.6, and -4.1, respectively).

It is unknown what effect, if any, the CFS may have on the expression of the *ica* operon in SH1000. Presumably, PIA does not play a significant role as its levels in the biofilm matrix in TSB-0.2G are low. The results presented in Figure 4.11 are in agreement with Haaber *et al.* in that SH1000, despite its ability to produce biofilms, has been reported to be unable to aggregate (Haaber *et al.*, 2012). This indicates that the processes behind aggregation and biofilm formation are not identical.

Mature *S. aureus* biofilms are notoriously difficult to treat due to the protection from the environment that the biofilm affords the cells within (Archer *et al.*, 2011). Preventing *S. aureus* biofilm is extremely difficult (Bhattacharya *et al.*, 2015) and is therefore important that researchers develop innovative ways to remove the protection of the existing biofilm, including targeting the matrix to prevent biofilm formation or induce biofilm dispersal.

In addition to *S. aureus* biofilm inhibition, *C. parapsilosis* CFS dispersed preformed biofilm in SA1 and SH1000 in TSB-0.2G media. No biofilm dispersal was observed in TSB-1G media in either strain. Similarly, to biofilm inhibition conditions, glucose concentration impacts the ability of the fungal CFS to detach preformed biofilm. The addition of 100% (v/v) *C. parapsilosis* CFS, SN1 or SN6, could detach *S. aureus* biofilm grown in TSB-1G. Reducing the glucose content of the growth media for subsequent incubation enabled detachment of the biofilm by the CFS. A reduction in glucose would

mean a reduction in lactic acid (final product of glycolysis) production. Perhaps pH may play a role in biofilm dispersal.

Biofilm dispersal occurs via a different mechanism to biofilm formation (Lister and Horswill, 2014). A different mechanism of action to biofilm inhibition by the fungal CFS is possible. Phenol soluble modulins and proteases play important roles in biofilm dispersal (Martí *et al.*, 2010; Periasamy *et al.*, 2012). It is possible that addition of *C. parapsilosis* CFS induces an upregulation of protease activity as it does during nascent biofilm formation. Further experimentation with biofilm supernatants collected from *C. parapsilosis* CFS-treated preformed *S. aureus* biofilm could confirm this.

As stated previously, protein is an important matrix component of the *S. aureus* strains used in this study. A study by Park *et al.*, used cell free supernatant of *Pseudomonas aeruginosa* which strongly inhibited *S. aureus* biofilm without bactericidal activity. They revealed that *P. aeruginosa* secreted a protease which induced endogenous *S. aureus* protease activity (Park *et al.*, 2012). In addition, *S. epidermidis* supernatants containing the serine proteinase Esp, were capable of inhibition of *S. aureus* biofilm as well as the destruction of preformed biofilm in a dose-dependent manner (Iwase *et al.*, 2010). *C. parapsilosis* is known to produce three secreted aspartyl proteases (Singh *et al.*, 2019) and protease activity is increased in CFS treated-SA1 in TSB-0.2G media at 24 h (Table 4.3). The aspartyl proteases produced by *C. parapsilosis* could be inducing endogenous *S. aureus* protease production. Treatment of the CFS with an aspartyl protease-specific inhibitor would confirm this. Further work is required to identify the possible mechanisms by which *C. parapsilosis* CFS is detaching *S. aureus* biofilm. This however was not the focus of this work.

The results presented here are suggestive of a strain-dependent mechanism of *S. aureus* biofilm inhibition exhibited by the *C. parapsilosis* CFS. Nuclease and protease activity may result with biofilm inhibition in SA1. In SH1000, no protease activity is seen and there is no significant change in nuclease activity due to treatment with CFS. Furthermore, the CFS can prevent aggregation in SA1 but the lack of ability to aggregate

in SH1000 has no impact on its ability to produce a biofilm. Thus, the CFS is not preventing biofilm formation in SH1000 via blocking aggregation. These results highlight the ability of *C. parapsilosis* CFS to target multiple physiological processes in *S. aureus*.

In conclusion, the aim of this chapter was to identify possible matrix targets by which the *C. parapsilosis* CFS is inhibiting biofilm maturation in *S. aureus*. A strain-dependent effect emerged suggesting that the CFS has pleotropic effects on several biofilm components in *S. aureus.* Further work is needed to fully elucidate the mechanisms by which *C. parapsilosis* inhibits *S. aureus* biofilm.

Chapter 5 - Characterising the *C. parapsilosis* Cell-Free Supernatant

5.1. Introduction

Faced with increasing frequencies of antimicrobial-resistant (AMR) strains, the search for new therapeutic agents effective against pathogens has become an emergency. Indiscriminate or overuse of antibiotics has led to resistance against almost all antimicrobial drugs (Blair *et al.*, 2015). Antibiotic resistance is heightened when bacteria grow as a biofilm. New treatments for these types of infections are needed. Screening of different microbial species (both fungal and bacterial) for biomolecules that show anti-biofilm properties is a promising approach.

Many studies focus on the cell-free supernatants (CFS) of probiotic bacteria such as lactic acid bacteria (LAB). CFS from lactic acid bacteria (LAB) can contain organic compounds, and fatty acids, among other compounds that have anti-microbial activity (Colombo *et al.*, 2018; Benmouna *et al.*, 2020). *L. agilis* CCUG31450 produces a glycoprotein with biosurfactant activity. A potential biomedical application for this could be as an anti-adhesive or anti-bacterial against *S. aureus* (Gudiña *et al.*, 2015; Satpute *et al.*, 2016). LAB strains have demonstrated their potential use against biofilm formation and dispersing preformed biofilm (Drumond *et al.*, 2023). Other microbial species, both commensal and pathogenic, can produce potentially useful biomolecules (Bandara *et al.*, 2009; Glatthardt *et al.*, 2020; Kim *et al.*, 2020). There is a potential therapeutic value for microbial supernatants. Microbial supernatant or the active molecules isolated from them could be used as an adjuvant therapy to reduce the use of or work in synergism with antibiotics.

The aim of this chapter was to characterise the *C. parapsilosis* CFS and the active factor(s) present. The activity of the *C. parapsilosis* CFS following heat and enzymatic treatments was investigated. The effect of *Candida albicans* CFS on *S. aureus* biofilm formation was also assessed to determine if the anti-biofilm effect was conserved between *Candida* species.

Next, targeted metabolomic analysis was used to identify a range of specific, chemically defined, and annotated metabolites in cell-free supernatant samples of *C. parapsilosis* and *C. albicans*. To our knowledge, few studies have analysed the metabolome and even fewer the extracellular metabolome of *C. parapsilosis* (López-Ramos *et al.*, 2021).

Metabolomic profiling, identifying and/or quantifying small molecules present in the CFS can help determine its biological activity and potential therapeutic value. A metabolite, in the context of metabolomics, is any molecule that is less than 1.5 kDa in size. These molecules are by-products of cellular metabolism. Metabolites secreted from the cells compose what is known as the extracellular metabolome (exo-metabolome) (Pinu and Villas-Boas, 2017). While a targeted metabolomics approach will only identify a limited number of metabolites, the resulting data is quantitative, and the data analysis and interpretation are simplified (Roberts *et al.*, 2012). Targeted metabolomics is useful as part of an initial investigation or characterisation experiment.

Finally, to assess the antibiofilm activity of *C. parapsilosis* CFS beyond *S. aureus*, its use on another *Staphylococcal* species, *Staphylococcus epidermidis* (*S. epidermidis*) was investigated.

5.2. Results

5.2.1. An alternative biofilm formation quantification method confirms *C. parapsilosis* CFS biofilm inhibitory effect.

An alternative method to confirm the inhibition of *S. aureus* biofilm formation and dispersal was utilised (Chapter 2, section 2.25). *S. aureus* was grown in 6-well Nunclon microtiter plates microtiter plates for 24 h at 37°C with or without *C. parapsilosis* CFS, SN1 (50% v/v). Biofilms were washed as normal, and 1 ml of PBS was added. Biofilms were removed from the plate surface by scraping and transferred to a pre-weighed microcentrifuge tube. The biofilms were dried overnight at 60°C to remove all water prior to weighing. The resulting weight was the biofilm dry weight.

Treatment with SN1 significantly inhibited SA1 biofilm by 80% ($P < 0.01$) in TSB-0.2G (Figure 5.1). No decrease in biofilm mass was measured in TSB-1G media. Likewise, at 24 h, a decrease in preformed biofilm of 63% ($P < 0.01$) was seen in 0.2% glucose, while there was no decrease in 1% glucose.

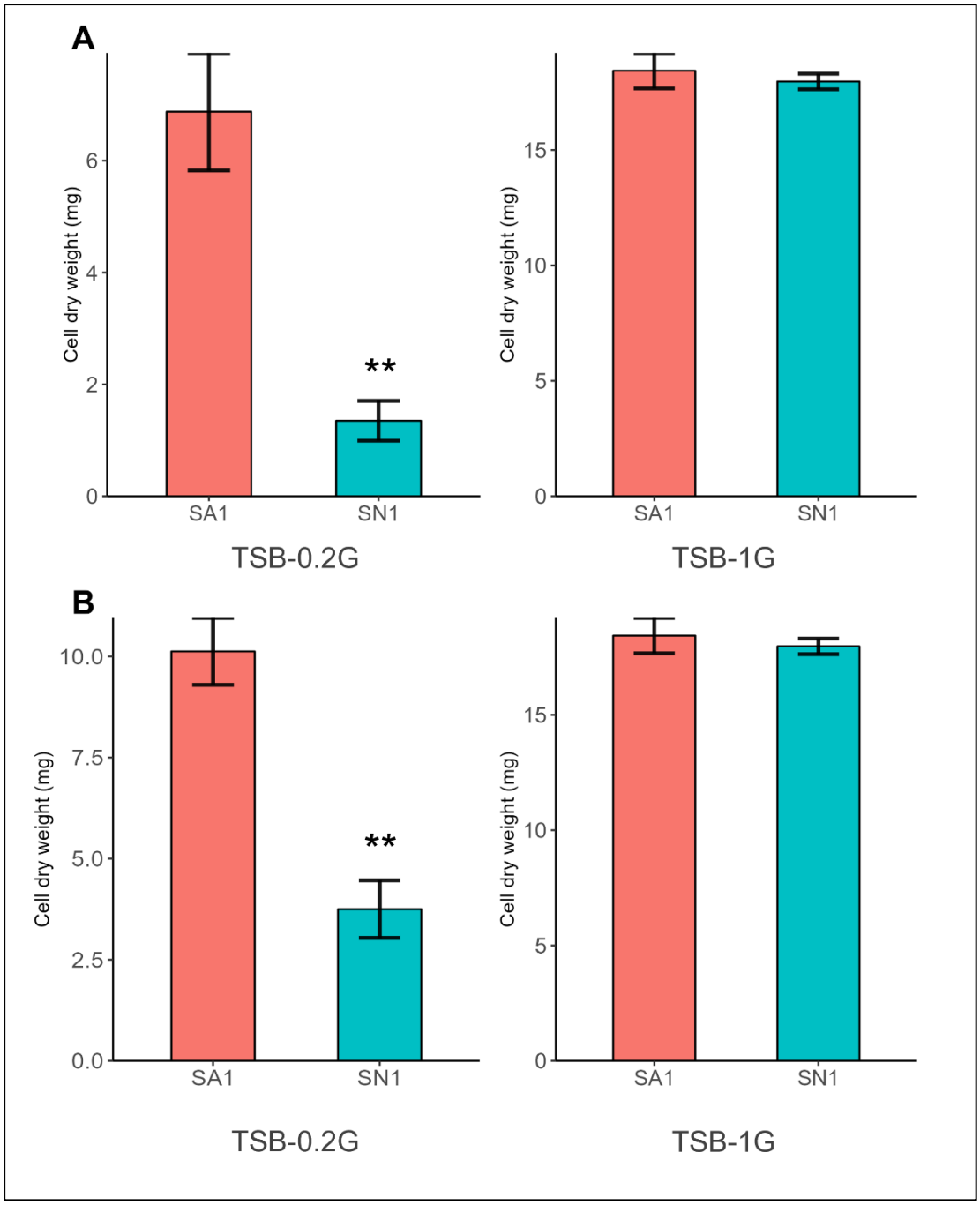

Figure 5.1. C. parapsilosis CFS effect on SA1 biofilm formation as measured by dry weight of biofilm. *A) Biofilm inhibition assay in TSB 0.2% glucose and TSB 1% glucose media. S. aureus biofilms were grown in the presence or absence of C. parapsilosis CFS, SN1 (50% (v/v)) in 6-well microtiter plates. The plates were incubated for 24 h at 37°C. Biofilms were collected, dried, and weighed. B) Biofilm dispersal in TSB-0.2G and TSB-1G media. S. aureus biofilms were grown for 24 h before adding SN1. The bars represent the mean dry weight (mg) of 3 combined wells. Errors bars represent ±SE. ** P < 0.01.*

5.2.2. The active factor is secreted by *C. parapsilosis* from an early timepoint.

Biologically active natural products can be made at different stages of microbial growth. To assess whether the active factor is secreted constitutively, *C. parapsilosis* was first grown under shaking conditions in TSB-0.2G media at 37°C for 28 h. *C. parapsilosis* CFS was sampled at an early (6 h) and a later (24 h) timepoint (Figure 5.2A). Both the CFS samples collected at 6 h and 24 h inhibited *S. aureus* biofilm formation ($P < 0.0001$) by 69% and 37%, respectively (Figure 5.2B). Biofilm inhibition by CFS collected after 6 h of *C. parapsilosis* growth resulted in greater *S. aureus* biofilm inhibition than CFS collected at 24 h after growth ($P < 0.0001$).

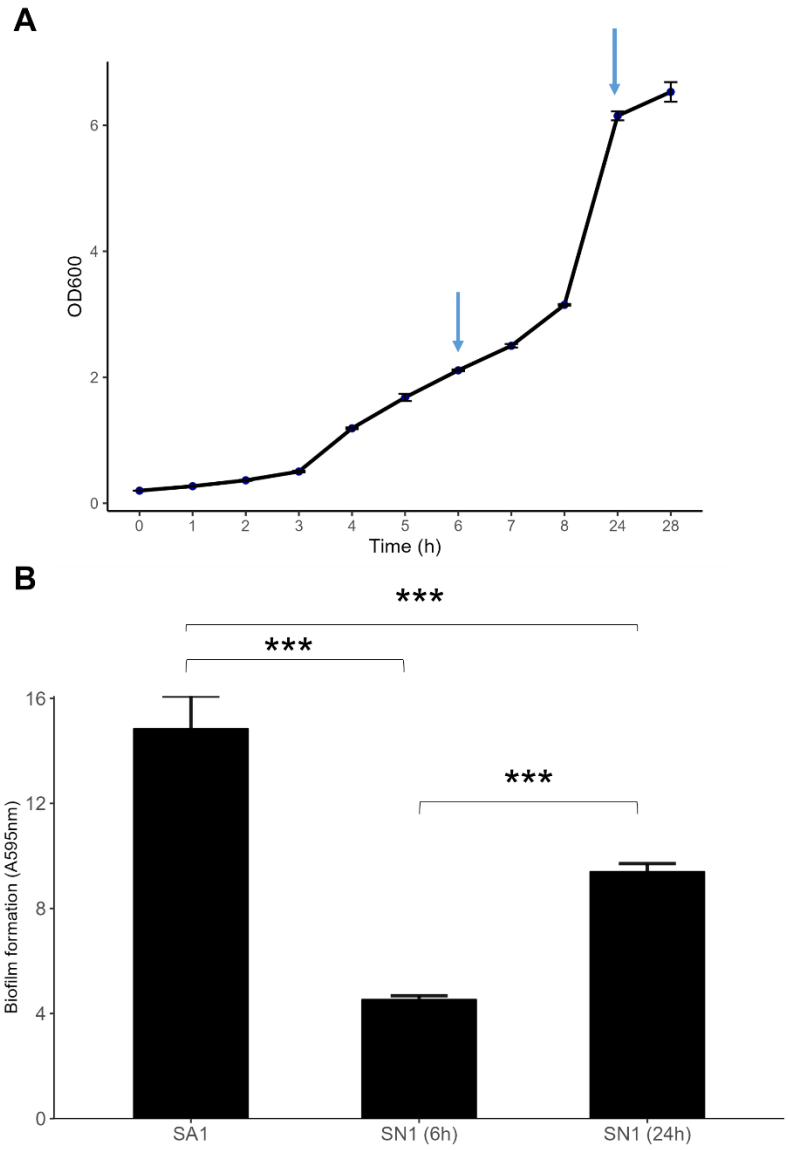

Figure 5.2. The active factor within the CFS is produced from at least 6 h of C. parapsilosis growth*. A) C. parapsilosis was grown in TSB 0.2% glucose (TSB-0.2G) media. The OD600 was recorded at the times indicated. C. parapsilosis CFS was collected at the indicated timepoints (blue arrows). B) S. aureus was grown in the presence or absence of C. parapsilosis CFS samples collected at different timepoints for 24 h at 37°C. Both supernatants inhibited S. aureus biofilm formation. Three biological replicates of S. aureus were tested against 4 biological replicates of C. parapsilosis from each timepoint. Biofilm biomass was quantified by crystal violet. Bars represent the mean value. Error bars represent ±SE. *** indicates P < 0.0001.*

5.2.3. The *C. parapsilosis* secreted anti-biofilm factor is not a secreted aspartyl protease.

C. parapsilosis produces three aspartyl proteases, Sapp1, Sapp2, and Sapp3 (Singh *et al.*, 2019). Pepstatin A, a potent inhibitor, was used to inactivate these aspartyl proteases. No significant difference in biofilm inhibition between untreated CFS and pepstatin A treated CFS was observed (Figure 5.3).

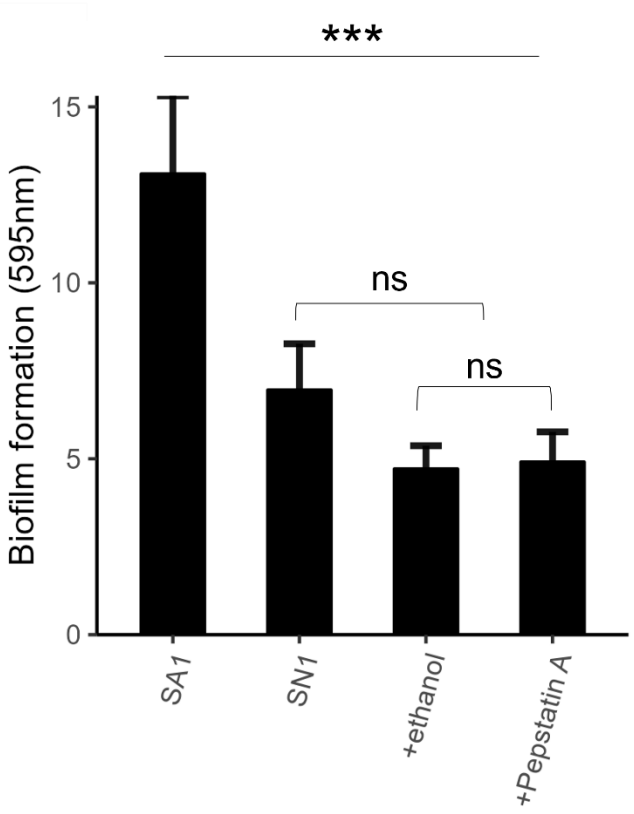

Figure 5.3. C. parapsilosis CFS pepstatin A treatment. *S. aureus biofilm assays were conducted in microtiter plates in TSB 0.2% glucose media and crystal violet staining was used to quantify biofilm biomass. Pepstatin A, an inhibitor of aspartyl proteases, was added to C. parapsilosis CFS before co-culture with S. aureus. + ethanol; SN1 with ethanol. An equal volume of ethanol was added as a control to account for it being used as the solvent for pepstatin A. +Pepstatin A; SN1 treated with pepstatin A prior to biofilm challenge. Bars represent the mean value. Error bars represent ±SE. P < 0.0001. SN1; C. parapsilosis CFS SN1. SA1; S. aureus.*

5.2.4. The *C. parapsilosis* secreted anti-biofilm factor is heat stable and proteinase K resistant.

Boiling the *C. parapsilosis* CFS had no effect on the anti-biofilm activity of the fungal supernatant (Figure 5.4), indicating that the secreted factor is heat stable.

The fungal CFS was also unaffected by proteinase K treatment (Figure 5.4) Due to the potency, pH stability, and low peptide bond specificity of proteinase K, the active factor in the CFS is unlikely to be proteinaceous in nature. This is further supported by the heat stability of the factor, as most proteins are denatured upon heat treatment.

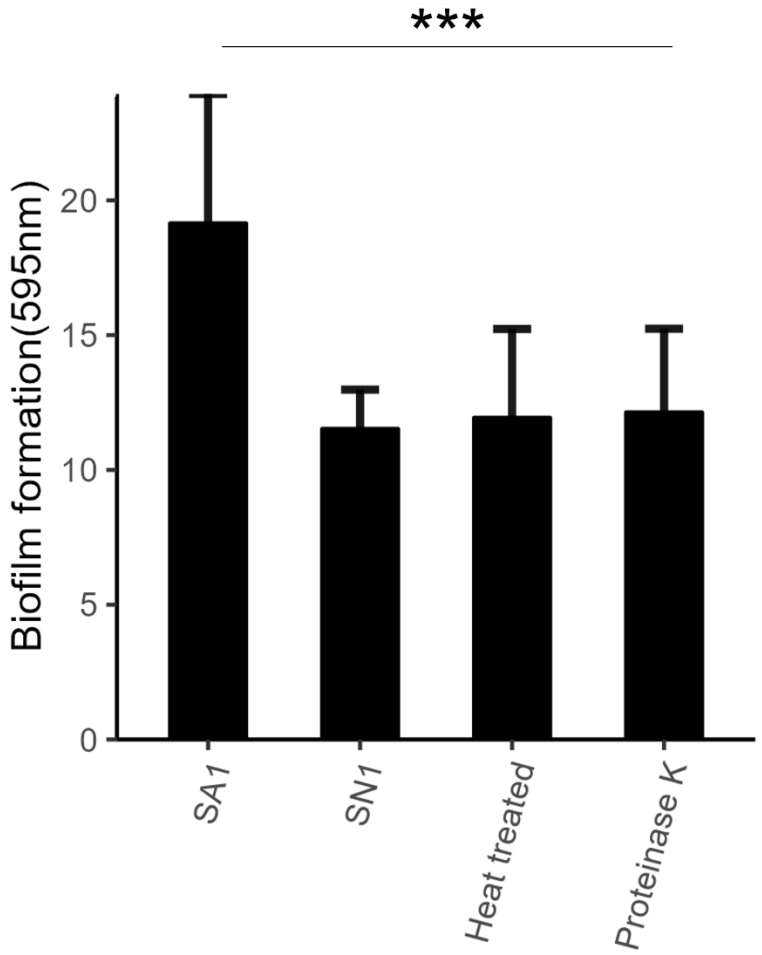

Figure 5.4. C. parapsilosis CFS biochemical treatment. *S. aureus biofilm assays were conducted in microtiter plates in TSB 0.2% glucose media and crystal violet staining was used to quantify biofilm biomass. C. parapsilosis CFS was boiled (heat treated) or treated with proteinase K prior to challenge of S. aureus biofilm formation. No effect on CFS activity was observed. Bars represent the mean value. Error bars represent ±SE. P < 0.0001. SN1; C. parapsilosis CFS SN1. SA1; S. aureus.*

5.2.5. There is evidence for more than one active factor in the *C. parapsilosis* CFS.

Sample fractionation is a useful tool in identifying unknown active molecules of interest. Different fractionation methods exist that separate a sample based on certain criteria. Here, size fractionation was used, where the *C. parapsilosis* CFS SN1 was divided into fractions based on their molecular weight. The CFS was fractionated using a 5000 molecular weight cut-off (MWCO) spin filter. The two resulting fractions contained molecules of either > 5 kDa or < 5 kDa in size. Crystal violet biofilm assays using size fractionated CFS showed that both fractions of the CFS were capable of inhibiting *S. aureus* biofilm ($P < 0.05$) (Figure 5.5). This may indicate that there is more than one active factor in the CFS.

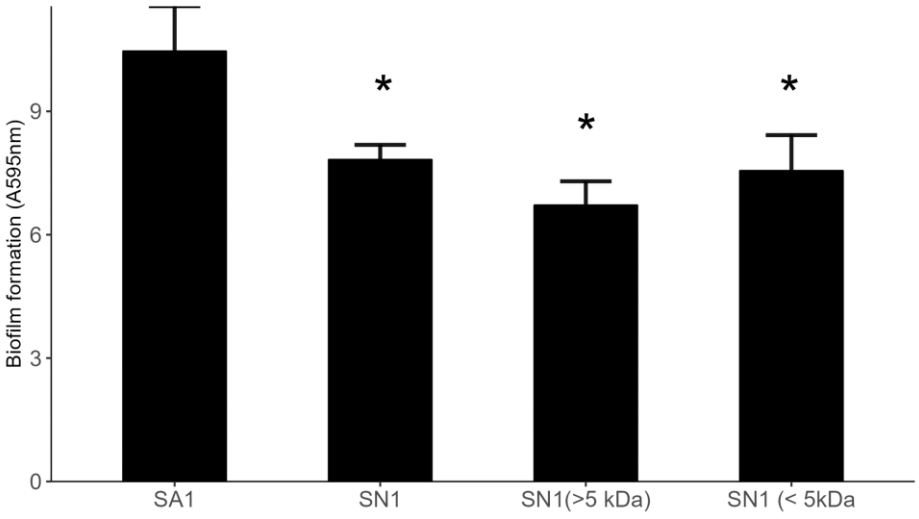

***Figure 5.5*. Biofilm formation of S. aureus grown in the presence of C. parapsilosis CFS fractionated by molecular weight (kDa).** *C. parapsilosis CFS was fractionated by a 5kDa filter. Both fractions were tested against S. aureus biofilm formation. S. aureus was grown with an equal volume of 50% (v/v) fractionated CFS in TSB media supplemented with 0.2% glucose. The plates were incubated for 24 h at 37°C. Biofilm biomass was quantified with crystal violet. Bars represent the mean value. Error bars represent ±SE. * indicates significance compared to the SA1 control (P < 0.05).*

5.2.6. *C. albicans* supernatant inhibits *S. aureus* biofilm formation.

C. albicans is a human fungal pathogen that belongs to the CTG clade alongside *C. parapsilosis*. The CTG clade includes species that translate the CTG codon to serine instead of leucine (Massey *et al.*, 2003). Unlike *C. parapsilosis*, *C. albicans* interaction with *S. aureus* and other *Staphylococci* is well-characterised (reviewed in (Carolus, Van Dyck and Van Dijck, 2019). Considering their relative relatedness, we wanted to investigate whether the *C. albicans* CFS could also inhibit *S. aureus* biofilm. *C. albicans* CFS (hereon referred to as CaSN; *Candida albicans* supernatant) was collected in the same way as *C. parapsilosis* CFS, SN1. *C. albicans* did not form hyphal cells in TSB-0.2G media when checked under a light microscope after 18 h of growth (data not shown).

Using the same set up for testing *C. parapsilosis* CFS, *S. aureus* was grown in the presence of CaSN (50% v/v) in TSB-0.2G or TSB-1G media in microtiter plates for 24 h at 37°C. The biofilms were collected and dried to remove all water. The dry weights of the resulting biofilms were measured. CaSN inhibited *S. aureus* biofilm by 69% ($P < 0.01$) in TSB-0.2G and had no significant effect on biofilm formation in TSB-1G (Figure 5.6).

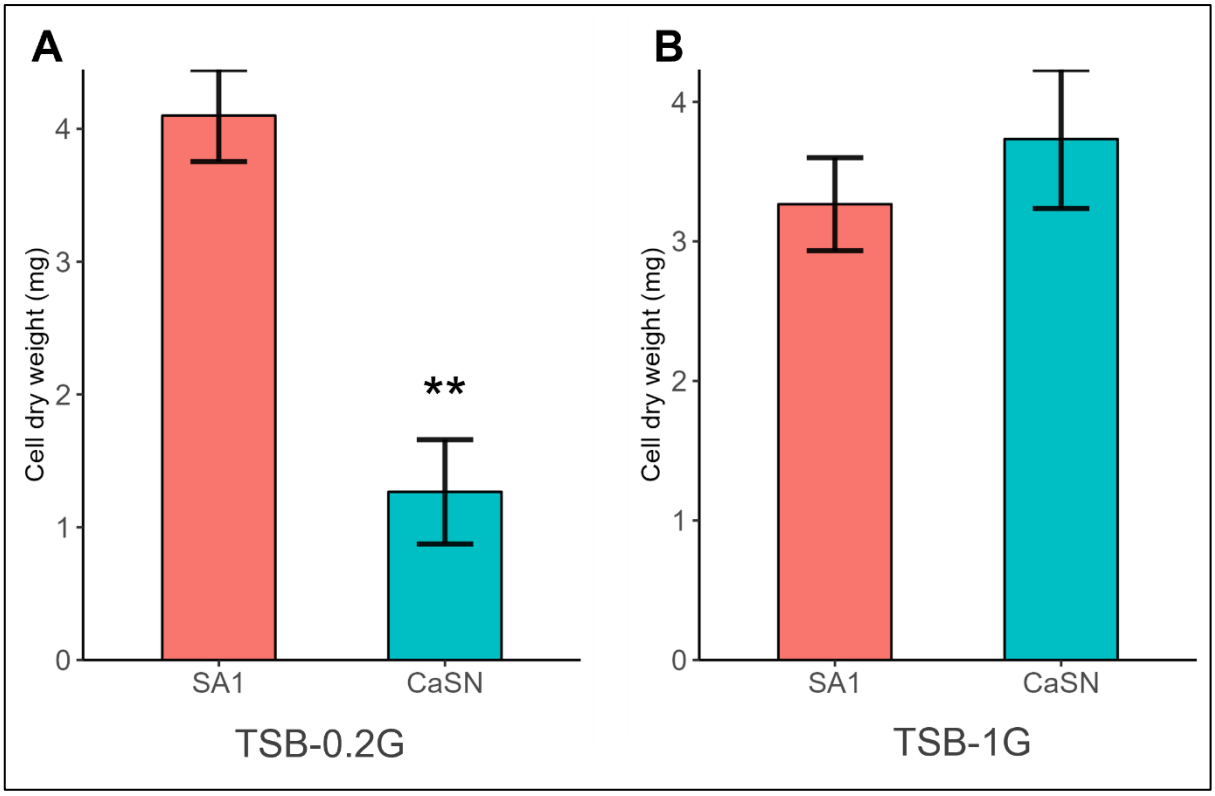

Figure 5.6. Dry weight of S. aureus biofilms grown in the presence of C. albicans CFS. *In 6 well microtiter plates, S. aureus (SA1) was grown with or without C. albicans CFS (CaSN) (50% v/v) for 24 h in A) TSB supplemented with 0.2% glucose (TSB-0.2G) or B) 1% glucose (TSB-1G) media. The biofilms were collected and dried before being weighed. The bars represent the mean dry weight (mg). Errors bars represent ±SE. ** P < 0.01.*

5.2.7. Targeted Metabolomic characterisation of the *Candida* cell-free supernatants.

5.2.7.1. Exo-metabolomic profile of each *Candida* CFS reveals similarity between sample groups.

The extracellular metabolome (exo-metabolome) is comprised of all metabolites and secondary metabolites that are secreted from the cell into the extracellular environment. Targeted metabolomics was utilised to identify the presence of various metabolites in *C. parapsilosis* CFS (SN1 and SN6), *C. albicans* CFS (CaSN) and TSB 0.2% glucose media control (TSB). This tandem mass spectrometry approach screened for > 600 metabolites. The concentrations (µM) of each metabolite identified in each sample were used for statistical analysis. The samples were analysed by the UCD Conway Metabolomic Facility.

PCA score plot was used to assess the quality of the data and identify any patterns (Figure 5.7). The SN1, SN6 and CaSN samples cluster within their respective biological replicates (groups) but SN6 and CaSN cluster close together. 18% of variance in the data is explained along Component 1, and 16% along Component 2. Only two control samples were analysed. An outlier sample in the CaSN group was identified (CaSN.5), however, it was included in the analysis upon advisement of our collaborating partners who specialise in metabolomics.

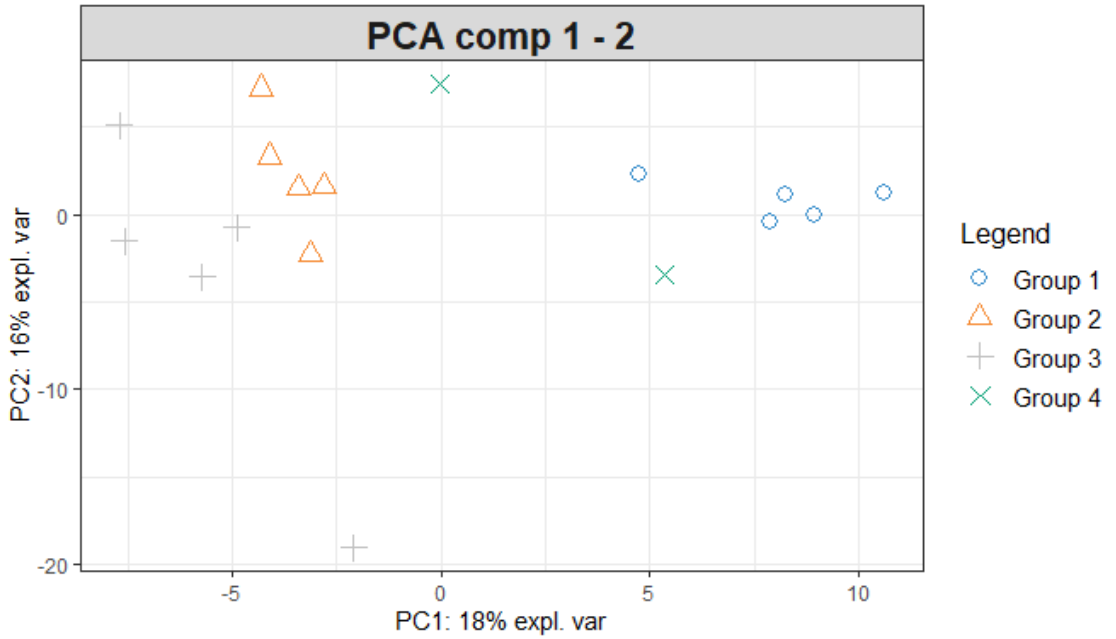

Figure 5.7. PCA plot of metabolomic analysis samples of the C. parapsilosis CFS. *PCA analysis of LC-MS/MS based metabolomics data analysis. The variance displayed in the plot above is the explained variance for the data in each group. Group 1; SN1. Group 2; SN6. Group 3; CaSN. Group 4; TSB 0.2% glucose media control.*

216 metabolites of 23 different classes were identified. A majority of the metabolites were of the triacylglycerols class (Figure 5.5.8A). Triacylglycerols are one of the two neutral lipid classes. Neutral lipids can be stored and then utilised for membrane formation when lipids are depleted (Wagner and Daum, 2005; Kohlwein, 2017). The other three classes that contained the most hits included, glycosylceramides (GlycCer), aminoacids related, and amino acids.

Unsupervised clustering on all samples was performed as initial data exploration to assess whether clustering of the groups could indicate the presence of a signature able to separate the groups. A reasonable clustering was observed between the groups with a good separation of media and SN1. We observed only partial separation of SN6, and

CaSN samples (Figure 5.8B). This suggests a closer similarity between the SN6 and CaSN samples than SN6 and SN1.

A

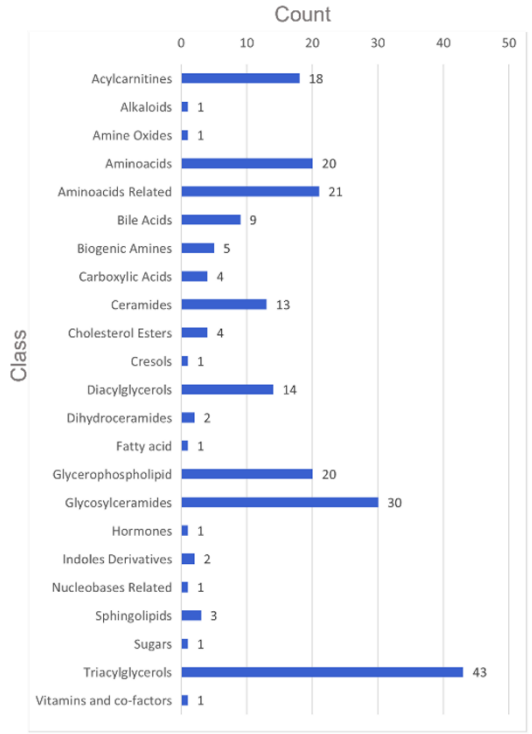
Count
0
10
20
30
40
50
Class
Acylcarnitines 18
Alkaloids 1
Amine Oxides 1
Aminoacids 20
Aminoacids Related 21
Bile Acids 9
Biogenic Amines 5
Carboxylic Acids 4
Ceramides 13
Cholesterol Esters 4
Cresols 1
Diacylglycerols 14
Dihydroceramides 2
Fatty acid 1
Glycerophospholipid 20
Glycosylceramides 30
Hormones 1
Indoles Derivatives 2
Nucleobases Related 1
Sphingolipids 3
Sugars 1
Triacylglycerols 43
Vitamins and co-factors 1

B

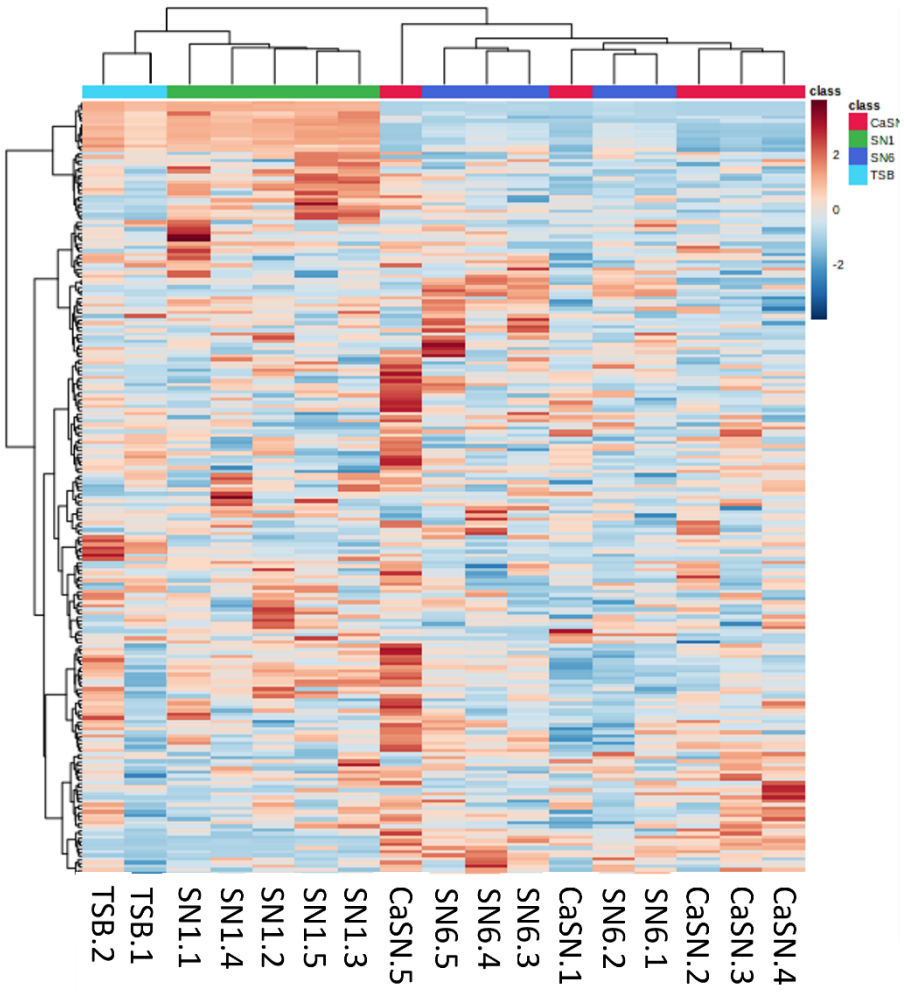
class
class
CaSN
SN1
SN6
TSB
2
0
-2
TSB.2
TSB.1
SN1.1
SN1.4
SN1.2
SN1.5
SN1.3
CaSN.5
SN6.5
SN6.4
SN6.3
CaSN.1
SN6.2
SN6.1
CaSN.2
CaSN.3
CaSN.4

Figure 5.8. Metabolites identified in C. parapsilosis and C. albicans CFS. *A) Table showing the counts of metabolites for each class identified by the analysis platform. B) Heat map of all metabolites showing hierarchical clustering on both columns and rows based on Euclidean mean distance. SN1; C. parapsilosis CP1 CFS. SN6; C. parapsilosis CP6 CFS. CaSN; C. albicans CFS.TSB; TSB 0.2% glucose media control.*

5.2.7.2. Comparison between *C. parapsilosis* and *C. albicans* CFS samples.

To identify metabolites increased in the three CFS sample groups, we analysed the differences of the concentrations of metabolites between TSB-0.2G media and each of the CFS samples. Metabolites were identified where the concentration was significantly increased ($P < 0.05$) in comparison to the media control. 12, 16, and 12 metabolites were significantly increased in SN1, SN6, and CaSN, respectively. SN6 showed greater similarity (in terms of common increased metabolites) to CaSN, with 10 metabolites in common compared to only three shared with SN1 (Figure 5.9).

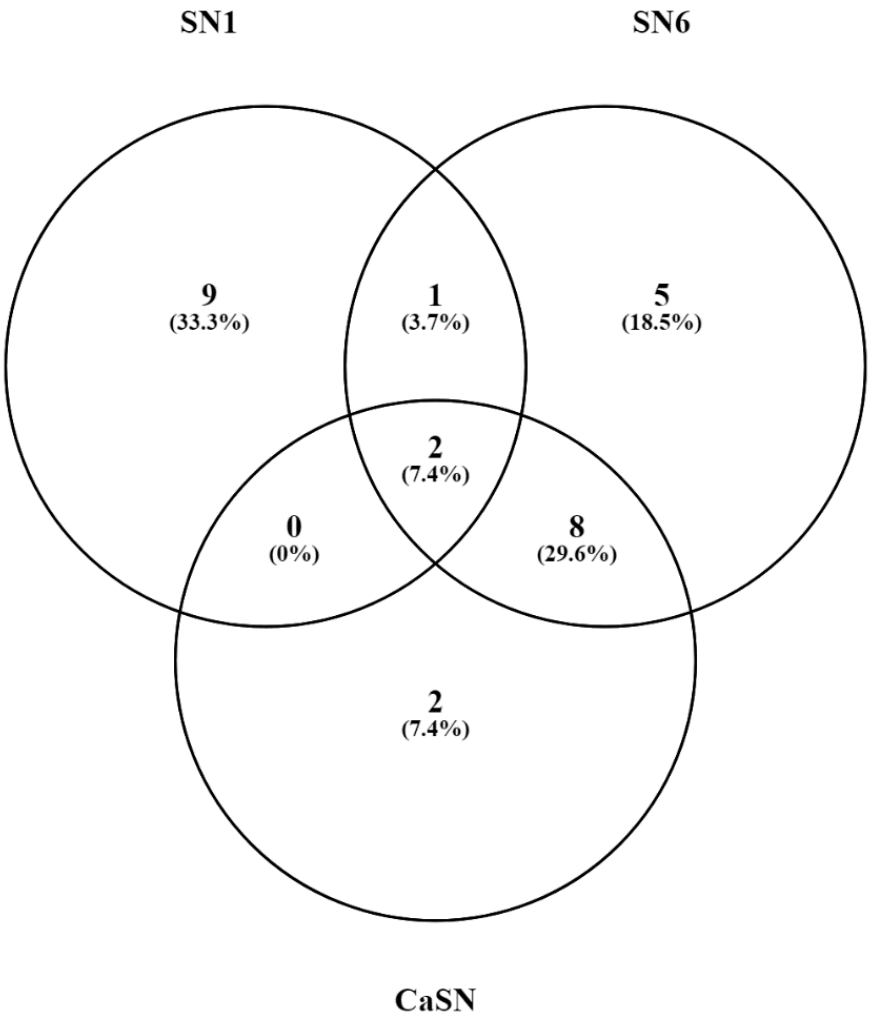

Figure 5.9. Venn diagram showing the overlap in significantly increased metabolites. *Metabolites were identified in the cell-free supernatants (CFS) of C. parapsilosis isolates (SN1 and SN6) and C. albicans (CaSN). The metabolites included in the Venn diagram were significantly increased in CFS samples compared to a background media control ($P < 0.05$). Percentages of the total number of significantly increased metabolites are also shown.*

Only one metabolite was shared between SN1 and SN6 but not CaSN (Figure 5.9). This was a triglyceride TG(18:2_38:4). Eight metabolites were increased in both SN6 and CaSN sample groups but not in the SN1 group. These were an acylcarnitine Glutaconylcarnitine (C5:1-DC), an amino acid-related compound homocysteine, two

carboxylic acids (aconitic acid and Succinic acid), a bile acid (Glycochenodeoxycholic acid), a lysophosphatidylcholine (lysoPC a C24:0), and two phosphatidylcholines (PC aa C34:4 and PC aa C36:3). These results suggest a greater similarity in terms of metabolites significantly increased in comparison to the TSB media control between SN6 and CaSN sample groups than SN6 and SN1 sample groups.

5.2.7.3. Glutamine and Indole acetic acid are significantly increased across *C. parapsilosis* and *C. albicans* CFS samples.

As the CFS of *C. parapsilosis* and *C. albicans* can inhibit *S. aureus* biofilm, metabolites in common between all three samples were of interest for further investigation. Two metabolites, glutamine (Gln) and Indole acetic acid (3-IAA), were identified as significantly increased in all three CFS sample groups (Table 5.1).

Glutamine is an important amino acid that supplies carbon and nitrogen to fuel the cell. Indole acetic acid is a plant hormone of the auxin class and so the terms “auxin” and “IAA” are sometimes interchangeable. It is a secondary metabolite that is produced by plants, bacteria, and fungi (Fu *et al.*, 2015).

Table 5.1. Glutamine and 3-IAA have increased concentration in *Candida* cell-free supernatant (CFS) samples compared to a TSB 0.2% glucose media control ($P < 0.05$).

	Fold change compared to TSB-0.2G ($P < 0.05$).		
Metabolite	SN1	SN6	CaSN
Glutamine Log2FC	2.1237	1.2451	1.1872
Indole acetic acid (3-IAA) Log2FC	0.61795	2.1939	1.8199
SN1; *C. parapsilosis* CP1 CFS. SN6; *C. parapsilosis* CP6 CFS. CaSN; *C. albicans* CFS.			

5.2.8. *C. parapsilosis* CFS can inhibit *Staphylococcus epidermidis* biofilm.

The effect of *C. parapsilosis* CFS was assessed against another *Staphylococcal* species. *S. epidermidis* has been regarded as a benign and sometimes helpful commensal bacteria of the skin. However, its role as a causative agent in various infections has become increasingly clear (Brown and Horswill, 2020; Zheng *et al.*, 2022; Severn and Horswill, 2023). Alongside *S. aureus*, it is among the most frequent causes of device/implant-related infections (Oliveira *et al.*, 2018). Here, *S. epidermis* was grown in salt media (TSB 1% NaCl), as it facilitated strong biofilm production. Biofilm biomass was quantified using crystal violet.

Treatment with SN1 (50% v/v) resulted in a 78% ($P < 0.0001$) decrease in biofilm formation (Figure 5.10A). *S. epidermidis* was allowed to grow under static biofilm growth conditions for 24 h, then treated with SN1 (50% v/v) for a further 24 h. This resulted in the detachment of preformed biofilm by 90% ($P < 0.0001$) (Figure 5.10B).

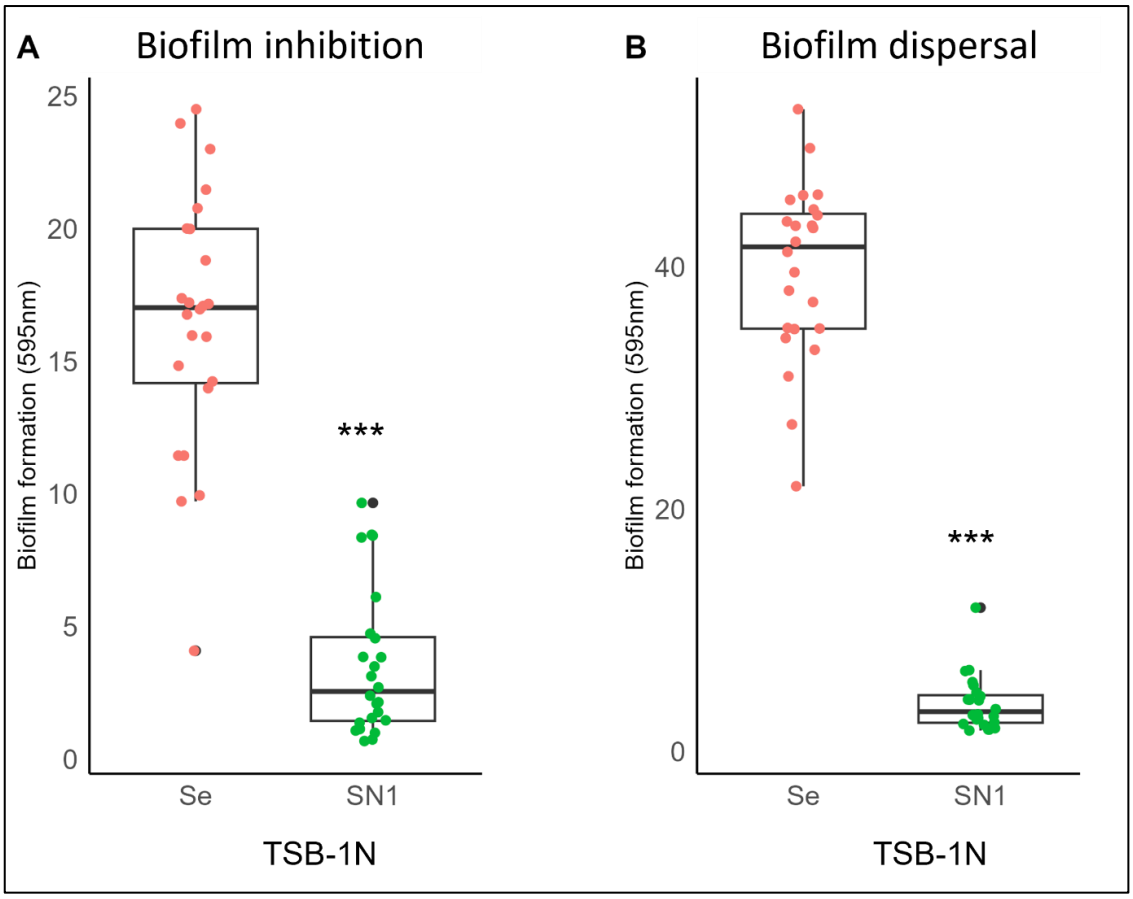

Figure 5.10. S. epidermidis biofilm formation and dispersal by C. parapsilosis CFS. *(A) C. parapsilosis CFS (SN1, 50% v/v) inhibits S. epidermidis biofilm formation in TSB media supplemented with 1% (w/v) NaCl (TSB-1N). (B) S. epidermidis biofilm was grown for 24 h and was dispersed by adding SN1 and incubating for a further 24 h. The biofilms were quantified with crystal violet staining. The boxes represent the interquartile range (IQR). The centre line in each box represents the median (50th percentile). The whiskers represent the largest or smallest absorbance values within 1.5 IQR above the 75th percentile or below the 25th percentile, respectively. The jitter points represent each single data point (n=24). Significance was calculated by students T-test (two-tailed). ***indicates P < 0.0001.*

The *S. epidermidis* biofilm matrix was assessed over time by dispersal with proteinase K, sodium metaperiodate and DNase I (Figure 5.11). The results show that while protein and eDNA seem to be important for the initial stages of biofilm formation in *S. epidermidis*, PIA and eDNA are the main constituents by 24 h (38% and 26%, respectively). Protein accounted for only 13% of the biofilm biomass at 24 h.

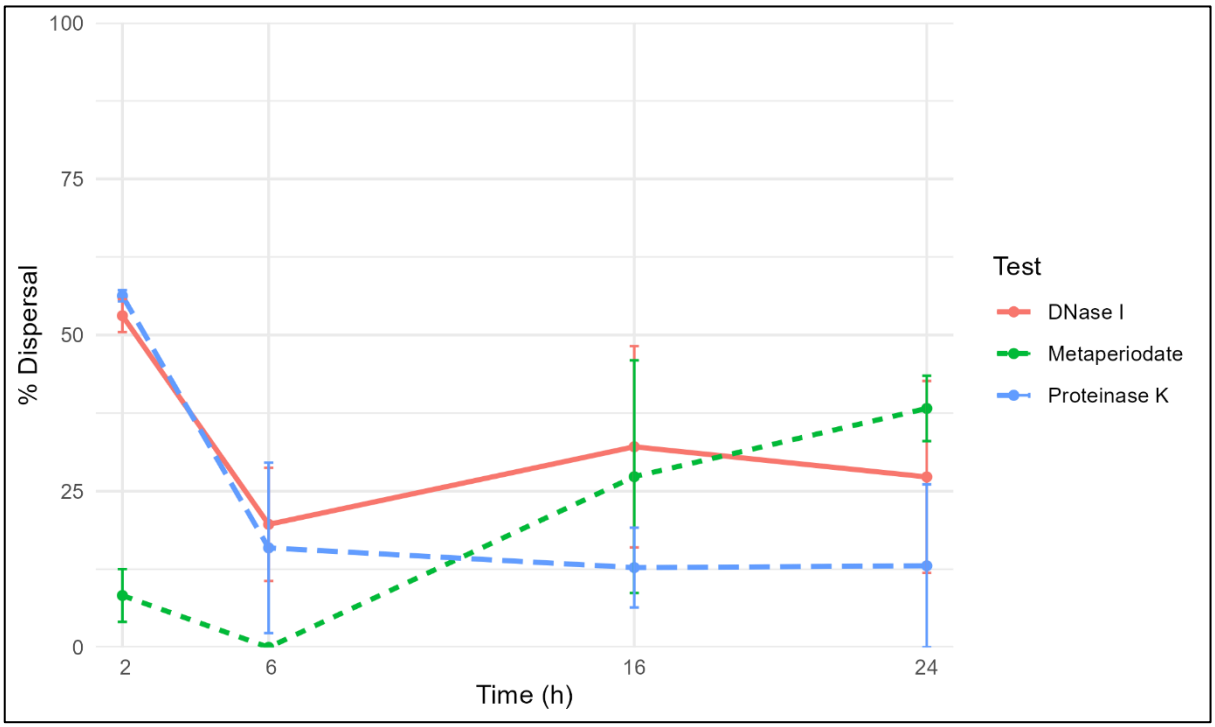

Figure 5.11. S. epidermidis biofilm matrix composition over 24 h*. Biofilm matrix composition was measured by percentage dispersal relative to the control at that time. Proteinase K, sodium metaperiodate, and DNase I were used to degrade protein, PIA (polysaccharide intracellular adhesin), and extracellular DNA, respectively. Error bars represent ±SE.*

5.2.9. *Candida albicans* supernatant is effective against *S. epidermidis*.

The effect on *S. epidermidis* by *C. albicans* CFS (CaSN) was measured using the crystal violet assay. *S. epidermidis* was grown in TSB-1N with or without the presence of CaSN

(50% v/v) at 37°C for 24 h (Figure 5.12). CaSN significantly inhibited the formation of *S. epidermidis* biofilm by 54% ($P < 0.0001$).

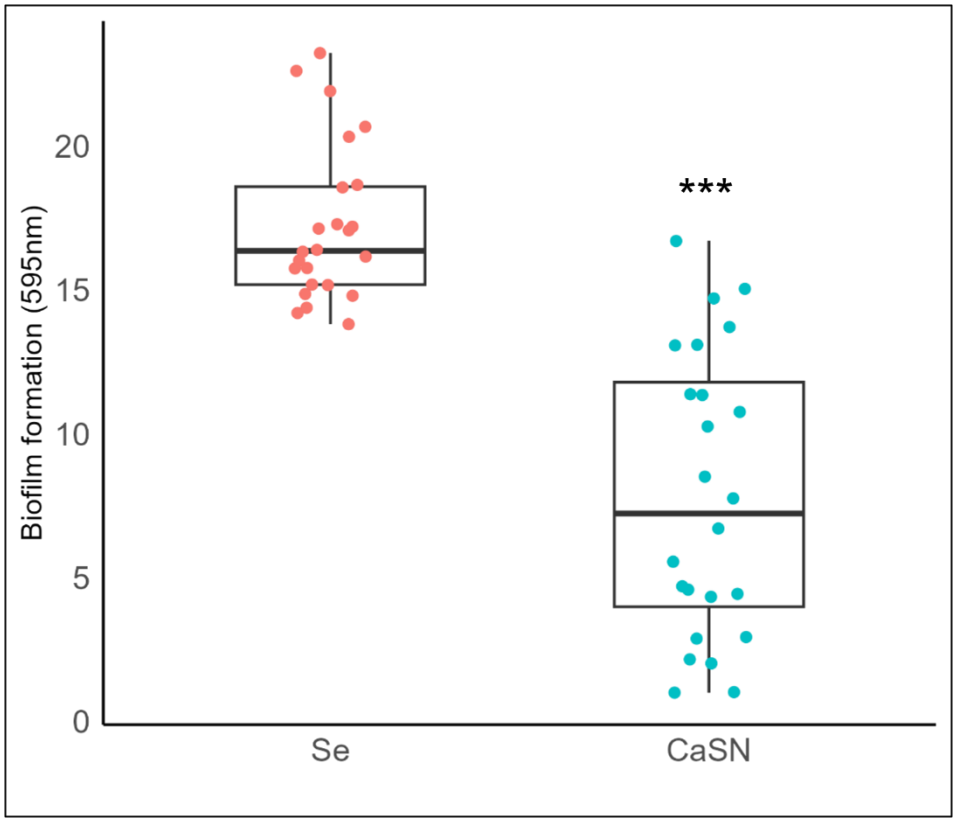

Figure 5.12. C. albicans CFS inhibitory effect on S. epidermidis biofilm formation. *S. epidermidis (Se) biofilm formation in TSB supplemented with 1% NaCl is inhibited when grown with C. albicans CFS (CaSN) (50% v/v). Biofilms were grown in 96 well plates for 24 h at 37°C. Biofilm biomass was quantified with crystal violet staining. The boxes represent the interquartile range (IQR). The centre line in each box represents the median (50th percentile). The whiskers represent the largest or smallest absorbance values within 1.5 IQR above the 75th percentile or below the 25th percentile, respectively. The jitter points represent each single data point (n=24). Significance was calculated by students T-test (two-tailed). **indicates P < 0.001.*

5.4. Discussion

Cell-free supernatant (CFS) derived from microorganisms have the potential as a source for novel therapeutics (Aminnezhad, Kermanshahi and Ranjbar, 2015; Glatthardt *et al.*, 2020; Alghofaili, 2022). This is far from a novel concept as the foundation of the biopharmaceutical industry is the use of microorganisms as cell-factories. Microbial interactions and competition are the source of potentially useful biomolecules (Tshikantwa *et al.*, 2018). The aim of this chapter was to characterise the fungal CFS and to determine the identity of the secreted anti-biofilm factor(s).

Crystal violet staining is a widely used biofilm quantitative method because it is a robust and cost-efficient method. Despite this, it is a variable method for biofilm quantification, with some researchers demonstrating poor reproducibility between experiments (Peeters, Nelis and Coenye, 2008; Kragh *et al.*, 2019). Confirmation of *S. aureus* biofilm inhibition by *C. parapsilosis* CFS was carried out by measuring the biofilm dry weights. Using this method, the *C. parapsilosis* CFS inhibition of *S. aureus* biofilm was measured at 80% ($P < 0.01$) in TSB-0.2G media (Figure 5.1). This method has its own difficulties, as it requires a standardised method to ensure each well is treated the same.

C. parapsilosis CFS collected at an early (6 h) and late (24 h) timepoint were effective at inhibiting SA1 biofilm (Figure 5.2). This indicates that *C. parapsilosis* is secreting the active factor by 6 h of growth in this media. CFS collected at 6 h reduced significantly ($P < 0.0001$) more biofilm than CFS collected at 24 h. This suggests that while the active factor is produced at early timepoints, its levels in the CFS may decrease or fluctuate over time.

The *Candida parapsilosis* CFS, like other microbial supernatants, is composed of a mixture of secreted proteins, metabolites, and other small molecules that are produced as the cells grow (Mani-López, Arrioja-Bretón and López-Malo, 2022). Various biochemical and fractionation methods can be used to characterise a mixture of interest. Here, size-fractionation of the supernatant revealed that there may be more than one active molecule in the *C. parapsilosis* CFS (Figure 5.5). Only a single cut-off (5

kDa) filter was used here to fractionate the fungal CFS. Using multiple molecular weight cut-offs would allow us to identify a size range. In addition, the active molecules were resistant to heat and treatment with proteinase K and pepstatin A (Figure 5.4 and 5.5, respectively). Therefore, it is unlikely the anti-biofilm molecules are proteinaceous in nature. A study by Glatthardt *et al*. demonstrated that *S. epidermidis* produces small molecules (between 3 – 10 kDa) that inhibited *S. aureus* biofilm (Glatthardt *et al.*, 2020). Comparable to the results presented here, these active molecules were also resistant to proteinase K and heat treatment.

C. albicans CFS inhibited SA1 biofilm formation by 69% (Figure 5.6). These results were very interesting as most published literature focuses on the synergism between *C. albicans* and *S. aureus* (Carlson and Johnson, 1985; Kong *et al.*, 2016). Our hypothesis is that the active factor(s), secreted by *C. parapsilosis* and *C. albicans*, result in a decrease in bacterial matrix formation. In contrast, a previous study has demonstrated that *C. albicans* (SC5314) induced *S. aureus* (USA300 strain) matrix formation by the upregulation of the *ica* operon and downregulation of *lrg* (Vila *et al.*, 2021). Furthermore, *nuc* (which encodes the *S. aureus* thermonuclease) was downregulated during co-culture. Therefore, matrix components PIA and eDNA were likely increased. The study by Vila *et al.* was conducted *in vivo* using a murine model (Vila *et al.*, 2021). Furthermore, while our results are contrary to this published study, we have already shown that there is a strain-dependent effect. Perhaps the inhibitory effect that *C. parapsilosis* and *C. albicans* can exert is only effective against a narrow range of MSSA *S. aureus* strains.

The importance of metabolism for biofilm survival has been highlighted (Lindgren *et al.*, 2014; Nassar *et al.*, 2021). Likewise, metabolites can be involved in inter-species communication. Fungal metabolites have previously been identified that control biofilm formation (reviewed in (Estrela and Abraham, 2016)). *C. parapsilosis* CFS samples SN1 and SN6, along with *C. albicans* CFS were analysed using a targeted metabolomic approach. A media control was included as previous studies have noted media-

dependent influences on metabolites (López-Ramos *et al.*, 2021; Fitzgerald *et al.*, 2022). Our hypothesis is that the active small molecules responsible for *S. aureus* biofilm inhibition may be metabolites.

For each sample group, metabolites with significantly increased concentration compared to the media control were identified (Figure 5.9). One metabolite, TG(18:2_38:4), was increased significantly compared to the media control between SN1 and SN6 only. TG(18:2_38:4) is a triglyceride. Triglycerides are composed of fatty acids and glycerol. They are a major form of stored lipids (Cecil and Jack, 1965). While studies that linked this particular triglyceride to biofilm formation in *S. aureus* or other bacteria were not identified, other fatty acids have been shown to inhibit *S. aureus* biofilm (Lee, Kim and Lee, 2022).

Eight metabolites were identified as increased in both SN6 and CaSN groups. One metabolite was identified that has been potentially flagged as an anti-biofilm compound. Aconitic acid was identified through molecular simulation as a potential inhibitor of diguanylate cyclases, which play a role in biofilm formation signalling (Pestana-Nobles, Leyva-Rojas and Yosa, 2020).

Bile acids have been demonstrated to have both enhancing and inhibiting effects on biofilm formation in different bacterial species (Hung *et al.*, 2006; Sanchez *et al.*, 2016). The bile acid identified in this metabolomics study, Glycochenodeoxycholic acid, was previously screened and demonstrated no antibiofilm activity against *Vibrio cholerae* or *Pseudomonas aeruginosa* (Sanchez *et al.*, 2016). Another of the metabolites identified, Homocysteine, is a sulphur -containing amino acid-related compound. Sulphur metabolism has been linked to positive biofilm formation in *S. aureus* and mycobacteria (Soutourina *et al.*, 2009; Virmani, Hasija and Singh, 2018).

The increased similarity between CaSN and SN6 sample groups over SN1 and SN6, despite the latter groups coming from the same species, was interesting and presents an opportunity for further analysis. One explanation for their similarity is that both *Candida albicans* and the *C. parapsilosis* CP6 isolate could form a biofilm in TSB-0.2G media, whereas the *C. parapsilosis* CP1 isolate could not. While an interesting avenue of research, the focus of this preliminary metabolomics study was to investigate any

similarity between all three sample groups, as all three fungal isolates produced a CFS with the ability to inhibit *S. aureus* biofilm.

Two metabolites (glutamine and indole acetic acid) were identified that were increased in concentration across all three CFS sample groups (Table 5.1). Amino acids are required by bacteria to support cell functions and alterations in amino acids have varied effects on the growth of pathogens and virulence factor expression (Ren *et al.*, 2018). While glucose and other sugars are the main carbon source preferentially utilised by *S. aureus*, when glucose becomes limited (e.g., during biofilm development) the bacteria can shift towards using amino acid metabolism for energy (Liebeke *et al.*, 2011).

As previously mentioned, glutamine is an amino acid that acts as a carbon and nitrogen source for cell biosynthetic pathways. Glutamine has been linked to increased virulence expression in bacteria. In *Listeria monocytogenes*, glutamine acted as an "on/off switch" for the induction of virulence genes (Haber *et al.*, 2017). Inactivation of a glutamine ABC transporter resulted in a dramatic decrease in virulence expression. This study demonstrated the importance of glutamine on the expression of virulence factors (Haber et al., 2017). In addition, elevated glutamine synthesis has been observed in *S. aureus* biofilm formation (Vudhya Gowrisankar *et al.*, 2021).

Indole acetic acid or Indole-3-Acetic Acid (IAA) was also significantly increased in SN1, SN6 and CaSN CFS samples. IAA was identified as a plant hormone that facilitates interactions between fungi, plants, and bacteria. Many bacteria (gram-positive and gram-negative) produce indole (Lee and Lee, 2010). It is a signalling molecule that facilitates interspecies and interkingdom communication. Though, there is no clearly defined target through which indole exerts its effects (Kim and Park, 2015). Indole molecules are of interest as bioactive molecules to control bacterial behaviour (reviewed in (Melander, Minvielle and Melander, 2014)).

IAA has antibiofilm activity against bacterial biofilms (Salini *et al.*, 2019). Interestingly, it has previously been demonstrated that IAA can have opposing effects depending on its concentration. At high concentrations it has a negative effect on biofilm and at low concentrations it can stimulate biofilm (Plyuta *et al.*, 2013). Under *in vitro* conditions, IAA acted synergistically with undecanoic acid to inhibit the biofilm formation of gram-

negative bacterial species, *Vibrio harveyi*. Few studies have investigated the effect of IAA on *S. aureus*. One study showed that IAA alone did not affect *S. aureus* viability, while combined IAA and horse radish peroxidase resulted in a bactericidal effect (Pugine *et al.*, 2010). However, IAA was produced in a marine bacterial strain that demonstrated antibacterial activity towards *S. aureus* (Bertrand *et al.*, 2023). An IAA-related molecule 3-Indole Acetonitrile exhibited anti-biofilm activity against *S. epidermidis* (Akbar *et al.*, 2023). In another study, the same 3-IA compound was used to decrease *E. coli* biofilm and reduce the virulence of *P. aeruginosa* (Lee, Cho and Lee, 2011).

The various fungal CFS sample groups showed similarity to the TSB media control (Figure 5.7 and Figure 5.8B). A greater separation was expected but this may be explained by TSB as a nutrient rich complex medium. A targeted metabolomics approach was used as an initial screen for potentially interesting metabolites in the fungal CFS that may explain the biofilm inhibition phenotype we observe. The focus was to identify metabolites that were significantly increased across all fungal samples compared to the control. However, chromatographic affinity fractionation may be a better approach to identify the anti-biofilm factor in *C. parapsilosis* and *C. albicans* CFS. Affinity columns, depending on the separation material used, can be used to tell researchers whether an unknown molecule of interest is polar, non-polar, its charge etc. This method can narrow the pool of target biomolecules. Previous studies have utilised these methods to investigate active factors within microbial supernatants. Fujiwara *et al.,* used gel filtration and ammonium sulphate fractionation to identify the molecular weight and proteinaceous nature of an inhibitory binding factor produced by Bifidobacteria (Fujiwara *et al.*, 1997). Another study utilised solvent extraction, where the active molecules in the CFS were soluble in ethyl acetate indicating they were nonpolar (Glatthardt *et al.*, 2020).

Untargeted metabolomics on samples already fractionated into a specific active fraction (demonstrating anti-biofilm activity) would aid in the identification of our active biomolecule(s). Furthermore, untargeted metabolomics could be used to identify possible novel metabolites. The metabolic study here was designed under the hypothesis that the active metabolites responsible for anti-biofilm activity were the

same in *C. parapsilosis* and *C. albicans*. It is possible that the active molecules secreted by *C. parapsilosis* are not the same as those secreted by *C. albican*s.

The ability of potential biomolecules to inhibit more than one target species is an attractive property. The *C. parapsilosis* CFS was effective against another *Staphylococcal* species. *S. epidermidis* is the fourth-most common species to be co-isolated with *C. albicans* from bloodstream infections (Klotz, Chasin, *et al.*, 2007). *S. epidermidis* biofilm was inhibited 78% by *C. parapsilosis* CFS (Figure 5.10). The *S. epidermidis* isolate produced a mixed matrix biofilm with higher levels of PIA and eDNA than protein, accounting for 38% and 26% of the biofilm biomass, respectively (Figure 5.11). PIA is the main functional component in most *S. epidermidis* biofilm (O'Gara, 2007). However, strains lacking the genes that encode PIA may still produce biofilm via the cell-wall linked protein Aap. This demonstrates the wide potential applicability of the CFS. *C. albicans* CFS was capable of inhibiting *S. epidermidis* biofilm formation (Figure 5.12) and our hypothesis that *C. albicans* produces the same or similar anti-biofilm factors as *C. parapsilosis*.

In conclusion, the data presented here indicate that the anti-biofilm molecules secreted by *C. parapsilosis* are heat-stable and not proteinaceous in nature. *C. albicans* may be producing similar active biomolecules to *C. parapsilosis* as it also inhibited SA1 biofilm formation. Targeted metabolomics identified two metabolites in common between the *C. parapsilosis* CFS samples and the *C. albicans* sample. In addition, these active biomolecules are effective in reducing biofilm formation in *S. epidermidis* demonstrating cross-species activity. While the potential metabolic nature of these biomolecules was investigated further characterisation and experimental investigation is required to identify the active biomolecules responsible for the bacterial biofilm inhibition.

Chapter 6 – Conclusions and Future Directions

The ability to produce a biofilm is a major virulence trait of many pathogens. Existence within a biofilm affords microorganisms enhanced protection compared to a planktonic lifestyle (Archer *et al.*, 2011). The antimicrobial resistance crisis is an imminent threat to human health. Biofilms represent a major hurdle in fighting this threat. *S. aureus* is a major source of device-related infection. These types of infections are extremely difficult to manage and have high rates of morbidity (Fätkenheuer, Cornely and Seifert, 2002). New therapies are needed to prevent biofilm formation in this bacterial pathogen.

Many biofilm infections are polymicrobial in nature, containing bacteria, fungi and viruses (Wolcott *et al.*, 2013; Anju *et al.*, 2022). The incidence of non-*albicans Candida* is rising. Few studies focus on the interaction between *S. aureus* and non-*albicans Candida*. The emerging fungal pathogen *Candida parapsilosis* is associated with neonatal infection and candidiasis (van Asbeck *et al.*, 2007; Trofa, Gácser and Nosanchuk, 2008). It is a common skin commensal and resides in similar niches on the human body, suggesting that *S. aureus* and *C. parapsilosis* may interact (Bonassoli, Bertoli and Svidzinski, 2005). Up to now, a very small number of studies have shown no interaction between these two species (Carlson and Johnson, 1985; Nash *et al.*, 2015).

In this thesis, investigations were undertaken to characterise and advance the understanding of the interactions that occur during *S. aureus* and *C. parapsilosis* co-culture. Interestingly we observed an antagonist relationship with *C. parapsilosis* inhibiting *S. aureus* biofilm formation.

6.1. *C. parapsilosis* inhibits *S. aureus* biofilm formation by targeting the biofilm matrix.

The incubation of *S. aureus* (SA1) in the presence of *C. parapsilosis* CFS under static biofilm growth conditions in TSB 0.2% glucose (TSB-0.2G) media resulted in decreased bacterial biofilm formation. The fungal CFS induced inhibition of biofilm formation was not a result of any growth defect or an inhibition of surface attachment (Figure 3.9 and

3.10). These data suggested that the *C. parapsilosis* CFS is targeting *S. aureus* biofilm maturation and not primary attachment. During maturation *S. aureus* produces a self-made extracellular matrix (ECM). Therefore, this is the likely target of the fungal CFS.

The ECM is generally composed of varying amount of carbohydrates, proteins (lysis-derived and secreted) and extracellular DNA (eDNA) (Fitzpatrick, Humphreys and O'Gara, 2005). Growth media can influence the type of ECM produced (Lade *et al.*, 2019). Altering the amount of glucose altered the levels of each matrix component (Table 6.1). In 1% and 0.2% glucose, the levels of protein were high. eDNA and PIA levels were altered depending on the levels of glucose, with SA1 having lower levels of both eDNA and PIA in 1% glucose media. Interestingly, the *C. parapsilosis* CFS had no effect on SA1 biofilm grown in 1% glucose. These data further indicate that a matrix component may be the target of the fungal CFS.

Table 6.1. Summary of the characterisation of *C. parapsilosis* CFS inhibition of *S. aureus* biofilm.

			Matrix component %		
	TSB media glucose	Inhibition (P <0.05)	protein	eDNA	PIA
SA1	0.2%	Yes	***	***	***
	1%	No	***	*	*
			***: 60-100%. **: 30-60%. *: <30%. % of biofilm dispersal by proteinase K, DNase I and metaperiodate, respectively.		

Incubation in the presence of *C. parapsilosis* cells or CFS led to a global effect on gene expression. RNA-sequencing detected hundreds of genes that were differentially expressed. The differential expression of so many genes may be explained by the various global regulators of biofilm and virulence that were differentially expressed; *agrAC*, *arlRS, mgrA,* and *SigB* (Table 3.3). Many of the genes that were significantly upregulated were virulence factors, like *nuc* (nuclease), *hla* (alpha toxin), and various proteases. In contrast, treatment of SA1 grown in TSB 1% glucose (TSB-1G) with *C. parapsilosis* CFS

did not have any effect on the amount of biofilm produced (Figure 4.1). Under these conditions only a handful of DEGs were identified. This data suggests that the anti-biofilm effect of the fungal CFS seen in TSB-0.2G media could be due to gene expression changes in *S. aureus.*

In SA1 there is evidence that eDNA is a target. RNA-sequencing revealed an increase in expression of the *nuc* gene in SA1 biofilm cells treated with fungal CFS in 0.2% glucose media but not 1% glucose media. This gene produces a thermonuclease that degrades eDNA. This suggests that the fungal CFS is increasing DNase levels in the supernatant leading to the degradation of matrix eDNA and less biofilm formation. Experiments using DNase agar also demonstrated the increase in DNase levels in fungal CFS treated biofilm supernatants in 0.2% glucose but not 1% glucose. Also, Table 6.1 shows that eDNA is not important for SA1 biofilm formation in 1% glucose. Therefore, the fungal CFS would not have any effect on biofilm formation under these conditions. The *lrgAB* operon, which is involved in autolysis repression and thus prevents release of eDNA, was differentially expressed. Furthermore, subinhibitory concentrations of oxacillin induced SA1 biofilm. The phenomenon of beta-lactam subinhibitory induced biofilm formation is known to be eDNA dependent (Kaplan *et al.*, 2012). This induction was prevented by the *C. parapsilosis* CFS. These data strengthen our hypothesis that eDNA is an important target of the CFS in SA1.

RNA-sequencing also revealed increased expression levels of protease genes. This was confirmed by protease activity assays. An increase in protease activity has been shown to result in matrix protein degradation and biofilm inhibition (Park *et al.*, 2012). Also, upregulation of proteases such as the metalloprotease aureolysin, a negative regulator of biofilm, can degrade proteins in the matrix (Loughran *et al.*, 2014). The upregulation of proteases and virulence factors by the Agr quorum sensing system can detach *S. aureus* biofilms and *agr* is activated by changes in the extracellular environment (Boles and Horswill, 2008). Here, the CFS modulates SA1 ability to alter its extracellular environment (Figure 4.6). The increase in pH was not enough to induce activation of the Agr QS system (Todd, Noverr and Peters, 2019), although it may still play a role in biofilm inhibition.

Finally, PIA, the carbohydrate matrix constituent, may also be a target of the fungal CFS. Genes that are involved in the production of the PIA were downregulated (*icaA*, *icaB* and *icaC*) suggesting the inhibitory effect may be due to lower levels of PIA.

As nuclease, protease and PIA expression may all play a role in the inhibition of SA1 biofilm, it is difficult to examine the contribution of each to the biofilm inhibition that we observe. Using genetically modified strains that lack target genes of interest (eg. *nuc*, *ica*, and *aur*) may be useful.

Overall, these data indicate that the fungal CFS is having pleiotropic effects on *S. aureus* biofilm formation and may have more than one matrix target.

6.2. *C. parapsilosis* may inhibit *S. aureus* biofilm formation via repression of a key metabolic pathway and modulating pH homeostasis.

Biofilms are complex communities with diverse metabolic niches within. Our RNA-seq experiment took total RNA from cells across the *S. aureus* biofilm. KEGG analysis led us to take a closer look at genes involved in arginine biosynthesis and the arginine deiminase (ADI) pathway. In TSB-0.2G media, genes of the ADI pathway (*arcABDC and arcR*) were significantly downregulated when SA1 was co-cultured with *C. parapsilosis* CFS. This was not the case in TSB-1G. To visualise this, a heatmap was created to compare specific genes across the two RNA experiments (Figure 6.1).

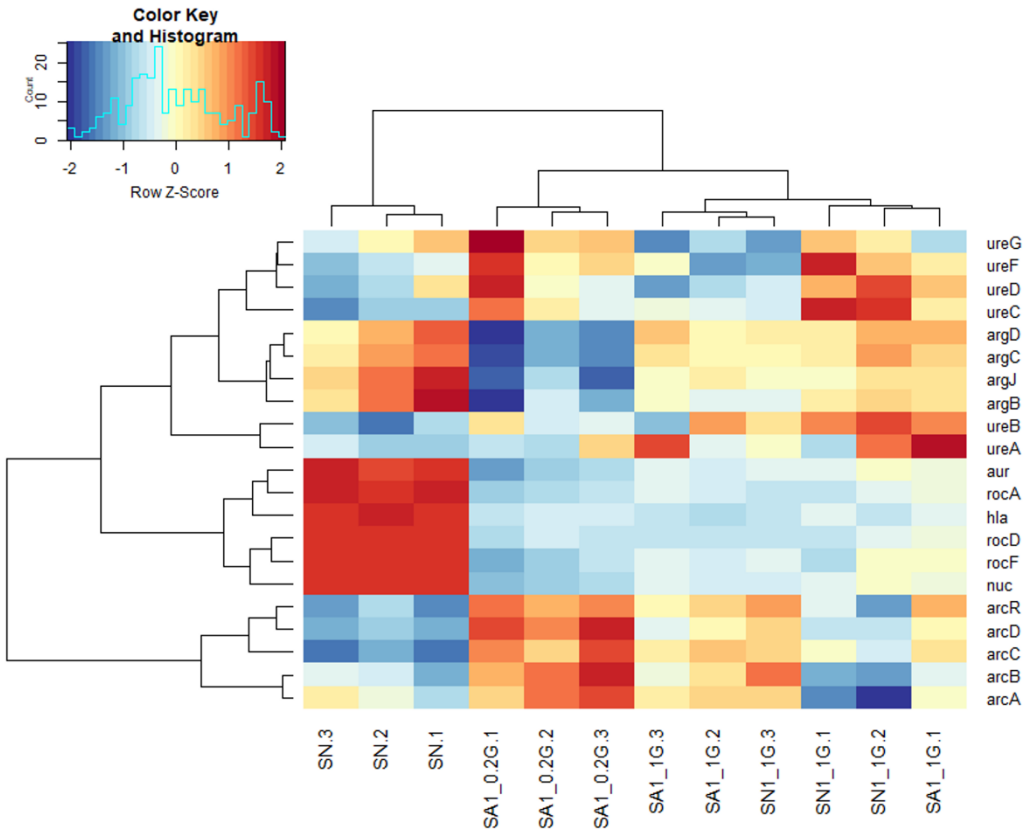

Figure 6.1. Heatmap of specific genes comparing gene expression across RNA-seq experiments. *RNA-sequencing sample gene counts from two experiments in two different media types (TSB 0.2% glucose and TSB 1% glucose) were compared. Specific differentially expressed genes of interest in the SN1-treated SA1 biofilm condition grown in TSB-0.2G were chosen. These include genes associated with the urea cycle (ureABCDEF), arginine biosynthesis (argBCDJ), the arginine deiminase pathway (arcABDC and arcR), the arginase pathway (rocA and rocF), and other highly upregulated genes (nuc, hla, and aur). SA1_1G and SN1_1G represent the control and CFS treated samples in TSB 1% glucose media, respectively. SA1_0.2G and SN represent the control and CFS treated samples in TSB 0.2% glucose media, respectively.*

C. parapsilosis CFS may be inhibiting *S. aureus* biofilm formation in part via modulation of the ADI pathway. The ADI pathway is required for energy production under anaerobic conditions (Makhlin *et al.*, 2007). When glucose becomes limited, arginine can be used as the sole source of energy (Cunin *et al.*, 1986). We hypothesise, that after 24 h of

growth when the availability of glucose is low, a functional ADI pathway is required for biofilm formation. This is supported by another study that reported that the ADI pathway was significantly upregulated under normal *S. aureus* biofilm conditions (Vlaeminck *et al.*, 2022). Inactivation of the arginine deiminase, ArcA, results in a marked decrease in biofilm (Vlaeminck *et al.*, 2022), and deletion of *arcD* resulted in a decrease in intercellular adhesin (PIA) deposition (Zhu *et al.*, 2007). It is reasonable to suggest that downregulation of these same genes due to the *C. parapsilosis* CFS could explain the downregulation of *ica* operon and the decrease in biofilm observed.

When we compare the 1% glucose condition to the 0.2% glucose condition, the ADI pathway is repressed in 1% glucose (Figure 6.1). This makes sense as the *arc* operon is under the control of catabolite repression and low glucose levels are required for de-repression (Makhlin *et al.*, 2007).

Arginine catabolism occurs via the arginase pathway also. Arginine is catabolised to L-glutamate. This then serves as a carbon source for the TCA cycle (Halsey *et al.*, 2017). Genes of this pathway (*rocA, rocD,* and *rocF*) were upregulated in the CFS-treated condition in TSB-0.2G only. This suggests that in low glucose and the absence of an active ADI pathway *S. aureus* utilises glutamate as a carbon source for energy. If the cells can maintain energy, it stands to reason that the other role of the ADI pathway is critical for biofilm formation.

The ADI pathway and urease metabolism play an additional role in pH regulation. Treatment with *C. parapsilosis* CFS resulted in an increase in the extracellular pH (Figure 4.6). As discussed above, we determined that this increase in pH was not responsible for the inhibition of biofilm as buffering the extracellular environment to a higher pH did not prevent biofilm inhibition (Figure 4.7). Instead, intracellular pH may play a role. Downregulation of the urease genes in CFS treated SA1 in TSB-0.2G is explained by the upregulation of *mgrA* (Crosby et al., 2016). Additionally, genes of the Kdp K+ uptake system were significantly downregulated by CFS treatment. These genes have been linked to pH homeostasis and are upregulated during *S. aureus* biofilm growth (Cotter and Hill, 2003; Beenken *et al.*, 2004; Price-Whelan *et al.*, 2013). Furthermore, pH homeostasis was crucial for biofilm maturation in *S. epidermidis* (Lindgren *et al.*, 2014). Together, the inactivation of these pH regulating systems during co-culture with *C.*

parapsilosis or its CFS may lead to the inability of *S. aureus* to regulate its intracellular pH environment and thus prevent biofilm maturation.

How *C. parapsilosis* CFS is repressing the ADI pathway and indeed triggering the differential expression of hundreds of other genes in TSB-0.2G media is unclear. As mentioned previously, in 1% glucose media (TSB-1G) we observed fewer changes in gene expression. A possible explanation is that the *C. parapsilosis* CFS may be targeting these pathways that are required in low glucose conditions (0.2%) but are already repressed in glucose abundant conditions (1%) and so their repression has no effect on *S. aureus*.

6.3. The *C. parapsilosis* inhibitory effect is conserved across *Staphylococcal* species.

In addition to SA1, biofilm formation of two more *S. aureus* strains, SH1000 and SA2, was also significantly inhibited by CFS. Our experiments with SH1000 and SA2 indicate that while the biofilm inhibitory effect is conserved, *C. parapsilosis* CFS may employ a strain-dependent mechanism of biofilm inhibition.

SH1000 biofilm was inhibited by the fungal CFS is both 0.2% and 1% glucose media. The inhibition in 1% glucose media was lesser than what was observed in 0.2% (30% inhibition) (Figure 4.8). Despite high levels of eDNA in the biofilm matrix in both 0.2% and 1% glucose media (Figure 4.9), no increase in DNase activity was seen in SH1000 (Table 4.4). Furthermore, no increase in protease activity was detected either (Figure 4.2). In addition, PIA is not an important matrix constituent in SH1000 making it an unlikely target in this strain. These data taken together suggest a strain dependent mechanism of inhibition by the *C. parapsilosis* CFS. Further analysis of the inhibitory effect in SH1000 is needed to identify the mechanism of biofilm inhibition. We do not have RNA-sequencing data for this strain. Future work could use RNA-sequencing or targeted qRT-PCR to examine the expression of genes of interest (i.e., *nuc*, *icaADBC*, or *agrAC*).

The inhibitory effect of *C. parapsilosis* CFS is conserved in another *Staphylococcal* species. In Chapter 5, we demonstrated that *C. parapsilosis* CFS is effective in reducing *S. epidermidis* biofilm. Considering the strain-dependent effects of the fungal CFS in *S. aureus*, a different mechanism in *S. epidermidis* may be likely. However, despite biofilm growth in TSB supplemented with NaCl instead of glucose, there were higher levels of PIA and eDNA compared to protein (Figure 5.12), which was similar to the trend we saw in SA1 and SH1000. Future work could expand on the effect observed in *S. epidermidis*.

6.4. Fungal anti-biofilm factors may be conserved between *Candida* species.

In chapter 5, characterisation of the *C. parapsilosis* CFS revealed that there are possibly multiple anti-biofilm factors. These factors are heat stable and potentially metabolic in nature. *C. albicans* CFS was also effective in reducing *S. aureus* biofilms. More than one active factor in the CFS may explain the global impact of the CFS on *S. aureus* gene expression or the strain dependent effect we see between SA1 and SH1000. There is much investigation still to be done.

Treatment of the CFS with proteinase K did not impact the anti-biofilm activity meaning that the active factors were not proteinaceous in nature (Figure 5.4). Therefore, as an initial screen, we used targeted metabolomics to identify a range of metabolites in the CFS samples. Glutamine and IAA were identified as potential metabolites responsible for biofilm inhibition, due to their common increased presence across the CFS samples we tested. Glutamine acts as a carbon source and its synthesis is important for biofilm formation in *S. aureus* (Vudhya Gowrisankar *et al.*, 2021). However, while IAA has been linked to anti-biofilm activity in other microbial species, including *S. epidermidis* (Lee, Cho and Lee, 2011; Salini *et al.*, 2019; Akbar *et al.*, 2023), there is no evidence to support antibiofilm activity in *S. aureus*. Further work is needed to confirm if either metabolite possesses anti-biofilm activity. This could be done by supplementing *S. aureus* growth media with glutamine or IAA.

Identification of the active components in the fungal CFS is needed to gain a fuller understanding of the anti-biofilm mechanism of action. Targeted metabolomics, as implied by the name, searches only for certain known metabolites. A preferred route of investigation would be to first extract the biologically active molecules with different solvents that can separate the CFS into biologically active fractions. For example, Glatthardt *et al*. (2020) used ethyl acetate to extract a molecule with anti-biofilm properties (Glatthardt *et al.*, 2020). Extraction with this solvent indicated the molecule was non-polar. Once the active molecules were separated from the *C. parapsilosis* CFS, size fractionation followed by untargeted metabolomics could be used to identify the unknown anti-biofilm factors.

A collection of gene knockouts in *C. parapsilosis* has previously been constructed (Holland *et al.*, 2014). This mutant library contains almost 100 strains carrying double allele deletions in transcription factors, protein kinases and species-specific genes. Using this knockout library, we could screen for a mutant that lacks the ability to produce a CFS that inhibits *S. aureus* biofilm. This would be interesting but presents challenges of its own. The crystal violet assay while high-throughput is highly variable and the inhibition trend that we investigated is sometimes difficult to spot due to inherent variability in biofilm formation. Therefore, it is likely that a researcher may miss something. Another method such as dry weight or increased replicates when using crystal violet would be needed.

The effect of the *C. parapsilosis* CFS on bacterial biofilm was dose dependent. As the type of biofilm matrix *S. aureus* made varied depending on the media used, we were unable to test alternate media backgrounds for producing the CFS. This media effect needs to be eliminated. Therefore, an approach whereby the SN is concentrated and dehydrated should be taken. Then the CFS could be grown in different media of choice then dehydrate it and resuspend in a neutral buffer.

6.5. Contributions and overall conclusion

Exploring the interactions between microorganisms presents a potential source of novel therapies against biofilm infections. Furthermore, characterising these interactions can give further insight into biofilm formation mechanisms employed by major pathogens like *S. aureus*.

The interaction between the human pathogens, *C. parapsilosis* and *S. aureus,* was characterised here for the first time, highlighting the novelty of the data presented here. A previous study investigated if, like *C. albicans*, *C. parapsilosis* would augment *S. aureus* virulence in a murine infection model and the researchers did not observe any increased virulence when a sub-lethal dose of *S. aureus* was co-infected with *C. parapsilosis* (Carlson and Johnson, 1985). However, their experimental design would not have identified any antagonistic behaviour. Data presented in this thesis demonstrate that an antagonistic relationship exists between *C. parapsilosis* and *S. aureus*.

C. parapsilosis is producing anti-biofilm factors that inhibit biofilm formation in *S. aureus*. It was demonstrated that the fungal CFS inhibitory effect is conserved in different *Staphylococcal* species. Furthermore, it was also shown for the first time that *C. albicans* produces an anti-biofilm factor effective against *Staphylococcal* species. These antibiofilm factors, with further investigation could potentially be used as biocontrol agents against *Staphylococcal* pathogens.

References

Abraham, N.M. and Jefferson, K.K. (2012) 'Staphylococcus aureus clumping factor B mediates biofilm formation in the absence of calcium', *Microbiology*, 158(Pt 6), pp. 1504–1512. Available at: https://doi.org/10.1099/mic.0.057018-0.

Afgan, E. *et al.* (2016) 'The Galaxy platform for accessible, reproducible and collaborative biomedical analyses: 2016 update', *Nucleic Acids Research*, 44(W1), pp. W3–W10. Available at: https://doi.org/10.1093/nar/gkw343.

Ahn, K.B. *et al.* (2018) 'Lipoteichoic Acid Inhibits Staphylococcus aureus Biofilm Formation', *Frontiers in Microbiology*, 9. Available at: https://www.frontiersin.org/articles/10.3389/fmicb.2018.00327 (Accessed: 7 February 2023).

Akbar, M.U. *et al.* (2023) 'Biofilm Formation by Staphylococcus epidermidis and Its Inhibition Using Carvacrol, 2-Aminobenzemidazole, and 3-Indole Acetonitrile', *ACS Omega*, 8(1), pp. 682–687. Available at: https://doi.org/10.1021/acsomega.2c05893.

Alghofaili, F. (2022) 'Use of bacterial culture supernatants as anti-biofilm agents against Pseudomonas aeruginosa and Klebsiella pneumoniae', *European Review for Medical and Pharmacological Sciences*, 26(4), pp. 1388–1397. Available at: https://doi.org/10.26355/eurrev_202202_28132.

Alves, D.R. *et al.* (2014) 'Combined Use of Bacteriophage K and a Novel Bacteriophage To Reduce Staphylococcus aureus Biofilm Formation', *Applied and Environmental Microbiology*, 80(21), pp. 6694–6703. Available at: https://doi.org/10.1128/AEM.01789-14.

Amador, C.I., Sternberg, C. and Jelsbak, L. (2018) 'Application of RNA-seq and Bioimaging Methods to Study Microbe-Microbe Interactions and Their Effects on Biofilm Formation and Gene Expression', *Methods in Molecular Biology (Clifton, N.J.)*, 1734, pp. 131–158. Available at: https://doi.org/10.1007/978-1-4939-7604-1_12.

Aminnezhad, S., Kermanshahi, R.K. and Ranjbar, R. (2015) 'Evaluation of Synergistic Interactions Between Cell-Free Supernatant of Lactobacillus Strains and Amikacin and Genetamicin Against Pseudomonas aeruginosa', *Jundishapur Journal of Microbiology*, 8(4), p. e16592. Available at: https://doi.org/10.5812/jjm.8(4)2015.16592.

Anders, S., Pyl, P.T. and Huber, W. (2015) 'HTSeq—a Python framework to work with high-throughput sequencing data', *Bioinformatics*, 31(2), pp. 166–169. Available at: https://doi.org/10.1093/bioinformatics/btu638.

Anju, V.T. *et al.* (2022) 'Polymicrobial Infections and Biofilms: Clinical Significance and Eradication Strategies', *Antibiotics*, 11(12), p. 1731. Available at: https://doi.org/10.3390/antibiotics11121731.

Archer, N.K. *et al.* (2011) 'Staphylococcus aureus biofilms', *Virulence*, 2(5), pp. 445–459. Available at: https://doi.org/10.4161/viru.2.5.17724.

Arya, R. and Princy, S.A. (2016) 'Exploration of Modulated Genetic Circuits Governing Virulence Determinants in Staphylococcus aureus', *Indian Journal of Microbiology*, 56(1), pp. 19–27. Available at: https://doi.org/10.1007/s12088-015-0555-3.

van Asbeck, E.C. *et al.* (2007) 'Candida parapsilosis fungemia in neonates: genotyping results suggest healthcare workers hands as source, and review of published studies', *Mycopathologia*, 164(6), pp. 287–293. Available at: https://doi.org/10.1007/s11046-007-9054-3.

Ashburner, M. *et al.* (2000) 'Gene Ontology: tool for the unification of biology', *Nature Genetics*, 25(1), pp. 25–29. Available at: https://doi.org/10.1038/75556.

Baelo, A. *et al.* (2015) 'Disassembling bacterial extracellular matrix with DNase-coated nanoparticles to enhance antibiotic delivery in biofilm infections', *Journal of Controlled Release: Official Journal of the Controlled Release Society*, 209, pp. 150–158. Available at: https://doi.org/10.1016/j.jconrel.2015.04.028.

Balibar, C.J. *et al.* (2010) 'cwrA, a gene that specifically responds to cell wall damage in Staphylococcus aureus', *Microbiology*, 156(5), pp. 1372–1383. Available at: https://doi.org/10.1099/mic.0.036129-0.

Bandara, H.M.H.N. *et al.* (2009) 'Escherichia coli and its lipopolysaccharide modulate in vitro Candida biofilm formation', *Journal of Medical Microbiology*, 58(12), pp. 1623–1631. Available at: https://doi.org/10.1099/jmm.0.012989-0.

Barbu, E.M. *et al.* (2014) 'SdrC induces staphylococcal biofilm formation through a homophilic interaction', *Molecular Microbiology*, 94(1), pp. 172–185. Available at: https://doi.org/10.1111/mmi.12750.

Bassetti, M. *et al.* (2015) 'Clinical and Therapeutic Aspects of Candidemia: A Five Year Single Centre Study', *PLOS ONE*, 10(5), p. e0127534. Available at: https://doi.org/10.1371/journal.pone.0127534.

Beenken, K.E. *et al.* (2004) 'Global Gene Expression in Staphylococcus aureus Biofilms', *Journal of Bacteriology*, 186(14), pp. 4665–4684. Available at: https://doi.org/10.1128/JB.186.14.4665-4684.2004.

Beenken, K.E., Blevins, J.S. and Smeltzer, M.S. (2003) 'Mutation of sarA in Staphylococcus aureus Limits Biofilm Formation', *Infection and Immunity*, 71(7), pp. 4206–4211. Available at: https://doi.org/10.1128/IAI.71.7.4206-4211.2003.

Begum, N. *et al.* (2022) 'Integrative functional analysis uncovers metabolic differences between Candida species', *Communications Biology*, 5(1), pp. 1–12. Available at: https://doi.org/10.1038/s42003-022-03955-z.

Benmouna, Z. *et al.* (2020) 'Ability of Three Lactic Acid Bacteria to Grow in Sessile Mode and to Inhibit Biofilm Formation of Pathogenic Bacteria', *Advances in Experimental Medicine and Biology*, 1282, pp. 105–114. Available at: https://doi.org/10.1007/5584_2020_495.

Berkow, E.L. and Lockhart, S.R. (2017) 'Fluconazole resistance in Candida species: a current perspective', *Infection and Drug Resistance*, 10, pp. 237–245. Available at: https://doi.org/10.2147/IDR.S118892.

Bertrand, C.D.F. *et al.* (2023) 'Saccharopolyspora sp. NFXS83 in Marine Biotechnological Applications: From Microalgae Growth Promotion to the Production of Secondary Metabolites', *Microorganisms*, 11(4), p. 902. Available at: https://doi.org/10.3390/microorganisms11040902.

Bhattacharya, M. *et al.* (2015) 'Prevention and treatment of Staphylococcus aureus biofilms', *Expert review of anti-infective therapy*, 13(12), pp. 1499–1516. Available at: https://doi.org/10.1586/14787210.2015.1100533.

Blair, J.M.A. *et al.* (2015) 'Molecular mechanisms of antibiotic resistance', *Nature Reviews Microbiology*, 13(1), pp. 42–51. Available at: https://doi.org/10.1038/nrmicro3380.

Boles, B.R. and Horswill, A.R. (2008) 'agr-Mediated Dispersal of Staphylococcus aureus Biofilms', *PLoS Pathogens*, 4(4). Available at: https://doi.org/10.1371/journal.ppat.1000052.

Boles, B.R. and Horswill, A.R. (2011) 'Staphylococcal biofilm disassembly', *Trends in microbiology*, 19(9), pp. 449–455. Available at: https://doi.org/10.1016/j.tim.2011.06.004.

Bonassoli, L.A., Bertoli, M. and Svidzinski, T.I.E. (2005) 'High frequency of Candida parapsilosis on the hands of healthy hosts', *The Journal of Hospital Infection*, 59(2), pp. 159–162. Available at: https://doi.org/10.1016/j.jhin.2004.06.033.

Bongomin, F. *et al.* (2017) 'Global and Multi-National Prevalence of Fungal Diseases—Estimate Precision', *Journal of Fungi*, 3(4). Available at: https://doi.org/10.3390/jof3040057.

Borges, K.R.A. *et al.* (2018) 'Adhesion and biofilm formation of Candida parapsilosis isolated from vaginal secretions to copper intrauterine devices', *Revista Do Instituto De Medicina Tropical De Sao Paulo*, 60, p. e59. Available at: https://doi.org/10.1590/S1678-9946201860059.

Borriello, G. *et al.* (2004) 'Oxygen Limitation Contributes to Antibiotic Tolerance of Pseudomonas aeruginosa in Biofilms', *Antimicrobial Agents and Chemotherapy*, 48(7), pp. 2659–2664. Available at: https://doi.org/10.1128/AAC.48.7.2659-2664.2004.

Bos, R., van der Mei, H.C. and Busscher, H.J. (1999) 'Physico-chemistry of initial microbial adhesive interactions – its mechanisms and methods for study', *FEMS*

Microbiology Reviews, 23(2), pp. 179–230. Available at: https://doi.org/10.1111/j.1574-6976.1999.tb00396.x.

Brown, J.W. and Grilli, A. (1998) 'An emerging superbug. Staphylococcus aureus becomes less susceptible to vancomycin', *MLO: medical laboratory observer*, 30(1), pp. 26–32; quiz 34–35.

Brown, M.M. and Horswill, A.R. (2020) 'Staphylococcus epidermidis—Skin friend or foe?', *PLOS Pathogens*, 16(11), p. e1009026. Available at: https://doi.org/10.1371/journal.ppat.1009026.

Brown, S., Santa Maria, J.P. and Walker, S. (2013) 'Wall Teichoic Acids of Gram-Positive Bacteria', *Annual review of microbiology*, 67, p. 10.1146/annurev-micro-092412–155620. Available at: https://doi.org/10.1146/annurev-micro-092412-155620.

Bu, D. *et al.* (2021) 'KOBAS-i: intelligent prioritization and exploratory visualization of biological functions for gene enrichment analysis', *Nucleic Acids Research*, 49(W1), pp. W317–W325. Available at: https://doi.org/10.1093/nar/gkab447.

Caiazza, N.C. and O'Toole, G.A. (2003) 'Alpha-Toxin Is Required for Biofilm Formation by Staphylococcus aureus', *Journal of Bacteriology*, 185(10), pp. 3214–3217. Available at: https://doi.org/10.1128/JB.185.10.3214-3217.2003.

Calderone, R.A. and Clancy, C.J. (2011) *Candida and Candidiasis*. American Society for Microbiology Press.

Camarillo-Márquez, O. *et al.* (2018) 'Antagonistic Interaction of Staphylococcus aureus Toward Candida glabrata During in vitro Biofilm Formation Is Caused by an Apoptotic Mechanism', *Frontiers in Microbiology*, 9. Available at: https://doi.org/10.3389/fmicb.2018.02031.

Campoccia, D., Montanaro, L. and Arciola, C.R. (2021) 'Extracellular DNA (eDNA). A Major Ubiquitous Element of the Bacterial Biofilm Architecture', *International Journal of Molecular Sciences*, 22(16), p. 9100. Available at: https://doi.org/10.3390/ijms22169100.

Carlson, E. and Johnson, G. (1985) 'Protection by Candida albicans of Staphylococcus aureus in the establishment of dual infection in mice.', *Infection and Immunity*, 50(3), pp. 655–659.

Carolus, H., Van Dyck, K. and Van Dijck, P. (2019) 'Candida albicans and Staphylococcus Species: A Threatening Twosome', *Frontiers in Microbiology*, 10, p. 2162. Available at: https://doi.org/10.3389/fmicb.2019.02162.

CDC (2021) *Candida auris | CDC*, *Candida auris | Candida auris | Fungal Diseases | CDC*. Available at: https://www.cdc.gov/fungal/candida-auris/index.html (Accessed: 23 January 2022).

Cecil, R. and Jack, M. (1965) 'Relation of triglycerides to phosphoglycerides in fungi', *Journal of the American Oil Chemists Society*, 42(12), pp. 1051–1053. Available at: https://doi.org/10.1007/BF02636903.

Cerca, N., Brooks, J.L. and Jefferson, K.K. (2008) 'Regulation of the Intercellular Adhesin Locus Regulator (icaR) by SarA, σB, and IcaR in Staphylococcus aureus', *Journal of Bacteriology*, 190(19), pp. 6530–6533. Available at: https://doi.org/10.1128/JB.00482-08.

Ceri, H. *et al.* (1999) 'The Calgary Biofilm Device: New Technology for Rapid Determination of Antibiotic Susceptibilities of Bacterial Biofilms', *Journal of Clinical Microbiology*, 37(6), pp. 1771–1776.

Chaignon, P. *et al.* (2007) 'Susceptibility of staphylococcal biofilms to enzymatic treatments depends on their chemical composition | SpringerLink', 75(1), pp. 125-132. Available at: https://doi.org/10.1007/s00253-006-0790-y.

Chambers, H.F. (1997) 'Methicillin resistance in staphylococci: molecular and biochemical basis and clinical implications.', *Clinical Microbiology Reviews*, 10(4), pp. 781–791.

Chanda, P.K. *et al.* (2010) 'Characterization of an unusual cold shock protein from Staphylococcus aureus', *Journal of basic microbiology*, 50(6), pp. 519–526. Available at: https://doi.org/10.1002/jobm.200900264.

Chen, Q. *et al.* (2019) 'Biofilm formation and prevalence of adhesion genes among Staphylococcus aureus isolates from different food sources', *MicrobiologyOpen*, 9(1), p. e00946. Available at: https://doi.org/10.1002/mbo3.946.

Chen, Y., Lun, A.T.L. and Smyth, G.K. (2016) 'From reads to genes to pathways: differential expression analysis of RNA-Seq experiments using Rsubread and the edgeR quasi-likelihood pipeline', *F1000Research*, 5, p. 1438. Available at: https://doi.org/10.12688/f1000research.8987.2.

Cheung, A.L. *et al.* (2001) 'SarS, a SarA Homolog Repressible by agr, Is an Activator of Protein A Synthesis in Staphylococcus aureus', *Infection and Immunity*, 69(4), pp. 2448–2455. Available at: https://doi.org/10.1128/IAI.69.4.2448-2455.2001.

Cheung, A.L. and Zhang, G. (2002) 'Global regulation of virulence determinants in Staphylococcus aureus by the SarA protein family', *Frontiers in Bioscience: A Journal and Virtual Library*, 7, pp. d1825-1842. Available at: https://doi.org/10.2741/A882.

Chiba, A. *et al.* (2022) 'Staphylococcus aureus utilizes environmental RNA as a building material in specific polysaccharide-dependent biofilms', *npj Biofilms and Microbiomes*, 8(1), pp. 1–10. Available at: https://doi.org/10.1038/s41522-022-00278-z.

Christensen, I.B. *et al.* (2021) 'Targeted Screening of Lactic Acid Bacteria With Antibacterial Activity Toward Staphylococcus aureus Clonal Complex Type 1 Associated With Atopic Dermatitis', *Frontiers in Microbiology*, 12. Available at:

https://www.frontiersin.org/articles/10.3389/fmicb.2021.733847 (Accessed: 7 February 2023).

Colombo, M. *et al.* (2018) 'Beneficial properties of lactic acid bacteria naturally present in dairy production', *BMC Microbiology*, 18(1), p. 219. Available at: https://doi.org/10.1186/s12866-018-1356-8.

Conlon, K.M., Humphreys, H. and O'Gara, J.P. (2002) 'icaR Encodes a Transcriptional Repressor Involved in Environmental Regulation of ica Operon Expression and Biofilm Formation in Staphylococcus epidermidis', *Journal of Bacteriology*, 184(16), pp. 4400–4408. Available at: https://doi.org/10.1128/JB.184.16.4400-4408.2002.

Corrigan, R.M. *et al.* (2007) 'The role of Staphylococcus aureus surface protein SasG in adherence and biofilm formation', *Microbiology*, 153(8), pp. 2435–2446. Available at: https://doi.org/10.1099/mic.0.2007/006676-0.

Costerton, J.W. *et al.* (1995) 'Microbial biofilms', *Annual Review of Microbiology*, 49, pp. 711–747.

Costerton, J.W., Geesey, G.G. and Cheng, K.-J. (1978) 'How Bacteria Stick', *Scientific American*, 238(1), pp. 86–95.

Cotter, P.D. and Hill, C. (2003) 'Surviving the Acid Test: Responses of Gram-Positive Bacteria to Low pH', *Microbiology and Molecular Biology Reviews*, 67(3), pp. 429–453. Available at: https://doi.org/10.1128/MMBR.67.3.429-453.2003.

Cramton, S.E. *et al.* (1999) 'The Intercellular Adhesion (ica) Locus Is Present in Staphylococcus aureus and Is Required for Biofilm Formation', *Infection and Immunity*, 67(10), pp. 5427–5433.

Creamer, E. *et al.* (2010) 'When are the hands of healthcare workers positive for methicillin-resistant Staphylococcus aureus?', *The Journal of Hospital Infection*, 75(2), pp. 107–111. Available at: https://doi.org/10.1016/j.jhin.2009.12.005.

Crosby, H.A. *et al.* (2016) 'The Staphylococcus aureus Global Regulator MgrA Modulates Clumping and Virulence by Controlling Surface Protein Expression', *PLOS Pathogens*, 12(5), p. e1005604. Available at: https://doi.org/10.1371/journal.ppat.1005604.

Crosby, H.A. *et al.* (2020) 'The Staphylococcus aureus ArlRS two-component system regulates virulence factor expression through MgrA', *Molecular Microbiology*, 113(1), pp. 103–122. Available at: https://doi.org/10.1111/mmi.14404.

Crosby, H.A., Kwiecinski, J. and Horswill, A.R. (2016) 'Staphylococcus aureus aggregation and coagulation mechanisms, and their function in host-pathogen interactions', *Advances in applied microbiology*, 96, pp. 1–41. Available at: https://doi.org/10.1016/bs.aambs.2016.07.018.

Cue, D., Lei, M.G. and Lee, C.Y. (2012) 'Genetic regulation of the intercellular adhesion locus in staphylococci', *Frontiers in Cellular and Infection Microbiology*, 2, p. 38. Available at: https://doi.org/10.3389/fcimb.2012.00038.

Cunin, R. *et al.* (1986) 'Biosynthesis and metabolism of arginine in bacteria', *Microbiological Reviews*, 50(3), pp. 314–352. Available at: https://doi.org/10.1128/mr.50.3.314-352.1986.

Das, T. *et al.* (2010) 'Role of Extracellular DNA in Initial Bacterial Adhesion and Surface Aggregation', *Applied and Environmental Microbiology*, 76(10), pp. 3405–3408. Available at: https://doi.org/10.1128/AEM.03119-09.

Dashtbani-Roozbehani, A. and Brown, M.H. (2021) 'Efflux Pump Mediated Antimicrobial Resistance by Staphylococci in Health-Related Environments: Challenges and the Quest for Inhibition', *Antibiotics*, 10(12), p. 1502. Available at: https://doi.org/10.3390/antibiotics10121502.

De Backer, S. *et al.* (2018) 'Enzymes Catalyzing the TCA- and Urea Cycle Influence the Matrix Composition of Biofilms Formed by Methicillin-Resistant Staphylococcus aureus USA300', *Microorganisms*, 6(4), p. 113. Available at: https://doi.org/10.3390/microorganisms6040113.

Dengler, V. *et al.* (2015) 'An Electrostatic Net Model for the Role of Extracellular DNA in Biofilm Formation by Staphylococcus aureus', *Journal of Bacteriology*, 197(24), pp. 3779–3787. Available at: https://doi.org/10.1128/JB.00726-15.

Donlan, R.M. (2002) 'Biofilms: Microbial Life on Surfaces', *Emerging Infectious Diseases*, 8(9), pp. 881–890. Available at: https://doi.org/10.3201/eid0809.020063.

Donlan, R.M. and Costerton, J.W. (2002) 'Biofilms: Survival Mechanisms of Clinically Relevant Microorganisms', *Clinical Microbiology Reviews*, 15(2), pp. 167–193. Available at: https://doi.org/10.1128/CMR.15.2.167-193.2002.

Drumond, M.M. *et al.* (2023) 'Cell-free supernatant of probiotic bacteria exerted antibiofilm and antibacterial activities against Pseudomonas aeruginosa: A novel biotic therapy', *Frontiers in Pharmacology*, 14. Available at: https://www.frontiersin.org/articles/10.3389/fphar.2023.1152588 (Accessed: 12 July 2023).

Dunne, W.M. (2002) 'Bacterial Adhesion: Seen Any Good Biofilms Lately?', *Clinical Microbiology Reviews*, 15(2), pp. 155–166. Available at: https://doi.org/10.1128/CMR.15.2.155-166.2002.

Eichelberger, K.R. and Cassat, J.E. (2021) 'Metabolic Adaptations During Staphylococcus aureus and Candida albicans Co-Infection', *Frontiers in Immunology*, 12, p. 797550. Available at: https://doi.org/10.3389/fimmu.2021.797550.

Estrela, A.B. and Abraham, W.-R. (2016) 'Fungal Metabolites for the Control of Biofilm Infections', *Agriculture*, 6(3), p. 37. Available at: https://doi.org/10.3390/agriculture6030037.

Fätkenheuer, G., Cornely, O. and Seifert, H. (2002) 'Clinical management of catheter-related infections', *Clinical Microbiology and Infection: The Official Publication of the European Society of Clinical Microbiology and Infectious Diseases*, 8(9), pp. 545–550. Available at: https://doi.org/10.1046/j.1469-0691.2002.00427.x.

Fazli, M. *et al.* (2009) 'Nonrandom distribution of Pseudomonas aeruginosa and Staphylococcus aureus in chronic wounds', *Journal of Clinical Microbiology*, 47(12), pp. 4084–4089. Available at: https://doi.org/10.1128/JCM.01395-09.

Fernández, L. *et al.* (2021) 'Environmental pH is a key modulator of Staphylococcus aureus biofilm development under predation by the virulent phage phiIPLA-RODI', *The ISME Journal*, 15(1), pp. 245–259. Available at: https://doi.org/10.1038/s41396-020-00778-w.

Ferreira, R.B.R. *et al.* (2019) 'Osmotic stress induces biofilm production by Staphylococcus epidermidis isolates from neonates', *Diagnostic Microbiology and Infectious Disease*, 94(4), pp. 337–341. Available at: https://doi.org/10.1016/j.diagmicrobio.2019.02.009.

Feuillie, C. *et al.* (2017) 'Molecular interactions and inhibition of the staphylococcal biofilm-forming protein SdrC', *Proceedings of the National Academy of Sciences*, 114(14), pp. 3738–3743. Available at: https://doi.org/10.1073/pnas.1616805114.

Fitzgerald, S. *et al.* (2022) 'Multi-Strain and -Species Investigation of Volatile Metabolites Emitted from Planktonic and Biofilm Candida Cultures', *Metabolites*, 12(5), p. 432. Available at: https://doi.org/10.3390/metabo12050432.

Fitzpatrick, F., Humphreys, H. and O'Gara, J.P. (2005) 'Evidence for icaADBC-Independent Biofilm Development Mechanism in Methicillin-Resistant Staphylococcus aureus Clinical Isolates', *Journal of Clinical Microbiology*, 43(4), pp. 1973–1976. Available at: https://doi.org/10.1128/JCM.43.4.1973-1976.2005.

Fleming, D. and Rumbaugh, K. (2018) 'The Consequences of Biofilm Dispersal on the Host', *Scientific Reports*, 8(1), p. 10738. Available at: https://doi.org/10.1038/s41598-018-29121-2.

Flemming, H.-C. *et al.* (2021) 'Who put the film in biofilm? The migration of a term from wastewater engineering to medicine and beyond', *npj Biofilms and Microbiomes*, 7(1), pp. 1–5. Available at: https://doi.org/10.1038/s41522-020-00183-3.

Foster, T.J. (2019) 'Surface Proteins of Staphylococcus aureus', *Microbiology Spectrum* [Preprint]. Available at: https://doi.org/10.1128/microbiolspec.GPP3-0046-2018.

Foulston, L. *et al.* (2014) 'The Extracellular Matrix of Staphylococcus aureus Biofilms Comprises Cytoplasmic Proteins That Associate with the Cell Surface in Response to Decreasing pH', *mBio*, 5(5). Available at: https://doi.org/10.1128/mBio.01667-14.

Frees, D. *et al.* (2004) 'Clp ATPases are required for stress tolerance, intracellular replication and biofilm formation in Staphylococcus aureus', *Molecular Microbiology*, 54(5), pp. 1445–1462. Available at: https://doi.org/10.1111/j.1365-2958.2004.04368.x.

Friedrich, R. *et al.* (2003) 'Staphylocoagulase is a prototype for the mechanism of cofactor-induced zymogen activation', *Nature*, 425(6957), pp. 535–539. Available at: https://doi.org/10.1038/nature01962.

Fu, S.-F. *et al.* (2015) 'Indole-3-acetic acid: A widespread physiological code in interactions of fungi with other organisms', *Plant Signaling & Behavior*, 10(8), p. e1048052. Available at: https://doi.org/10.1080/15592324.2015.1048052.

Fujiwara, S. *et al.* (1997) 'Proteinaceous factor(s) in culture supernatant fluids of bifidobacteria which prevents the binding of enterotoxigenic Escherichia coli to gangliotetraosylceramide', *Applied and Environmental Microbiology*, 63(2), pp. 506–512. Available at: https://doi.org/10.1128/aem.63.2.506-512.1997.

Fux, C.A., Wilson, S. and Stoodley, P. (2004) 'Detachment Characteristics and Oxacillin Resistance of Staphyloccocus aureus Biofilm Emboli in an In Vitro Catheter Infection Model', *Journal of Bacteriology*, 186(14), pp. 4486–4491. Available at: https://doi.org/10.1128/JB.186.14.4486-4491.2004.

Galié, S. *et al.* (2018) 'Biofilms in the Food Industry: Health Aspects and Control Methods', *Frontiers in Microbiology*, 9. Available at: https://www.frontiersin.org/articles/10.3389/fmicb.2018.00898 (Accessed: 15 September 2022).

Ganeshnarayan, K. *et al.* (2009) 'Poly-N-Acetylglucosamine Matrix Polysaccharide Impedes Fluid Convection and Transport of the Cationic Surfactant Cetylpyridinium Chloride through Bacterial Biofilms', *Applied and Environmental Microbiology*, 75(5), pp. 1308–1314. Available at: https://doi.org/10.1128/AEM.01900-08.

Garcia, L.M. *et al.* (2020) 'A Two-Way Road: Antagonistic Interaction Between Dual-Species Biofilms Formed by Candida albicans/Candida parapsilosis and Trichophyton rubrum', *Frontiers in Microbiology*, 11, p. 1980. Available at: https://doi.org/10.3389/fmicb.2020.01980.

García-Álvarez, L. *et al.* (2011) 'Meticillin-resistant Staphylococcus aureus with a novel mecA homologue in human and bovine populations in the UK and Denmark: a descriptive study', *The Lancet. Infectious Diseases*, 11(8), pp. 595–603. Available at: https://doi.org/10.1016/S1473-3099(11)70126-8.

Gee Neoh, K. *et al.* (2017) 'Surface modification strategies for combating catheter-related complications: recent advances and challenges', *Journal of Materials Chemistry B*, 5(11), pp. 2045–2067. Available at: https://doi.org/10.1039/C6TB03280J.

Geoghegan, J.A. *et al.* (2010) 'Role of Surface Protein SasG in Biofilm Formation by Staphylococcus aureus', *Journal of Bacteriology*, 192(21), pp. 5663–5673. Available at: https://doi.org/10.1128/JB.00628-10.

Geoghegan, J.A. *et al.* (2013) 'Subdomains N2N3 of Fibronectin Binding Protein A Mediate Staphylococcus aureus Biofilm Formation and Adherence to Fibrinogen Using Distinct Mechanisms', *Journal of Bacteriology* [Preprint]. Available at: https://doi.org/10.1128/JB.02128-12.

Ghosh, A., Jayaraman, N. and Chatterji, D. (2020) 'Small-Molecule Inhibition of Bacterial Biofilm', *ACS Omega*, 5(7), pp. 3108–3115. Available at: https://doi.org/10.1021/acsomega.9b03695.

Gibson, R.L., Burns, J.L. and Ramsey, B.W. (2003) 'Pathophysiology and Management of Pulmonary Infections in Cystic Fibrosis', *American Journal of Respiratory and Critical Care Medicine*, 168(8), pp. 918–951. Available at: https://doi.org/10.1164/rccm.200304-505SO.

Gjødsbøl, K. *et al.* (2006) 'Multiple bacterial species reside in chronic wounds: a longitudinal study', *International Wound Journal*, 3(3), pp. 225–231. Available at: https://doi.org/10.1111/j.1742-481X.2006.00159.x.

Glatthardt, T. *et al.* (2020) 'Small Molecules Produced by Commensal Staphylococcus epidermidis Disrupt Formation of Biofilms by Staphylococcus aureus', *Applied and Environmental Microbiology*, 86(5), pp. e02539-19. Available at: https://doi.org/10.1128/AEM.02539-19.

Gonia, S. *et al.* (2017) 'Candida parapsilosis Protects Premature Intestinal Epithelial Cells from Invasion and Damage by Candida albicans', *Frontiers in Pediatrics*, 5. Available at: https://doi.org/10.3389/fped.2017.00054.

Gordon, R.J. and Lowy, F.D. (2008) 'Pathogenesis of Methicillin-Resistant Staphylococcus aureus Infection', *Clinical infectious diseases : an official publication of the Infectious Diseases Society of America*, 46(Suppl 5), pp. S350–S359. Available at: https://doi.org/10.1086/533591.

Gottrup, F. (2004) 'A specialized wound-healing center concept: importance of a multidisciplinary department structure and surgical treatment facilities in the treatment of chronic wounds', *The American Journal of Surgery*, 187(5), pp. S38–S43. Available at: https://doi.org/10.1016/S0002-9610(03)00303-9.

Gross, M. *et al.* (2001) 'Key Role of Teichoic Acid Net Charge in Staphylococcus aureus Colonization of Artificial Surfaces', *Infection and Immunity*, 69(5), pp. 3423–3426. Available at: https://doi.org/10.1128/IAI.69.5.3423-3426.2001.

Gudiña, E.J. *et al.* (2015) 'Antimicrobial and anti-adhesive activities of cell-bound biosurfactant from Lactobacillus agilis CCUG31450', *RSC Advances*, 5(110), pp. 90960–90968. Available at: https://doi.org/10.1039/C5RA11659G.

Guggenberger, C. *et al.* (2012) 'Two Distinct Coagulase-Dependent Barriers Protect Staphylococcus aureus from Neutrophils in a Three Dimensional in vitro Infection Model', *PLoS Pathogens*, 8(1), p. e1002434. Available at: https://doi.org/10.1371/journal.ppat.1002434.

Guinea, J. (2014) 'Global trends in the distribution of Candida species causing candidemia', *Clinical Microbiology and Infection*, 20, pp. 5–10. Available at: https://doi.org/10.1111/1469-0691.12539.

Gulati, M. and Nobile, C.J. (2016) 'Candida albicans biofilms: development, regulation, and molecular mechanisms', *Microbes and infection / Institut Pasteur*, 18(5), pp. 310–321. Available at: https://doi.org/10.1016/j.micinf.2016.01.002.

Haaber, J. *et al.* (2012) 'Planktonic Aggregates of Staphylococcus aureus Protect against Common Antibiotics', *PLOS ONE*, 7(7), p. e41075. Available at: https://doi.org/10.1371/journal.pone.0041075.

Haag, A.F. and Bagnoli, F. (2017) 'The Role of Two-Component Signal Transduction Systems in Staphylococcus aureus Virulence Regulation', *Current Topics in Microbiology and Immunology*, 409, pp. 145–198. Available at: https://doi.org/10.1007/82_2015_5019.

Haber, A. *et al.* (2017) 'L-glutamine Induces Expression of Listeria monocytogenes Virulence Genes', *PLOS Pathogens*, 13(1), p. e1006161. Available at: https://doi.org/10.1371/journal.ppat.1006161.

Haiko, J. *et al.* (2019) 'Coexistence of Candida species and bacteria in patients with cystic fibrosis', *European Journal of Clinical Microbiology & Infectious Diseases*, 38(6), pp. 1071–1077. Available at: https://doi.org/10.1007/s10096-019-03493-3.

Hall-Stoodley, L., Costerton, J.W. and Stoodley, P. (2004) 'Bacterial biofilms: from the Natural environment to infectious diseases', *Nature Reviews Microbiology*, 2(2), pp. 95–108. Available at: https://doi.org/10.1038/nrmicro821.

Halsey, C.R. *et al.* (2017) 'Amino Acid Catabolism in Staphylococcus aureus and the Function of Carbon Catabolite Repression', *mBio*, 8(1), pp. e01434-16. Available at: https://doi.org/10.1128/mBio.01434-16.

Han, G. and Ceilley, R. (2017) 'Chronic Wound Healing: A Review of Current Management and Treatments', *Advances in Therapy*, 34(3), pp. 599–610. Available at: https://doi.org/10.1007/s12325-017-0478-y.

Hancock, V., Witsø, I.L. and Klemm, P. (2011) 'Biofilm formation as a function of adhesin, growth medium, substratum and strain type', *International journal of medical*

microbiology: IJMM, 301(7), pp. 570–576. Available at: https://doi.org/10.1016/j.ijmm.2011.04.018.

Health Protection Surveillance Centre (2022) 'Data on S. aureus/MRSA bloodstream infections from acute hospitals, 2016-2020 (all public and private hospitals, complete datasets of historic data and interactive database with trends)'. Available at: https://www.hpsc.ie/a-z/microbiologyantimicrobialresistance/europeanantimicrobialresistancesurveillancesystemearss/referenceandeducationalresourcematerial/saureusmrsa/latestsaureusmrsadata/SAU%20BSI%20Report%20by%20Hospital_with%20Interactive%20Database_20220325.xlsx.

Heilmann, C. *et al.* (1996) 'Molecular basis of intercellular adhesion in the biofilm-forming Staphylococcus epidermidis', *Molecular Microbiology*, 20(5), pp. 1083–1091. Available at: https://doi.org/10.1111/j.1365-2958.1996.tb02548.x.

Herman-Bausier, P. *et al.* (2018) 'Staphylococcus aureus clumping factor A is a force-sensitive molecular switch that activates bacterial adhesion', *Proceedings of the National Academy of Sciences of the United States of America*, 115(21), pp. 5564–5569. Available at: https://doi.org/10.1073/pnas.1718104115.

Hobley, L. *et al.* (2015) 'Giving structure to the biofilm matrix: an overview of individual strategies and emerging common themes', *FEMS Microbiology Reviews*, 39(5), pp. 649–669. Available at: https://doi.org/10.1093/femsre/fuv015.

Høiby, N. *et al.* (2015) 'ESCMID ∗ guideline for the diagnosis and treatment of biofilm infections 2014', *Clinical Microbiology and Infection*, 21, pp. S1–S25. Available at: https://doi.org/10.1016/j.cmi.2014.10.024.

Høiby, N. (2017) 'A short history of microbial biofilms and biofilm infections', *APMIS*, 125(4), pp. 272–275. Available at: https://doi.org/10.1111/apm.12686.

Holland, L.M. *et al.* (2014) 'Comparative Phenotypic Analysis of the Major Fungal Pathogens Candida parapsilosis and Candida albicans', *PLOS Pathogens*, 10(9), p. e1004365. Available at: https://doi.org/10.1371/journal.ppat.1004365.

Horsburgh, M.J. *et al.* (2002) 'σB Modulates Virulence Determinant Expression and Stress Resistance: Characterization of a Functional rsbU Strain Derived from Staphylococcus aureus 8325-4', *Journal of Bacteriology*, 184(19), pp. 5457–5467. Available at: https://doi.org/10.1128/JB.184.19.5457-5467.2002.

Houston, P. *et al.* (2010) 'Essential Role for the Major Autolysin in the Fibronectin-Binding Protein-Mediated Staphylococcus aureus Biofilm Phenotype', *Infection and Immunity* [Preprint]. Available at: https://doi.org/10.1128/IAI.00364-10.

Hung, D.T. *et al.* (2006) 'Bile acids stimulate biofilm formation in Vibrio cholerae', *Molecular Microbiology*, 59(1), pp. 193–201. Available at: https://doi.org/10.1111/j.1365-2958.2005.04846.x.

Hunt, S.M. *et al.* (2004) 'Hypothesis for the Role of Nutrient Starvation in Biofilm Detachment', *Applied and Environmental Microbiology*, 70(12), pp. 7418–7425. Available at: https://doi.org/10.1128/AEM.70.12.7418-7425.2004.

Huseby, M.J. *et al.* (2010) 'Beta toxin catalyzes formation of nucleoprotein matrix in staphylococcal biofilms', *Proceedings of the National Academy of Sciences*, 107(32), pp. 14407–14412. Available at: https://doi.org/10.1073/pnas.0911032107.

Ingavale, S. *et al.* (2005) 'Rat/MgrA, a Regulator of Autolysis, Is a Regulator of Virulence Genes in Staphylococcus aureus', *Infection and Immunity* [Preprint]. Available at: https://doi.org/10.1128/IAI.73.3.1423-1431.2005.

Ireland and SARI Infection Control Subcommittee (2001) *The control and prevention of MRSA in hospitals and in the community*. Dublin: HSE, Protection Surveillance Centre.

Iwase, T. *et al.* (2010) 'Staphylococcus epidermidis Esp inhibits Staphylococcus aureus biofilm formation and nasal colonization', *Nature*, 465(7296), pp. 346–349. Available at: https://doi.org/10.1038/nature09074.

Jacques, M., Marrie, T.J. and Costerton, J.W. (1987) 'Review: Microbial colonization of prosthetic devices', *Microbial Ecology*, 13(3), pp. 173–191. Available at: https://doi.org/10.1007/BF02024996.

James, G.A. *et al.* (2008) 'Biofilms in chronic wounds', *Wound Repair and Regeneration: Official Publication of the Wound Healing Society [and] the European Tissue Repair Society*, 16(1), pp. 37–44. Available at: https://doi.org/10.1111/j.1524-475X.2007.00321.x.

Jefferson, K.K. (2004) 'What drives bacteria to produce a biofilm?', *FEMS Microbiology Letters*, 236(2), pp. 163–173. Available at: https://doi.org/10.1111/j.1574-6968.2004.tb09643.x.

Jenul, C. and Horswill, A.R. (2018) 'Regulation of Staphylococcus aureus virulence', *Microbiology spectrum*, 6(1), p. 10.1128/microbiolspec.GPP3-0031–2018. Available at: https://doi.org/10.1128/microbiolspec.GPP3-0031-2018.

Jiang, Q., Jin, Z. and Sun, B. (2018) 'MgrA Negatively Regulates Biofilm Formation and Detachment by Repressing the Expression of psm Operons in Staphylococcus aureus', *Applied and Environmental Microbiology*, 84(16), pp. e01008-18. Available at: https://doi.org/10.1128/AEM.01008-18.

Johnson, M., Cockayne, A. and Morrissey, J.A. (2008) 'Iron-regulated biofilm formation in Staphylococcus aureus Newman requires ica and the secreted protein Emp', *Infection and Immunity*, 76(4), pp. 1756–1765. Available at: https://doi.org/10.1128/IAI.01635-07.

Kanehisa, M. and Goto, S. (2000) 'KEGG: Kyoto Encyclopedia of Genes and Genomes', *Nucleic Acids Research*, 28(1), pp. 27–30. Available at: https://doi.org/10.1093/nar/28.1.27.

Kaplan, J.B. *et al.* (2003) 'Detachment of Actinobacillus actinomycetemcomitans Biofilm Cells by an Endogenous β-Hexosaminidase Activity', *Journal of Bacteriology*, 185(16), pp. 4693–4698. Available at: https://doi.org/10.1128/JB.185.16.4693-4698.2003.

Kaplan, J.B. *et al.* (2012) 'Low Levels of β-Lactam Antibiotics Induce Extracellular DNA Release and Biofilm Formation in Staphylococcus aureus', *mBio*, 3(4), pp. e00198-12. Available at: https://doi.org/10.1128/mBio.00198-12.

Kateete, D.P. *et al.* (2010) 'Identification of Staphylococcus aureus: DNase and Mannitol salt agar improve the efficiency of the tube coagulase test', *Annals of Clinical Microbiology and Antimicrobials*, 9(1), p. 23. Available at: https://doi.org/10.1186/1476-0711-9-23.

Kavanaugh, J.S. *et al.* (2019) 'Identification of Extracellular DNA-Binding Proteins in the Biofilm Matrix', *mBio*, 10(3). Available at: https://doi.org/10.1128/mBio.01137-19.

Kelly, D. *et al.* (2012) 'Prevention of Staphylococcus aureus biofilm formation and reduction in established biofilm density using a combination of phage K and modified derivatives', *Letters in Applied Microbiology*, 54(4), pp. 286–291. Available at: https://doi.org/10.1111/j.1472-765X.2012.03205.x.

Khatoon, Z. *et al.* (2018) 'Bacterial biofilm formation on implantable devices and approaches to its treatment and prevention', *Heliyon*, 4(12). Available at: https://doi.org/10.1016/j.heliyon.2018.e01067.

Kim, D. *et al.* (2019) 'Graph-based genome alignment and genotyping with HISAT2 and HISAT-genotype', *Nature Biotechnology*, 37(8), pp. 907–915. Available at: https://doi.org/10.1038/s41587-019-0201-4.

Kim, J. and Park, W. (2015) 'Indole: a signaling molecule or a mere metabolic byproduct that alters bacterial physiology at a high concentration?', *Journal of Microbiology (Seoul, Korea)*, 53(7), pp. 421–428. Available at: https://doi.org/10.1007/s12275-015-5273-3.

Kim, Y.J. *et al.* (2020) 'Anti-Biofilm Activity of Cell-Free Supernatant of Saccharomyces cerevisiae against Staphylococcus aureus', 30(12), pp. 1854–1861. Available at: https://doi.org/10.4014/jmb.2008.08053.

Klotz, S.A., Gaur, N.K., *et al.* (2007) 'Candida albicans Als proteins mediate aggregation with bacteria and yeasts', *Medical Mycology*, 45(4), pp. 363–370. Available at: https://doi.org/10.1080/13693780701299333.

Klotz, S.A., Chasin, B.S., *et al.* (2007) 'Polymicrobial bloodstream infections involving Candida species: analysis of patients and review of the literature', *Diagnostic Microbiology and Infectious Disease*, 59(4), pp. 401–406. Available at: https://doi.org/10.1016/j.diagmicrobio.2007.07.001.

Köck, R. *et al.* (2010) 'Methicillin-resistant Staphylococcus aureus (MRSA): burden of disease and control challenges in Europe', *Eurosurveillance*, 15(41), p. 19688. Available at: https://doi.org/10.2807/ese.15.41.19688-en.

Kogan, G. *et al.* (2006) 'Biofilms of clinical strains of Staphylococcus that do not contain polysaccharide intercellular adhesin', *FEMS Microbiology Letters*, 255(1), pp. 11–16. Available at: https://doi.org/10.1111/j.1574-6968.2005.00043.x.

Kohlwein, S.D. (2017) 'Analyzing and Understanding Lipids of Yeast: A Challenging Endeavor', *Cold Spring Harbor Protocols*, 2017(5), p. pdb.top078956. Available at: https://doi.org/10.1101/pdb.top078956.

Kong, E.F. *et al.* (2016) 'Commensal Protection of Staphylococcus aureus against Antimicrobials by Candida albicans Biofilm Matrix', *mBio*, 7(5), pp. e01365-16. Available at: https://doi.org/10.1128/mBio.01365-16.

Kostakioti, M., Hadjifrangiskou, M. and Hultgren, S.J. (2013) 'Bacterial Biofilms: Development, Dispersal, and Therapeutic Strategies in the Dawn of the Postantibiotic Era', *Cold Spring Harbor Perspectives in Medicine*, 3(4), p. a010306. Available at: https://doi.org/10.1101/cshperspect.a010306.

Kozik, A. *et al.* (2015) 'Fibronectin-, vitronectin- and laminin-binding proteins at the cell walls of Candida parapsilosis and Candida tropicalis pathogenic yeasts', *BMC Microbiology*, 15, p. 197. Available at: https://doi.org/10.1186/s12866-015-0531-4.

Kragh, K.N. *et al.* (2019) 'Into the well—A close look at the complex structures of a microtiter biofilm and the crystal violet assay', *Biofilm*, 1, p. 100006. Available at: https://doi.org/10.1016/j.bioflm.2019.100006.

Kroh, H.K., Panizzi, P. and Bock, P.E. (2009) 'Von Willebrand factor-binding protein is a hysteretic conformational activator of prothrombin', *Proceedings of the National Academy of Sciences of the United States of America*, 106(19), pp. 7786–7791. Available at: https://doi.org/10.1073/pnas.0811750106.

Kulshrestha, A. and Gupta, P. (2023) 'Secreted aspartyl proteases family: a perspective review on the regulation of fungal pathogenesis', *Future Microbiology*, 18(5), pp. 295–309. Available at: https://doi.org/10.2217/fmb-2022-0143.

Kumar, M.S. and Philominathan, P. (2009) 'The physics of flagellar motion of E. coli during chemotaxis', *Biophysical Reviews*, 2(1), pp. 13–20. Available at: https://doi.org/10.1007/s12551-009-0024-5.

Kumari, A. and Singh, R. (2019) 'Medically important interactions of staphylococci with pathogenic fungi', *Future Microbiology* [Preprint]. Available at: https://doi.org/10.2217/fmb-2019-0155.

Lade, H. *et al.* (2019) 'Biofilm Formation by Staphylococcus aureus Clinical Isolates is Differentially Affected by Glucose and Sodium Chloride Supplemented Culture Media',

Journal of Clinical Medicine, 8(11), p. 1853. Available at: https://doi.org/10.3390/jcm8111853.

Laffey, S.F. and Butler, G. 2005 (2005) 'Phenotype switching affects biofilm formation by Candida parapsilosis', *Microbiology*, 151(4), pp. 1073–1081. Available at: https://doi.org/10.1099/mic.0.27739-0.

Lamret, F. *et al.* (2022) 'Human Osteoblast-Conditioned Media Can Influence Staphylococcus aureus Biofilm Formation', *International Journal of Molecular Sciences*, 23(22), p. 14393. Available at: https://doi.org/10.3390/ijms232214393.

Larsen, J. *et al.* (2022) 'Emergence of methicillin resistance predates the clinical use of antibiotics', *Nature*, pp. 1–7. Available at: https://doi.org/10.1038/s41586-021-04265-w.

Lattif, A.A. *et al.* (2010) 'Characterization of biofilms formed by Candida parapsilosis, C. metapsilosis, and C. orthopsilosis', *International Journal of Medical Microbiology*, 300(4), pp. 265–270. Available at: https://doi.org/10.1016/j.ijmm.2009.09.001.

Lauderdale, K.J. *et al.* (2009) 'Interconnections between Sigma B, agr, and Proteolytic Activity in Staphylococcus aureus Biofilm Maturation', *Infection and Immunity*, 77(4), pp. 1623–1635. Available at: https://doi.org/10.1128/IAI.01036-08.

Laura Estela, C.R. and Ramos, P. (2012) 'Biofilms: A Survival and Resistance Mechanism of Microorganisms', in M. Pana (ed.). InTech. Available at: https://doi.org/10.5772/28504.

Lee, J.-H., Cho, M.H. and Lee, J. (2011) '3-indolylacetonitrile decreases Escherichia coli O157:H7 biofilm formation and Pseudomonas aeruginosa virulence', *Environmental Microbiology*, 13(1), pp. 62–73. Available at: https://doi.org/10.1111/j.1462-2920.2010.02308.x.

Lee, J.-H., Kim, Y.-G. and Lee, J. (2022) 'Inhibition of Staphylococcus aureus Biofilm Formation and Virulence Factor Production by Petroselinic Acid and Other Unsaturated C18 Fatty Acids', *Microbiology Spectrum*, 10(3), pp. e01330-22. Available at: https://doi.org/10.1128/spectrum.01330-22.

Lee, J.-H. and Lee, J. (2010) 'Indole as an intercellular signal in microbial communities', *FEMS microbiology reviews*, 34(4), pp. 426–444. Available at: https://doi.org/10.1111/j.1574-6976.2009.00204.x.

Liebeke, M. *et al.* (2011) 'A metabolomics and proteomics study of the adaptation of Staphylococcus aureus to glucose starvation', *Molecular bioSystems*, 7(4), pp. 1241–1253. Available at: https://doi.org/10.1039/c0mb00315h.

Lim, Y. *et al.* (2004) 'Control of Glucose- and NaCl-Induced Biofilm Formation by rbf in Staphylococcus aureus', *Journal of Bacteriology*, 186(3), pp. 722–729. Available at: https://doi.org/10.1128/JB.186.3.722-729.2004.

Lindgren, J.K. *et al.* (2014) 'Arginine Deiminase in Staphylococcus epidermidis Functions To Augment Biofilm Maturation through pH Homeostasis', *Journal of Bacteriology*, 196(12), pp. 2277–2289. Available at: https://doi.org/10.1128/JB.00051-14.

Lister, J.L. and Horswill, A.R. (2014) 'Staphylococcus aureus biofilms: recent developments in biofilm dispersal', *Frontiers in Cellular and Infection Microbiology*, 4. Available at: https://doi.org/10.3389/fcimb.2014.00178.

Liu, J. *et al.* (2021) 'Destruction of Staphylococcus aureus biofilms by combining an antibiotic with subtilisin A or calcium gluconate', *Scientific Reports*, 11(1), p. 6225. Available at: https://doi.org/10.1038/s41598-021-85722-4.

Liu, S. *et al.* (2016) 'Understanding, Monitoring, and Controlling Biofilm Growth in Drinking Water Distribution Systems', *Environmental Science & Technology*, 50(17), pp. 8954–8976. Available at: https://doi.org/10.1021/acs.est.6b00835.

Liu, Y., Zhang, J. and Ji, Y. (2020) 'Environmental factors modulate biofilm formation by Staphylococcus aureus', *Science Progress*, 103(1), p. 0036850419898659. Available at: https://doi.org/10.1177/0036850419898659.

Lohse, M.B. *et al.* (2018) 'Development and regulation of single- and multi-species Candida albicans biofilms', *Nature Reviews Microbiology*, 16(1), pp. 19–31. Available at: https://doi.org/10.1038/nrmicro.2017.107.

López, D., Vlamakis, H. and Kolter, R. (2010) 'Biofilms', *Cold Spring Harbor Perspectives in Biology*, 2(7), p. a000398. Available at: https://doi.org/10.1101/cshperspect.a000398.

López-Ramos, J.E. *et al.* (2021) 'Analysis of Volatile Molecules Present in the Secretome of the Fungal Pathogen Candida glabrata', *Molecules*, 26(13), p. 3881. Available at: https://doi.org/10.3390/molecules26133881.

Loughran, A.J. *et al.* (2014) 'Impact of individual extracellular proteases on Staphylococcus aureus biofilm formation in diverse clinical isolates and their isogenic sarA mutants', *MicrobiologyOpen*, 3(6), pp. 897–909. Available at: https://doi.org/10.1002/mbo3.214.

Lowy, F.D. (1998) 'Staphylococcus aureus Infections', *http://dx.doi.org/10.1056/NEJM199808203390806* [Preprint]. Available at: https://doi.org/10.1056/NEJM199808203390806.

Luo, Z. *et al.* (2020) 'Reduced Growth of Staphylococcus aureus Under High Glucose Conditions Is Associated With Decreased Pentaglycine Expression', *Frontiers in Microbiology*, 11. Available at: https://www.frontiersin.org/articles/10.3389/fmicb.2020.537290 (Accessed: 16 June 2023).

Mack, D. *et al.* (1996) 'The intercellular adhesin involved in biofilm accumulation of Staphylococcus epidermidis is a linear beta-1,6-linked glucosaminoglycan: purification and structural analysis', *Journal of Bacteriology*, 178(1), pp. 175–183. Available at: https://doi.org/10.1128/jb.178.1.175-183.1996.

MacKintosh, E.E. *et al.* (2006) 'Effects of biomaterial surface chemistry on the adhesion and biofilm formation of Staphylococcus epidermidis in vitro', *Journal of Biomedical Materials Research Part A*, 78A(4), pp. 836–842. Available at: https://doi.org/10.1002/jbm.a.30905.

Makhlin, J. *et al.* (2007) 'Staphylococcus aureus ArcR Controls Expression of the Arginine Deiminase Operon', *Journal of Bacteriology*, 189(16), pp. 5976–5986. Available at: https://doi.org/10.1128/JB.00592-07.

Manfredi, M. *et al.* (2002) 'The isolation, identification and molecular analysis of Candida spp. isolated from the oral cavities of patients with diabetes mellitus', *Oral Microbiology and Immunology*, 17(3), pp. 181–185. Available at: https://doi.org/10.1034/j.1399-302X.2002.170308.x.

Mani-López, E., Arrioja-Bretón, D. and López-Malo, A. (2022) 'The impacts of antimicrobial and antifungal activity of cell-free supernatants from lactic acid bacteria in vitro and foods', *Comprehensive Reviews in Food Science and Food Safety*, 21(1), pp. 604–641. Available at: https://doi.org/10.1111/1541-4337.12872.

Mann, E.E. *et al.* (2009) 'Modulation of eDNA Release and Degradation Affects Staphylococcus aureus Biofilm Maturation', *PLOS ONE*, 4(6), p. e5822. Available at: https://doi.org/10.1371/journal.pone.0005822.

Mariam, S.H. *et al.* (2014) 'Potential of cell-free supernatants from cultures of selected lactic acid bacteria and yeast obtained from local fermented foods as inhibitors of Listeria monocytogenes, Salmonella spp. and Staphylococcus aureus', *BMC Research Notes*, 7(1), p. 606. Available at: https://doi.org/10.1186/1756-0500-7-606.

Martí, M. *et al.* (2010) 'Extracellular proteases inhibit protein-dependent biofilm formation in Staphylococcus aureus', *Microbes and Infection*, 12(1), pp. 55–64. Available at: https://doi.org/10.1016/j.micinf.2009.10.005.

Massey, S.E. *et al.* (2003) 'Comparative Evolutionary Genomics Unveils the Molecular Mechanism of Reassignment of the CTG Codon in Candida spp.', *Genome Research*, 13(4), pp. 544–557. Available at: https://doi.org/10.1101/gr.811003.

Maya, I.D. *et al.* (2007) 'Treatment of dialysis catheter-related Staphylococcus aureus bacteremia with an antibiotic lock: a quality improvement report', *American Journal of Kidney Diseases: The Official Journal of the National Kidney Foundation*, 50(2), pp. 289–295. Available at: https://doi.org/10.1053/j.ajkd.2007.04.014.

McAdow, M., Missiakas, D.M. and Schneewind, O. (2012) '*Staphylococcus aureus* Secretes Coagulase and von Willebrand Factor Binding Protein to Modify the

Coagulation Cascade and Establish Host Infections', *Journal of Innate Immunity*, 4(2), pp. 141–148. Available at: https://doi.org/10.1159/000333447.

Melander, R.J., Minvielle, M.J. and Melander, C. (2014) 'Controlling bacterial behavior with indole-containing natural products and derivatives', *Tetrahedron*, 70(37), pp. 6363–6372. Available at: https://doi.org/10.1016/j.tet.2014.05.089.

Michael, C.A., Dominey-Howes, D. and Labbate, M. (2014) 'The Antimicrobial Resistance Crisis: Causes, Consequences, and Management', *Frontiers in Public Health*, 2, p. 145. Available at: https://doi.org/10.3389/fpubh.2014.00145.

Miller, M.B. and Bassler, B.L. (2001) 'Quorum Sensing in Bacteria', *Annual Review of Microbiology*, 55(1), pp. 165–199. Available at: https://doi.org/10.1146/annurev.micro.55.1.165.

Mishra, R. *et al.* (2020) 'Natural Anti-biofilm Agents: Strategies to Control Biofilm-Forming Pathogens', *Frontiers in Microbiology*, 11. Available at: https://www.frontiersin.org/article/10.3389/fmicb.2020.566325 (Accessed: 26 January 2022).

Mlynek, K.D. *et al.* (2020) 'Genetic and Biochemical Analysis of CodY-Mediated Cell Aggregation in Staphylococcus aureus Reveals an Interaction between Extracellular DNA and Polysaccharide in the Extracellular Matrix', *Journal of Bacteriology*, 202(8), pp. e00593-19. Available at: https://doi.org/10.1128/JB.00593-19.

Moormeier, D.E. *et al.* (2013) 'Use of Microfluidic Technology To Analyze Gene Expression during Staphylococcus aureus Biofilm Formation Reveals Distinct Physiological Niches', *Applied and Environmental Microbiology*, 79(11), pp. 3413–3424. Available at: https://doi.org/10.1128/AEM.00395-13.

Moormeier, D.E. *et al.* (2014) 'Temporal and Stochastic Control of Staphylococcus aureus Biofilm Development', *mBio*, 5(5). Available at: https://doi.org/10.1128/mBio.01341-14.

Moormeier, D.E. and Bayles, K.W. (2017) 'Staphylococcus aureus Biofilm: A Complex Developmental Organism', *Molecular microbiology*, 104(3), pp. 365–376. Available at: https://doi.org/10.1111/mmi.13634.

Mulani, M.S. *et al.* (2019) 'Emerging Strategies to Combat ESKAPE Pathogens in the Era of Antimicrobial Resistance: A Review', *Frontiers in Microbiology*, 10, p. 539. Available at: https://doi.org/10.3389/fmicb.2019.00539.

Naglik, J.R., Challacombe, S.J. and Hube, B. (2003) 'Candida albicans Secreted Aspartyl Proteinases in Virulence and Pathogenesis', *Microbiology and Molecular Biology Reviews*, 67(3), pp. 400–428. Available at: https://doi.org/10.1128/MMBR.67.3.400-428.2003.

Nakamura, S. and Minamino, T. (2019) 'Flagella-Driven Motility of Bacteria', *Biomolecules*, 9(7), p. 279. Available at: https://doi.org/10.3390/biom9070279.

Nash, E.E. *et al.* (2015) 'Morphology-Independent Virulence of Candida Species during Polymicrobial Intra-abdominal Infections with Staphylococcus aureus', *Infection and Immunity*, 84(1), pp. 90–98. Available at: https://doi.org/10.1128/IAI.01059-15.

Nassar, R. *et al.* (2021) 'Microbial Metabolic Genes Crucial for S. aureus Biofilms: An Insight From Re-analysis of Publicly Available Microarray Datasets', *Frontiers in Microbiology*, 11. Available at: https://www.frontiersin.org/articles/10.3389/fmicb.2020.607002 (Accessed: 23 July 2023).

Nealson, K.H., Platt, T. and Hastings, J.W. (1970) 'Cellular Control of the Synthesis and Activity of the Bacterial Luminescent System1', *Journal of Bacteriology*, 104(1), pp. 313–322.

Neji, S. *et al.* (2017) 'Virulence factors, antifungal susceptibility and molecular mechanisms of azole resistance among Candida parapsilosis complex isolates recovered from clinical specimens', *Journal of Biomedical Science*, 24, p. 67. Available at: https://doi.org/10.1186/s12929-017-0376-2.

Nemeth, T.M., Gacser, A. and Nosanchuk, J.D. (2018) 'Candida psilosis Complex', in *Reference Module in Life Sciences*. Elsevier. Available at: https://doi.org/10.1016/B978-0-12-809633-8.20709-7.

Novick, R.P. and Jiang, D. (2003) 'The staphylococcal saeRS system coordinates environmental signals with agr quorum sensing', *Microbiology (Reading, England)*, 149(Pt 10), pp. 2709–2717. Available at: https://doi.org/10.1099/mic.0.26575-0.

O'Gara, J.P. (2007) 'ica and beyond: biofilm mechanisms and regulation in Staphylococcus epidermidis and Staphylococcus aureus', *FEMS Microbiology Letters*, 270(2), pp. 179–188. Available at: https://doi.org/10.1111/j.1574-6968.2007.00688.x.

Ogston, A. and Witte, W. (1984) 'On Abscesses', *Reviews of Infectious Diseases*, 6(1), pp. 122–128.

Oliveira, W.F. *et al.* (2018) 'Staphylococcus aureus and Staphylococcus epidermidis infections on implants', *Journal of Hospital Infection*, 98(2), pp. 111–117. Available at: https://doi.org/10.1016/j.jhin.2017.11.008.

O'Neill, E. *et al.* (2007) 'Association between Methicillin Susceptibility and Biofilm Regulation in Staphylococcus aureus Isolates from Device-Related Infections', *Journal of Clinical Microbiology* [Preprint]. Available at: https://doi.org/10.1128/JCM.02280-06.

O'Neill, E. *et al.* (2008) 'A Novel Staphylococcus aureus Biofilm Phenotype Mediated by the Fibronectin-Binding Proteins, FnBPA and FnBPB', *Journal of Bacteriology*, 190(11), pp. 3835–3850. Available at: https://doi.org/10.1128/JB.00167-08.

Orazi, G. and O'Toole, G.A. (2017) 'Pseudomonas aeruginosa Alters Staphylococcus aureus Sensitivity to Vancomycin in a Biofilm Model of Cystic Fibrosis Infection', *mBio*, 8(4). Available at: https://doi.org/10.1128/mBio.00873-17.

Otto, M. (2013) 'Staphylococcal Infections: Mechanisms of Biofilm Maturation and Detachment as Critical Determinants of Pathogenicity', *Annual Review of Medicine*, 64(1), pp. 175–188. Available at: https://doi.org/10.1146/annurev-med-042711-140023.

Otto, M. (2014) 'Staphylococcus aureus toxins', *Current opinion in microbiology*, 0, pp. 32–37. Available at: https://doi.org/10.1016/j.mib.2013.11.004.

Paharik, A.E. and Horswill, A.R. (2016) 'The Staphylococcal Biofilm: Adhesins, regulation, and host response', *Microbiology spectrum*, 4(2). Available at: https://doi.org/10.1128/microbiolspec.VMBF-0022-2015.

Pané-Farré, J. *et al.* (2006) 'The sigmaB regulon in Staphylococcus aureus and its regulation', *International journal of medical microbiology: IJMM*, 296(4–5), pp. 237–258. Available at: https://doi.org/10.1016/j.ijmm.2005.11.011.

Pannanusorn, S. *et al.* (2014) 'Characterization of Biofilm Formation and the Role of BCR1 in Clinical Isolates of Candida parapsilosis', *Eukaryotic Cell*, 13(4), pp. 438–451. Available at: https://doi.org/10.1128/EC.00181-13.

Pannanusorn, S., Fernandez, V. and Römling, U. (2013) 'Prevalence of biofilm formation in clinical isolates of Candida species causing bloodstream infection', *Mycoses*, 56(3), pp. 264–272. Available at: https://doi.org/10.1111/myc.12014.

Park, J.-H. *et al.* (2012) 'Acceleration of protease effect on Staphylococcus aureus biofilm dispersal', *FEMS Microbiology Letters*, 335(1), pp. 31–38. Available at: https://doi.org/10.1111/j.1574-6968.2012.02635.x.

Peeters, E., Nelis, H.J. and Coenye, T. (2008) 'Comparison of multiple methods for quantification of microbial biofilms grown in microtiter plates', *Journal of Microbiological Methods*, 72(2), pp. 157–165. Available at: https://doi.org/10.1016/j.mimet.2007.11.010.

Pena, R.T. *et al.* (2019) 'Relationship Between Quorum Sensing and Secretion Systems', *Frontiers in Microbiology*, 10. Available at: https://www.frontiersin.org/article/10.3389/fmicb.2019.01100 (Accessed: 23 January 2022).

Peng, Q. *et al.* (2023) 'A Review of Biofilm Formation of Staphylococcus aureus and Its Regulation Mechanism', *Antibiotics*, 12(1), p. 12. Available at: https://doi.org/10.3390/antibiotics12010012.

Periasamy, S. *et al.* (2012) 'How Staphylococcus aureus biofilms develop their characteristic structure', *Proceedings of the National Academy of Sciences of the*

United States of America, 109(4), pp. 1281–1286. Available at: https://doi.org/10.1073/pnas.1115006109.

Pessione, E. (2012) 'Lactic acid bacteria contribution to gut microbiota complexity: lights and shadows', *Frontiers in Cellular and Infection Microbiology*, 2. Available at: https://www.frontiersin.org/article/10.3389/fcimb.2012.00086 (Accessed: 18 February 2022).

Pestana-Nobles, R., Leyva-Rojas, J.A. and Yosa, J. (2020) 'Searching Hit Potential Antimicrobials in Natural Compounds Space against Biofilm Formation', *Molecules*, 25(22), p. 5334. Available at: https://doi.org/10.3390/molecules25225334.

Peters, B.M. *et al.* (2012) 'Staphylococcus aureus adherence to Candida albicans hyphae is mediated by the hyphal adhesin Als3p', *Microbiology*, 158(Pt 12), pp. 2975–2986. Available at: https://doi.org/10.1099/mic.0.062109-0.

Pfaller, M.A. and Diekema, D.J. (2007) 'Epidemiology of Invasive Candidiasis: a Persistent Public Health Problem', *Clinical Microbiology Reviews*, 20(1), pp. 133–163. Available at: https://doi.org/10.1128/CMR.00029-06.

Pinu, F.R. and Villas-Boas, S.G. (2017) 'Extracellular Microbial Metabolomics: The State of the Art', *Metabolites*, 7(3), p. 43. Available at: https://doi.org/10.3390/metabo7030043.

Plyuta, V.A. *et al.* (2013) 'Effect of salicylic, indole-3-acetic, gibberellic, and abscisic acids on biofilm formation by Agrobacterium tumefaciens C58 and Pseudomonas aeruginosa PAO1', *Applied Biochemistry and Microbiology*, 49(8), pp. 706–710. Available at: https://doi.org/10.1134/S000368381308005X.

Pollitt, E.J.G., Crusz, S.A. and Diggle, S.P. (2015) 'Staphylococcus aureus forms spreading dendrites that have characteristics of active motility', *Scientific Reports*, 5. Available at: https://doi.org/10.1038/srep17698.

Post, V. *et al.* (2017) 'Vancomycin displays time-dependent eradication of mature Staphylococcus aureus biofilms', *Journal of Orthopaedic Research*, 35(2), pp. 381–388. Available at: https://doi.org/10.1002/jor.23291.

Price-Whelan, A. *et al.* (2013) 'Transcriptional Profiling of Staphylococcus aureus During Growth in 2 M NaCl Leads to Clarification of Physiological Roles for Kdp and Ktr K+ Uptake Systems', *mBio*, 4(4), pp. e00407-13. Available at: https://doi.org/10.1128/mBio.00407-13.

Pugine, S.M.P. *et al.* (2010) 'Toxicity Of Indole-3-acetic Acid Combined With Horseradish Peroxidase On Staphylococcus Aureus'. Available at: http://www.webmedcentral.com/ (Accessed: 11 December 2023).

Quan, K. *et al.* (2021) 'Water in bacterial biofilms: pores and channels, storage and transport functions', *Critical Reviews in Microbiology*, 0(0), pp. 1–20. Available at: https://doi.org/10.1080/1040841X.2021.1962802.

R Core Team (2022) ‘R: A language and environment for statistical computing.’ R Foundation for Statistical Computing, Vienna, Austria. Available at: https://www.R-project.org/.

Rani, S.A. *et al.* (2007) ‘Spatial Patterns of DNA Replication, Protein Synthesis, and Oxygen Concentration within Bacterial Biofilms Reveal Diverse Physiological States’, *Journal of Bacteriology*, 189(11), pp. 4223–4233. Available at: https://doi.org/10.1128/JB.00107-07.

Rao, M.S. *et al.* (2019) ‘Comparison of RNA-Seq and Microarray Gene Expression Platforms for the Toxicogenomic Evaluation of Liver From Short-Term Rat Toxicity Studies’, *Frontiers in Genetics*, 9. Available at: https://www.frontiersin.org/articles/10.3389/fgene.2018.00636 (Accessed: 26 June 2023).

Reddinger, R.M. *et al.* (2016) ‘Host Physiologic Changes Induced by Influenza A Virus Lead to Staphylococcus aureus Biofilm Dispersion and Transition from Asymptomatic Colonization to Invasive Disease’, *mBio*, 7(4), pp. e01235-16. Available at: https://doi.org/10.1128/mBio.01235-16.

Reffuveille, F. *et al.* (2017) ‘Staphylococcus aureus Biofilms and their Impact on the Medical Field’, *The Rise of Virulence and Antibiotic Resistance in* Staphylococcus aureus [Preprint]. Available at: https://doi.org/10.5772/66380.

Regassa, L.B., Novick, R.P. and Betley, M.J. (1992) ‘Glucose and nonmaintained pH decrease expression of the accessory gene regulator (agr) in Staphylococcus aureus’, *Infection and Immunity*, 60(8), pp. 3381–3388. Available at: https://doi.org/10.1128/iai.60.8.3381-3388.1992.

Ren, W. *et al.* (2018) ‘Amino Acids As Mediators of Metabolic Cross Talk between Host and Pathogen’, *Frontiers in Immunology*, 9, p. 319. Available at: https://doi.org/10.3389/fimmu.2018.00319.

Renner, L.D. and Weibel, D.B. (2011) ‘Physicochemical regulation of biofilm formation’, *MRS bulletin / Materials Research Society*, 36(5), pp. 347–355. Available at: https://doi.org/10.1557/mrs.2011.65.

Rice, K.C. *et al.* (2007) ‘The cidA murein hydrolase regulator contributes to DNA release and biofilm development in Staphylococcus aureus’, *Proceedings of the National Academy of Sciences of the United States of America*, 104(19), pp. 8113–8118. Available at: https://doi.org/10.1073/pnas.0610226104.

Rice, L.B. (2008) ‘Federal Funding for the Study of Antimicrobial Resistance in Nosocomial Pathogens: No ESKAPE’, *The Journal of Infectious Diseases*, 197(8), pp. 1079–1081. Available at: https://doi.org/10.1086/533452.

Roberts, L.D. *et al.* (2012) ‘Targeted Metabolomics’, *Current Protocols in Molecular Biology*, CHAPTER, p. Unit30.2. Available at: https://doi.org/10.1002/0471142727.mb3002s98.

Robinson, M.D., McCarthy, D.J. and Smyth, G.K. (2010) 'edgeR: a Bioconductor package for differential expression analysis of digital gene expression data', *Bioinformatics*, 26(1), pp. 139–140. Available at: https://doi.org/10.1093/bioinformatics/btp616.

Roche, F.M., Meehan, M. and Foster, T.J. (2003) 'The Staphylococcus aureus surface protein SasG and its homologues promote bacterial adherence to human desquamated nasal epithelial cells', *Microbiology,* 149(10), pp. 2759–2767. Available at: https://doi.org/10.1099/mic.0.26412-0.

Rodrigues, M.L. and Nosanchuk, J.D. (2020) 'Fungal diseases as neglected pathogens: A wake-up call to public health officials', *PLOS Neglected Tropical Diseases*, 14(2), p. e0007964. Available at: https://doi.org/10.1371/journal.pntd.0007964.

Römling, U. *et al.* (2014) 'Microbial biofilm formation: a need to act', *Journal of Internal Medicine*, 276(2), pp. 98–110. Available at: https://doi.org/10.1111/joim.12242.

Rupp, C.J., Fux, C.A. and Stoodley, P. (2005) 'Viscoelasticity of Staphylococcus aureus Biofilms in Response to Fluid Shear Allows Resistance to Detachment and Facilitates Rolling Migration', *Applied and Environmental Microbiology*, 71(4), pp. 2175–2178. Available at: https://doi.org/10.1128/AEM.71.4.2175-2178.2005.

Sadykov, M.R. and Bayles, K.W. (2012) 'The control of death and lysis in staphylococcal biofilms: a coordination of physiological signals', *Current Opinion in Microbiology*, 15(2), pp. 211–215. Available at: https://doi.org/10.1016/j.mib.2011.12.010.

Salgado-Pabón, W. and Schlievert, P.M. (2014) 'Models matter: the search for an effective Staphylococcus aureus vaccine', *Nature Reviews Microbiology*, 12(8), pp. 585–591. Available at: https://doi.org/10.1038/nrmicro3308.

Salini, R. *et al.* (2019) 'Synergistic antibiofilm efficacy of undecanoic acid and auxins against quorum sensing mediated biofilm formation of luminescent Vibrio harveyi', *Aquaculture*, 498, pp. 162–170. Available at: https://doi.org/10.1016/j.aquaculture.2018.08.038.

Sanchez, L.M. *et al.* (2016) 'Biofilm Formation and Detachment in Gram-Negative Pathogens Is Modulated by Select Bile Acids', *PLoS ONE*, 11(3), p. e0149603. Available at: https://doi.org/10.1371/journal.pone.0149603.

Satpute, S.K. *et al.* (2016) 'Biosurfactant/s from Lactobacilli species: Properties, challenges and potential biomedical applications', *Journal of Basic Microbiology*, 56(11), pp. 1140–1158. Available at: https://doi.org/10.1002/jobm.201600143.

Schlecht, L.M. *et al.* (2015) 'Systemic Staphylococcus aureus infection mediated by Candida albicans hyphal invasion of mucosal tissue', *Microbiology*, 161(Pt 1), pp. 168–181. Available at: https://doi.org/10.1099/mic.0.083485-0.

Schroeder, K. *et al.* (2009) 'Molecular Characterization of a Novel Staphylococcus Aureus Surface Protein (SasC) Involved in Cell Aggregation and Biofilm Accumulation', *PLOS ONE*, 4(10), p. e7567. Available at: https://doi.org/10.1371/journal.pone.0007567.

Secor, P.R. *et al.* (2011) 'Staphylococcus aureus Biofilm and Planktonic cultures differentially impact gene expression, mapk phosphorylation, and cytokine production in human keratinocytes', *BMC Microbiology*, 11, p. 143. Available at: https://doi.org/10.1186/1471-2180-11-143.

Sellam, A. *et al.* (2009) 'A Candida albicans early stage biofilm detachment event in rich medium', *BMC Microbiology*, 9(1), p. 25. Available at: https://doi.org/10.1186/1471-2180-9-25.

Severn, M.M. and Horswill, A.R. (2023) 'Staphylococcus epidermidis and its dual lifestyle in skin health and infection', *Nature Reviews Microbiology*, 21(2), pp. 97–111. Available at: https://doi.org/10.1038/s41579-022-00780-3.

She, P. *et al.* (2020) 'Antibiofilm efficacy of the gold compound auranofin on dual species biofilms of Staphylococcus aureus and Candida sp.', *Journal of Applied Microbiology*, 128(1), pp. 88–101. Available at: https://doi.org/10.1111/jam.14443.

Short, B. *et al.* (2021) 'Investigating the Transcriptome of Candida albicans in a Dual-Species Staphylococcus aureus Biofilm Model', *Frontiers in Cellular and Infection Microbiology*, 11. Available at: https://www.frontiersin.org/article/10.3389/fcimb.2021.791523 (Accessed: 22 February 2022).

Silva, S. *et al.* (2009) 'Biofilms of non-Candida albicans Candida species: quantification, structure and matrix composition', *Medical Mycology*, 47(7), pp. 681–689. Available at: https://doi.org/10.3109/13693780802549594.

Silva, S. *et al.* (2012) 'Candida glabrata, Candida parapsilosis and Candida tropicalis: biology, epidemiology, pathogenicity and antifungal resistance', *FEMS Microbiology Reviews*, 36(2), pp. 288–305. Available at: https://doi.org/10.1111/j.1574-6976.2011.00278.x.

Singh, D.K. *et al.* (2019) 'Functional Characterization of Secreted Aspartyl Proteases in Candida parapsilosis', *mSphere*, 4(4). Available at: https://doi.org/10.1128/mSphere.00484-19.

Singh, R. *et al.* (2016) 'Penetration barrier contributes to bacterial biofilm-associated resistance against only select antibiotics, and exhibits genus-, strain- and antibiotic-specific differences', *Pathogens and Disease*, 74(6), p. ftw056. Available at: https://doi.org/10.1093/femspd/ftw056.

Sollid, J.U.E. *et al.* (2014) 'Staphylococcus aureus: Determinants of human carriage', *Infection, Genetics and Evolution*, 21, pp. 531–541. Available at: https://doi.org/10.1016/j.meegid.2013.03.020.

Soutourina, O. *et al.* (2009) 'CymR, the master regulator of cysteine metabolism in Staphylococcus aureus, controls host sulphur source utilization and plays a role in biofilm formation', *Molecular Microbiology*, 73(2), pp. 194–211. Available at: https://doi.org/10.1111/j.1365-2958.2009.06760.x.

Speziale, P. *et al.* (2014) 'Protein-based biofilm matrices in Staphylococci', *Frontiers in Cellular and Infection Microbiology*, 4, p. 171. Available at: https://doi.org/10.3389/fcimb.2014.00171.

Stapleton, P.D. and Taylor, P.W. (2002) 'Methicillin resistance in Staphylococcus aureus', *Science progress*, 85(Pt 1), pp. 57–72.

Stauff, D.L. *et al.* (2008) 'Staphylococcus aureus HrtA Is an ATPase Required for Protection against Heme Toxicity and Prevention of a Transcriptional Heme Stress Response', *Journal of Bacteriology*, 190(10), pp. 3588–3596. Available at: https://doi.org/10.1128/JB.01921-07.

Stewart, P.S. and Franklin, M.J. (2008) 'Physiological heterogeneity in biofilms', *Nature Reviews Microbiology*, 6(3), pp. 199–210. Available at: https://doi.org/10.1038/nrmicro1838.

Stock, A.M., Robinson, V.L. and Goudreau, P.N. (2000) 'Two-component signal transduction', *Annual Review of Biochemistry*, 69, pp. 183–215. Available at: https://doi.org/10.1146/annurev.biochem.69.1.183.

Subhadra, B. *et al.* (2018) 'Control of Biofilm Formation in Healthcare: Recent Advances Exploiting Quorum-Sensing Interference Strategies and Multidrug Efflux Pump Inhibitors', *Materials*, 11(9). Available at: https://doi.org/10.3390/ma11091676.

Sugimoto, S. *et al.* (2018) 'Broad impact of extracellular DNA on biofilm formation by clinically isolated Methicillin-resistant and -sensitive strains of Staphylococcus aureus', *Scientific Reports*, 8(1), p. 2254. Available at: https://doi.org/10.1038/s41598-018-20485-z.

Suresh, M.K., Biswas, R. and Biswas, L. (2019) 'An update on recent developments in the prevention and treatment of Staphylococcus aureus biofilms', *International Journal of Medical Microbiology*, 309(1), pp. 1–12. Available at: https://doi.org/10.1016/j.ijmm.2018.11.002.

Tacconelli, E. *et al.* (2018) 'Discovery, research, and development of new antibiotics: the WHO priority list of antibiotic-resistant bacteria and tuberculosis', *The Lancet Infectious Diseases*, 18(3), pp. 318–327. Available at: https://doi.org/10.1016/S1473-3099(17)30753-3.

Taei, M., Chadeganipour, M. and Mohammadi, R. (2019) 'An alarming rise of non-albicans Candida species and uncommon yeasts in the clinical samples; a combination of various molecular techniques for identification of etiologic agents', *BMC Research Notes*, 12(1), p. 779. Available at: https://doi.org/10.1186/s13104-019-4811-1.

Tan, L. *et al.* (2018) 'Therapeutic Targeting of the Staphylococcus aureus Accessory Gene Regulator (agr) System', *Frontiers in Microbiology*, 9. Available at: https://www.frontiersin.org/article/10.3389/fmicb.2018.00055 (Accessed: 16 February 2022).

Tan, X. *et al.* (2015) 'Transcriptome analysis of the biofilm formed by methicillin-susceptible Staphylococcus aureus', *Scientific Reports*, 5(1), p. 11997. Available at: https://doi.org/10.1038/srep11997.

Tanwar, J. *et al.* (2014) 'Multidrug Resistance: An Emerging Crisis', *Interdisciplinary Perspectives on Infectious Diseases*, 2014, p. 541340. Available at: https://doi.org/10.1155/2014/541340.

Tegmark, K., Karlsson, A. and Arvidson, S. (2000) 'Identification and characterization of SarH1, a new global regulator of virulence gene expression in Staphylococcus aureus', *Molecular Microbiology*, 37(2), pp. 398–409. Available at: https://doi.org/10.1046/j.1365-2958.2000.02003.x.

Thammavongsa, V., Missiakas, D.M. and Schneewind, O. (2013) 'Staphylococcus aureus Degrades Neutrophil Extracellular Traps to Promote Immune Cell Death', *Science*, 342(6160), pp. 863–866. Available at: https://doi.org/10.1126/science.1242255.

Theis, T.J. *et al.* (2023) 'Staphylococcus aureus persisters are associated with reduced clearance in a catheter-associated biofilm infection', *Frontiers in Cellular and Infection Microbiology*, 13. Available at: https://www.frontiersin.org/articles/10.3389/fcimb.2023.1178526 (Accessed: 2 August 2023).

Thoendel, M. *et al.* (2011) 'Peptide signaling in the Staphylococci', *Chemical reviews*, 111(1), pp. 117–151. Available at: https://doi.org/10.1021/cr100370n.

Thomas, V.C. and Hancock, L.E. (2009) 'Suicide and Fratricide in Bacterial Biofilms', *The International Journal of Artificial Organs*, 32(9), pp. 537–544. Available at: https://doi.org/10.1177/039139880903200902.

Thomer, L., Schneewind, O. and Missiakas, D. (2016) 'Pathogenesis of Staphylococcus aureus Bloodstream Infections', *Annual review of pathology*, 11, pp. 343–364. Available at: https://doi.org/10.1146/annurev-pathol-012615-044351.

Thurlow, L.R. *et al.* (2011) 'Staphylococcus aureus Biofilms Prevent Macrophage Phagocytosis and Attenuate Inflammation In Vivo', *The Journal of Immunology*, 186(11), pp. 6585–6596. Available at: https://doi.org/10.4049/jimmunol.1002794.

Todd, O.A. *et al.* (2019) 'Candida albicans Augments Staphylococcus aureus Virulence by Engaging the Staphylococcal agr Quorum Sensing System', *mBio* [Preprint]. Available at: https://doi.org/10.1128/mBio.00910-19.

Todd, O.A., Noverr, M.C. and Peters, B.M. (2019) 'Candida albicans Impacts Staphylococcus aureus Alpha-Toxin Production via Extracellular Alkalinization', *mSphere*, 4(6), pp. e00780-19. Available at: https://doi.org/10.1128/mSphere.00780-19.

Tong, S.Y.C. *et al.* (2015) 'Staphylococcus aureus Infections: Epidemiology, Pathophysiology, Clinical Manifestations, and Management', *Clinical Microbiology Reviews*, 28(3), pp. 603–661. Available at: https://doi.org/10.1128/CMR.00134-14.

Tormo, M.Á. *et al.* (2005) 'SarA Is an Essential Positive Regulator of Staphylococcus epidermidis Biofilm Development', *Journal of Bacteriology*, 187(7), pp. 2348–2356. Available at: https://doi.org/10.1128/JB.187.7.2348-2356.2005.

Trofa, D., Gácser, A. and Nosanchuk, J.D. (2008) 'Candida parapsilosis, an Emerging Fungal Pathogen', *Clinical Microbiology Reviews*, 21(4), pp. 606–625. Available at: https://doi.org/10.1128/CMR.00013-08.

Trotonda, M.P. *et al.* (2005) 'SarA Positively Controls Bap-Dependent Biofilm Formation in Staphylococcus aureus', *Journal of Bacteriology*, 187(16), pp. 5790–5798. Available at: https://doi.org/10.1128/JB.187.16.5790-5798.2005.

Trunk, T. *et al.* (2018) 'Bacterial autoaggregation', *AIMS Microbiology*, 4(1), pp. 140–164. Available at: https://doi.org/10.3934/microbiol.2018.1.140.

Tshikantwa, T.S. *et al.* (2018) 'Current Trends and Potential Applications of Microbial Interactions for Human Welfare', *Frontiers in Microbiology*, 9, p. 1156. Available at: https://doi.org/10.3389/fmicb.2018.01156.

Uruén, C. *et al.* (2020) 'Biofilms as Promoters of Bacterial Antibiotic Resistance and Tolerance', *Antibiotics*, 10(1), p. 3. Available at: https://doi.org/10.3390/antibiotics10010003.

Valle, J. *et al.* (2003) 'SarA and not σB is essential for biofilm development by Staphylococcus aureus', *Molecular Microbiology*, 48(4), pp. 1075–1087. Available at: https://doi.org/10.1046/j.1365-2958.2003.03493.x.

Valle, J., Echeverz, M. and Lasa, I. (2019) 'σB Inhibits Poly-N-Acetylglucosamine Exopolysaccharide Synthesis and Biofilm Formation in Staphylococcus aureus', *Journal of Bacteriology*, 201(11), pp. e00098-19. Available at: https://doi.org/10.1128/JB.00098-19.

Vandecandelaere, I. *et al.* (2017) 'Metabolic activity, urease production, antibiotic resistance and virulence in dual species biofilms of Staphylococcus epidermidis and Staphylococcus aureus', *PLOS ONE*, 12(3), p. e0172700. Available at: https://doi.org/10.1371/journal.pone.0172700.

VanEpps, J.S. and Younger, J.G. (2016) 'Implantable Device Related Infection', *Shock (Augusta, Ga.)*, 46(6), pp. 597–608. Available at: https://doi.org/10.1097/SHK.0000000000000692.

Vestby, L.K. *et al.* (2020) 'Bacterial Biofilm and its Role in the Pathogenesis of Disease', *Antibiotics*, 9(2), p. 59. Available at: https://doi.org/10.3390/antibiotics9020059.

Vila, T. *et al.* (2021) 'Therapeutic implications of C. albicans-S. aureus mixed biofilm in a murine subcutaneous catheter model of polymicrobial infection', *Virulence*, 12(1), pp. 835–851. Available at: https://doi.org/10.1080/21505594.2021.1894834.

Virmani, R., Hasija, Y. and Singh, Y. (2018) 'Effect of Homocysteine on Biofilm Formation by Mycobacteria', *Indian Journal of Microbiology*, 58(3), pp. 287–293. Available at: https://doi.org/10.1007/s12088-018-0739-8.

Vlaeminck, J. *et al.* (2022) 'The dynamic transcriptome during maturation of biofilms formed by methicillin-resistant Staphylococcus aureus', *Frontiers in Microbiology*, 13. Available at: https://www.frontiersin.org/articles/10.3389/fmicb.2022.882346 (Accessed: 27 June 2023).

Vudhya Gowrisankar, Y. *et al.* (2021) 'Staphylococcus aureus grown in anaerobic conditions exhibits elevated glutamine biosynthesis and biofilm units', *Canadian Journal of Microbiology*, 67(4), pp. 323–331. Available at: https://doi.org/10.1139/cjm-2020-0434.

Wagner, A. and Daum, G. (2005) 'Formation and mobilization of neutral lipids in the yeast Saccharomyces cerevisiae', *Biochemical Society Transactions*, 33(Pt 5), pp. 1174–1177. Available at: https://doi.org/10.1042/BST20051174.

Wang, X., Preston, J.F. and Romeo, T. (2004) 'The pgaABCD Locus of Escherichia coli Promotes the Synthesis of a Polysaccharide Adhesin Required for Biofilm Formation', *Journal of Bacteriology*, 186(9), pp. 2724–2734. Available at: https://doi.org/10.1128/JB.186.9.2724-2734.2004.

Wang, Yaqi *et al.* (2021) 'Metabolism Characteristics of Lactic Acid Bacteria and the Expanding Applications in Food Industry', *Frontiers in Bioengineering and Biotechnology*, 9. Available at: https://www.frontiersin.org/articles/10.3389/fbioe.2021.612285 (Accessed: 6 March 2023).

Weinstein, R.A. and Darouiche, R.O. (2001) 'Device-Associated Infections: A Macroproblem that Starts with Microadherence', *Clinical Infectious Diseases*, 33(9), pp. 1567–1572. Available at: https://doi.org/10.1086/323130.

Wijesinghe, G. *et al.* (2019) 'Influence of Laboratory Culture Media on in vitro Growth, Adhesion, and Biofilm Formation of Pseudomonas aeruginosa and Staphylococcus aureus', *Medical Principles and Practice*, 28(1), pp. 28–35. Available at: https://doi.org/10.1159/000494757.

Wolcott, R. *et al.* (2013) 'The polymicrobial nature of biofilm infection', *Clinical Microbiology and Infection*, 19(2), pp. 107–112. Available at: https://doi.org/10.1111/j.1469-0691.2012.04001.x.

Wolcott, R.D., Kennedy, J.P. and Dowd, S.E. (2009) 'Regular debridement is the main tool for maintaining a healthy wound bed in most chronic wounds', *Journal of Wound Care*, 18(2), pp. 54–56. Available at: https://doi.org/10.12968/jowc.2009.18.2.38743.

World Health Organization (2019) 'Thirteenth General Programme of Work, 2019–2023'. Available at: https://apps.who.int/ iris/bitstream/handle/10665/324775/WHO-PRP-18.1-eng.pdf (Accessed: 19 September 2022).

World Health Organization (2021) *Surveillance of antimicrobial resistance in Europe, 2020 data*. Available at: https://www.ecdc.europa.eu/en/publications-data/surveillance-antimicrobial-resistance-europe-2020 (Accessed: 5 January 2022).

Wu, Y.-M. *et al.* (2021) 'Enhanced Virulence of Candida albicans by Staphylococcus aureus: Evidence in Clinical Bloodstream Infections and Infected Zebrafish Embryos', *Journal of Fungi*, 7(12), p. 1099. Available at: https://doi.org/10.3390/jof7121099.

Yarwood, J.M. *et al.* (2004) 'Quorum Sensing in Staphylococcus aureus Biofilms', *Journal of Bacteriology*, 186(6), pp. 1838–1850. Available at: https://doi.org/10.1128/JB.186.6.1838-1850.2004.

Yonemoto, K. *et al.* (2019) 'Redundant and Distinct Roles of Secreted Protein Eap and Cell Wall-Anchored Protein SasG in Biofilm Formation and Pathogenicity of Staphylococcus aureus', *Infection and Immunity*, 87(4), pp. e00894-18. Available at: https://doi.org/10.1128/IAI.00894-18.

Yu, J. *et al.* (2021) 'Thermonucleases Contribute to Staphylococcus aureus Biofilm Formation in Implant-Associated Infections–A Redundant and Complementary Story', *Frontiers in Microbiology*, 12. Available at: https://www.frontiersin.org/article/10.3389/fmicb.2021.687888 (Accessed: 16 February 2022).

Zapotoczna, M. *et al.* (2015) 'An Essential Role for Coagulase in Staphylococcus aureus Biofilm Development Reveals New Therapeutic Possibilities for Device-Related Infections', *The Journal of Infectious Diseases*, 212(12), pp. 1883–1893. Available at: https://doi.org/10.1093/infdis/jiv319.

Zapotoczna, M., O'Neill, E. and O'Gara, J.P. (2016) 'Untangling the Diverse and Redundant Mechanisms of Staphylococcus aureus Biofilm Formation', *PLOS Pathogens*, 12(7), p. e1005671. Available at: https://doi.org/10.1371/journal.ppat.1005671.

Zhang, F. *et al.* (2021) 'Bacillus subtilis revives conventional antibiotics against Staphylococcus aureus osteomyelitis', *Microbial Cell Factories*, 20(1), p. 102. Available at: https://doi.org/10.1186/s12934-021-01592-5.

Zhao, G. *et al.* (2013) 'Biofilms and Inflammation in Chronic Wounds', *Advances in Wound Care*, 2(7), pp. 389–399. Available at: https://doi.org/10.1089/wound.2012.0381.

Zheng, Y. *et al.* (2022) 'Commensal Staphylococcus epidermidis contributes to skin barrier homeostasis by generating protective ceramides', *Cell host & microbe*, 30(3), pp. 301-313.e9. Available at: https://doi.org/10.1016/j.chom.2022.01.004.

Zhou, C. *et al.* (2019) 'Urease is an essential component of the acid response network of Staphylococcus aureus and is required for a persistent murine kidney infection', *PLoS Pathogens*, 15(1), p. e1007538. Available at: https://doi.org/10.1371/journal.ppat.1007538.

Zhou, C. and Fey, P.D. (2020) 'The Acid Response Network of Staphylococcus aureus', *Current opinion in microbiology*, 55, pp. 67–73. Available at: https://doi.org/10.1016/j.mib.2020.03.006.

Zhu, Y. *et al.* (2007) 'Staphylococcus aureus Biofilm Metabolism and the Influence of Arginine on Polysaccharide Intercellular Adhesin Synthesis, Biofilm Formation, and Pathogenesis', *Infection and Immunity*, 75(9), pp. 4219–4226. Available at: https://doi.org/10.1128/IAI.00509-07.

Appendix

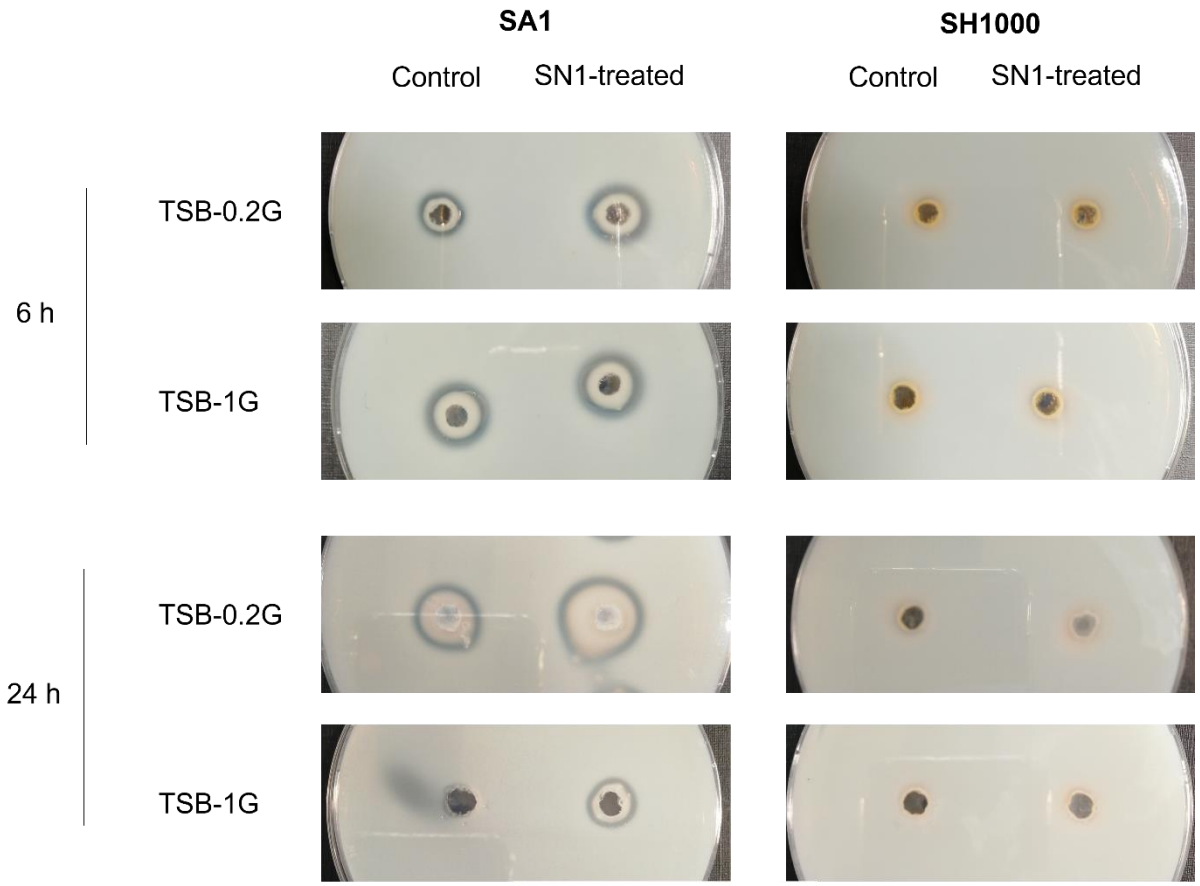

Figure A1. Protease activity of *C. parapsilosis* CFS-treated *S. aureus* biofilm supernatants. Two *S. aureus* strains, SA1 and SH1000 were grown in TSB-0.2G or TSB-1G media with or without SN1 (*C. parapsilosis* CFS). Biofilm supernatant samples were taken at 6 h and 24 h. Zones of clearing indicate protease activity. The diameter of each well is 5 mm.

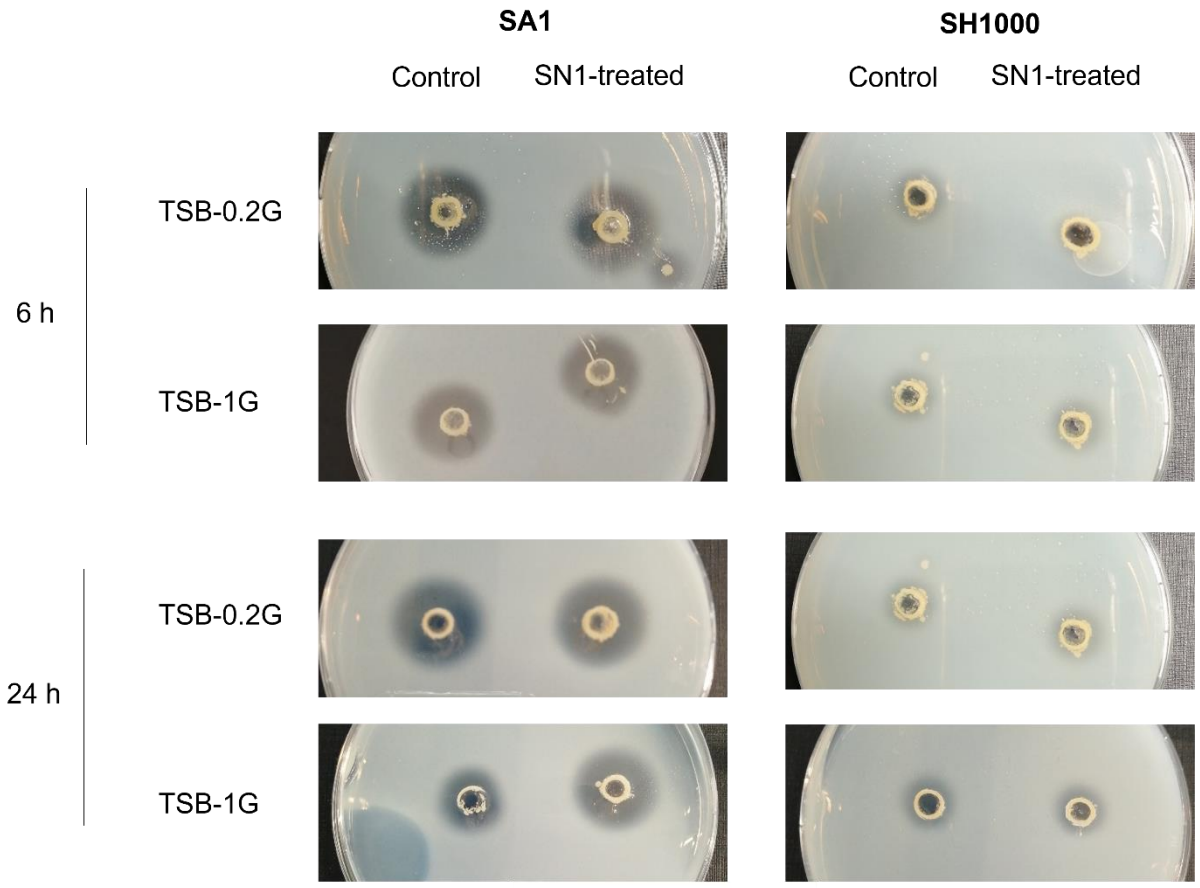

Figure A2. DNase activity of *C. parapsilosis* CFS-treated *S. aureus* biofilm supernatants. Two *S. aureus* strains, SA1 and SH1000 were grown in TSB-0.2G or TSB-1G media with or without SN1 (*C. parapsilosis* CFS). Biofilm supernatant samples were taken at 6 h and 24 h. Zones of clearing indicate DNase activity. The diameter of each well is 5 mm.

Table A1. Strain names and origin information for the *Candida parapsilosis* clinical isolates.

Number	Name	Origin	Isolated from	Reference
CP1	CLIB214	Puerto Rico	Faeces	Type strain
CP2	CDC317	USA	Health care workers hand	Clark et al 2004 doi: 10.1128/JCM.42.10.4468-4472.2004
CP3	CDC173	USA	Blood or catheter cultures	Kuhn et al 2004 doi: 10.3201/eid1006.030873
CP4	711701	Aberdeen, UK	Unknown	Tavanti et al doi 10.1128/JCM.43.1.284-292.2005
CP5	CDC167	USA	Blood or catheter cultures	Kuhn et al 2004 doi: 10.3201/eid1006.030873
CP6	J961250	Lisbon, Portugal	Nail	Tavanti et al doi 10.1128/JCM.43.1.284-292.2005
CP7	CDC179	USA	Blood or catheter cultures	Kuhn et al 2004 doi: 10.3201/eid1006.030873
CP8	J930733	Beerse, Belgium	Cat hair	Tavanti et al doi 10.1128/JCM.43.1.284-292.2005
CP9	103	London, UK	Anus	Tavanti et al doi 10.1128/JCM.43.1.284-292.2005
CP10	J930631/1	Africa	Cat hair	Tavanti et al doi 10.1128/JCM.43.1.284-292.2005
CP11	J960578	Hong Kong	Nail	Tavanti et al doi 10.1128/JCM.43.1.284-292.2005
CP12	81/040(s)	London, UK	Toe	Tavanti et al doi 10.1128/JCM.43.1.284-292.2005
CP13	81/041	Mayo Clinic, USA	Vagina	Tavanti et al doi 10.1128/JCM.43.1.284-292.2005
CP14	CDC177	USA	Blood or catheter cultures	Kuhn et al 2004 doi: 10.3201/eid1006.030873
CP15	90-137	San Jose, USA	Orbital Tissue	Tavanti et al doi 10.1128/JCM.43.1.284-292.2005

CP16	02-203	Bergamo, Italy	Blood	Tavanti et al doi 10.1128/JCM.43.1.284-292.2005
CP17	73/107	London, UK	Mouth	Tavanti et al doi 10.1128/JCM.43.1.284-292.2005
CP18	CDC165	USA	Blood or catheter cultures	Kuhn et al 2004 doi: 10.3201/eid1006.030873
CP19	81/253	London, UK	Nail	Tavanti et al doi 10.1128/JCM.43.1.284-292.2005
CP20	81/040 (C)	London, UK	Toe	Tavanti et al doi 10.1128/JCM.43.1.284-292.2005
CP21	J931058	Belgium	Nail	Tavanti et al doi 10.1128/JCM.43.1.284-292.2005
CP22	J951066	Korea	Nail	Tavanti et al doi 10.1128/JCM.43.1.284-292.2005
CP23	J950218	USA	Unknown	Tavanti et al doi 10.1128/JCM.43.1.284-292.2005
CP24	J931845	Japan	Unknown	Tavanti et al doi 10.1128/JCM.43.1.284-292.2005